



# University of HUDDERSFIELD

## University of Huddersfield Repository

Kakadia, Pratibha G.

Formulation and Evaluation of Nanoencapsulated Antimicrobial Agents for Dermal Delivery

### Original Citation

Kakadia, Pratibha G. (2016) Formulation and Evaluation of Nanoencapsulated Antimicrobial Agents for Dermal Delivery. Doctoral thesis, University of Huddersfield.

This version is available at <http://eprints.hud.ac.uk/id/eprint/28705/>

The University Repository is a digital collection of the research output of the University, available on Open Access. Copyright and Moral Rights for the items on this site are retained by the individual author and/or other copyright owners. Users may access full items free of charge; copies of full text items generally can be reproduced, displayed or performed and given to third parties in any format or medium for personal research or study, educational or not-for-profit purposes without prior permission or charge, provided:

- The authors, title and full bibliographic details is credited in any copy;
- A hyperlink and/or URL is included for the original metadata page; and
- The content is not changed in any way.

For more information, including our policy and submission procedure, please contact the Repository Team at: [E.mailbox@hud.ac.uk](mailto:E.mailbox@hud.ac.uk).

<http://eprints.hud.ac.uk/>

**FORMULATION AND EVALUATION OF  
NANOENCAPSULATED ANTIMICROBIAL  
AGENTS FOR DERMAL DELIVERY**

**PRATIBHA KAKADIA**

A thesis submitted in partial fulfilment of the requirements for the degree of  
Doctor of Philosophy

**THE UNIVERSITY OF HUDDERSFIELD  
2016**

## SUMMARY

Healthcare associated infections are a major concern within the health services as they inflict a significant financial burdens and time constraints on the healthcare system. Effective skin antisepsis prior to incision of the skin, for example, during surgery, is essential in preventing subsequent infection. Current evidence-based guidelines recommend the use of 2 % (w/v) chlorhexidine digluconate (CHG), preferably in 70 % (v/v) isopropyl alcohol (IPA) prior to incision of the skin. However, many antimicrobial agents poorly permeate into the skin and microorganisms residing in the deeper layers and around hair follicles, may survive the procedure and cause infection. Lipid-based nanocarriers are promising drug delivery system with the potential to improve chemical stability, control drug release and alter drug pharmacokinetics.

In present study, the ability of lipid-based nanocarriers to enhance the skin retention of antimicrobial agents was accessed. The solid lipid nanoparticles (SLNs) and nanoemulsions (NEs) of triclosan (TSN) and chlorhexidine digluconate (CHG) were prepared and compared based on their physicochemical parameter and better skin retention properties. SLNs of TSN was prepared using glyceryl behenate (GB) and glyceryl palmitostearate (GP) solid lipids, while NEs of TSN and CHG were prepared using eucalyptus oil (EO) and olive oil (OO) with combination of surfactants Tween<sup>®</sup> 80 and Span<sup>®</sup> 80. Characterisation and optimisation of SLN and NE formulations to find better skin retention ability is described with various other studies within this thesis.

Skin permeation of TSN and CHG was subsequently investigated by *in vitro* Franz diffusion model using artificial membrane and full thickness porcine ear skin and the penetration profile were determined by differential stripping technique to quantify the amount of drug retained within skin. In both SLN and NE formulations, no detectable level of TSN and CHG was found in receiver medium through full thickness porcine ear skin in 24 h, which is advantageous for topical drug delivery system.

SLNs prepared with GP, as solid lipid was able to produce smaller size formulation along with better skin penetration compared with GB-SLNs formulation. SLNs and NEs of TSN was analysed and compared for enhanced skin retention properties. The results demonstrated a significantly enhanced skin penetration of TSN for NE formulations compared to SLNs, which might be due to difference in composition and physical state of lipids and physicochemical parameter of formulations. In case of CHG-loaded NEs, the results demonstrated EO show better skin penetration compared to OO formulations due to its skin penetration enhancing property, which might be beneficial for skin antisepsis prior to invasive procedure to reduce the microorganisms on and within the skin. However, further studies are required to study antibacterial effects of nanoformulations against various skin microorganisms, to analyse skin permeation and retention ability of prepared nanoformulations in *in vivo* diffusion studies and further studies to analyse toxicity and skin tolerance of EO alone or in combination with antimicrobial agents.

Key words: skin permeation, solid lipid nanoparticles, nanoemulsions, chlorhexidine digluconate, triclosan, eucalyptus oil, olive oil, Franz diffusion cell

## **DEDICATION**

This thesis is dedicated to my family, especially to my mom, without their love, support and encouragement; this would not have been possible.

## **ACKNOWLEDGEMENT**

The study of doctorate degree at University of Huddersfield possesses me a very valuable experience. This thesis would not have been possible without the selfless support, encouragement and useful advises from my supervisor, colleagues, family and friends; therefore I take this opportunity to thank everyone and express my sincere appreciation.

Foremost, I would like to express my sincere gratitude to my supervisor, Prof. Barbara Conway, with whom it has been my absolute privilege and pleasure to work, her kind guidance, affectionate encouragement and excellent support throughout my PhD studies made my research journey memorable. I sincerely thank you for making my doctoral degree a wonderful learning experience with not only the technical content but also the philosophical aspects. I would also like to thank my second supervisor Dr. Hassane Larhrib for his beneficial advice and helpful suggestion during my early year of research degree.

I must also extend my thanks to Dr. Alan Smith, Dr. Hamid Merchant, Dr. Kofi Asare-Addo and Miss Hayley Markham for their support, friendship and help. I also like to thank Dr. Jeremy Hopwood for his specialist advice, time and immense support with obtaining transmission electron microscopy images of my work within this thesis. Thanks also must go to all the staff, colleagues and my friends and to the other persons who I have not mentioned individually, for their support, assistance and valuable friendship to cherish forever.

Most importantly, I would like to convey my sincere thanks and gratitude to my family members; my thesis would not have completed without their patience, encouragement and support. My parents, my maternal uncle gave me the strength and support during my research. Finally I like to thank my sister and brother for their moral support and confidence on me. All your confidence gave me the strength to have this wonderful achievement.

I appreciate all of you for being so kind and supportive on me. Thank you!

# LIST OF CONTENTS

SUMMARY.....	2
ACKNOWLEDGEMENT .....	4
LIST OF FIGURES .....	11
LIST OF TABLES.....	15
LIST OF ABBREVIATIONS.....	17
1. CHAPTER – INTRODUCTION.....	19
1.1 Healthcare associated infections.....	19
1.1.1 Surgical site infections.....	19
1.1.1.1 Risk of developing surgical site infections.....	20
1.1.1.2 Cost of surgical site infections.....	20
1.1.1.3 Microorganisms .....	20
1.2 Wounds .....	22
1.2.1 Classification of wounds.....	22
1.2.1.1 Acute wounds .....	22
1.2.1.2 Chronic wounds .....	23
1.2.2 Wound infection .....	24
1.2.3 Wound healing.....	25
1.2.3.1 Haemostasis phase .....	25
1.2.3.2 Inflammatory phase .....	25
1.2.3.3 Proliferation .....	26
1.2.3.4 Remodeling phase.....	26
1.2.4 Wound dressings.....	27
1.2.5 Types of wound dressings .....	27
1.3 Skin .....	31
1.3.1 Structure of skin.....	31
1.3.1.1 Stratum corneum.....	32
1.3.1.2 Epidermis .....	32
1.3.1.3 Dermis.....	33
1.3.1.4 Skin appendages .....	33
1.3.2 Penetration pathways into the skin .....	34
1.3.3 Skin penetration enhancers .....	35

1.3.3.1 Chemical approach .....	35
1.3.3.2 Physical approach .....	39
1.3.4 Techniques for quantification of drug retained into skin.....	39
1.3.5 Topical antimicrobial agents.....	41
1.3.5.1 Alcohols .....	41
1.3.5.2 Povidone – iodine .....	42
1.3.5.3 Chlorhexidine digluconate.....	43
1.3.5.4 Triclosan .....	44
1.3.5.5 Essential oils .....	45
1.3.5.6 Silver compounds .....	46
1.4 Novel carriers for dermal drug delivery .....	47
1.4.1 Solid Lipid Nanoparticles .....	47
1.4.1.2 Advantages and disadvantages of solid lipid nanoparticles.....	48
1.4.1.3 Production methods .....	49
1.4.2 Nanoemulsions .....	49
1.4.2.1 Production methods .....	50
1.5 Aims of the thesis .....	51
<b>2. CHAPTER: MATERIALS AND GENERAL METHODS .....</b>	<b>52</b>
2.1 Materials .....	52
2.1.1 Compritol® 888 ATO .....	52
2.2.2 Precirol® ATO5 .....	53
2.2.3 Eucalyptus oil .....	54
2.2.4 Olive oil .....	54
2.2.5 Tween® 80 .....	55
2.2.6 Span® 80 .....	56
2.2.7 Transcutol® P .....	56
2.2.8 Sodium lauryl sulphate .....	57
2.2 General Methods.....	59
2.2.1 High performance liquid chromatography method development and validation	59
2.2.1.1 Method development for triclosan.....	59
2.2.1.2 Method development for chlorhexidine digluconate .....	60
2.2.1.3 High performance liquid chromatography method validation.....	60
2.2.1.3.1 Specificity .....	60
2.2.1.3.2 Accuracy .....	63

2.2.1.3.3 Linearity.....	64
2.2.1.3.4 Precision .....	66
2.2.2 Skin diffusion mechanism .....	68
2.2.2.1 <i>In vitro</i> skin permeation model.....	70
2.2.2.2 Membrane selection.....	71
2.2.3 Construction of pseudoternary phase diagrams .....	75
<b>3. CHAPTER: FORMULATION AND EVALUATION OF SOLID LIPID NANOPARTICLES FOR DERMAL DELIVERY .....</b>	<b>77</b>
3.1 Introduction.....	77
3.2 Aims of the study.....	80
3.3 Materials and methods .....	81
3.3.1 Materials .....	81
3.3.2 Methods .....	81
3.3.2.1 Solubility studies of triclosan in buffer .....	81
3.3.2.2 Formulation of solid lipid nanoparticles.....	81
3.3.2.3 Lyophilisation of solid lipid nanoparticles .....	84
3.3.3 Physicochemical characterisation.....	84
3.3.3.1 Particle size analysis .....	84
3.3.3.2 Determination of drug entrapment efficiency.....	84
3.3.3.3 Zeta potential measurement.....	85
3.3.3.4 Thermal analysis of solid lipid nanoparticles .....	85
3.3.3.5 Powder X-ray diffraction analysis .....	86
3.3.3.6 Transmission electron microscopy .....	86
3.3.3.7 Fourier transform infrared spectrometry .....	86
3.3.3.8 Stability study .....	86
3.3.3.9 Skin permeation study .....	87
3.3.3.9.1 <i>In vitro</i> skin diffusion studies .....	87
3.3.3.9.2 Quantification of triclosan from skin using differential stripping technique.....	88
3.3.3.9.3 <i>In vitro</i> comparison study of follicular penetration using differential stripping technique.....	89
3.3.3.10 Statistical analysis.....	90
3.4 Results and Discussion .....	91
3.4.1 Solubility studies of triclosan in buffer .....	91



3.4.2 Preparation and optimisation of solid lipid nanoparticles .....	92
3.4.2.1 Effect of homogenisation speed and time.....	92
3.4.2.3 Effect of surfactant and cosurfactant ratio.....	95
3.4.3 Physicochemical characterisation.....	97
3.4.3.1 Determination of particle size, zeta potential and percent drug entrapment efficiency .....	97
3.4.3.2 Thermal analysis of solid lipid nanoparticles .....	101
3.4.3.3 Powder X-ray diffraction analysis .....	103
3.4.3.4 Transmission electron microscopy .....	104
3.4.3.5 Fourier Transform infrared spectrometry .....	105
3.4.3.6 Stability study .....	107
3.4.3.7 Skin permeation study.....	110
3.4.3.7.1 <i>In vitro</i> skin permeation studies.....	110
3.4.3.7.2 Quantification of triclosan from skin using differential stripping techniques .....	112
3.4.3.7.3 <i>In vitro</i> comparison studies of follicular penetration using differential stripping technique.....	114
3.5 Conclusion .....	116
4. CHAPTER: DESIGNS AND DEVELOPMENT OF ANTIBACTERIAL NANOEMULSIONS FOR TOPICAL DELIVERY .....	118
4.1 Introduction.....	118
4.3 Materials and Methods .....	121
4.3.1 Solubility study of triclosan.....	121
4.3.2 Construction of pseudoternary phase diagrams .....	121
4.3.3 Formulation of triclosan nanoemulsions .....	122
4.3.4 Physicochemical characterisation of the nanoemulsion formulations.....	124
4.3.4.1 Accelerated stability studies .....	124
4.3.4.2 pH determination .....	124
4.3.4.3 Determination of viscosity.....	125
4.3.4.4 <i>In vitro</i> drug release and skin permeation studies .....	125
4.3.4.5 Quantification of triclosan in skin using an adhesive tape stripping method .....	125
4.3.4.6 Statistical analysis.....	126
4.4 Results and Discussion .....	127

4.4.1 Determination of triclosan solubility .....	127
4.4.2 Construction of pseudoternary phase diagrams .....	128
4.4.3 Preparation of nanoemulsions.....	132
4.4.3.1 Impact of homogenisation time .....	132
4.4.3.2. Impact of formulation variables.....	133
4.4.4 Accelerated stability study.....	136
4.4.5 Physicochemical characterisation of nanoemulsions.....	139
4.4.6 Morphological study .....	140
4.4.7 Thermal analysis .....	142
4.4.8 Fourier transform infrared analysis .....	143
4.4.9 <i>In vitro</i> release study.....	145
4.4.10 <i>In vitro</i> skin permeation study .....	146
4.4.10.1 Quantification of triclosan from skin using adhesive tape stripping method .....	148
4.4.11 Comparison of skin penetration of lipid nanocarriers for topical delivery of triclosan using <i>in vitro</i> diffusion studies.....	150
4.5 Conclusion .....	153
<b>5. CHAPTER – NANOEMULSIONS AS CARRIERS OF HYDROPHILIC COMPOUNDS FOR TOPICAL DELIVERY .....</b>	<b>154</b>
5.1 Introduction.....	154
5.2 Aims of the study.....	157
5.3 Materials and Method .....	158
5.3.1 Construction of pseudoternary phase diagrams .....	158
5.3.2 Formulation of chlorhexidine digluconate nanoemulsions.....	158
5.3.3 Physicochemical characterisation of nanoemulsion formulations.....	160
5.3.3.1 <i>In vitro</i> drug release and skin permeation studies .....	160
5.3.3.2 Quantification of chlorhexidine digluconate in skin using adhesive tape stripping method .....	161
5.3.3.3 <i>In vitro</i> skin diffusion studies of chlorhexidine digluconate nanoemulsions using methacrylate dressing powder.....	161
5.3.3.5 <i>In vitro</i> diffusion studies of chlorhexidine digluconate permeation using porcine ear skin and Strat- M <sup>®</sup> membrane .....	162
5.3.3.6 Studies of chlorhexidine digluconate penetration into barrier-intact and barrier-impaired porcine ear skin.....	162

5.3.3.7 Statistical analysis.....	162
5.4 Results and Discussion .....	163
5.4.1 Pseudoternary phase diagrams.....	163
5.4.2 Preparation and characterisation of nanoemulsions .....	166
5.4.2.1 Influence of homogenisation stirring speed and processing time.....	166
5.4.2.2. Influence of surfactant concentration .....	168
5.4.3 Thermal stability study .....	169
5.4.4 Physicochemical characterisation of nanoemulsions.....	172
5.4.5 Morphological study .....	173
5.4.6 Fourier transform infrared spectrometry .....	174
5.4.7 <i>In vitro</i> drug release study .....	176
5.4.8 <i>In vitro</i> skin diffusion studies .....	177
5.4.8.1 Quantification of chlorhexidine digluconate in skin using adhesive tape stripping method .....	179
5.4.9 <i>In vitro</i> skin diffusion studies of chlorhexidine digluconate nanoemulsions using methacrylate dressing powder .....	181
5.4.10 <i>In vitro</i> diffusion studies of chlorhexidine digluconate permeation using porcine ear skin and Strat- M <sup>®</sup> membrane .....	184
5.4.11 Studies of chlorhexidine digluconate penetration into barrier-intact and barrier-impaired porcine ear skin.....	187
6. CHAPTER: FINAL DISCUSSION AND FUTURE WORK .....	192
7. REFERENCES .....	198
8. PUBLICATIONS AND PROFESSIONAL ACTIVITIES .....	240

## LIST OF FIGURES

Figure 1.1 Schematic diagram of mammalian skin. ....	31
Figure 1.2 Schematic representation of drug penetration routes through the skin. ....	34
Figure 1.3 Povidone-iodine, the iodine complex with neutral polyvinylpyrrolidone polymer carrier. ....	42
Figure 1.4 Chemical structure of chlorhexidine digluconate [1,6-Bis(N5-[p-chlorophenyl]-N1-biguanido)hexane digluconate].....	43
Figure 1.5 Structure of triclosan. ....	44
Figure 1.6 Structure of solid lipid nanoparticles. ....	48
Figure 2.1 Chemical structure of glyceryl behenate. ....	52
Figure 2.2 Chemical structure of glyceryl palmitostearate.....	53
Figure 2.3 Chemical structure of polyoxyethylene sorbitan ester. ....	55
Figure 2.4 Chemical structure of sorbitan monooleate.....	56
Figure 2.5 Chemical structure of diethylene glycol monoethyl ether. ....	57
Figure 2.6 Chemical structure of sodium lauryl sulphate.....	57
Figure 2.7 Chromatogram of triclosan standard solution. ....	61
Figure 2.8 Chromatogram of triclosan test sample.....	61
Figure 2.9 Chromatogram of chlorhexidine digluconate standard solution. ....	62
Figure 2.10 Chromatogram of chlorhexidine digluconate test sample.....	62
Figure 2.11 Standard calibration curve for triclosan. ....	65
Figure 2.12 Standard calibration curve for chlorhexidine digluconate. ....	65
Figure 2.13 Molecular transport mechanism across a membrane. ....	68
Figure 2.14 Schematic diagram of Franz diffusion cell. ....	71
Figure 2.15 Schematic representation of pseudoternary phase diagram. ....	75
Figure 3.1 Experimental set up showing TSN skin retention study using unsliced full thickness porcine ear skin by GP-SLNs.....	90
Figure 3.2 Effect of homogenisation speed on mean particle size of GB-SLNs (GB5-2) and GP-SLNs (GP5-2).....	93
Figure 3.3 Effect of homogenisation time on mean particle size of GB-SLNs (GB5-2) and GP-SLNs (GP5-2) .....	93
Figure 3.4 Particle size distributions of GB-SLNs and GP-SLNs using NTA system.....	97
Figure 3.5 DSC thermograms of TSN, GB, physical mixture of GB and TSN, TSN-loaded GB-SLNs (GB3-2, GB5-2).....	101

Figure 3.6 DSC thermograms of TSN, GP, physical mixture of GP and TSN, TSN-loaded GP-SLNs (GP3-2, GP5-2).....	102
Figure 3.7 XRD pattern showing TSN, GB, TSN-loaded GB-SLNs (GB3-2, GB5-2).....	103
Figure 3.8 XRD pattern showing TSN, GP, TSN-loaded GP-SLNs (G53-2, GP5-2).....	103
Figure 3.9 TEM images (10,000 x) of TSN loaded SLNs.....	105
Figure 3.10 FTIR spectrums of TSN, GB and TSN-loaded GB-SLNs (GB3-2, GB5-2)...	105
Figure 3.11 FTIR spectrums of TSN, GP and TSN-loaded GP-SLNs (GP3-2, GP5-2).....	106
Figure 3.12 <i>In vitro</i> cumulative amount of triclosan permeated following 24 h topical application of SLN formulations and control solution through porcine ear skin.....	110
Figure 3.13 Triclosan uptake into skin treated with GB-SLNs (GB3-2, GB5-2), GP-SLNs (GP3-2, GP5-2) and control solution.....	112
Figure 3.14 Amount of triclosan recovered from full thickness unsliced and excised porcine ear skin.....	114
Figure 4.1 Pseudoternary phase diagrams of a) eucalyptus oil and b) olive oil with surfactant (T80) and water.....	129
Figure 4.2 Pseudoternary phase diagrams of eucalyptus oil, water and different ratios of surfactant mixture (T80:S80).....	130
Figure 4.3 Pseudoternary phase diagrams of olive oil, water and different ratios of surfactant mixture (T80:S80).....	131
Figure 4.4 Impact of homogenisation time on mean droplet size of EO-NEs and OO-NEs.....	132
Figure 4.5 TEM image of TSN-loaded NEs (EO-5;5).....	141
Figure 4.6 DSC thermograms for TSN, blank EO-NEs, and TSN-loaded EO-NEs (EO-5;5, EO-10;5).....	142
Figure 4.7 DSC thermograms for TSN, blank OO-NEs, and TSN-loaded OO-NEs (OO-5;5, OO-10;5).....	142
Figure 4.8 FTIR spectra for TSN, EO, Blank EO-NEs and the TSN-loaded EO-NEs (EO-5;5, EO-10;5).....	144
Figure 4.9 FTIR spectra for TSN, OO, Blank OO-NEs and the TSN-loaded OO-NEs (OO-5;5, OO-10;5).....	144
Figure 4.10 <i>In vitro</i> release profiles of TSN from EO-NEs (EO-5;5, EO-10;5), OO-NEs (OO-5;5, OO-10;5) and control solution.....	146
Figure 4.11 <i>In vitro</i> skin permeation profile of NE formulations (EO-5;5, EO-10;5, OO-5;5, OO-10;5) and control solution.....	147

Figure 4.12 <i>In vitro</i> profile of TSN accumulation in skin layers 24 h following topical application of control, EO-NEs (EO-5;5, EO-10;5) and OO-NEs (OO-5;5, OO-10;5).....	149
Figure 4.13 Amount of triclosan in the skin following application of GP-SLNs (GP5-2) and EO-NEs (EO-5;5).....	151
Figure 5.1 Hydrogel conversion of methacrylate powder dressing following the addition of CHG-NEs [C-EO-70(10)].....	161
Figure 5.2 Pseudoternary phase diagrams of a) eucalyptus oil and b) olive oil with surfactant (S80) and water.....	163
Figure 5.3 Pseudoternary phase diagrams of eucalyptus oil, water and different ratios of surfactant mixture (S80:T80).....	164
Figure 5.4 Pseudoternary phase diagrams of olive oil, water and different ratios of surfactant mixture (S80:T80).....	165
Figure 5.5 Influence of homogenisation speed on droplet size of CHG-loaded EO-NEs [C-EO-70(10)] and CHG-OO NEs [C-OO-70(10)].....	167
Figure 5.6 Influence of duration of homogenisation on droplet size of CHG-loaded OO-NEs [C-EO-70(10)] and CHG-OO NEs [C-OO-70(10)].....	168
Figure 5.7 TEM image of CHG-loaded NEs [C-EO-70(10)].....	173
Figure 5.8 FTIR spectra for CHG, EO, Blank EO-NEs and CHG-loaded EO-NEs [C-EO-70(10), C-EO-75(10)].....	175
Figure 5.9 FTIR spectra for CHG, OO, Blank OO-NEs and CHG-loaded OO-NEs [C-OO-70(10), C-OO-75(10)].....	175
Figure 5.10 <i>In vitro</i> release profiles of CHG from NE formulations [C-EO-70(10), C-EO-75(10), C-OO-70(10), C-OO-75(10)] and control solution.....	176
Figure 5.11 <i>In vitro</i> skin permeation of CHG from NE formulations [C-EO-70(10), C-EO-75(10), C-OO-70(10), C-OO-75(10)] and control solution.....	178
Figure 5.12 Penetration profiles showing the concentrations of CHG ( $\mu\text{g}/\text{mg}$ tissue) in porcine ear skin after 24 h exposure to the NE formulations [C-EO-70(10), C-EO-75(10), C-OO-70(10), C-OO-75(10)] and control solution.....	180
Figure 5.13 <i>In vitro</i> skin permeation of CHG in presence of methacrylate powder dressing from NE formulations [C-EO-70(10), C-EO-75(10), C-OO-70(10), C-OO-75(10)] and control solution.....	182
Figure 5.14 Penetration profiles showing the concentrations of CHG ( $\mu\text{g}/\text{mg}$ tissue) in presence of methacrylate powder dressing from NE formulations [C-EO-70(10), C-EO-75(10), C-OO-70(10), C-OO-75(10)] and control solution.....	183

Figure 5.15 <i>In vitro</i> skin diffusion studies of CHG through Strat-M membrane from NE formulations [C-EO-75(10), C-OO-75(10)] and control solution.....	185
Figure 5.16 <i>In vitro</i> skin diffusion of CHG through barrier impaired skin from NE formulations [C-EO-70(10), C-EO-75(10), C-OO-70(10), C-OO-75(10)] and control solution .....	187

## LIST OF TABLES

Table 2.1 Recovery of triclosan from spiked samples for determination of assay accuracy.....	63
Table 2.2 Recovery of chlorhexidine digluconate from spiked samples for determination of assay accuracy.....	63
Table 2.3 Intra-day and inter-day precision of HPLC methods for triclosan.....	66
Table 2.4 Intra-day and inter-day precision of HPLC method for chlorhexidine digluconate.....	67
Table 2.5 Chromatographic characteristics of HPLC system suitability.....	67
Table 3.1 Composition of preliminary TSN-loaded SLN formulations.....	83
Table 3.2 Solubility profile of triclosan in buffer.....	91
Table 3.3 Effect of concentration of lipid on percent drug entrapment efficiency of SLNs.....	94
Table 3.4 Effect of different ratios of surfactant and cosurfactant on mean particle size and percent drug entrapment efficiency of SLNs.....	96
Table 3.5 Physicochemical characterisation of GB-SLNs.....	98
Table 3.6 Physicochemical characterisation of GP-SLNs.....	99
Table 3.7 Particle size, PDI and zeta potential of GP-SLN formulations stored at room temperature and accelerated humidity conditions.....	108
Table 3.8 Particle size, PDI and zeta potential of GB-SLN formulations stored at room temperature and accelerated humidity conditions.....	109
Table 3.9 <i>In vitro</i> permeability parameters of TSN-loaded SLN formulations and control solution in porcine ear skin.....	112
Table 4.1 Compositions of preliminary TSN-loaded NE formulations.....	123
Table 4.2 Solubility of triclosan obtained in different oils and surfactants after 48 h equilibration at 25°C.....	127
Table 4.3 Effect of oil and surfactant concentrations on droplet size and distribution in EO-NE and OO-NE formulations.....	134
Table 4.4 Accelerated stability assessment of EO-NE and OO-NE formulations. ....	138
Table 4.5 Physicochemical characterisation of optimised NE formulations.....	140
Table 4.6 <i>In vitro</i> skin permeation parameters for NEs and control solution.....	148
Table 5.1 Composition of preliminary CHG-loaded NE formulations.....	159



Table 5.2 Influence of surfactant concentration on droplet size and distribution of CHG-loaded EO-NEs and OO-NEs.....	169
Table 5.3 Thermal stability assessments of CHG-loaded EO-NE and OO-NE formulations.....	171
Table 5.4 Physicochemical characterisation of NE formulations.....	172
Table 5.5 <i>In vitro</i> permeability parameters of CHG from NE formulations and control solution.....	179
Table 5. 6 Permeability parameters for CHG from control solution and NEs in porcine ear skin and Strat-M membrane.....	186
Table 5. 7 Amount of CHG recovered from the SC (15 tapes) and homogenised tissue following barrier-intact and barrier-impaired skin permeation studies.....	188

## LIST OF ABBREVIATIONS

AUC	Area under curve
BSIs	Blood stream infections
°C	Degree Celsius
CHG	Chlorhexidine digluconate
cm	Centimetre
cm <sup>2</sup>	Centimetre squared
cm <sup>-1</sup>	Reciprocal centimetre or wavenumber
CMC	Critical micelle concentration
cP	Centipoise
DEE	Drug entrapment efficiency
DSC	Differential scanning calorimetry
EO	Eucalyptus oil
FTIR	Fourier transform infrared
g	Gram
GB	Glyceryl behenate
GP	Glyceryl palmitostearate
h	Hour
HAIs	Healthcare associated infections
IgA	Immunoglobulin A
IPA	Isopropyl Alcohol
J <sub>ss</sub>	Steady state flux
kDa	Kilo dalton
K <sub>p</sub>	Permeability coefficient
LOD	Limit of detection
LOQ	Limit of quantification
mg	Milligram
MIC	Minimum inhibitory concentration
Min	Minute
ml	Millilitre
mM	Millimolar
MRSA	<i>Methicillin resistant staphylococcus aureus</i>
mV	Millivolt
NHS	National Health Service

NICE	National Institute for Health and Care Excellence
nm	Nanometre
OO	Olive oil
O/W	Oil-in-water
PBS	Phosphate buffer saline
PDI	Polydispersity Index
PG	Propylene Glycol
RH	Relative humidity
rpm	Revolution per minute
S80	Span 80
SC	Stratum corneum
SD	Standard deviation
Sec	Second
SLS	Sodium lauryl sulphate
T80	Tween 80
TEM	Transmission electron microscopy
TP	Transcutol P
W/O	Water-in-oil
w/w	Weight per weight
µg	Microgram
µg/mg	Microgram per milligram
µg/ml	Microgram per millilitre
µL	Microlitre
µm	Micrometre
XRD	X-ray diffractometry
ZP	Zeta potential

# 1. CHAPTER – INTRODUCTION

## 1.1 Healthcare associated infections

Healthcare associated infections (HAIs) are a major concern within the health services. These are defined as infections acquired either inside hospitals or as a direct result of a healthcare intervention. They inflict significant financial burdens and time constraints on the healthcare system due to increased morbidity and mortality rates, prolonged hospital occupancy and intensified treatment regimes, including repeated surgeries (Vilela *et al.*, 2007). The National Institute for Health and Care Excellence (NICE) estimates that HAIs account for approximately 300,000 infections per year in England, and contribute to 5,000 deaths per year, with an estimated extra cost to the National Health Service (NHS) of £1 billion annually. A significant number of HAIs (15 %) are thought to be preventable through compliance with infection control practices and adequate hygiene, including appropriate skin antisepsis prior to invasive procedures (Morse, 2009). There are many types of HAIs, which includes skin and soft tissue infections, primary bloodstream infections (BSIs), gastrointestinal infections and urinary tract infections (UTIs).

### 1.1.1 Surgical site infections

Surgical site infections (SSIs), are defined as infection that occurs at or near body parts after surgery. SSIs occurs due to microbial contamination and these microorganisms are may originated from either internal or external sources, which includes the patient's skin, mucous membranes or any contaminated item in the sterile surgical field, including surgical team members, instruments, air, or materials (De Lissovoy *et al.*, 2009). Infection only occurs if the number and virulence of bacteria or fungi overwhelm natural host defence mechanisms. SSIs represent the most common infection which account for 15 % of total infections among surgical patients (Reichman and Greenberg, 2009).

#### 1.1.1.1 Risk of developing surgical site infections

In 1999, the Hospital Infection Control Practices Advisory Committee of the Centres for Disease Control and Prevention published guidelines for the prevention of SSIs. To identify risk and to prevent the SSIs, there is a need of consideration of factors related to both patient and surgery (Mangram *et al.*, 1999). Several patient related factors which increase the risk of SSIs may include but not limited to diabetes, cigarette smoking, malnutrition, prolonged preoperative hospital stays, microorganisms colonisation (Blam *et al.*, 2003). In addition age, obesity and body site infection may also increase the risk of SSIs. Various pre and post-surgery related factors includes blood transfusion, length of hospital stay, duration of surgery and antibiotic prophylaxis (Triantafyllopoulos *et al.*, 2015).

#### 1.1.1.2 Cost of surgical site infections

SSIs raise health care cost due to prolonged hospitalisation, additional diagnostic tests, therapeutic antibiotic treatment, and, rarely, additional surgery. In 2009, it was estimated that SSIs extend the length of hospital stays by 9.7 days on average and increase costs by \$20,842 per admission, along with readmission into the hospital due to SSIs for an additional \$700 million of total health care cost (Reichman and Greenberg, 2009; Wilson *et al.*, 2015). Deep incisional SSIs cost more than the superficial infections. A study performed involving 16 patients to analyse SSIs cost, reported average increase of 115 % in the total treatment cost of SSIs compared to non-infected patients (Broex *et al.*, 2009).

#### 1.1.1.3 Microorganisms

Microorganisms responsible for SSIs are mainly originate from patients own flora. Most common isolated bacteria are *Staphylococcus aureus*, *Escherichia coli* and *Enterococcus species* (Schaberg, *et al.*, 1991). The increase in SSIs is caused by the antibiotic resistant pathogen such as *methicillin-resistant Staphylococcus aureus* (MRSA) or *Candida Albicans*, which increases the number of severely ill patients and hence the need to use broad

spectrum antimicrobial agents (Schaberg, 1994). Sudden outbreak of infections might also cause by the uncommon microorganisms such as *Clostridium perfringens*, *Rhodococcus bronchialis*, *Nocardia farcinica* and *Legionella pneumophila* due to the contaminated dressings, tap water, elastic bandages or contaminated disinfectant solution (Mangram *et al.*, 1999).

## 1.2 Wounds

A wound is defined as damage or disruption in the protective function of skin caused by loss of barrier property of epithelium followed by cuts, surgery, chemicals, friction force and pressure or as a result of disease.

### 1.2.1 Classification of wounds

Wounds can be classified in various methods, their location, type of injury or symptoms and the time require for healing. Based on the time require for healing wounds can be classified either acute or chronic.

#### 1.2.1.1 Acute wounds

Acute wounds are common health problems involving process of tissue repair immediately after injury. It is well-organised process with predictable healing which damages only epidermis and superficial dermis layer (Korting *et al.*, 2011a).

The acute wounds occur due to sudden loss of tissue or after surgery, which usually takes up to 30 days for healing process. Acute wounds are categorised based on cause (surgical incisions, abrasions, lacerations, thermal burns) and type (size and depth of tissue damage).

**Surgical incision wounds:** Surgical wounds are cuts through skin during surgery, which might be small or long depending upon the type of surgery. Incision wounds in blood vessels, heart or lungs can be painful and life threatening (Richardson, 2004).

**Abrasion wounds:** Abrasion wounds caused due to minor cuts or friction of injured skin with other surface results in damaged or removal of surface layer of skin. These wounds are generally small, pain free and less to no bleeding (Korting *et al.*, 2011b).

**Laceration wounds:** Laceration wounds occurs due to sudden trauma or accident forms an deeper cuts than the abrasion wounds with severe pain and more bleeding (Monaco and Lawrence, 2003).

**Thermal burn wounds:** A thermal burn is a damage of surface skin along with deeper layers of skin tissues, caused by contact with heat, electricity, chemicals, light, radiation or friction. Severe loss of skin can lead to infection and the loss of skin functions such as thermoregulation and immunity. Wounds caused by sun exposure or heat surface can be managed by first aid treatment while burns with heat flame or electric charge needs to be hospitalised (Li *et al.*, 2007).

#### 1.2.1.2 Chronic wounds

Multiple local disturbances and systemic disease, impaired wound healing, prolonged inflammation and a toxic environment are the main reasons for transition of acute wound to chronic state (Eming *et al.*, 2002). Some of the most common types of chronic wounds are as follows (Degreef, 1998; Robson *et al.*, 2001a; Szycher and Lee, 1992):

**Infectious wounds:** Infectious wounds are caused by bacterial, fungal or viral. They usually have drainage of pus, debris, bad odour and inflammation symptoms such as pain, fever or redness.

**Ischemic wounds:** Ischemic wound occurs due to lack of blood supply to tissue. The area will usually be pale and cold. Wound healing can be delayed due to less oxygen and nutrients supply.

**Surgical wounds:** Incision or cuts made during surgery results in surgical wounds, which might turn into chronic wounds if proper medical treatment or care is not provided.

Ulcers are the most common type of chronic wound, and can be further divided into categories as follows:

**1. Venous ulcers:** It is a most common vascular ulcer especially in lower legs including deep vein thrombosis, varicose veins and venous hypertension. Patients often have a history of lower limb oedema (swollen legs) or damaged leaking veins.



**2. Diabetic ulcers:** These are chronic, painless and clean ulcerations that develop due to vascular, neurological and metabolic disorders in diabetes. It results in nerve damage, poor blood supply and impaired immune function, which cause skin damage and ulceration. Even in the absence of infection, poor blood supply can lead to the establishment of dry diabetic gangrene.

**3. Pressure ulcers:** Pressure ulcers are also known as pressure sores and decubitus ulcers, which causes injury to skin or underlying tissue. These ulcers mainly develop over bony area that are close to skin due to the pressure or friction, which prevents the blood flow to soft tissue. These ulcers show symptoms such as redness followed by itching, blistering, swelling and discoloration of the area.

#### 1.2.2 Wound infection

Wound infection occurs due to colonisation of microorganisms at or near wounds, delaying process of wound healing. Wounds or insertion or insertion of intravascular lines and catheters causes disruption of epidermis, which can lead to pathogenic infection.. Infected wounds usually occur due to microorganisms present within skin and other areas of body or from external sources (Klimek, 1985). If the skin is intact microorganisms present within skin are normally harmless, but in wound the protective barrier of skin is disrupted and these microorganisms accumulate at injured area resulting in delay in wound healing.

The most common bacteria that lead to wound infection are *Staphylococcus aureus* and other groups of *Streptococci* (Williford, 1999). The microorganisms such as *Pseudomonas aeruginosa*, *Escherichia coli*, and *Staphylococcus epidermis* are also known to contribute to skin infections (Percival *et al.*, 2012). In terms of the treatment of contaminated burns, pathogenic bacteria that are resistant to multiple drugs are an increasing problem (Dai *et al.*, 2009). Inadequate care of wound infections may lead to reduced healing response, loss of soft tissue, limb amputation and death (Edward and Harding, 2004). A recent report

suggests that microbial infection is the cause of death for at least 10,000 in every million wound patients (Percival *et al.*, 2012).

### 1.2.3 Wound healing

Wound healing is a continuous process taking place in all the damaged tissue which is categorised into four different phase to understand the mechanism of tissue healing (Richardson, 2004). Healing proceeds *via* four overlapping phases: haemostasis, inflammation, proliferation and remodelling; each phase is characterised by the infiltration of specific cell types into the wound site (Diegelmann and Evans, 2004).

#### 1.2.3.1 Haemostasis phase

Immediately following injury, haemostasis takes place in the wound to prevent further tissue loss from damaged blood vessels (Broughton *et al.*, 2006; Pool, 1977). This provides the matrix for incoming cells that are needed for the later phases of healing (Lawrence, 1998; Robson *et al.*, 2001). Haemostasis is achieved upon platelet adhesion and aggregation through the synthesis of insoluble fibrin; adhesive molecules such as fibronectin and vitronectin are deposited onto the fibrin mesh. The formation of fibrin-based clots within damaged blood vessels facilitates cessation of haemorrhage, whereas discharge from blood vessels into the surrounding tissue provides a provisional matrix over which cells responsible for repair can migrate. In the final stages of haemostasis, fibrin degradation products, together with platelet-derived growth factors activates the inflammatory cells.

#### 1.2.3.2 Inflammatory phase

The haemostasis phase is followed by cellular inflammatory phase to create an immune barrier against microorganisms. In this phase, a variety of leukocytes are released from blood vessels in response to cellular signals. Inflammation is traditionally separated into an early and late stage, each of which is characterised by the predominance of particular leucocytes (Hart, 2002). The early stage features wound debridement, facilitated by the

phagocytosis and eventual destruction of bacteria and cell debris by neutrophils, whereas the late stage consists of macrophage predominance and the eventual infiltration of lymphocytes into the wound site.

#### 1.2.3.3 Proliferation

Stimulated growth and migration of neighbouring dermal and epidermal cells to the site of injury is the hallmark of the proliferative phase. This phase is characterised by migration of fibroblast and deposition of newly synthesised extracellular matrix, which replaces the provisional network of fibrin and fibronectin and last for about 2 weeks. Central to proliferative phase of wound healing is the formation of granulation tissue. Dermal fibroblast proliferation, migration and differentiation (into contractile myofibroblast) occur under the influence of growth factors (Traversa and Sussman, 2001). Fibroblasts are crucial for the production of extracellular matrix, which is comprised of collagen, glycosaminoglycans, proteoglycans, fibronectin and elastin (Wild *et al.*, 2010). During the proliferative phase, wound contraction is an important process that occurs through the action of myofibroblast differentiated from mesenchymal fibroblast cell lines (Gilbane *et al.*, 2013).

#### 1.2.3.4 Remodeling phase

As the final phase of wound healing, the remodelling phase is responsible for the development of new epithelium and the formation of final scar tissue. Traditionally, it has been treated as a separate phase, primarily because it continues for up to two years following injury, long after the proliferation phase has ended (Ramasastry, 2005; Witte and Barbul, 1997). During remodelling phase, nutrient requirement of wound decreases, which is characterised by reduced proliferation and inflammation, active re-organisation of the extracellular matrix and regression of newly formed capillaries (O'Toole, 2001). During

remodelling, collagen becomes more organised, fibronectin disappears and hyaluronic acid and glycosaminoglycan are replaced by proteoglycans (Guo and Dipietro, 2010).

#### 1.2.4 Wound dressings

Until the 1960s, traditional wound dressings used for wound healing were based on technologies to absorb wound exudates and keep the wound dry, but later it was found that maintenance of hydration and moisture helps in faster wound healing. As a result of these findings, several modern dressings have been formulated to retain the moisture *via* occlusion (Boateng *et al.*, 2008; Fan *et al.*, 2011a; Schultz *et al.*, 2003).

Wound dressings are local therapeutic agents widely used as the first line of treatment for minor superficial wounds as well as for complicated exuding or infected wounds. Besides arresting bleeding, wound dressings function as an artificial barrier to protect the wound against further trauma or environmental bacterial contamination, while promoting healing by preventing the presence of excessive wound exudates (Quinn *et al.*, 1985).

The ideal properties of wound dressings are directly related to the physiological condition of the wound. The functions of wound dressings are described as follows (Lawrence and Diegelmann, 1994):

- Preservation of humid environment
- Absorption of exudates and microorganisms
- Formation of mechanical barrier against secondary infections and thermal isolation
- Promotion of debridement

#### 1.2.5 Types of wound dressings

Wound dressings can be generally divided into traditional and modern dressings. Gauzes, natural or synthetic bandages, and cotton wool are referred as traditional dressings, while hydrocolloids, alginates, hydrogels, biological dressings, semipermeable adhesive film dressings and foam dressings are modern dressings (Falabella, 2006; Queen *et al.*, 2004).

Further classification is based on the function of dressings for the wound (debridement,

antibacterial, occlusive, absorbent, adherence) (Purner and Babu, 2000). Dressings that make physical contact with the wound surface are referred to as primary dressings, while secondary dressings cover the primary dressings (Van Rijswijk, 2006).

**Gauze** dressings are made from fibres of cotton, rayon polyester or a combination of both. They have been widely used in wound care throughout history due to their ability to offer good absorption and the fact that they are affordable and easily accessible (Jones, 2006). However, as later research has revealed the importance of maintaining a moist wound bed, traditional cotton gauze has been found to be inappropriate for wounds that produce little wound exudate. In addition, the drying nature of gauze can potentially lead to discomfort and trauma during removal. It has been suggested that traditional dressings should be employed only for wounds that are clean and dry, or be used as secondary dressings to absorb exudates and protect the wound (Harding *et al.*, 2000; Morgan, 2002).

**Films** are thin, adhesive and semi-occlusive membranes that can be used as both primary and secondary dressings. They manage moisture *via* vapour transmission and are good barriers against foreign liquid and bacteria. As film dressings are non-absorbent and hence may lead to trapping of fluid and subsequent maceration of wound tissue, they are recommended for wounds with minimal wound exudate or as secondary dressings. Patients using films can also benefit from the fact that the dressings can be left in place without being changed for up to 7 days (Fonder *et al.*, 2008; Schultz *et al.*, 2004).

**Hydrocolloid** dressings are most commonly used dressings and are usually composed of gelatin, pectin and carboxymethylcellulose. These dressings are available in the form of thin sheets or films and adhesive hydrocolloid gel form (Bethell, 2003). In the intact state, the outer dressing layer is impermeable to bacteria, oxygen and water vapour, but as the gelling process takes place and the dressing becomes progressively more permeable. This keeps wound at an optimal stable temperature and moisture level. Therefore, hydrocolloids are recommended for wounds with low to moderate amounts of exudate (Barnea *et al.*, 2004).

Branded hydrocolloid products include Granuflex<sup>®</sup> and Aquacel<sup>®</sup> (ConvaTec, UK), Comfeel<sup>®</sup> (Coloplast, UK) and Tegaserb<sup>®</sup> (3M Healthcare, UK).

**Foam** dressings are prepared with porous polyurethane foam have the ability to absorb moderate amounts of fluid, making them useful for the management of wounds with light and moderate levels of exudate (Morgan, 2002). Foam dressings have been found to be useful for treatment of granulating wounds but are not suitable for dry epithelising wounds or dry scars, as foam dressings rely on exudates (Marcia and Castro, 2002; Morgan, 1999). Foam dressing products include Lyofoam<sup>®</sup> (ConvaTec) and Allevyn<sup>®</sup> (Smith and Nephew).

**Alginate** dressings are composed of sodium and calcium salts of alginic acid, an anionic polysaccharide and are available in the form of a plate or a band. When applied to wounds, calcium ions present in the alginate fibre are exchanged with sodium ions present in the blood to form a protective gel film (Thomas, 2000). Examples of alginate dressings available in the market are Sorbsan<sup>®</sup> (Maersk, UK), Kaltostat<sup>®</sup> (ConvaTec, UK).

**Hydrogels** were first developed in the 1950s, and applied to wound therapy about 30 years later (Kennedy-Evans and Lutz, 2010). They are insoluble, swellable hydrophilic materials made from synthetic polymers such as poly(methacrylates) and polyvinylpyrrolidone, and have ability to transfer vapour and water and provide moisture to the wound (Fan *et al.*, 2011b). Hydrogel dressings work by rehydrating dead tissues and enhancing autolytic debridement for the treatment of dry, necrotic wounds. The dressings are non-reactive with biological tissue, are permeable to metabolites and are non-irritating (Wichterle and Lim, 1960). Recently, a flexible methacrylate dressing (Altrazeal<sup>®</sup>, Uluru Inc., US) was introduced. Altrazeal is available as sterile dressing powder which is used for treatment of exuding wounds such as burns, abrasions, surgical wounds and chronic wounds (Fitzgerald *et al.*, 2009). Altrazeal powder is composed of small particles containing a poly-2-hydroxyethyl-/poly-2-hydroxypropyl (pHEMA/pupa)-methacrylate backbone and a terminal hydroxyl group, which is transformed into a porous gel matrix once in contact with wound

exudate. Hence, it can be directly applied to a wound, transforming in the presence of wound exudate, or can be hydrated using saline or other sterile solutions, becoming a flexible dressing.

**Biological** dressings are made from biomaterials that play an active part in the wound healing process; hence, they are also known as bioactive dressings. Bioactive dressings are prepared using polymers such as collagen, hyaluronic acid, chitosan, alginates and elastin (Ishihara *et al.*, 2002; Ramshaw *et al.*, 1995). The biomaterials incorporated into biological dressings have the advantage of forming part of the natural tissue matrix in the normal wound healing process (Ueno *et al.*, 1999).

**Antimicrobial** dressings are used to minimise the growth of microorganisms in wounds. They provide local treatment and have a therapeutic effect on the dermis and superficial dermis, since the active ingredients are concentrated at the skin surface and less reaches the subcutaneous fat. The ideal antimicrobial drug for topical treatment should have broad activity, and be microbicide, non-toxic, and non-allergenic (Kaye, 2000). Topical treatment with antimicrobial agents can limit and reduce the risk of wound infections. These dressings can be used on both acute and chronic wounds that are critically infected, which can lead to compromised wound healing (Flores and Kingsley, 2007). Different antiseptics such as silver, iodine, polyhexamethyl biguanide (PHMB), and chlorhexidine have been used in antimicrobial dressings (McDonnell and Russell, 1999).

## 1.3 Skin

### 1.3.1 Structure of skin

Skin is a complex organ that primarily functions as a protective barrier and a sensory organ and is also involved in maintenance of haemostasis. The skin has a layered structure, which is broadly categorised into the outermost layer of tissue (non-viable epidermis), the stratum corneum (SC); the viable epidermis; the overlying dermis; and the innermost subcutaneous hypodermis (Figure 1.1). The skin is the largest organ of the body, accounting for approximately 10 % of the total body mass (Mills and Cross, 2006). The structure (such as the number of sebaceous glands, hair density and thickness) and physiology (such as metabolic activity, pH and humidity) of skin may display both inter-individual and even intra-individual variability, depending on the body site and age (Waller and Maibach, 2009, 2005). The normal pH of skin has been estimated at 4.7. However, many external factors such as the use of water and soap affect the skin surface pH, and therefore it ranges between 4 to 7 (Lambers *et al.*, 2006).

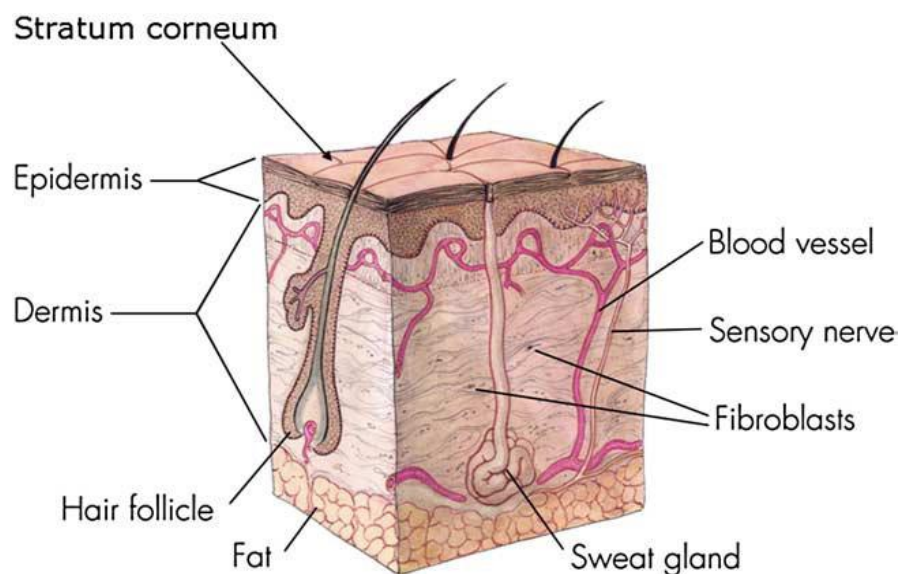


Figure 1.1 Schematic diagram of mammalian skin (Visscher, 2009).



#### 1.3.1.1 Stratum corneum

The outermost layer of skin, the SC, is generated by the epidermis and is about 10 to 20  $\mu\text{m}$  in thickness and is known as non-viable epidermis composed of flattened, hexagonal and cornified cells. SC is surrounded by extracellular lamellar lipid matrix of mostly ceramides, free fatty acids and cholesterol, which is known the brick and mortar model (Waller and Maibach, 2005). In this model, the bricks represent the corneocytes embedded in the mortar, the lipid phase. The corneocytes are tightly packed and flattened (approximately 0.5  $\mu\text{m}$  thick) due to contraction of keratin filaments and loss of intracellular organelles such as the nucleus, and are connected by corneodesmosomes, enhancing the SC barrier properties (Haftik *et al.*, 1998; Korting *et al.*, 2011). Furthermore, the cell membrane of keratinocytes in the SC is covered by a protective cornified envelope, which provides additional strength. The intercellular spaces in the SC are filled with lipid bilayers (lamellae), composed of non-polar lipids, including ceramides (47 %), free fatty acids (9 %) and esters, as well as cholesterol (27 %) and its sulphates. The structure of the lipid bilayer displays heterogeneity, having both lipophilic and hydrophilic domains (Rosso and Levin, 2011).

#### 1.3.1.2 Epidermis

The epidermis is composed of stratified squamous epithelium, which contains keratinocytes, melanocytes, Langerhans cells and Merkel cells. The epidermis is divided into four different layers depending on the status of keratinocyte differentiation (Mills and Cross, 2006). The thickness of epidermis varies from 0.05 mm on the eyelids to  $0.8 \pm 1.5$  mm on the soles of feet and palm. It is composed of different sub-layers: the uppermost granular cell layer, the central spinous cell layer and the basal layer at the bottom. The basal cells undergo several stages of differentiation during progressive movement up through the layers towards the SC, replacing the dead SC cells that are shed from the skin surface. The

entire process from a basal cell layer to SC shedding takes around 28 days (Blanpain and Fuchs, 2009).

#### 1.3.1.3 Dermis

The dermis is an underlying layer of connective tissue consisting of thick fibrous and elastic layer containing blood vessels, lymphatic channels and sensory nerves. Below the dermis lie papillary layers of loose collagenous and elastic fibres, which extend from the base of the papillary layer to subcutaneous tissue. The dermis is made up of fibroblasts, which produce collagen, elastin and structural proteoglycans, together with immune-competent mast cells and macrophages (Cevc and Vierl, 2010). The fibrous tissue of dermis also contains sweat glands, nerve endings, sebaceous glands and hair follicles.

#### 1.3.1.4 Skin appendages

Skin appendages include the hair follicles and the sebaceous, apocrine and eccrine glands, which are located within the skin. The follicles are derived from the epidermis and the dermis, and are very dense on the scalp and face. The pilosebaceous unit is composed of hair follicles, the hair shaft and the associated sebaceous glands. The hair shaft is composed of the medulla, the cortex with melanosomes, and the cuticula, represented by flat cornified cells arranged similarly to roof tiles (Gawkrodger and Arden-Jones, 2002; Jakubovic and Ackerman, 1992).

Human skin contains two types of hair: terminal hairs are pigmented, long and thick (>2 cm) with roots deep in the dermis (>3 mm depth), while the thinner and shorter vellus hairs reach a depth of 1 mm. Each hair follicle is lined by germinative cells, which produce keratin and melanocytes and synthesise pigment (Lauer, 2005). The hair shaft consists of an outer cuticle, a cortex of keratinocytes and an inner medulla. The outer root sheath that

surrounds the hair follicle is a stratified epithelium that is continuous with the epidermis (Knaggs, 2007; Otberg *et al.*, 2007; Schaefer and Lademann, 2001).

Sebaceous glands are closely associated with hair follicles, especially those of the scalp, face, chest and back. They produce an oily sebum *via* holocrine secretion, in which the cells break down and release their lipid cytoplasm (Meidan *et al.*, 2005; Tobin, 2001). Apocrine and eccrine glands are sweat glands; the eccrine glands produce sweat and for temperature regulation, and apocrine glands produce lipid-rich secretions (Mills and Cross, 2006).

### 1.3.2 Penetration pathways into the skin

Skin penetration is a passive process that is affected by drug solubility and partitioning in the vehicle, skin structures, and diffusion of the drug into the skin. Generally, the penetration of topically applied substances through the skin occurs *via* three separate pathways, as illustrated in Figure 1.2 (Bunge *et al.*, 1999). The first is the transcellular pathway, which encompasses the direct transportation of substances through the lipophilic and hydrophilic domains. The second is the intercellular pathway, by which substances passively diffuse between cells along the tortuous lipid matrix around the corneocytes. The third is the transappendageal pathway, which involves the penetration of substances through skin appendages such as hair follicles and sweat glands.

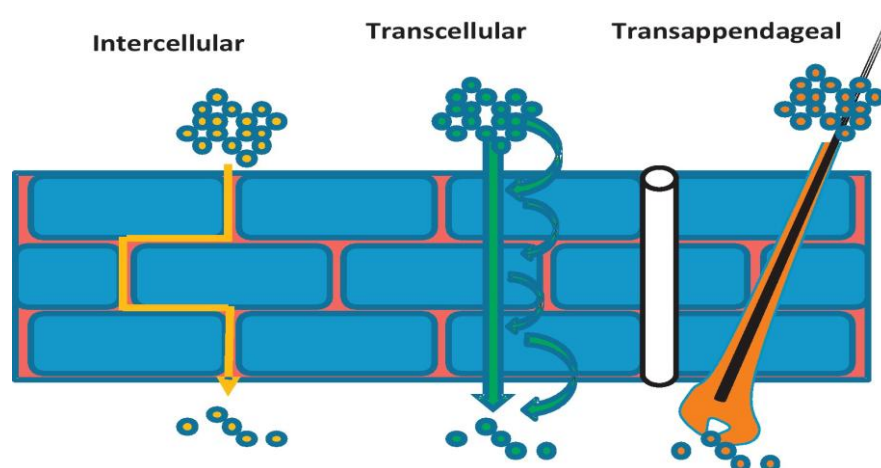


Figure 1.2 Schematic representation of drug penetration routes through the skin (Lane, 2013).

Lipophilic compounds are thought to travel along the lipid domains of the lipid bilayer (hydrocarbon chains), while hydrophilic compounds travel along the polar head group regions. The transappendageal route, which includes hair follicles and sweat glands, is called the 'shunt route,' as there are less lipid membranes to be crossed compared to the transcellular and intercellular pathways (Otberg *et al.*, 2004). The important role of hair follicles in skin penetration and reservoir function has already been validated and reported in literature (Knorr *et al.*, 2009). In present research work, importance of follicular pathway to enhance the skin penetration of triclosan has been studied using differential stripping technique which is described in detail in chapter 3 (Refer section 3.4.3.7).

### 1.3.3 Skin penetration enhancers

Penetration enhancers are defined as substances or strategies that promote penetration of drugs into the skin, or drug permeation through the skin. Penetration enhancers are the most common agents used for increasing dermal absorption of antimicrobial agent to the deeper layers of the skin (Sapra *et al.*, 2008). Several physical and chemical penetration enhancers have been reported in the literature; these have successfully resulted in elevated levels of drugs delivered across and into the skin (Ghosh *et al.*, 1997).

#### 1.3.3.1 Chemical approach

The chemical approach to penetration enhancement includes the use of chemicals such as surfactants (e.g. Tween or propylene glycol), solvents (e.g. alcohols), fatty acids (e.g. lauric acid, palmitic acid and oleic acid), esters, glycols, and sulphoxides. Chemical penetration enhancers can reversibly alter the barrier properties of the skin through several mechanisms such as reversible disruption of lipid structure in SC, enhancing partition of vehicle or transport of solvent into the skin (Barry, 1987; Guy and Hadgraft, 1987):

**Alcohols, fatty alcohols and glycols:**

Alcohols such as ethanol, methanol and fatty acids like oleic acids are commonly used in many dermal formulations. Ethanol can also be used as a co-solvent during *in vitro* permeation experiments to maintain sink condition and it has been shown to enhance the flux of levonorgestrel, estradiol, hydrocortisone and 5-fluorouracil through rat skin (Friend *et al.*, 1988) and of estradiol through human skin *in vivo* (Pershing *et al.*, 1990). The permeation enhancing ability of oleic acid and palmitoleic acid has been studied using propylene glycol (PG) as co-solvent, which has shown approximately a 10-fold increase in permeation across skin (Yokomizo and Sagitani, 1996). Since 1932, PG has been used either as a co-solvent for poorly soluble materials or to enhance drug permeation through skin from topical preparations (Barrett *et al.*, 1965; Hoelgaard and Mollgaard, 1985).

**Azone:**

Azone (1-dodecylazacycloheptan-2-one or laurocapram), the first molecule or agent specifically designed as a skin penetration enhancer (Stoughton and McClure, 1983), was investigated extensively in the 1980s and 1990s (Harrison *et al.*, 1996). Azone is a highly lipophilic material that is soluble and compatible with the most organic solvents, including alcohol and PG. Azone interacts with lipid domains of SC by partitioning into the lipid bilayer (Williams and Barry, 2004). Azone has low irritation and toxicity with nearly no pharmacological activity. It can be used as a penetration enhancers for hydrophilic and lipophilic substances (Wiechers *et al.*, 1987). Azone and its derivatives acts effectively as penetration enhancers when used in low concentrations between 1 – 5 %.

**Glycol ethers – Transcutol® P**

Transcutol P (TP), a monoethyl ether of diethylene glycol, has also been reported to increase the solubility of drugs in the skin. Harrison *et al.*, (1996) demonstrated the effects of TP on

the diffusivity and solubility of 4-cyanophenol in human skin in an *in vitro* skin diffusion study. Although many reports in the literature have demonstrated the ability of this molecule to enhance penetration (El Nabarawi *et al.*, 2013; Pandey *et al.*, 2014; Prasanthi and Lakshmi, 2012), further mechanistic studies are required to elucidate its exact interaction with skin components.

### **Sulphoxides:**

Dimethyl sulphoxide (DMSO) has been extensively reported in the literature as a co-solvent and penetration enhancer (Coldman *et al.*, 1971; Maibach and Feldmann, 1967; Roth and Fuller, 2011). It is typically considered to be a 'universal solvent' in many areas of pharmaceutical science. Recent work using molecular simulations has suggested that DMSO must be present in high concentrations in the skin in order to be efficacious as a chemical penetration enhancer (Junyaprasert *et al.*, 2013). Because of the relatively high amounts of DMSO needed for penetration enhancement, as well as the associated issues of irritation and production of a malodourous metabolite in the breath, this compound has very limited use in commercial topical products.

### **Surfactants:**

There are many surfactants that are capable of interacting with the SC to enhance the absorption of drugs and other active compounds from products applied to the skin. When surfactants are deposited onto the SC, they cause disruption of the SC structure. Anionic surfactants, such as sodium lauryl sulphate (SLS), induce fluidisation of SC lipids and increase skin absorption (Van-der Valk *et al.*, 1985). Kushla and Zatz (1991) investigated a range of cationic surfactants for their ability to act as chemical penetration enhancers for water and lidocaine *in vitro*. Results showed a greater enhancement ratio for both water and lidocaine with higher concentrations of surfactants.

Cationic surfactants such as benzalkonium chloride (Basketter *et al.*, 2004) and cetylpyridinium chloride (Lin and Hemming, 1996) are reported as irritant to the skin and hence they are not suitable for dermal delivery. Non-ionic surfactants are generally considered to be less irritating than ionic surfactants and the most often reported compounds used as permeation enhancers include the polyoxyethylene alkyl ether (Brij) and polyoxyethylenesorbitan fatty acid ester (Tween) series. Ashton *et al.*, (1986) investigated the influence of Brij 36T on the time of erythema induced by nicotine when applied as gel. Another study reported by Ryan and Mezei (1975) observed that the application of 10 % Tween 85 in petrolatum to the forearm of human subjects increases epidermal permeability due to water loss.

#### **Essential oils, terpenes and terpenoids:**

The application of monoterpenes and sesquiterpenes in dermal drug delivery has been extensively investigated over the years (Cornwell and Barry, 1994; Williams and Barry, 1991; Yamane *et al.*, 1995). Terpenes act by modification of the SC, improving drug partitioning into the skin. They are found in essential oils, and the compounds comprise of only carbon, hydrogen and oxygen atoms. Menthol is traditionally used in inhalation pharmaceuticals and has mild antipruritic effects when added to emollient preparations. The essential oils of eucalyptus and chenopodium have been shown to be effective penetration enhancers for 5-fluorouracil in human skin *in vivo* (Williams and Barry, 1989). L-menthol has been shown to enhance the *in vitro* permeation of morphine hydrochloride through hairless rat skin (Morimoto *et al.*, 2002), imipramine hydrochloride across rat skin (Jain *et al.*, 2002) and hydrocortisone through hairless mouse skin (El-Kattan *et al.*, 2000).

However, the success of chemical enhancers is limited to low molecular mass permeants and their inclusion in the formulation may enhance the absorption of components other than

the permeants, which can lead to skin damage and irritation problems (Prausnitz *et al.*, 2004).

#### 1.3.3.2 Physical approach

Physical enhancement utilises external energy to physically reduce the SC biological barrier, promoting penetration of exogenous compounds. This approach can be further categorised based on the energy force used, such as electrical (iontophoresis, electroporation); mechanical (abrasion and microneedles); and miscellaneous methods (ultrasound and laser wave) (Brown *et al.*, 2006). These approaches are mainly used for large and hydrophilic molecules such as peptides and proteins. Furthermore, some of these techniques are associated with a sensation of discomfort and mechanical damage to the skin barrier (Lau *et al.*, 2008). It has been proposed that using a combination of physical and chemical enhancers may achieve synergistic effects. For example, enhanced transdermal permeation of insulin has been achieved by combining iontophoresis with chemical enhancers, compared to the individual techniques employed separately (Pillai *et al.*, 2004).

#### 1.3.4 Techniques for quantification of drug retained into skin

The skin absorption of drugs from various topical formulations is studied using a variety of experimental approaches that permit the measurement of either *in vivo* or *ex vivo* penetration or the permeation profiles of substances that pass through the SC barrier.

The well-known tape stripping technique, first introduced in 1951 by Pinkus, is widely used as a minimally invasive technique for evaluating the localisation and distribution of substances within the SC (Pinkus, 1951). The development of the differential stripping technique enabled quantitative evaluation of the hair follicular penetration process by combining the classical tape stripping process with cyanoacrylate skin surface stripping technique (Teichmann *et al.*, 2005). Briefly, after application of a substance onto the skin, the tape stripping process is performed, which removes the portion of substance present



within the SC and the rest of the substance, located inside the hair follicle orifices, is removed by the cyanoacrylate skin surface stripping technique. Thus, substances accessing the intercellular, transcellular and transfollicular pathways can be quantitatively evaluated by region. A further technique was developed in 2006, in which the hair follicle orifices are artificially blocked by nail varnish or wax within a predetermined skin region (Teichmann *et al.*, 2006). This approach allows the evaluation of skin penetration *in vivo* by detecting and comparing the blood concentrations of substance in both blocked and unblocked hair follicle orifices.

For *ex vivo* studies, the skin mounted in Franz diffusion cells is exposed to the drug for defined time periods. The skin is then removed and drug penetration is quantified, either in full-thickness skin or in horizontally sliced skin of defined thickness. The amount of drug present in the receiver fluid is normally analysed using high-pressure liquid chromatography (HPLC) (Gysler *et al.*, 1999). Other quantification methods include infrared (IR) imaging, confocal laser scanning microscopy (CLSM) and Raman spectroscopy (Alvarez-Román *et al.*, 2004; Mao *et al.*, 2012; Tanja *et al.*, 2010).

Most of these approaches, however, do not reach a spatial resolution at the subcellular level. In some skin absorption studies, dyes are used in place of drug as a suitable model for visualizing the uptake and transport of substances by fluorescence microscopy (Küchler *et al.*, 2009). Confocal laser scanning microscopy and two-photon microscopy, for example, have the inherent advantage of high sensitivity, reaching single-molecule detection (Peter *et al.*, 2000). However, fluorescence microscopy can rarely be used to probe the uptake of drugs into skin because it requires the drug to display fluorescence.

Mass spectroscopy based techniques, such as matrix assisted desorption/ionisation mass spectrometry imaging (MALDI-MSI) (Brendan *et al.*, 2007; Philippa *et al.*, 2011) and time-of-flight secondary ion mass spectrometry (TOF-SIMS) (Judd *et al.*, 2013) have also been used. These techniques mainly focus on the characterisation of skin (Tanja *et al.*, 2010) or

the penetration of fluorescent molecules (Alvarez-Román *et al.*, 2004), surfactants (Mao *et al.*, 2012) or non-active ingredients (e.g. solvents) (Kazarian and Chan, 2013) into the skin. Mass spectroscopy has the advantage of high chemical specificity without requiring the use of labels such as isotopes or fluorescence (Michell *et al.*, 2003).

### 1.3.5 Topical antimicrobial agents

Appropriate and effective skin antisepsis is essential in preventing infections that can arise from a breach of the skin, such as during surgery or prior to insertion of intravascular devices. A variety of topical antimicrobial agents for skin antisepsis are currently available in different concentrations and formulations. The antiseptics used most commonly for skin preparation before surgery are alcohols, chlorhexidine digluconate (CHG) and povidone-iodine (PVP-I), of which CHG and PVP-I have shown more persistent antimicrobial activity compared to alcohols.

#### 1.3.5.1 Alcohols

Various alcohols such as ethanol, isopropyl alcohol and n-propanol have been used effectively as antimicrobials against bacteria, viruses and fungi (Morton, 1983). Current uses of alcohol within the hospital environment include alcohol-based hand rubs for general antisepsis, alcoholic CHG solution for cutaneous decontamination prior to catheter insertion and for skin preparation before invasive procedures due to rapid volatile nature. The mechanism of action of alcohols is non-specific but they denature proteins and cause membrane damage and cell lysis. Alcohols, if used alone for skin antisepsis, does not exhibit prolonged action on the skin. Therefore, it is recommended to use alcohols in combination with another antimicrobials such as CHG or iodine to enhance the longevity of the antimicrobial effect. Combining CHG with isopropyl alcohol, for example, has

demonstrated superior activity compared to IPA alone in preventing infections associated with peripheral venous catheters (Small *et al.*, 2008).

#### 1.3.5.2 Povidone – iodine

Povidone-iodine (PVP-I) is the most common iodophor used in the healthcare environment (Figure 1.3), which is a complex of iodine and polyvinylpyrrolidone. It releases concentration of free iodine, whose exact mode of action is not known but is thought to involve multiple cellular effects by binding to proteins, nucleotides and fatty acids. Iodine likely reacts with the phenolic groups of tyrosine and the N-H groups of amino acids (such as arginine, histidine and lysine) to block hydrogen bonding and also oxidises the S-H bonds of cysteine and methionine. It reacts with the bases of nucleotides (such as adenine, cytosine and guanine) to prevent hydrogen bonding, and reacts with C=C bonds in fatty acids to alter the membrane structure (McDonnell and Russell, 1999). It has a broad spectrum of activity against bacteria, mycobacteria, fungi, protozoa and viruses.

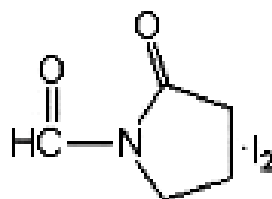


Figure 1.3 Povidone-iodine, the iodine complex with neutral polyvinylpyrrolidone polymer carrier.

Alcoholic solutions of CHG have been reported to exhibit superior antimicrobial activity compared to PVP-I; these studies have compared, for example, PVP-I and alcoholic 0.5 % (w/v) CHG in reducing catheter-related blood stream infections (CR-BSI), central venous catheter (CVC) tip colonisation and CVC skin site colonisation (Humar *et al.*, 2000), tincture of iodine and CHG in reducing blood culture contamination (Traunter *et al.*, 2002)

and alcoholic and aqueous CHG and PVP-I against *Staphylococcus epidermis* in a planktonic and a biofilm modes of growth *in vitro* (Small *et al.*, 2008).

### 1.3.5.3 Chlorhexidine digluconate

CHG is the most commonly used broad spectrum topical antimicrobial agent for skin preparations available in different salt forms such as diacetate, digluconate and dihydrochloride (Block, 1991; Rosenberg *et al.*, 1976). CHG shows antimicrobial activity against both Gram-positive and Gram-negative bacteria. At very low concentrations, CHG exerts bacteriostatic effects and at high concentrations, CHG shows bactericidal effects, but however the effects vary from species to species. CHG acts by binding to bacterial cell walls and a rapid electrostatic attraction between the negatively charged bacterial cell wall and positively charged CHG, leads to leakage of bacterial cytoplasm showing rapid bactericidal effects (Paulson, 2014). Studies have also reported a biphasic effect of higher concentrations of CHG on protoplast lysis (Hiom *et al.*, 1996).

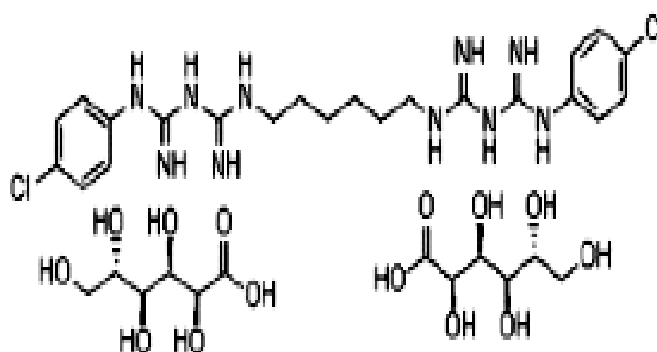


Figure 1.4 Chemical structure of chlorhexidine digluconate [1,6-Bis(N5-[p-chlorophenyl]-N1-biguanido)hexane digluconate] (Rosenberg *et al.*, 1976).

CHG is thought to be an inhibitor of both membrane-bound and soluble ATPase, as well as net K<sup>+</sup> uptake in *Enterococcus faecalis* (Harold *et al.*, 1969). However, only high biguanide

concentrations inhibit membrane-bound ATPase (Chopra, 1987). The effect of CHG and other biocides on *Acanthamoeba* was reviewed by Furr (2013) which showed that membrane damage to protozoa is a significant factor in their inactivation. CHG activity against yeast is similar to its activity against bacterial cells, with the targeting of yeast cell membranes. However, the yeast cell wall reduces its activity, as there is limited diffusion through the cell wall to the target cell membranes (McDonnell and Russell, 1999).

#### 1.3.5.4 Triclosan

Triclosan (TSN), also known as 2,4,4-trichloro-2-hydroxydiphenyl ether, is a strong, broad-spectrum, antimicrobial agent. It is bacteriostatic at low concentrations, where it blocks lipid synthesis, whereas at high concentrations, membrane destabilisation and triclosan-induced  $K^+$  leakage causes a rapid bactericidal effect.

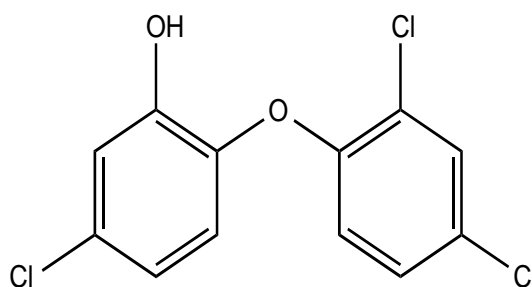


Figure 1.5 Structure of triclosan (Bhargava and Leonard, 1995).

TSN is highly lipophilic ( $\log P$  4.8) and insoluble in water, but is easily solubilised in most organic solvents. It has a ionisation constant ( $pK_a$ ) of 7.9 and a molecular weight of 289.5 Da. TSN is known to inhibit fatty acid synthesis through interaction with the enoyl-acyl carrier protein enzyme reductase (Savage, 1971). Furthermore, incorporation of TSN into formulations can significantly enhance their efficacy against Gram-negative bacteria and

yeasts (Leive, 1974). It has also been reported that TSN exhibits anti-inflammatory activity (Barkvoll and Rolla., 1994; Waaler *et al.*, 1993). While specific mode of action for TSN is unknown, it has been suggested that it primarily affects the cytoplasmic membrane.

#### 1.3.5.5 Essential oils

Essential oils are volatile aromatic oils obtained from various parts of plant contains complex mixtures of terpenes and their oxygenated compounds (Guenther, 1948). Many essential oils, such as camphor, cinnamon, clove, eucalyptus, geranium, lavender, lemon, lime, mint, rosemary and basil, are used in foods, beverages, cosmetics and healthcare products such as soaps, mouthwashes and toothpastes. They have not only been used as aromatic substances but also as natural preservatives (due to their antioxidant or radical scavenging properties) as well as antimicrobial agents (Cowan, 1999).

Many essential oils, and their terpene constituents, have demonstrated broad-spectrum activity (Cowan, 1999). Tea tree oil (TTO) (from the leaves of *Melaleuca alternifolia*), for example, has been shown to efficiently eradicate MRSA from skin (Caelli *et al.*, 2000; Dryden *et al.*, 2004), as well as treat pulmonary tuberculosis (Sherry *et al.*, 2004) and diabetic foot ulcers (Sherry *et al.*, 2003). Eucalyptus oil (from the leaves of *Eucalyptus globulus*) has been successfully used to treat pulmonary tuberculosis (Sherry and Warnke, 2004). Anti-inflammatory activity has been found for basil (Singh and Majumdar, 1999). Lemon and rosemary oils possess antioxidant properties (Aruoma *et al.*, 1996; Calabrese *et al.*, 1999). Peppermint and orange oils have shown anticancer activity (Kumar *et al.*, 2004). Essential oils are generally regarded as safe when used at low doses. However, some cases of toxicity and skin irritation have been reported. For example, skin irritation and toxicity of TTO has been described. However, the use of TTO diluted for topical use (Hammer *et al.*, 2006) and the protection of TTO from oxidation or other damage through proper storage

(Hausen *et al.*, 1999) reduces the risk of adverse effects. Studies on irritation and toxicity caused by other essential oils and terpenes are not well documented.

The antimicrobial activity reported for many of the essential oils is not yet fully understood. However, they are thought to act on the plasma membranes of microorganisms, increasing cell membrane permeability and leakage of intracellular constituents (Cowan, 1999). Other studies have demonstrated membrane damage by lipophilic cyclic monoterpenes such as  $\alpha$ -pinene and limonene, as well as their partitioning within the lipid membranes, which increases membrane fluidity, affecting the respiration and function of cell membrane enzyme activity and increasing permeability to protons and ions (Sikkema *et al.*, 1995).

#### 1.3.5.6 Silver compounds

Silver, and its compounds, have long been used as antimicrobial agents (Brown and Anderson, 1968; Russell and Hugo, 1994). Presently, silver sulfadiazine is the most commonly used silver compound, although silver metal, silver acetate, silver nitrate have also shown antimicrobial properties (Brayfield, 2014). Silver compounds has various medical applications in dental work, catheters, and the healing of burn wounds (Klasen, 2000; Silver and Phung, 1996) and non-medical applications such as in electrical appliances (Jung *et al.*, 2007). More recently, silver has been also incorporated in wound dressings to reduce bacterial infection (Gemmell *et al.*, 2006). The antimicrobial action of silver ions is closely related to their interaction with thiol groups (Belly and Kydd., 1982; Bragg and Rainnie., 1974; Furr *et al.*, 1994), although other target sites remain a possibility (Richards *et al.*, 1984). Amino acids, such as cysteine, and other compounds containing thiol groups, such as sodium thioglycolate, neutralise the action of silver against bacteria (Aziz *et al.*, 2012; Leaper, 2006; Sepideh *et al.*, 2013).

## 1.4 Novel carriers for dermal drug delivery

To improve drug delivery into skin, there is always a need to modify existing, or formulate new, drug delivery system for drugs with poor solubility or permeability. Polymeric drug delivery system are the most common formulations for long term delivery of therapeutic agents as they also have the potential for chemical modification. Nevertheless, the number of products on the market that are based on polymeric microparticles and nanoparticles remains limited because of the toxicity of polymers and the solvent residues left over from their production, the high cost of biodegradable polymers, the potentially toxic or allergenic end products of biodegradable polymers, and the lack of suitable large scale production methods (Shegokar *et al.*, 2011; Yadav *et al.*, 2013).

In order to overcome these problems, a great deal of interest has been focused on lipid-based carriers such as lipid emulsions, liposomes and lipid nanoparticles (Chen *et al.*, 2010). Lipid based delivery systems are an accepted approach and constitute an emerging field for drug delivery. They have attracted the interest of a number of research groups because of their inherent properties, the biocompatibility and biodegradability of physiologically tolerated lipids, their physiochemical diversity, lower toxicity, high incorporation efficiency of lipophilic drugs, their ability to protect drugs from degradation, improved bioavailability, and controlled release characteristics. However, there are challenges regarding stability and manufacturing at the commercial scale and their suitability for drug delivery at different sites of administration (Liu *et al.*, 2010b).

### 1.4.1 Solid Lipid Nanoparticles

Lipid nanoparticles have gained more interest in pharmaceutical applications due to their small sizes as it influences *in vitro* and *in vivo* skin penetration. Solid lipid nanoparticles (SLNs) refer to colloidal carriers in size ranges from 10 to 1000 nm prepared by physiologically biocompatible solid lipids, which are stabilised by surfactants. SLNs are



mostly used for lipophilic drugs as an alternative carrier system to emulsions and liposomes (Chimmiri *et al.*, 2012; Ramadan, 2010). SLNs are composed of well tolerated biocompatible lipids which reduces the risk of toxicity for dermal application.

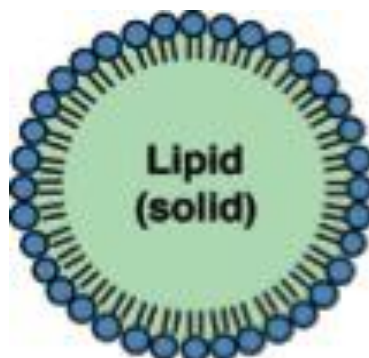


Figure 1.6 Structure of solid lipid nanoparticles (Ekambaram *et al.*, 2012).

A typical solid lipid used in such delivery systems melts at temperatures exceeding body temperature (37°C). Examples of some of the lipids that have been investigated include fatty acids, steroids, waxes, triglycerides and acylglycerols alone or in combinations. Many classes of emulsifiers, either by themselves or in combination, have been utilised to stabilise the lipid dispersion. Examples of emulsifiers include lecithin, bile salts such as sodium taurocholate, nonionic emulsifiers such as ethylene oxide, propylene oxide copolymers, sorbitan esters, fatty acid ethoxylates, and combinations of these (Rupenganta *et al.*, 2011).

#### 1.4.1.2 Advantages and disadvantages of solid lipid nanoparticles

SLNs has many advantages such as solid lipid matrix offers protection of chemically labile drugs from external environment. Preparation of SLNs avoids use of organic solvents hence minimise the skin irritation and also use of biodegradable lipids avoids toxicity. SLNs can be used to controlled and targeted drug delivery systems. SLNs offer improved storage stability compared to liposomes as they can be easily freeze-dried (Fahr and Liu, 2007; Rupenganta *et al.*, 2011). However, they also have some challenges such as the potential for

expulsion of drug from lipid matrix during storage and modification of lipid structure to transform into a crystal lattice (Ekambaram *et al.*, 2012).

#### 1.4.1.3 Production methods

SLNs are formulated using various methods described in literature. These methods include high shear homogenisation (HSH) (Liedtke *et al.*, 2000), microemulsion techniques (Priano *et al.*, 2007), emulsion solvent evaporation (Mehnert *et al.*, 2001b), high pressure homogenisation (HPH) and emulsion solvent diffusion (Trotta *et al.*, 2003), solvent injection or a solvent displacement (Schubert, 2003), phase inversion (Heurtault *et al.*, 2002), multiple emulsion techniques (García-Fuentes *et al.*, 2002), probe ultrasonication (Puglia *et al.*, 2006) and a membrane contractor technique (Charcosset *et al.*, 2005). All these methods work on same principle of generation of a nanoemulsion by replacing oil with a molten lipid phase using high and low energy methods. Then cooling of molten lipid formulations causes generation of SLNs. HSH is most commonly used technique due to its ease of scale up, relatively low production cost and time. HSH production methods in general consist of premixing the heated lipid phase to 5-10°C above its melting point. An hot aqueous surfactant solution heated at the same temperature is added and the mixture is homogenised under HSH followed by cooling to room temperature or rapid cooling using dry ice to form SLNs (Ekambaram *et al.*, 2012; Kakadia and Conway, 2014).

#### 1.4.2 Nanoemulsions

Nanoemulsions (NEs) were introduced during 1950's, and are heterogeneous mixtures of two immiscible liquids, one of which is dispersed uniformly as fine droplets throughout the external continuous phase. Based on the size of droplets they are also termed emulsions, microemulsions and sub-microemulsions. NEs have many advantages as they are a kinetically stable system due to their small droplet size, larger surface area which reduces the occurrence of creaming, flocculation and sedimentation. NEs can be incorporated into

various formulations such as creams, gels, liquids and foams. NEs offers easy large scale up production techniques. Non-toxic and non-irritant nature of NEs makes it greater choice for skin and mucous application. It enhances drug solubility and absorption due to lipophilic nature (Bali *et al.*, 2010; Bouchemal *et al.*, 2004). NEs can be oil-in-water (O/W), water-in-oil (W/O) and multiple NEs based on composition of the dispersed and continuous phases (Sharma *et al.*, 2010).

#### 1.4.2.1 Production methods

Various methods have been suggested to prepare NE formulations. Production of NEs require high amount of energy which can either provide by mechanical equipment or chemical potential present within the NE system. Methods used to prepare NEs includes microfluidisation, HPH, HSH and probe ultrasonication that generates intense cavitation forces to produce very fine droplets (Azevedo *et al.*, 2015).

## 1.5 Aims of the thesis

The aims of this thesis were

- To determine the potential for lipid nanocarriers, i.e. SLNs and NEs, to be used as novel drug delivery systems for dermal delivery using antimicrobial agents such as TSN and CHG.
- To study the suitability of SLNs and NEs as drug carrier systems within the scope of topical dermal delivery, especially for the treatment and prevention of skin infections.
- To formulate TSN-loaded SLNs using glyceryl behenate and glyceryl palmitostearate as solid lipids to study the effects of composition and concentration of lipids on physicochemical parameter and skin retention properties of SLNs.
- To assess the ability of SLNs to target hair follicles by performing *in vitro* skin diffusion studies using a cyanoacrylate adhesive tape stripping method.
- To study NEs as drug carrier for various antimicrobial agents for topical delivery of CHG using eucalyptus oil and olive oil.
- To compare skin permeation and retention abilities of SLNs and NEs containing eucalyptus oil and olive oil.
- To compare CHG skin permeation data obtained using Strat-M membrane and porcine ear skin.
- To analyse the ability of methacrylate dressing powder as drug delivery vehicle for CHG controlled and prolonged release.

## 2. CHAPTER: MATERIALS AND GENERAL METHODS

### 2.1 Materials

All the excipients used in the formulation of SLNs and NEs are of analytical grade. Lipids and oils used are biocompatible and well tolerated, are of generally regarded as safe (GRAS) status, are accepted for human use.

#### 2.1.1 Compritol<sup>®</sup> 888 ATO

Compritol<sup>®</sup> 888 ATO is a marketed product from Gattefossé GmbH (Weil am Rhein, Germany) is also known as glyceryl behenate (GB). The chemical structure of GB is based on the glycerol esters of behenic acid (C<sub>22</sub>) (Figure 2.1) and is composed of a mixture of glycerol tribehenate (28-32 %), glycerol dibehenate (52-54 %) and glycerol monobehenate (12-18 %). While the main fatty acid is behenic acid (>85 %), other fatty acids (C<sub>16</sub>-C<sub>20</sub>) are also present (Raymond *et al.*, 2009).

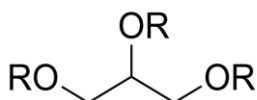


Figure 2.1 Chemical structure of glyceryl behenate.

The melting point of GB is between 69°C and 74°C. Due to the presence of partial acylglycerols, this lipid has an amphiphilic character. Its hydrophilic lipophilic balance (HLB) value is about 2 and its density is 0.94 g/cm<sup>3</sup>. GB, when heated, is soluble in chloroform, methylene chloride, xylene and insoluble in ethanol, ethyl ether, mineral oils and water. It is used in various pharmaceutical applications as a lubricant and binding agent for tablets and capsules, and as a viscosity enhancer in emulsion formulations for dermal

delivery (Brossard, 1991). GB is used in oral enteric-coated pellets, powders, suspensions and as a hot-melt coating agent sprayed onto a powder (Jannin *et al.*, 2003). It has been used for the formulation of SLNs as a colloidal drug carrier (Negi *et al.*, 2014; Reddy *et al.*, 2006).

### 2.2.2 Precirol<sup>®</sup> ATO5

Precirol<sup>®</sup> ATO5, also known as known as glyceryl palmitostearate (GP), and 1,2,3-propane triol is available as a marketed product from Gattefossé GmbH (Weil am Rhein, Germany). It is a mixture of the mono-, di- and triglycerides of the C<sub>16</sub> and C<sub>18</sub> fatty acids (Figure 2.2) (Raymond *et al.*, 2009). The melting point of GP is between 52°C and 55°C. GP has a peroxide value lower than 0.3 mEq O<sub>2</sub>/kg, indicating high chemical stability. It is freely soluble in chloroform, dichloromethane and practically insoluble in ethanol (95 %), mineral oil, and water.

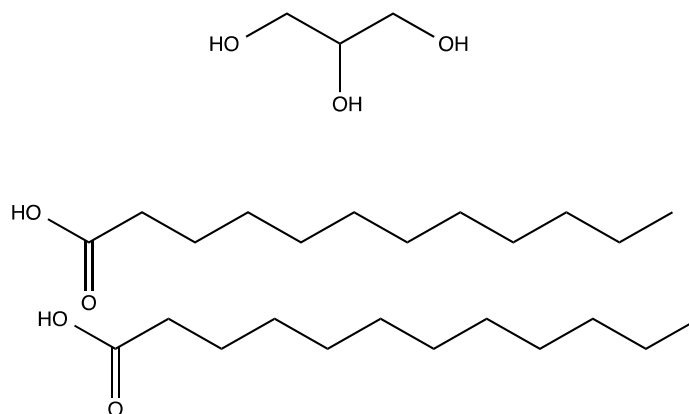


Figure 2.2 Chemical structure of glyceryl palmitostearate.

GP is used to form microspheres, which may be used in capsules or be compressed to form tablets (Edimo, 1993; Shaikh, 1991), pellets (Hamdani, 2003) and biodegradable gels (Gao, 1995). It is used in lipophilic matrices for sustained release tablet and capsule formulations (Saraiya and Bolton, 1990). It has been used to formulate SLNs of paclitaxel (Shenoy *et al.*, 2009), proteins and peptides (Yang *et al.*, 2010).

### 2.2.3 Eucalyptus oil

Eucalyptus oil (EO) is obtained from the leaf of the eucalyptus tree, which belongs to the family Myrtaceae (Ogunwande *et al.*, 2003). EO is pale yellow in colour and has a distinctive odour. It contains cineole (eucalyptol) as a major active ingredient. EO contains cineole, pinene and other types of terpenes along with small quantities of phellandrene, which has been used for medicinal purposes (Reynolds, 1982). Up to forty-one compounds have been detected in EO, depending on the source and purity (Brophy *et al.*, 1985). EO is insoluble in water, soluble in 1:5 alcohol (70 %), and miscible with fats, paraffin, ether, and chloroform. The boiling point of EO is from 176°C to 177°C. Because of its antibacterial activity, EO has been widely used in food, perfume, cosmetic, pharmaceutical and chemical applications (Ghalem and Mohamed, 2008; Hendry *et al.*, 2009; Takahashi *et al.*, 2004). Eucalyptus leaf extracts have been used as food additives.

Various studies have shown that EO has antimicrobial activity against a range of microorganisms (Cimanga *et al.*, 2002). EO is used for respiratory tract infections such as coughs, asthma, throat infections and sinusitis (Salari *et al.*, 2006). EO has various skin care applications for wound infections, cuts, burns and insect bites (Mulyaningsih *et al.*, 2011; Sadlon and Lamson, 2010). In addition, EO has also shown antibacterial (Cimanga *et al.*, 2002), antifungal (Su *et al.*, 2006), analgesic, anti-inflammatory effects (Silva *et al.*, 2003), as well as antioxidative activities (Siramon and Ohtani, 2007).

### 2.2.4 Olive oil

Olive oil (OO) is clear, a pale yellow liquid obtained from the ripe drupes of *Olea europaea* (Romero-García *et al.*, 2014). OO is a mixture of fatty acid glycerides. Analysis of OO shows a high proportion of unsaturated fatty acids, such as palmitic acid, oleic acid, stearic acid, myristic acid and behenic acid. OO is miscible with ether, ethanol (95 %) chloroform, light petroleum, and carbon disulfide.

OO is widely used as an edible oil, in food preparations and products such as cooking oils and salad dressings. It is also used in topical pharmaceutical formulations and cosmetics as a solvent and hair conditioner. OO is used in various formulations such as soaps, liniments, plasters, oral capsules and as a vehicle for oily injections (Jakate *et al.*, 2003). It is used to soften ear wax (Realdon *et al.*, 2001) and in combination with soybean oil to prepare a lipid emulsion for use in premature infants (Koletzko *et al.*, 2003).

### 2.2.5 Tween<sup>®</sup> 80

Tween<sup>®</sup> 80 (T80) is chemically known as polysorbate 80, polyoxyethylene sorbate or polyoxyethylene sorbitan fatty acid esters. T80 contains a series of partial fatty acid esters of sorbitol and its anhydrides copolymerised with approximately 20, 5, or 4 moles of ethylene oxide for each mole of sorbitol and its anhydrides (Figure 2.3). T80 is hydrophilic in nature has a HLB value of 15 and CMC value of 0.015 mM at 25°C in water (Mahmood and Al-Koofee, 2013).

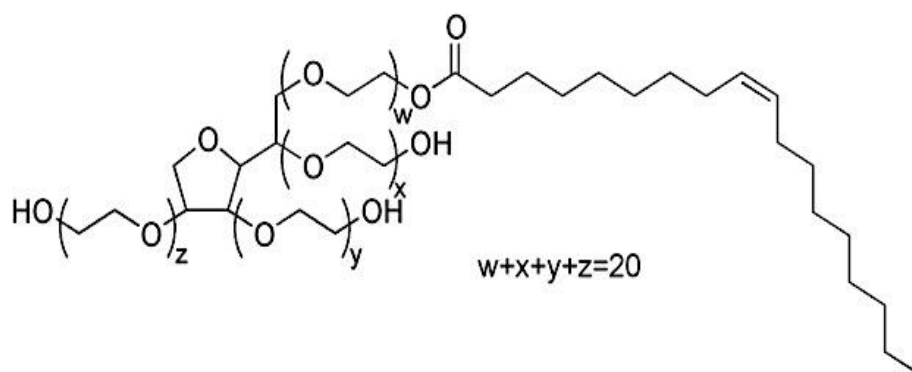


Figure 2.3 Chemical structure of polyoxyethylene sorbitan ester.

T80 is commonly used as an emulsifier in foods, particularly in ice cream, to make it smoother and easier to handle (Goff, 1997). It is also used as an excipient for stabilising aqueous formulations for parenteral administration. It is widely used as an emulsifying agent in the preparation of stable oil-in-water pharmaceutical emulsions (Nerurkar, 1996). T80 is used as a solubilising agent for essential oils, oil-soluble vitamins, and as a wetting



agent for oral and parenteral suspension formulation (Zhang, 2003).

### 2.2.6 Span<sup>®</sup> 80

Span<sup>®</sup> 80, (S80) chemically known as sorbitan monooleate or sorbitan oleate, belongs to the sorbitan esters group. S80 is a mixture of partial esters of sorbitol and its mono and di-anhydrides with fatty acids (Figure 2.4). S80 is hydrophobic in nature and is generally soluble or dispersible in oils; it is also soluble in most organic solvents. Although insoluble in water, it is generally dispersible. S80 has HLB value of 4.3.

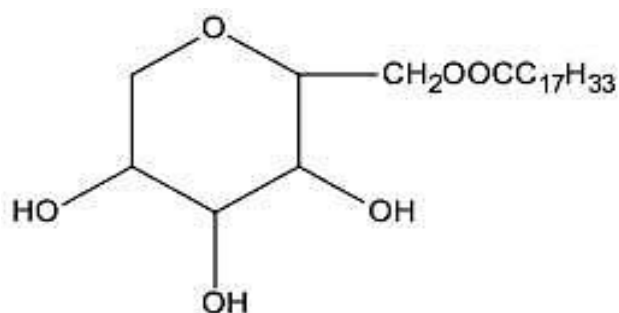


Figure 2.4 Chemical structure of sorbitan monooleate.

S80 is used as a nonionic surfactant in various pharmaceutical formulations, cosmetics and food products. It is also used as an emulsifying agent for topical formulations such as creams, emulsions, and ointments. S80 is either used alone or in combination with polysorbate to produce stable emulsions. S80 is also used in self-emulsifying drug delivery systems for poorly soluble compounds (Fatouros *et al.*, 2007). Although S80 is non-toxic and non-irritant in nature, hypersensitivity has been reported after topical application (Rowe *et al.*, 2012).

### 2.2.7 Transcutol<sup>®</sup> P

Transcutol<sup>®</sup> P (TP), also known as diethylene glycol monoethyl ether, ethoxy diglycol, ethyl dioxytol, or ethyl carbitol (Figure 2.5), is a marketed product from Gattefossé GmbH (Weil am Rhein, Germany).

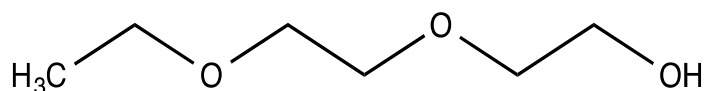


Figure 2.5 Chemical structure of diethylene glycol monoethyl ether.

TP is a clear, colourless liquid having boiling point 198°C. It is freely soluble in water, miscible in acetone, benzene, chloroform, and insoluble in mineral oils. TP has been widely used as solubiliser in various pharmaceutical products such as oral, topical, transdermal and injectables in the United States, Asia, and Europe (Osborne, 2011). It is used as a skin penetration enhancer for skin products such as lotions, gels, creams and cosmetic formulations (Puglia and Bonina, 2008). Topical solutions and a spray containing TP are used as anti-parasitic agents for veterinary applications (Strickley, 2004).

#### 2.2.8 Sodium lauryl sulphate

Sodium lauryl sulphate (SLS) is chemically known as dodecyl alcohol hydrogen sulphate, sodium dodecyl sulphate or sulphuric acid monododecyl ester (Figure 2.6). It is an anionic surfactant with a bitter taste and a faint odour of fatty substances.

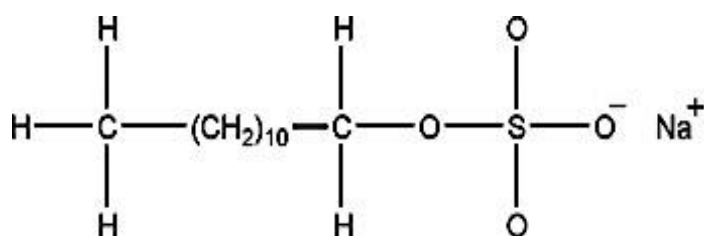


Figure 2.6 Chemical structure of sodium lauryl sulphate.

SLS takes the form of white or cream to pale yellow coloured crystals, flakes, or a smooth feeling powder with melting point of 204°C - 207°C. It is freely soluble in water, giving an

opalescent solution, and is practically insoluble in chloroform and ether. The HLB value of SLS is  $\approx 40$  and its CMC value is 8.1 mM at 25°C in water (Mukerjee and Mysels, 1971). It is widely used in non-parenteral formulations and cosmetics at different concentrations. It is effective as a wetting agent in both acidic and alkaline conditions and is also used as an emulsifying agent, tablet and capsule lubricant. It has been used as a solubilising agent for improving the solubility of poorly water soluble drugs, like montelukast (Priyanka and Abdul, 2012), and TSN (Grove *et al.*, 2003).

## 2.2 General Methods

### 2.2.1 High performance liquid chromatography method development and validation

An objective of this study was to develop and validate rapid and sensitive methods for quantitative analysis of TSN and CHG. The reverse phase high performance liquid chromatography (RP-HPLC) methods developed were validated in terms of precision, accuracy, sensitivity, linearity, range and recovery (ICH, 2005). Applications of this method include determination of drug content and encapsulation efficiency and evaluation of the *in vitro* release of TSN and CHG from the developed nanoformulations.

#### 2.2.1.1 Method development for triclosan

**Materials:** Triclosan was a gift from Vivimed Labs (India). HPLC grade acetonitrile was obtained from Fisher Scientific (UK) and ultrapure water generated in-house was used in the study.

**Method:** The HPLC system was obtained from Shimadzu Corporation (UK) and comprised an LC-10AT pump, an auto injector (LC-20AT) and a UV-Visible detector (SPD-20AV). The chromatographic analysis of TSN standard solution samples was carried out on a pentafluorophenyl (PFP) column (Phenomenex, UK). The column was 250 mm long with an internal diameter of 4.6 mm and a particle size of 5  $\mu\text{m}$ . The mobile phase used was acetonitrile and water (60:40, % v/v) and analysis was performed at 30°C.

To enhance the separation of TSN, the amount of the ionised form of the drug was kept to a minimum by maintaining the mobile phase pH at 6 (based on the  $\text{pK}_a$  of TSN (see section 1.3.5.4)). The samples were run at a constant flow rate of 1 ml/min. Detection of the samples was carried out at a maximum absorption wavelength of 280 nm. A stock solution of 100  $\mu\text{g/ml}$  was prepared. This was then diluted with the mobile phase to prepare 1, 5, 10, 20, 30, 40 and 50  $\mu\text{g/ml}$  samples and responses were measured using HPLC.

### 2.2.1.2 Method development for chlorhexidine digluconate

**Materials:** Chlorhexidine digluconate (20 % w/v) solution, sodium heptane sulphonate and diethylamine were purchased from Sigma Aldrich (UK). HPLC grade methanol was obtained from Fisher Scientific (UK) and ultrapure water generated in-house was used in the study.

**Method:** The same HPLC system as described in Section 2.2.1.1 was used. The chromatographic analysis of the CHG containing samples was carried out using a Synergi C<sub>18</sub> column (250 mm x 4.6 mm ID, 4µm) from Phenomenex, UK. The isocratic mobile phase consisted of methanol: water mixture (75:25, % v/v) with 0.005 M sodium heptane sulphonate and 0.1 % (v/v) diethylamine, adjusted to pH 4 with glacial acetic acid. The samples were run at a constant flow rate of 1 ml/min. Detection of the samples was carried out at a wavelength of 254 nm. A stock solution of 100 µg/ml was prepared for CHG. This was further diluted with the mobile phase to prepare 1, 5, 10, 20, 30 and 40 µg/ml samples and responses were measured using HPLC.

### 2.2.1.3 High performance liquid chromatography method validation

#### 2.2.1.3.1 Specificity

The analytical specificity of a method is its ability to accurately identify and measure an analyte in the presence of other closely related compounds. Specificity shows how well an assay can detect only a specific substance and not the other closely related substances in the sample during an analysis. The analytical specificities of the RP-HPLC methods for TSN and CHG were determined by comparing the chromatograms obtained from the injection of standard drug solution and the injection of a test sample containing all inactive excipients along with the drug. Figure 2.7 and Figure 2.8 shows typical HPLC chromatograms of TSN standard solution and TSN test sample, while Figure 2.9 and Figure 2.10 shows typical HPLC chromatograms of CHG standard solution and CHG test sample respectively.

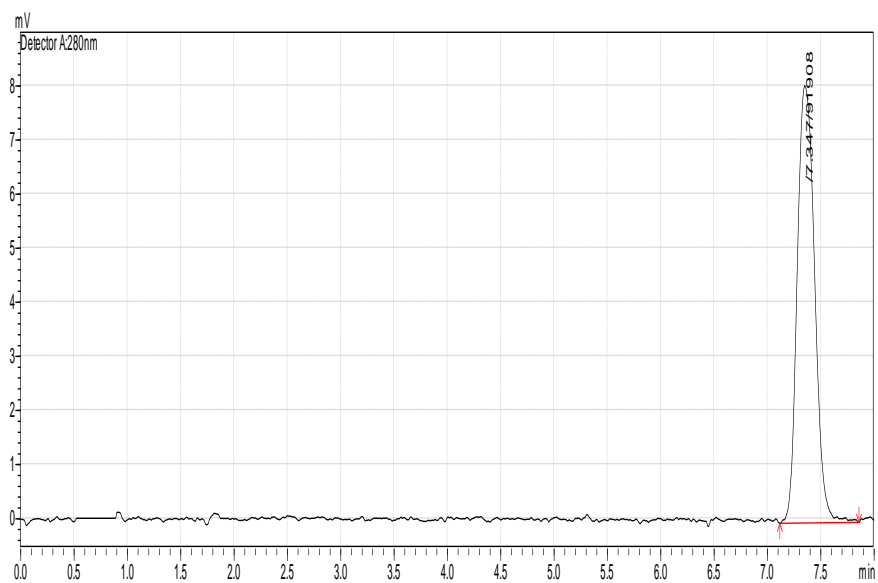


Figure 2.7 Chromatogram of triclosan standard solution (20 µg/ml).

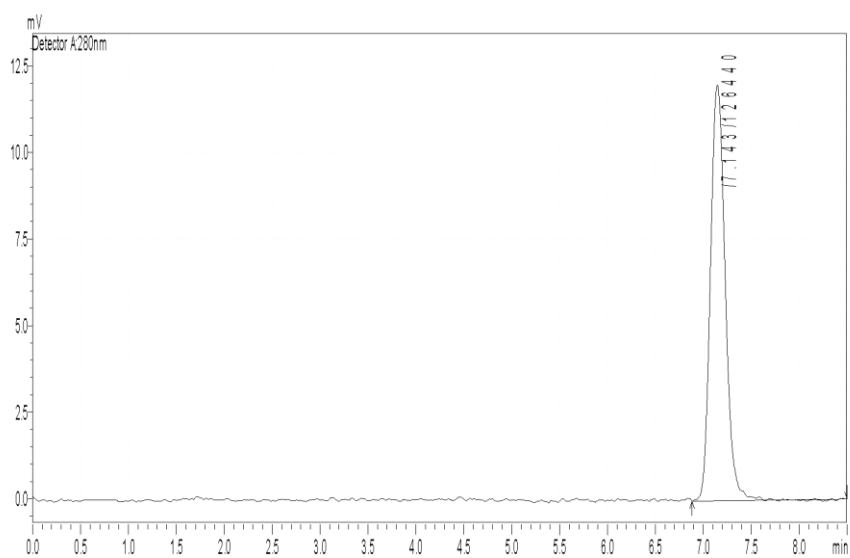


Figure 2.8 Chromatogram of triclosan test sample.

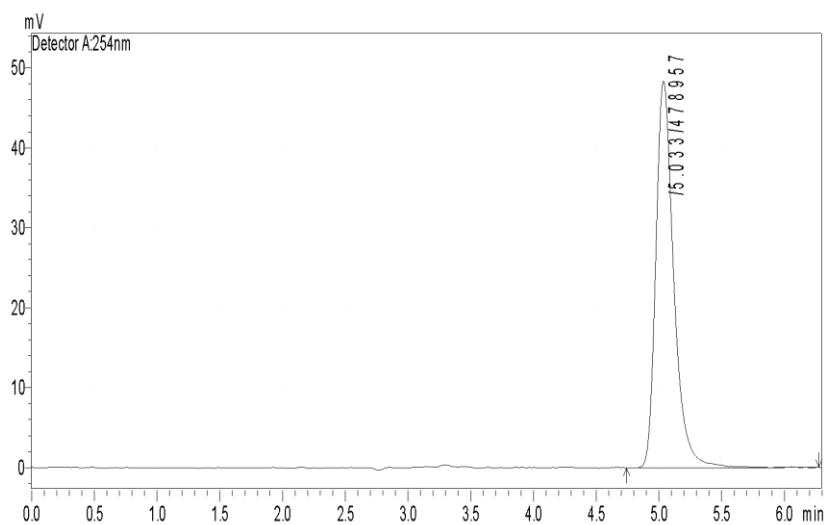


Figure 2.9 Chromatogram of chlorhexidine digluconate standard solution (20 µg/ml).

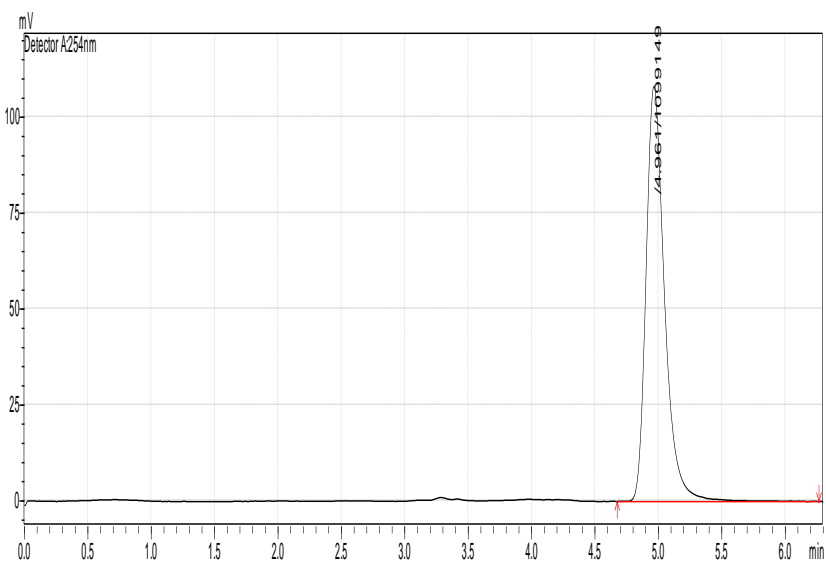


Figure 2.10 Chromatogram of chlorhexidine digluconate test sample.

The HPLC chromatograms for mixtures of inactive ingredients revealed no extra peaks near the retention times of 7.34 min for TSN and 5.03 min for CHG, showing the HPLC

methods specificity for their respective drugs.

#### 2.2.1.3.2 Accuracy

The accuracy of an analytical method represents the closeness of the test results obtained using the method to the true value Accuracy was evaluated by determining the recovery of a sample of the analyte spiked into the matrix of the sample to be analysed. Drug solutions were prepared that contained known amounts of drug, at 50 %, 100 % and 150 % of the assay concentrations. These were compared with reference standards of known purity for both drugs and percent recoveries (mean  $\pm$  SD) were calculated. The TSN and CHG solutions were spiked with known amounts of excipients used in formulations and samples were analysed by comparing the estimated concentrations with the known concentrations of TSN and CHG to calculate the percentage recovered.

Table 2.1 Recovery of triclosan from spiked samples for determination of assay accuracy (Mean  $\pm$  SD, n=3).

Levels	Amount added ( $\mu\text{g/ml}$ )	Amount recovered ( $\mu\text{g/ml}$ )	% Recovery
50 %	25	24.82	99.23 $\pm$ 0.06
100 %	50	50.87	101.65 $\pm$ 0.12
150 %	75	74.61	99.46 $\pm$ 0.08

Table 2.2 Recovery of chlorhexidine digluconate from spiked samples for determination of assay accuracy (Mean  $\pm$  SD, n=3).

Levels	Amount added ( $\mu\text{g/ml}$ )	Amount recovered ( $\mu\text{g/ml}$ )	% Recovery
50 %	20	20.32	101.51 $\pm$ 0.03
100 %	40	39.84	99.58 $\pm$ 0.09
150 %	60	60.53	100.85 $\pm$ 0.15



### 2.2.1.3.3 Linearity

The linearity of HPLC method is the ability to detect the upper and lower concentration range of analyte through the system. To determine the linearity and range of an assay, a calibration curve must be prepared over the range of concentrations appropriate to the assay and the regression coefficient determined.

The linearity was analysed for TSN in the concentration range of 1 – 50 µg/ml, whereas for CHG the concentration range was 1 – 40 µg/ml (all samples were prepared in triplicate). The regression equation for TSN (Figure 2.11) was found to be  $y = 5153.3x - 1085.3$  ( $R^2 > 0.9999$ ), while the regression equation for CHG (Figure 2.12) was found to be  $y = 23045x + 10195$  ( $R^2 > 0.9995$ ). The limit of detection (LOD) and limit of quantification (LOQ) were calculated from the standard curve according to Equations 2.1 and Equation 2.2 below:

$$\text{LOD} = \frac{3\text{XSD}}{\text{slope}} \quad \text{Equation 2.1}$$

$$\text{LOQ} = \frac{10\text{xSD}}{\text{slope}} \quad \text{Equation 2.2}$$

All the parameters such as LOD, LOQ, capacity factor, tailing factor, theoretical plates, peak resolution and column efficiency were calculated for both TSN and CHG to test the system suitability for analysis (Table 2.5).

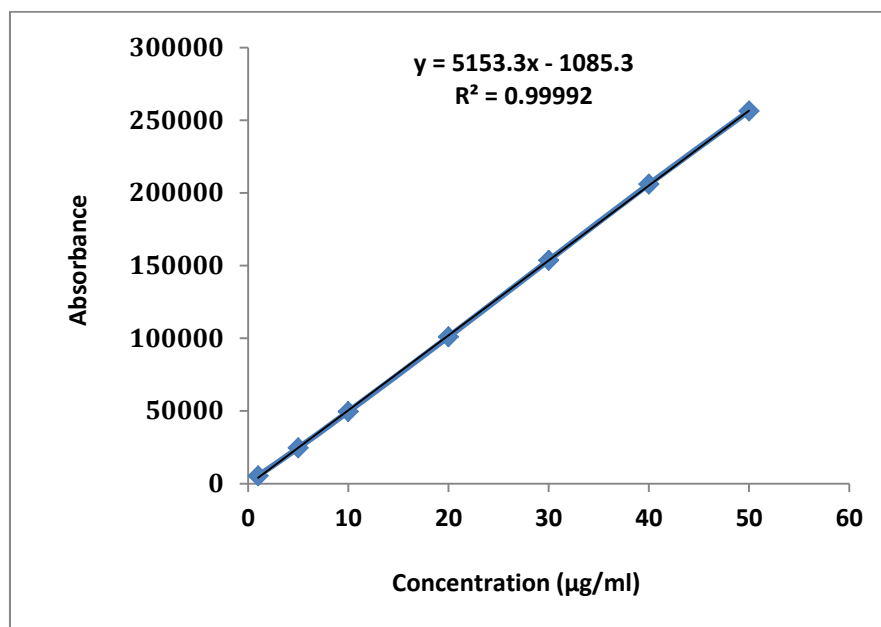


Figure 2.11 Standard calibration curve for triclosan (Mean  $\pm$  SD, n=3).

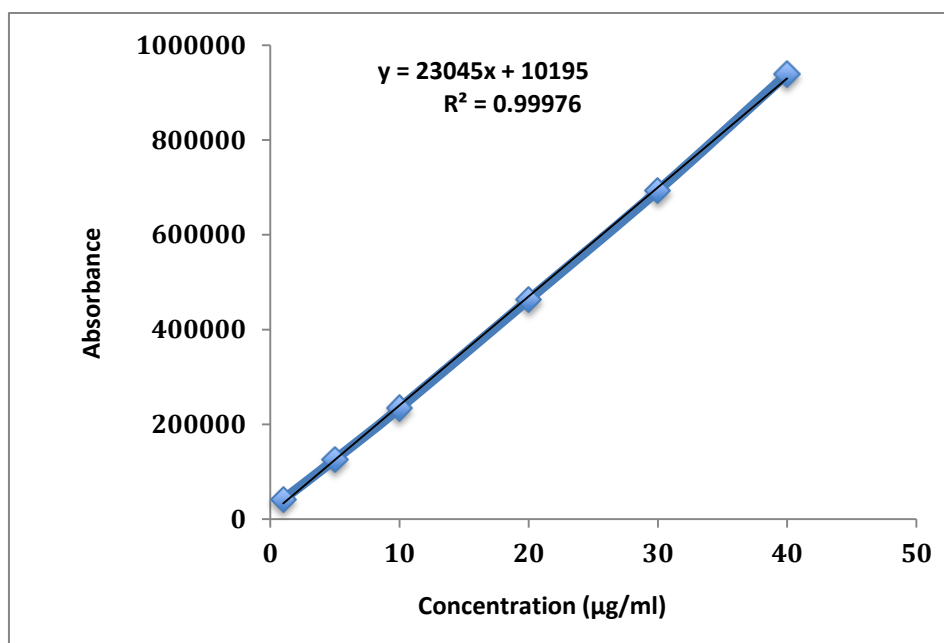


Figure 2.12 Standard calibration curve for chlorhexidine digluconate (Mean  $\pm$  SD, n=3).

#### 2.2.1.3.4 Precision

The precision data of analytical methods shows close agreement between repeated test results of the same samples. The precision of the method measures reproducibility of results of analytical including sample preparation and sampling under specified operating conditions. Precision of HPLC methods used for both TSN and CHG was determined using six replicas of the TSN and CHG standard solutions, on the same day (intra-day precision) and once a day over a period of one week (inter-day precision). The results are expressed as the mean area under the curve (AUC) and percent relative standard deviation (% RSD) measurements (Tables 2.3 and Table 2.4).

Table 2.3 Intra-day and inter-day precision of HPLC methods for triclosan (Mean  $\pm$  SD, n=3).

Concentration ( $\mu\text{g/ml}$ )	Intra-day precision		Inter-day precision	
	Mean AUC $\pm$ SD	% RSD	Mean AUC $\pm$ SD	% RSD
1	6232.1 $\pm$ 142.1	0.45	6217.8 $\pm$ 274.6	0.71
5	27116.7 $\pm$ 109.3	0.21	27032.1 $\pm$ 163.2	0.42
10	51534.2 $\pm$ 252.5	0.05	51741.9 $\pm$ 192.5	0.62
20	102860.7 $\pm$ 178.5	0.09	102891.4 $\pm$ 316.1	0.6
30	155005.5 $\pm$ 214.3	0.03	154008.4 $\pm$ 287.3	0.56
40	207583.3 $\pm$ 149.7	0.08	206714.1 $\pm$ 174.2	0.38
50	261832.5 $\pm$ 317.2	0.10	261198.2 $\pm$ 185.3	0.74

Table 2.4 Intra-day and inter-day precision of HPLC method for chlorhexidine digluconate (Mean  $\pm$  SD, n=3).

Concentration ( $\mu\text{g/ml}$ )	Intra-day precision		Inter-day precision	
	Mean AUC $\pm$ SD	% RSD	Mean AUC $\pm$ SD	% RSD
1	9438.2 $\pm$ 362.1	0.17	9321.6 $\pm$ 283.1	0.18
5	31284.6 $\pm$ 273.6	0.36	32835.2 $\pm$ 253.4	0.26
10	56930.8 $\pm$ 241.2	0.14	55628.1 $\pm$ 195.2	0.62
20	116839.3 $\pm$ 316.3	0.24	114636.6 $\pm$ 184.7	0.58
30	174582.7 $\pm$ 212.6	0.37	175391.4 $\pm$ 196.2	0.35
40	235826.5 $\pm$ 325.5	0.18	237293.4 $\pm$ 314.7	0.27

Table 2.5 Chromatographic characteristics of HPLC system suitability.

HPLC Parameter	TSN	CHG
LOD	0.60 $\mu\text{g/ml}$	0.63 $\mu\text{g/ml}$
LOQ	1.83 $\mu\text{g/ml}$	1.93 $\mu\text{g/ml}$
Theoretical plate number (N)	5230.13 cm	2564.47 cm
Tailing factor (T)	1.25	1.57
Capacity Factor (K)	2.92	3.96
Height equivalent theoretical plate	0.04	0.09

### 2.2.2 Skin diffusion mechanism

For most chemicals, the main transport mechanism through the skin is passive diffusion, as is the case with most other biological membrane barriers of physiological or pharmaceutical relevance. Passive diffusion is a mechanism by which a substance moves from one region of a system to another, following random molecular motions (Figure 2.13). In other words, there is a random walk of an ensemble of molecules from a region of high concentration to regions of low concentration. The diffusion process can be expressed through Fick's first law and the second law of diffusion.

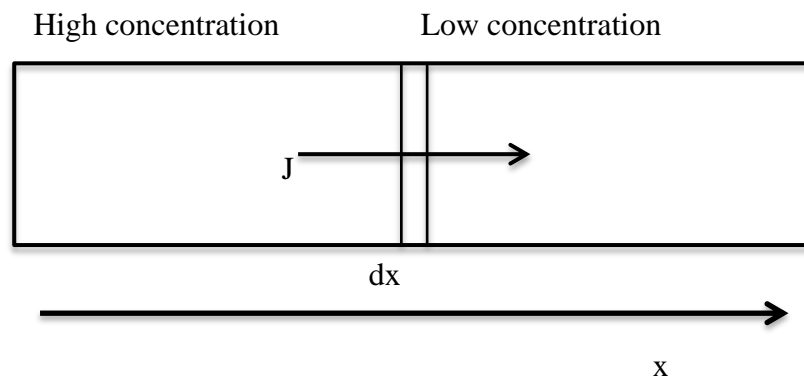


Figure 2.13 Molecular transport mechanism across a membrane.

#### A. Fick's first law of diffusion

For a given medium, the particle flux ( $J$ ), or the number of particles travelling through a unit of perpendicular area per unit time, is proportional to the concentration gradient. This is expressed through Fick's first law of diffusion (Equation 2.3),

$$J = -D \frac{dC}{dx} \quad \text{Equation 2.3}$$

Where,  $J$  = rate of transfer per unit surface area (the flux),  $dC/dX$  = concentration gradient per unit length, and  $D$  = diffusion coefficient or diffusivity.

The proportionality constant in Equation 2.3 is the diffusion coefficient ( $D$ ) of the corresponding medium, or a rough measure of the ease with which a molecule can move

about within a medium, in this case, the SC. Since diffusion through the SC is passive, large molecules diffuse more slowly than small ones. In general, drugs with a molecular weight smaller than 500 Da have acceptable permeation rates (Aulton and Taylor, 2013). However, diffusivity is not only dependent on molecular weight and volume but on the degree of interaction between the drug and the SC. The concentration gradient across the SC will depend primarily upon the chemical characteristics of the drug, including solubility, lipophilicity, ionisation and stability.

### **B. Fick's second law of diffusion**

When a formulation is placed on the skin surface, it partitions into the lipids and diffuses *via* intercellular channels. Following a short period of exposure, a nonlinear concentration gradient develops across the SC, the slope of which is described by Fick's second law of diffusion (Equation 2.4). Fick's second law relates the rate of change in concentration with time at a given point in a system to the rate of change in concentration gradient at that point.

$$\frac{dc}{dt} = \frac{dJ}{h} \quad \text{Equation 2.4}$$

The rate of permeation across the skin ( $dQ/dt$ ) is given by:

$$\frac{dQ}{dt} = P_s (C_d - C_r) \quad \text{Equation 2.5}$$

Where  $C_d$  = concentration of skin penetrant in the donor compartment (e.g., on the surface of the SC)

$C_r$  = concentration in receiver compartment (e.g., body)

$P_s$  = the overall permeability constant of skin tissue to the penetrant

$$P_s = \frac{K_s D_{ss}}{h_s} \quad \text{Equation 2.6}$$

Where  $K_s$  represent the partition coefficient of the penetrant molecule from a formulation to SC,  $D_{ss}$  is apparent diffusivity of the steady-state diffusion of the penetrant molecule and  $h_s$  is the thickness of skin.

From Equation 2.5, it can be seen that the constant rate of drug permeation can be obtained only when  $C_d \gg C_r$ , i.e., the drug concentration at the surface of the SC, i.e.  $C_d$ , is consistently higher than the drug concentration in the body ( $C_r$ ). Hence, the equation 2.5 thus becomes:

$$\frac{dQ}{dt} = P_s C_s \quad \text{Equation 2.7}$$

The membrane-limited flux (J) under this steady-state condition is described by the equation:

$$J = \frac{D K_{o/w} C}{h} \quad \text{Equation 2.8}$$

Where

J = Amount of drug passing through the membrane system *per unit area per unit time*.

D = Diffusion coefficient within the membrane

$K_{o/w}$  = Membrane / vehicle partition coefficient

C = Concentration gradient across the membrane

h = Membrane thickness

### 2.2.2.1 *In vitro* skin permeation model

*In vitro* diffusion models include simple two-compartment “static” diffusion cells or multi-jacketed “flow-through” cells which are normally inert and made of glass material. The membrane, in this case excised skin or the artificial membrane, is mounted as a the barrier between a donor and a receiver compartment of the diffusion cell and the amount drug diffusing from the donor to the receiver compartment is analysed as a function of time. The static diffusion cell is usually a Franz upright diffusion model (Figure 2.14) or side-by-side model.

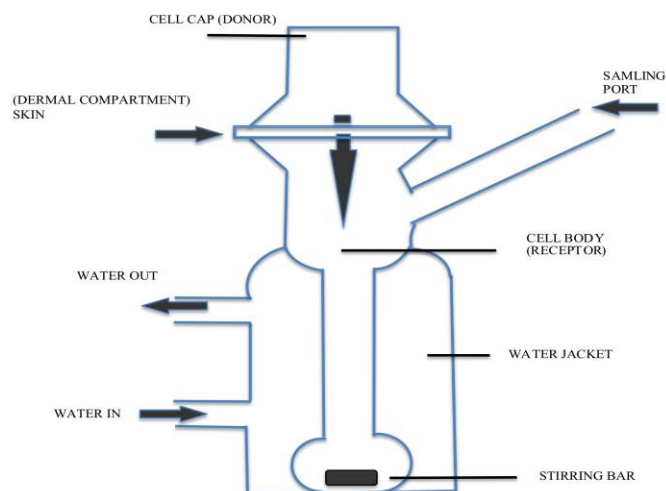


Figure 2.14 Schematic diagram of Franz diffusion cell.

The receiver compartment is filled with physiological saline or buffer solution which can provide ions and pH require to diffuse the drug from the donor compartment. The temperature of diffusion cell is always maintained at a constant temperature, usually at 37°C, to maintain a surface skin temperature at 32°C as an *in vivo* mimic. The receiver compartment is stirred continuously and analyte is sampled at regular intervals. This helps to avoid saturation of the receiver solution and maintain sink conditions.

#### 2.2.2.2 Membrane selection

Human skin is clearly the most relevant model for evaluating the dermal drug delivery of various formulations. Skin obtained from various sources, including plastic surgery, amputation and cadavers, has been used for *ex vivo* evaluation of drug penetration (Godin and Touitou, 2007). Skin samples are mostly taken from the abdomen, back, leg or breast (Schaefer *et al.*, 2008) and varies in thickness depending on the bodysite .

Moreover, skin permeability varies greatly between specimens taken from the same and different anatomical sites of the same donor and between the specimens of different subjects or different age groups (Haigh and Smith, 1994). These variations may be due to



differences in lipid composition, skin thickness or hydration, which are determined by the body site, sex, race, and the age of the donor, and disease state. Another limitation of using human skin is the metabolism and biotransformation of chemicals applied to the skin that occurs after excision of the tissue from the donor. Therefore, many *in vitro* permeation studies have used animal skin rather than human skin as a rate-limiting membrane. Various animal skins such as hairless mouse, rabbit, guinea pig, rat, pig and shed snake skin have been tested as a model for human skin (Gomes *et al.*, 2014; Ngawhirunpat *et al.*, 2008).

Domestic porcine skin is reported as the most appropriate animal model due to the numerous anatomical, histological and physiological similarities with human skin. These include epidermal thickness, the dermal-epidermal thickness ratio, the resemblance of hair follicles and blood vessel density in the skin, as well as the content of SC glycosphingolipids, ceramides, dermal collagen and elastin (Dick and Scott, 1992; Godin and Touitou, 2007). Porcine skin is readily obtained as a waste material from animals slaughtered for food. The comparison of drug permeability using human and porcine skin has demonstrated good correlation, particularly for lipophilic substances, while skin from rodents has generally exhibited higher permeation rates. In addition, porcine skin exhibits less donor variability than human skin (Barbero and Frasch, 2009).

In comparison to porcine skin models, the use of rodent skin requires ethical permission to be granted. The use of rodents have advantages such as their small size, low cost and easy handling, however, conventional rodents have the disadvantage of an extremely high density of hair follicles, which necessitates hair removal prior to the formulation administration (Godin and Touitou, 2007). Rodent skin is believed to be more permeable to molecules compared to human skin due to differences in SC thickness, the number of corneocyte layers, hair density, water content, lipid profile and morphology (Schaefer *et al.*,

2008).

Shed snake skin has been proposed as an alternative skin model and as it is non-living tissue hence it can be stored at room temperature for relatively long periods of time (Haigh and Smith, 1994). Similarities with the human SC have been confirmed in terms of structure, composition of lipid content and water permeability. However, the lack of hair follicles could influence drug permeability (Godin and Touitou, 2007). Therefore, this model is not appropriate for investigating dermal absorption of drugs that penetrate the skin *via* the follicular route. Rigg and Barry (1990) compared a shed snake membrane with both hairless mouse and human skin by evaluating the effect of different penetration enhancers on the permeability of 5-fluorouracil indicating non-suitability of shed snake skin as a model for human skin.

Most current methods for investigating formulations destined for topical treatment rely on the use of animal models. The use of isolated epidermis or SC sheets of human or animal origin has a number of disadvantages, including high intra-individual and inter-individual variation, particularly in relation to the diseased skin for which most topical drug formulations are developed. The majority of artificial models are used to mimic healthy skin with intact barrier properties. Relatively few models offer the potential to mimic the compromised skin. Poly(dimethylsiloxane) (PDMS) or silicone membranes have been used for decades in screening the effects of different vehicles and assessing their impact on the overall mechanisms of drug transport across human skin (Dias *et al.*, 2007; Nakano and Patel, 1970; Oliveira *et al.*, 2011). Although these membranes can be used to predict the skin permeability of lipophilic compounds, it has been concluded that they are not useful for hydrophilic compounds (Miki *et al.*, 2015). To improve their hydrophilic permeability, polyethylene glycol 6000 copolymer-impregnated membrane has been developed. So far, the adapted model has only been tested using drugs in aqueous solutions; its potential in

formulation development still needs to be elucidated. The parallel artificial membrane permeability assay (PAMPA) was introduced as a rapid *in vitro* model for assessing transcellular intestinal permeability (Kansy *et al.*, 1998). The original PAMPA system consists of an artificial membrane containing a hydrophobic filter, coated with phosphatidylcholine dissolved in n-dodecane, as a membrane barrier that separates the donor and acceptor compartments. The model has a high throughput screening format and could be modified by adjusting the membrane composition. Lipid and solvent mixtures in the membrane are not well characterised and lack the true lipid bilayers found in biological membranes (Faller, 2008). Sinko and colleagues developed skin-PAMPA composites containing synthetic ceramides, which are analogues for ceramides and are proposed as replacements for naturally occurring ceramides found in SC (Sinko *et al.*, 2012). Ceramides are cheaper alternatives to natural ceramides, with the potential to prolong the storage time (Tsinman and Sinko, 2013). Although the ceramides are structurally different from ceramides, their comparable molecular mass and hydrogen acceptor and donor capacity enable them to act as the lipid constituents in the PAMPA sandwich membrane, together with cholesterol, stearic acid and silicone oil (Sinko *et al.*, 2009).

Another synthetic model called Strat-M<sup>®</sup> is predictive of diffusion in human skin without lot-to-lot variability or safety and storage limitations (Joshi *et al.*, 2012). Strat-M<sup>®</sup> is constructed of two layers of polyethersulfone (PES), which acts as a tight surface layer, creating more resistance to the entry of the drug molecule. On top of this layer, one layer of polyolefin forms a more porous and diffusive membrane. These polymeric layers form a porous structure with similar morphology to human skin (Karadzovska and Riviere, 2013).

### 2.2.3 Construction of pseudoternary phase diagrams

For nanoemulsions, the water titration method of Baboota *et al.*, (2007) was used to develop pseudoternary phase diagrams for investigating the concentration ranges of components for monophasic region formation at room temperature. Surfactant and cosurfactant ( $S_{mix}$ ) were mixed at different weight ratios of increasing concentrations of surfactant with respect to cosurfactant for a detailed phase study. For each phase diagram, a predetermined amount of oil, surfactant and cosurfactant were mixed thoroughly at room temperature using different ratios of oil to  $S_{mix}$  (1:9, 2:8, 3:7, 4:6, 5:5, 6:4, 7:3, 8:2 and 9:1) using a magnetic stirrer. Different weight ratios covered the full range so as to delineate the boundaries of phases precisely in the phase diagrams. These mixtures were continuously titrated with water. After each addition, the system was visually examined for physical appearance. Phase boundaries were determined by the end point of titration, at which the solution became turbid. The quantity of water required to make the solution turbid was recorded and phase diagram plotted (JPM 5 Software, USA), with one axis represents oil phase, second representing the water phase and third axis representing the  $S_{mix}$  at a fixed ratio.

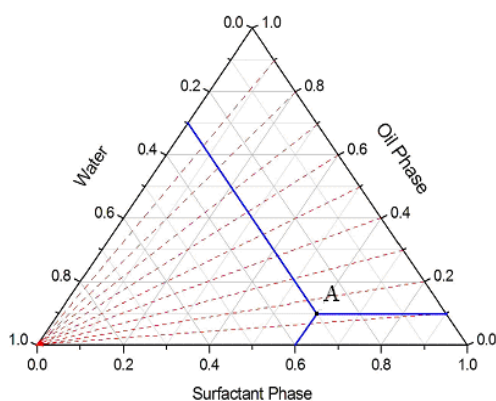


Figure 2.15 Schematic representation of pseudoternary phase diagram.

A typical pseudoternary phase diagram representing a three-component system of oil, water and surfactant can be read following the solid lines, as shown in Figure 2.15. In this work,

phase diagrams are referred to as “pseudoternary” phase diagrams, as the surfactant phase was a mixture of surfactant and cosurfactant. The titration procedure began with a zero loading of water and ended at a point of 100 % water loading. An infinite number of tie lines can be drawn in any pseudoternary phase diagram (Li *et al.*, 2005). In the present work, the titration was initiated using different ratios of surfactant phase to oil phase and followed by drop wise addition of water. The  $S_{\text{mix}}$  was fixed at a 2:1 ratio.

### **3. CHAPTER: FORMULATION AND EVALUATION OF SOLID LIPID NANOPARTICLES FOR DERMAL DELIVERY**

#### 3.1 Introduction

Considering non-invasive routes of administration, the dermal route seems to be one of the most attractive approaches for drug delivery. However, one of the challenges in dermal drug delivery is the requirement to overcome the barrier properties of the skin and to deliver effective amounts of drug for the desired therapeutic action. In addition, prediction of adequate skin delivery of drugs from formulations has always been difficult. It is well understood that the SC acts as a rate-controlling barrier for percutaneous drug delivery and the challenges become more pronounced in the case of poorly soluble drugs.

The basic factors of the skin affecting the absorption of drug include a) skin integrity and regional variation, b) dimensions of orifices, aqueous pores and lipidic fluid paths, and c) density of appendages. Several approaches have been used to overcome the skin barrier and allow drugs to reach their site of action. Different formulation approaches such as microparticles, SLNs and nano-lipid carriers have been evaluated (Filon *et al.*, 2015; Jana *et al.*, 2009). Although these carriers are not able to penetrate the SC at high concentrations, they may be able to deliver drugs to the skin surface and into the hair follicles. In one study it was shown that when the particle size was larger than 5  $\mu\text{m}$ , almost no penetration of drug was observed through the SC, however particles with diameters of about 750 nm demonstrated better permeation into hair follicle of the human skin (Lademan *et al.*, 2007). On the other hand, it has been claimed that ethosomes, niosomes and transferosomes change their morphology and squeeze past the SC cells and achieve systemic delivery (Rai *et al.*, 2010). Studies have also shown that hair follicles and sweat ducts provide routes for SLNs to penetrate through the skin (Hamishehkar *et al.*, 2015). The hair follicles are an important

target for drug delivery, due to being surrounded by a close network of blood capillaries and dendritic cells (Hung *et al.*, 2015; Larese *et al.*, 2015; Mittal *et al.*, 2015). The relevance of the hair follicles for the percutaneous penetration process has been identified in several investigations using split or full thickness porcine ear skin or other animal models such as mice (Fan *et al.*, 1999), mouse (Mahe *et al.*, 2009) and human skin (Vogt *et al.*, 2006). Thus, follicular transport is considered to be a potential pathway for dermal and cosmetic formulations. There are many reports on different results about drug permeation through excised and intact full thickness skin which might be explained by differences in size, type and density of the follicles, lipid composition and SC thickness (Lauterbach and Müller-Goymann, 2014). Irrespective of individual skin differences, the excision of the skin may also have an influence on the penetration rate. After cutting a piece of skin and removing the subcutaneous fatty tissue, the skin contracts to a certain degree (Starcher *et al.*, 2005). This may be due to several physiological factors such as water loss and the sudden absence of blood flow. Additionally, the elastic fibres, which endow the skin with resilience presumably contract after being cut. On one hand, this means that the hair follicle density per  $\text{cm}^2$  increases, possibly influencing the follicular penetration rate. However, it is possible that after cutting the skin, the hair follicles are constricted by the contracting elastic fibres and therefore, are significantly less receptive to the penetration process (Patzelt *et al.*, 2008).

SLNs with diameters about 200 nm were found to improve the penetration of diclofenac sodium through rat skin (Liu *et al.*, 2010a). The importance of particle size on drug delivery to skin was emphasised, but in addition, absorption was also influenced by type of excipients used in the formulation. Irrespective of the penetration route, the uptake of particles requires adequate wetting and thus the use of surfactants in the formulation plays a very important role. In the present work T80 and TP were used as surfactant and

cosurfactant in different ratios to study their effect on particle size and drug encapsulation. Two solid lipids, GB and GP, were used in different concentrations to compare their effect on drug permeability while TSN was used as the model drug. There are limited reports on TSN formulations for delivery to the skin, however, topical lipid formulations hold great promise for delivery of this very poorly soluble drug.



### 3.2 Aims of the study

The aims of this study were,

- To develop TSN-loaded SLNs for topical drug delivery using the solid lipids GB and GP. To analyse effect of type and concentration of lipid and surfactants on physicochemical properties of SLNs by formulating various compositions of preliminary formulations.
- To analyse prepared SLN formulations based on physicochemical properties and stability studies to select optimised SLNs to perform *in vitro* skin diffusion using Franz diffusion model.
- To evaluate and compare the ability of GB-SLNs and GP-SLNs to permeate through, and retain the TSN within skin using an *in vitro* diffusion study using frozen excised full thickness porcine ear skin.
- To evaluate the ability of SLNs to enhance the delivery of TSN to deeper layers within the skin and hair follicles using differential stripping techniques.

### 3.3 Materials and methods

#### 3.3.1 Materials

Triclosan was obtained from Vivimed Ltd. (Mumbai, India). Glyceryl behenate, glyceryl palmitostearate and Transcutol<sup>®</sup>P were a kind gift from Gattefossé (Weil am Rhein, Germany). Phosphate buffered saline tablets (pH 7.4), sodium lauryl sulphate and Parafilm<sup>®</sup>M were purchased from Sigma Aldrich (UK). Tween<sup>®</sup>80 was obtained from Fisher Scientific Ltd (UK). All other solvents and chemicals were of analytical grade.

#### 3.3.2 Methods

##### 3.3.2.1 Solubility studies of triclosan in buffer

The solubility of TSN was determined in phosphate buffer solution (PBS, pH 7.4). Approximately 10 ml of buffer solution was added to a vial, an excess quantity of TSN was placed in each vial, which was greater than the quantity expected to dissolve in the receiver medium. Solubility was also determined in PBS solution containing various concentrations of 1 % w/v SLS (50 mM, 100 mM, 150 mM, 200 mM and 250 mM) to find a suitable concentration of SLS require to enhance TSN solubility and maintain sink conditions in the receiver medium during diffusion studies. All vials were tightly closed and placed in a shaking water bath (GLS aqua 12 plus, Grant, UK) at  $25 \pm 1^\circ\text{C}$ , 350 rpm for 24 h after which time, the samples were filtered through a 0.45  $\mu\text{m}$  syringe filter (Fisher Scientific, UK) and analysed by HPLC (Section 2.2.1.1).

##### 3.3.2.2 Formulation of solid lipid nanoparticles

TSN-loaded SLNs were prepared by hot HSH followed by probe ultrasonication (Nerella *et al.*, 2014; Patel *et al.*, 2012). Briefly, the lipid phase was prepared by heating lipids (GB and GP) to 5°C above their melting points and TSN (equivalent to 10 mg/g of formulation) was added to the lipids while the aqueous phase was prepared by mixing  $S_{\text{mix}}$  (T80 and TP) and water heated to same temperature. The hot lipid phase was slowly added to the hot aqueous

phase under HSH (Silverson, UK). This hot primary emulsion was then subjected to probe ultrasonication (Sonics and Materials Inc., USA) for 10 min at 70 % frequency amplitude. The resultant dispersion was cooled to room temperature to solidify the lipids and form SLN dispersions. The impact of homogenisation conditions on the SLNs was investigated (i.e. homogenisation speed was varied from 6000 rpm to 10,000 rpm and duration of homogenisation time from 5 min to 15 min). Also, the effect of various formulation parameters, such as ratio of surfactant to cosurfactant and lipid to drug on mean particle size and entrapment efficiency were also studied.

Table 3.1 Composition of preliminary TSN-loaded SLN formulations.

Formulation Code	Lipid		T80: TP (% w/w)
	Type	Concentration (% w/w)	
GB3-1	Glyceryl behenate	3	1:1
GB3-2			2:1
GB3-3			3:1
GB3-4			4:1
GB5-1		5	1:1
GB5-2			2:1
GB5-3			3:1
GB5-4			4:1
GB7.5-1		7.5	1:1
GB7.5-2			2:1
GB7.5-3			3:1
GB7.5-4			4:1
GB10-1		10	1:1
GB10-2			2:1
GB10-3			3:1
GB10-4			4:1
GP3-1	Glyceryl palmitostearate	3	1:1
GP3-2			2:1
GP3-3			3:1
GP3-4			4:1
GP5-1		5	1:1
GP5-2			2:1
GP5-3			3:1
GP5-4			4:1
GP7.5-1		7.5	1:1
GP7.5-2			2:1
GP7.5-3			3:1
GP7.5-4			4:1
GP10-1		10	1:1
GP10-2			2:1
GP10-3			3:1
GP10-4			4:1

### 3.3.2.3 Lyophilisation of solid lipid nanoparticles

The primary purpose of drying the SLN dispersion was to obtain a powder for further solid state characterisation. The TSN loaded SLNs were frozen overnight at – 20°C before freeze drying under vacuum at atmospheric pressure for 24 h. (Christ LD 2-4 plus, UK).

### 3.3.3 Physicochemical characterisation

#### 3.3.3.1 Particle size analysis

The particle size and polydispersity index (PDI) of TSN-loaded SLNs were measured using nanoparticle tracking analysis (NTA, Nanosight LM10, UK). This technique utilises both light scattering and Brownian motion in order to obtain particle size distributions of samples in liquid suspensions. The laser beam is passed through a prism-edged flat glass surface within the sample chamber into the nanoparticle suspension. Suspended particles in the path of this beam scatter light in such a manner that they can be easily visualised *via* a microscope (Filipe *et al.*, 2010). Particle size distribution within formulations is expressed as the PDI, which can be calculated from 10 %, 50 % and 90 % of total volume of sample. All the samples were measured in triplicate to obtain the mean particle size and PDI, which was calculated using Equation 3.1,

$$\text{PDI} = \frac{D_{90\%} - D_{10\%}}{D_{50\%}} \quad \text{Equation 3.1}$$

#### 3.3.3.2 Determination of drug entrapment efficiency

The percentage drug entrapment efficiency (% DEE), which corresponds to the percentage of TSN encapsulated within the SLNs, was determined by measuring the concentration of free TSN in the dispersion medium. The free TSN was determined by adding 500 µl of TSN loaded SLNs to 9.5 ml chloroform and methanol (1:1) mixture and centrifuged at 5000 rpm (Eppendorf AG 5702, Germany) for 20 min. The supernatant was filtered through a syringe

filter (0.45 µm) and analysed for unencapsulated TSN at 280 nm using HPLC after suitable dilution (Khurana *et al.*, 2010). The analysis was performed in triplicate. The % DEE was calculated according to Equation 3.2 as follows,

$$\% \text{ DEE} = \frac{W_{\text{initial drug}} - W_{\text{free drug}}}{W_{\text{initial drug}}} \times 100 \quad \text{Equation 3.2}$$

#### 3.3.3.3 Zeta potential measurement

In order to quantify the surface charge on nanoparticles, the zeta potential (ZP) was measured using a Zetasizer Nano Z (Malvern Instruments Ltd, UK). Each sample was suitably diluted with the aqueous phase of the formulation and placed in a disposable zeta cell. Zeta limits ranged from -200 mV to +200 mV. The average of three measurements of each sample was used to derive the average ZP.

#### 3.3.3.4 Thermal analysis of solid lipid nanoparticles

The thermal behavior of drug and SLNs was analysed by differential scanning calorimetry (DSC) using a Mettler Toledo DSC1 (STAR<sup>e</sup> system, UK), calibrated using an indium standard. Samples (8-10 mg) of pure TSN, GB and GP lipids, equivalent ratio of physical mixtures of drug and lipids (PM) and lyophilised TSN-loaded SLNs were analysed in sealed 40 µl aluminum pans. The thermograms were recorded over a temperature range of 25-160°C at a heating rate of 10°C/min under a continuous nitrogen gas purge, maintained at a flow rate of 50 ml/min (Kotikalapudi *et al.*, 2012).

#### 3.3.3.5 Powder X-ray diffraction analysis

The effect of the encapsulation process on the crystallinity of the TSN was investigated using powder X-ray diffractometry (XRD, Bruker D2 Phase, UK). XRD patterns were obtained by analysing samples of pure TSN, GB and GP lipids, lyophilised TSN-loaded SLNs. Samples were placed in the stainless steel holder and the surface powder was leveled manually. The sample was scanned between 5 and 40° of 2θ with step size of 0.019° and a step time of 32.5 Sec.

#### 3.3.3.6 Transmission electron microscopy

The morphology of SLNs was confirmed by transmission electron microscopy (TEM) using a JEOL 3010, which was operated at 300 kV. The SLNs dispersion was diluted with water and placed on a carbon film supported by a copper grid (200 mesh carbon coated copper grid, Agar Scientific, UK). Excess sample was removed with filter paper and to achieve a better imaging contrast, the samples were negatively stained with 1 % (w/w) phosphotungstic acid for 1 min. Stained samples were air dried at room temperature before analysis (Kupetz and Bunjes, 2014).

#### 3.3.3.7 Fourier transform infrared spectrometry

The freeze dried SLN formulations and samples of pure TSN, GB and GP lipids were evaluated using Fourier transform infrared spectrometry (FTIR, Frontier TM, PerkinElmer; Santa Clara, CA, USA) equipped with a diamond crystal. All samples were run in triplicate; a background run (to remove the background noise of the instrument) was carried out as a negative control. Spectra were recorded between 4,000 and 600  $\text{cm}^{-1}$  with a spectral resolution of 4  $\text{cm}^{-1}$ .

#### 3.3.3.8 Stability study

TSN-loaded SLNs were stored for 3 months at room temperature (~20°C) and at elevated temperature and relative humidity (40°C/75 % RH). The samples were characterised for

particle size, PDI and ZP following storage. The samples were studied in triplicate and results were expressed as mean  $\pm$  SD. Statistical analysis of the data was performed using a student t-test. A probability of less than 0.05 ( $p < 0.05$ ) was considered significant in this study.

### 3.3.3.9 Skin permeation study

#### 3.3.3.9.1 *In vitro* skin diffusion studies

Porcine skin is reported to share similar permeation characteristics to human skin (see section 2.2.2.2) (Flaten *et al.*, 2015). Fresh porcine ears were obtained from a local abattoir (Leonard Wood and Sons, Huddersfield, UK) and cleaned under cold running water. The outer region of the skin was separated from the cartilage and subcutaneous fat and placed into a sealed bag and stored in a freezer at  $-20^{\circ}\text{C}$  for maximum storage period of one week. Frozen excised full thickness porcine ear skin was thoroughly thawed before use and visually inspected for defects and punctures. *In vitro* permeation studies were carried out over a period of 24 h using vertical Franz diffusion cells with a diffusion area of  $3.8\text{ cm}^2$  and a receiver compartment volume of 30 ml. The skin was hydrated by immersing in PBS (pH 7.4) solution for 60 min prior to the start of each experiment. The skin was then cut into appropriate sections and mounted on the Franz diffusion cells, with the SC facing the donor compartment (where the formulation was applied) and the dermis facing the receiver compartment. The receiver compartment was filled with PBS solution (pH 7.4) containing 1 % w/w SLS (150 mM) water circulated at  $37^{\circ}\text{C}$  to maintain a skin surface temperature at  $32^{\circ}\text{C}$ , with stirring speed of 200 rpm for 24 h. The skin was equilibrated for 30 min before loading with SLNs formulation (equivalent to 10 mg/g TSN concentration) or aqueous saturated solution of TSN as control to each donor compartment and covered with Parafilm to prevent evaporation. Samples (500  $\mu\text{l}$ ) were withdrawn at regular intervals from receiver compartment (normally 2, 4, 6, 8, 10, 12 and 24 h) and replaced by an equal volume of



fresh PBS solution to maintain sink conditions. The amount of TSN permeated through skin over 24 h was analysed by HPLC (Section 2.2.1.1).

#### 3.3.3.9.2 Quantification of triclosan from skin using differential stripping technique

The differential stripping technique allows the quantification of drug retained in the SC and in the hair follicles, differentiating between transepidermal and transfollicular penetration. The differential stripping technique consists of adhesive tape stripping followed by cyanoacrylate biopsy (Teichmann *et al.*, 2005; Wosika and Cal, 2010). The adhesive tape stripping method is a commonly used method, which allows removal of the SC layer by layer, and can be used to determine the amount of substance retained in the skin surface both *in vitro* and *in vivo*. Cyanoacrylate skin surface biopsy is a non-invasive method, which consists of applying superglue on the skin surface and removing it after polymerisation, thus entrapping corneocytes and follicular casts. Hence with the differential stripping technique, it is possible to quantify drug SC retention by tape stripping and follicular retention by cyanoacrylate biopsy, making it a complete quantification method. After *in vitro* skin permeation studies, the skin surface was washed thoroughly with distilled water to remove any excess formulation followed by differential stripping technique.

##### Adhesive tape stripping technique and cyanoacrylate skin surface biopsy

The skin was stripped using an adhesive surgical tape (3M Transpore, UK) and was cut into 3x3 cm<sup>2</sup> pieces and applied to the SC side of the treated skin surface. The tape strips were pressed onto the skin by applying uniform pressure in order to obtain an intimate contact between tape and skin. The procedure was repeated with 15 tapes for each skin tissue. Following the removal of 15 tape strips, a drop of superglue was placed on the stripped area and the glue was covered with adhesive tape under slight pressure. After 10 min, the cyanoacrylate polymerised and the strip was removed with a quick motion, entrapping the

casts of hair follicles. Two such cyanoacrylate tapes were used for each skin sample and analysed individually.

After differential stripping, the porcine skin was weighed accurately and cut into fine pieces. Minced skin tissue along with adhesive tape and cyanoacrylate tape samples were placed into vials. The first adhesive strip was analysed separately as this would represent unabsorbed materials on the skin surface whereas tapes 2-5, 6-10 and 11-15 were pooled together for analysis (Nagelreitera *et al.*, 2015). 10 ml of methanol was added to all the vials and samples were sonicated for 30 min. After sonication (Transonic UK), the samples were centrifuged for 20 min at 400 rpm (Eppendorf centrifuge 5702, UK). The supernatant obtained after centrifugation was collected and analysed for amount of TSN recovered using HPLC (Section 2.2.1.1).

#### 3.3.3.9.3 *In vitro* comparison study of follicular penetration using differential stripping technique

The aim of the present study was to investigate the hypothesis that in excised skin separated from cartilage and subcutaneous fats, the hair follicle reservoir is significantly reduced compared to intact skin. Therefore, drug retention data in both excised and intact full thickness porcine ear skin was compared using the differential adhesive tape stripping technique. GP-SLN formulation (GP5-2) was selected to compare the drug retention between intact and excised porcine ear skin.

To study skin retention of TSN in intact, unsliced porcine ear skin, an area of 4x4 cm<sup>2</sup> was marked in the inner side of the ear using permanent marker, and a plastic cap having an open compartment on both sides was used to form donor cell sample reservoir during the experiment (Figure 3.1). Subsequently, 1 ml of the SLN dispersion (equivalent to 10 mg/g of TSN concentration) was applied. After 24 h of contact time, excess formulation was removed from skin and the treated area was subjected to differential adhesive stripping (Section 3.3.3.9.2).

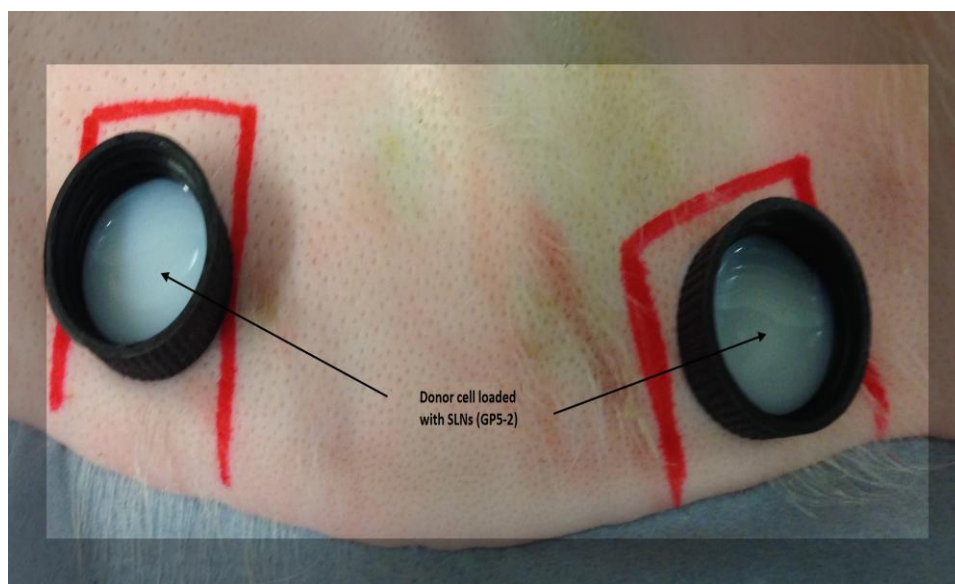


Figure 3.1 Experimental set up showing TSN skin retention study using unsliced full thickness porcine ear skin by GP-SLNs (GP5-2).

Similarly, excised full thickness porcine skin was prepared by cutting a  $4 \times 4 \text{ cm}^2$  area of porcine ear skin by removing cartilage and other subcutaneous fat. Skin samples were mounted on Franz cells to perform the diffusion experiment. After 24 h, samples were subjected to the differential stripping technique. Samples from both intact and excised porcine ear skin were analysed using HPLC to quantify the amount of TSN recovered from skin and compared for follicular penetration. Experiments were repeated in triplicate and data obtained was represented as mean  $\pm$  SD.

#### 3.3.3.10 Statistical analysis

All the data obtained from physicochemical characterisations were performed in triplicate. Mean values were tested using one way analysis of variance (ANOVA) using GraphPad Prism 6 software and differences were considered to be statistically significant when  $p < 0.05$ .

### 3.4 Results and Discussion

#### 3.4.1 Solubility studies of triclosan in buffer

SLS, an anionic surfactant, possesses skin penetration enhancing properties and increases drug penetration into the skin by increasing the fluidity of epidermal lipids (Leveque *et al.*, 1993). Many studies also include SLS in the receiver medium in order to increased solubility of lipophilic drug and to maintain sink conditions throughout the diffusion experiment (Shumaia *et al.*, 2014). This is due to the formation of micelles with hydrophobic molecules. A micelle is a group of surfactant aggregates, which in aqueous solution forms a hydrophilic head with surrounding solvent and hydrophobic tails in the micelle centre. Micelle formation occurs due to presence of SLS above its CMC i.e. the concentration above which micelles start to form, which is reported as 8.1 mM at 25°C (Aguiar *et al.*, 2003; Elisabet *et al.*, 2005). Solubility data obtained after 24 h shows that TSN solubility increases with increasing SLS concentrations from 50 mM, 100 mM, 150 mM, 200 mM and 250 mM (Table 3.2).

Table 3.2 Solubility profile of triclosan in buffer (Mean  $\pm$  SD, n = 3).

SLS concentration (mM)	Solubility (mg/ml)
50	2.61 $\pm$ 0.74
100	3.73 $\pm$ 0.52
150	5.25 $\pm$ 0.81
200	6.27 $\pm$ 0.35
250	6.39 $\pm$ 0.23

Priyanka and Sathali (2012) reported the ability of SLS (0.5 % w/w) to increase the release of montelukast sodium into dissolution media from SLNs. Another study reported by

Rahman *et al.*, (2009) showed increase in rate of curcumin release with increase in concentration of SLS into dissolution media with results indicated maximum increase was found in water containing 2 % w/v of SLS. For most poorly water soluble drugs addition of surfactants in diffusion media improves the solubility of drugs significantly, which is necessary to maintain sink conditions during diffusion experiment. Hence, based on the results obtained and to prevent formation of excess air bubbles, 150 mM concentration of 1 % w/v SLS was selected for the diffusion studies.

### 3.4.2 Preparation and optimisation of solid lipid nanoparticles

A very simple, economical and reproducible method was used for the preparation of SLNs (Chen *et al.*, 2010; Fang *et al.*, 2008). TSN-loaded SLN formulations were prepared using GB and GP as core matrices at different concentrations of 3, 5, 7.5 and 10 % (w/w). These lipid carrier systems were stabilised by T80 and TP in different ratios, i.e. 1:1, 2:1, 3:1 and 4:1 respectively (Table 3.1).

#### 3.4.2.1 Effect of homogenisation speed and time

To optimise homogenisation speed and time, GB-SLNs (GB5-2) and GP-SLNs (GP5-2) were prepared and the effect of different homogenisation speed and time on the mean particle size was determined. It was observed that when homogenisation speed was increased from 4000 to 10,000 rpm, the mean particle size decreased from  $520 \pm 10.34$  nm to  $193 \pm 17.3$  nm for GB5-2, while in case of GP5-2, mean particle size decreased from  $584 \pm 19.4$  to  $173 \pm 12.5$  nm (Figure 3.2). Therefore, 10,000 rpm was selected for obtaining SLNs for both GB and GP lipids.

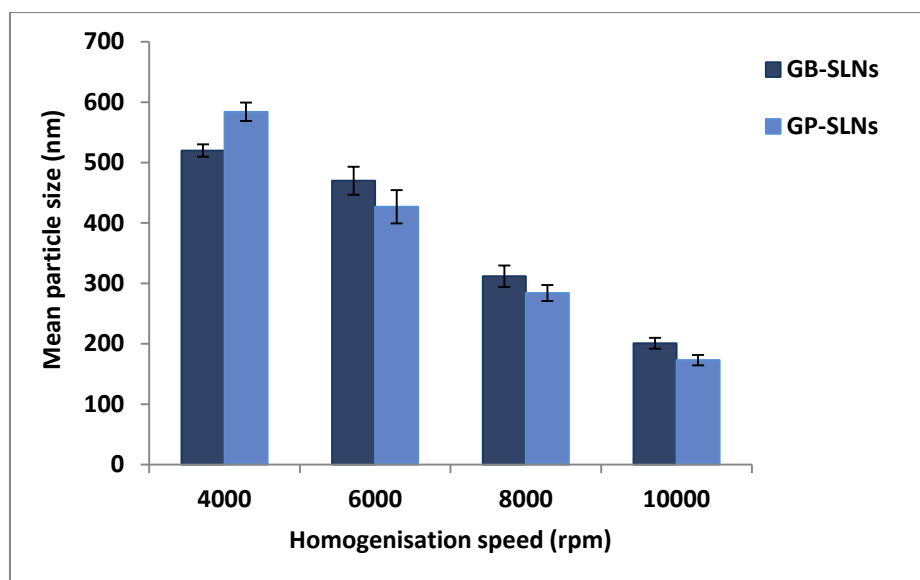


Figure 3.2 Effect of homogenisation speed on mean particle size of GB-SLNs (GB5-2) and GP-SLNs (GP5-2) (Mean  $\pm$  SD, n = 3).

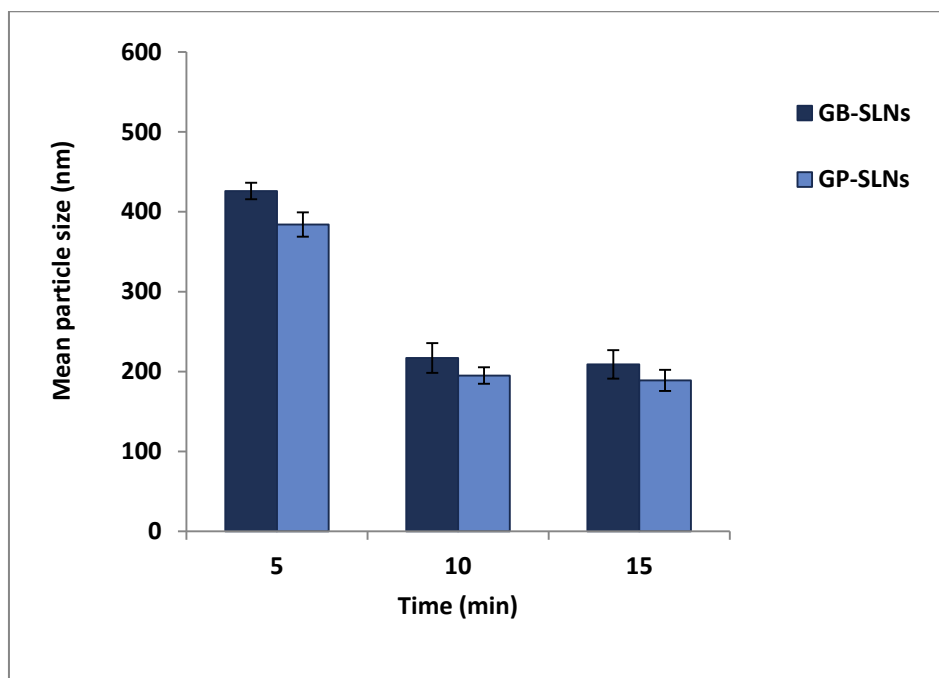


Figure 3.3 Effect of homogenisation time on mean particle size of GB-SLNs (GB5-2) and GP-SLNs (GP5-2) (Mean  $\pm$  SD, n = 3).

The influence of homogenisation time on the mean particle size of SLNs was studied by homogenising SLNs for 5, 10 and 15 min. Figure 3.3 shows the decrease in particle size for

both GB-SLNs and GP-SLNs when homogenisation time increased from 5 min to 10 min, but when homogenisation time increased to 15 min there was no further decrease in particle size for both GB-SLNs and GP-SLNs. The reason may be that each system has its own optimum homogenisation speed and time during which SLNs can undergo particle size reduction and beyond which, exposure of SLNs to excess cavitation forces lead to collision and therefore aggregation (Mehnert *et al.*, 2001a). Thus optimised parameters selected for preparation of SLNs was homogenisation at 10,000 rpm for 10 min.

#### 3.4.2.2 Effect of lipid and drug ratio

Increase in lipid concentrations with respect to drug for both lipids (GB and GP) causes an increase in % DEE (Table 3.3). As the lipid concentration was increased from 3 to 5 % (w/w), there was an increase in % DEE for both GB-SLNs and GP-SLNs, which subsequently decreased with further increases in lipid concentrations up to 10 % (w/w).

Table 3.3 Effect of concentration of lipid on percent drug entrapment efficiency of SLNs (Mean  $\pm$  SD, n = 3).

Lipid: drug	% DEE	
	GB-SLNs	GP-SLNs
3: 1	76.23 $\pm$ 1.63	79.34 $\pm$ 1.86
5: 1	83.61 $\pm$ 2.47	87.27 $\pm$ 1.48
7.5: 1	77.56 $\pm$ 1.06	75.12 $\pm$ 1.94
10: 1	68.23 $\pm$ 2.18	65.86 $\pm$ 2.4

This might be because during crystallisation of the lipids, a partial expulsion of drug occurs on particle surface. Furthermore, the higher viscosity at the interface produced by high lipid concentrations may cause a decrease in diffusion and hence few lipid molecules will be

carried into the aqueous phase and therefore reduce the entrapment of drug (Abdelbary and Fahmy, 2009).

#### 3.4.2.3 Effect of surfactant and cosurfactant ratio

The type of surfactant and its concentration has a great impact on the particle size distribution and stability of SLNs (Han *et al.*, 2008). Low levels of surfactant can result in particle aggregation leading to an increase in particle size, however the use of excess amounts of surfactant should be avoided to prevent a decrease in % DEE, burst release, toxicity and any irritant effects. Literature study showed T80 as commonly used nonionic stabiliser for SLN formulations for various drug delivery systems (Salminen *et al.*, 2014; Shah *et al.*, 2015; Soares *et al.*, 2013). The choice of surfactant used in preparation of SLNs has great influence on the physical stability of the nanoparticles, extent of drug dissolution and drug permeability into skin. It can also contribute to the safety of SLNs when administered to the body (Karn-orachaia *et al.*, 2016). For SLNs prepared for targeted drug delivery system, surface modification of nanoparticles is required (Müller *et al.*, 1995). Polymeric nanoparticles coated with T80 are able to deliver dalargin, the leu-enkephalin analogue through blood brain barrier (Alyautdin *et al.*, 1998). Another study reported ability of T80 to prevent the loss of drug after filtration of SLNs by enhancing the emulsification of lipophilic drug compounds (Rassua *et al.*, 2015). Addition of a cosurfactant to the surfactant in formulations was reported to improve dispersibility and solubility in formulation (Chen, 2008). TP has included as a cosurfactant to improve stability of formulations (Prajapati *et al.*, 2013; Salunkhe *et al.*, 2013).



Table 3.4 Effect of different ratios of surfactant and cosurfactant on mean particle size and percent drug entrapment efficiency of SLNs (Mean  $\pm$  SD, n = 3).

T80: TP	Mean particle size (nm)		% DEE	
	GB-SLN <sub>s</sub>	GP-SLN <sub>s</sub>	GB-SLN <sub>s</sub>	GP-SLN <sub>s</sub>
1: 1	315 $\pm$ 1.33	286 $\pm$ 1.27	81.3 $\pm$ 0.79	84.5 $\pm$ 1.53
2: 1	217 $\pm$ 2.12	184 $\pm$ 1.78	79.6 $\pm$ 1.38	81.7 $\pm$ 1.04
3: 1	196 $\pm$ 0.93	171 $\pm$ 2.04	68.4 $\pm$ 1.73	73.5 $\pm$ 2.18
4: 1	163 $\pm$ 1.64	154 $\pm$ 2.36	60.1 $\pm$ 1.28	66.2 $\pm$ 1.57

On increasing the ratio of surfactant and cosurfactant from 1:1 to 4:1, the mean particle size of GB-SLN<sub>s</sub> decreased from 315  $\pm$  1.33 nm to 163  $\pm$  1.64 nm and the mean particle size of GP-SLN<sub>s</sub> decreased from 286  $\pm$  1.27 nm to 154  $\pm$  2.36 nm (Table 3.4). This decrease in particle size is due to an effective reduction in interfacial tension between aqueous and lipid phases leading to formation of smaller particles ( Liu *et al.*, 2007). Hence addition of cosurfactant helps reduce the amount of surfactant required (Kreilgaard *et al.*, 2000) and it further reduces the interfacial tension and increase the fluidity of interface (Tenjarla, 1999). Higher surfactant concentrations stabilise particles by forming a steric barrier on the particle surface thereby preventing their coalescence.

A similar effect was observed for % DEE of TSN into SLNs, which decreased with an increase in ratio of surfactant and cosurfactant (Table 3.4). This can be explained by the partition phenomenon. High surfactant levels in the aqueous phase might increase partition of drug from internal lipid phase to the external aqueous phase, decreasing drug encapsulation (Rahman *et al.*, 2010).

### 3.4.3 Physicochemical characterisation

#### 3.4.3.1 Determination of particle size, zeta potential and percent drug entrapment efficiency

Prepared formulations were characterised based on their particle size, PDI, ZP, % DEE and results are shown in Table 3.5 and Table 3.6 respectively. Figure 3.4 shows a typical NTA image showing the particle size distribution of both GB-SLNs and GP-SLNs. The mean particle size of both lipid formulations ranged from  $178.38 \pm 12.45$  nm to  $942.17 \pm 6.35$  nm. The results clearly show an increase in particle size with increase in lipid concentration, which may be related to the viscosity of the samples, and a decrease in particle size with increasing surfactant concentration which might be due to reduction in interfacial tension between lipid and aqueous phases forming smaller, stable nanoparticles (Rahman *et al.*, 2010).

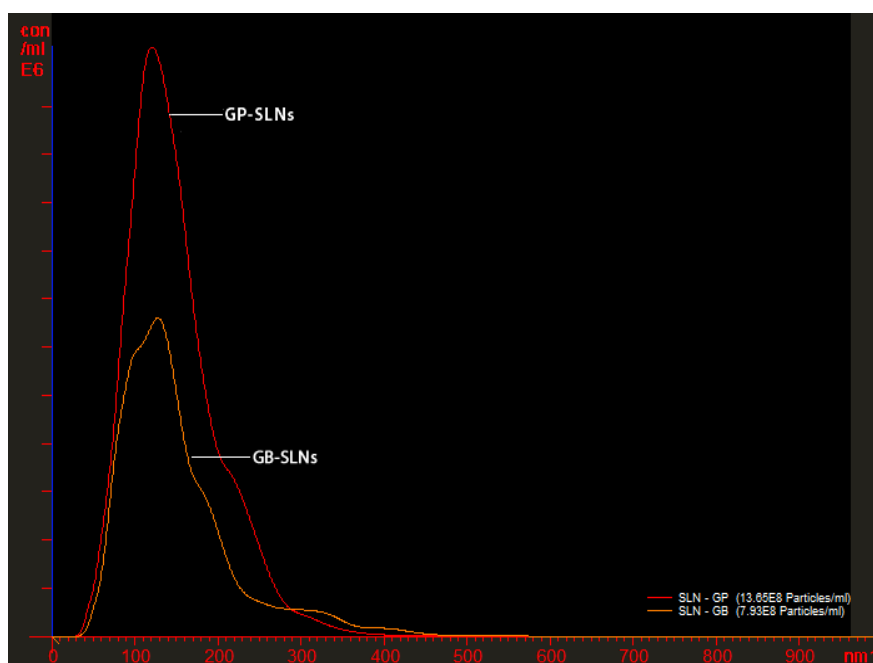


Figure 3.4 Particle size distributions of GB-SLNs and GP-SLNs using NTA system.

Table 3.5 Physicochemical characterisation of GB-SLNs (Mean  $\pm$  SD, n = 3).

Formulation Batch	Particle size (nm)	PDI	% DEE	ZP (mV)
GB3-1	350.23 $\pm$ 2.36	0.46	78.21 $\pm$ 0.82	-19.2 $\pm$ 1.2
GB3-2	224.15 $\pm$ 5.28	0.57	77.17 $\pm$ 0.26	-20.3 $\pm$ 0.9
GB3-3	198.03 $\pm$ 1.62	0.82	73.84 $\pm$ 2.17	-27.7 $\pm$ 1.5
GB3-4	191.37 $\pm$ 5.58	0.71	69.10 $\pm$ 1.31	-29.3 $\pm$ 2.1
GB5-1	419.29 $\pm$ 3.47	0.63	80.62 $\pm$ 0.88	-24.8 $\pm$ 2.5
GB5-2	231.72 $\pm$ 6.52	0.72	78.28 $\pm$ 0.24	-25.9 $\pm$ 0.6
GB5-3	201.42 $\pm$ 2.61	0.76	75.32 $\pm$ 0.56	-28.8 $\pm$ 0.9
GB5-4	195.04 $\pm$ 7.72	0.77	74.14 $\pm$ 0.16	-30.1 $\pm$ 1.4
GB7.5-1	729.43 $\pm$ 2.63	0.84	73.45 $\pm$ 0.68	-27.9 $\pm$ 1.6
GB7.5-2	683.91 $\pm$ 8.69	0.81	71.23 $\pm$ 0.91	-28.4 $\pm$ 1.1
GB7.5-3	604.38 $\pm$ 9.81	0.62	70.47 $\pm$ 0.39	-31.3 $\pm$ 2.8
GB7.5-4	592.12 $\pm$ 11.03	0.72	69.52 $\pm$ 0.90	-34.7 $\pm$ 1.9
GB10-1	942.17 $\pm$ 6.35	0.64	67.28 $\pm$ 0.52	-32.1 $\pm$ 1.4
GB10-2	904.63 $\pm$ 8.72	0.85	67.26 $\pm$ 0.39	-33.5 $\pm$ 2.5
GB10-3	839.59 $\pm$ 3.43	0.77	66.37 $\pm$ 1.29	-36.5 $\pm$ 1.7
GB10-4	821.82 $\pm$ 9.86	0.82	65.21 $\pm$ 1.68	-35.2 $\pm$ 1.3

Table 3.6 Physicochemical characterisation of GP-SLNs (Mean  $\pm$  SD, n = 3).

Formulation Batch	Particle size (nm)	PDI	% DEE	ZP (mV)
GP3-1	420.11 $\pm$ 5.34	0.43	84.12 $\pm$ 1.28	-21.8 $\pm$ 0.8
GP3-2	201.56 $\pm$ 9.23	0.51	82.19 $\pm$ 1.42	-24.4 $\pm$ 1.2
GP3-3	185.38 $\pm$ 13.45	0.79	79.08 $\pm$ 1.03	-26.3 $\pm$ 1.6
GP3-4	178.38 $\pm$ 12.45	0.81	76.19 $\pm$ 0.98	-25.8 $\pm$ 1.1
GP5-1	389.07 $\pm$ 15.23	0.61	81.29 $\pm$ 1.29	-27.2 $\pm$ 0.9
GP5-2	192.23 $\pm$ 6.39	0.59	77.26 $\pm$ 2.17	-29.9 $\pm$ 2.1
GP5-3	184.78 $\pm$ 18.43	0.72	75.03 $\pm$ 2.53	-24.2 $\pm$ 2.6
GP5-4	179.13 $\pm$ 8.39	0.65	73.28 $\pm$ 2.81	-24.9 $\pm$ 1.5
GP7.5-1	621.92 $\pm$ 12.57	0.73	76.21 $\pm$ 1.38	-31.6 $\pm$ 1.3
GP7.5-2	597.39 $\pm$ 23.53	0.81	73.81 $\pm$ 1.44	-29.4 $\pm$ 1.7
GP7.5-3	562.82 $\pm$ 1.54	0.56	70.42 $\pm$ 1.72	-30.1 $\pm$ 2.2
GP7.5-4	538.03 $\pm$ 3.62	0.61	68.32 $\pm$ 1.03	-32.1 $\pm$ 1.8
GP10-1	843.28 $\pm$ 17.52	0.69	70.17 $\pm$ 1.28	-34.5 $\pm$ 2.9
GP10-2	829.31 $\pm$ 13.56	0.72	69.11 $\pm$ 2.16	-30.6 $\pm$ 2.3
GP10-3	792.85 $\pm$ 26.39	0.78	68.25 $\pm$ 2.62	-28.4 $\pm$ 1.2
GP10-4	753.17 $\pm$ 21.04	0.84	65.57 $\pm$ 2.84	-29.3 $\pm$ 1.9

SLNs formed using GB were larger in size than corresponding GP formulations (Table 3.5 and Table 3.6). This may be due to differences in chain lengths and viscosities of the lipids. GB contains glycerol esters of behenic acid (C<sub>22</sub>), where the main fatty acid is behenic acid (> 85 %) along with other fatty acids (C<sub>16</sub>-C<sub>20</sub>). GP is composed of palmitic acid (C<sub>16</sub>) and stearic acid (C<sub>18</sub>) >90 %. A higher viscosity (Section 2.1.1) and longer hydrocarbon chain length may affect packing of GB resulting in a larger particle size compared to GP lipid.

ZP indicates the degree of charge present on suspended particles in dispersion. A suitably high value of ZP (positive or negative) confers stability because the particles resist aggregation. As depicted in Tables 3.5 and Table 3.6, the ZP of all formulations were negative, ranging from -19.2 mV to -36.5 mV indicating relatively good stability and dispersion quality (Essa *et al.*, 2011). The ZP values obtained for both GB-SLNs and GP-SLNs are similar to those mentioned in literature (Negi *et al.*, 2014; Padhye and Nagarsenker, 2013). The % DEE for all SLN formulations was high, ranging from 65.31 ± 1.24 % to 85.16 ± 2.19 % (Table 3.5 and Table 3.6). % DEE is dependent upon the nature of the lipids. For example, crystalline lipids (e.g. monoacid triglycerides) form a perfect lattice and this can lead to drug expulsion (Westesen *et al.*, 1997). However more complex lipids as GB and GP, being the mixture of mono, di and triglycerides form less perfect crystals with many imperfections offering more space to accommodate drugs (Müller *et al.*, 2000).

Hence, based on the results obtained for mean particle size, PDI, % DEE and also considering minimum use of surfactant mixture to avoid skin irritation for topical application, SLN formulations prepared with 3 % and 5 % w/w GB and GP lipids with T80 and TP (2:1) as S<sub>mix</sub> were selected for further characterisation and *in vitro* skin permeation studies.

### 3.4.3.2 Thermal analysis of solid lipid nanoparticles

DSC was used to investigate the melting behavior of SLNs. Figure 3.5 and Figure 3.6 represent DSC curves of pure TSN, GB and GP lipids, PM of drug with both lipids and TSN-loaded SLNs respectively. TSN has a relatively sharp melting endotherm at 61°C indicating its crystallinity. An endothermic peak for the drug was detected for physical mixtures at 56.5°C and 56.2°C for mixtures with GB and GP lipids respectively, which may reflect an interaction with lipids or may be a change in the crystal form. The lipids have peaks at 76.8°C and 57°C for GB and GP respectively, representing their melting points, but in the PM the endothermic peaks were detected at 72°C and 52°C for GB and GP lipids respectively.

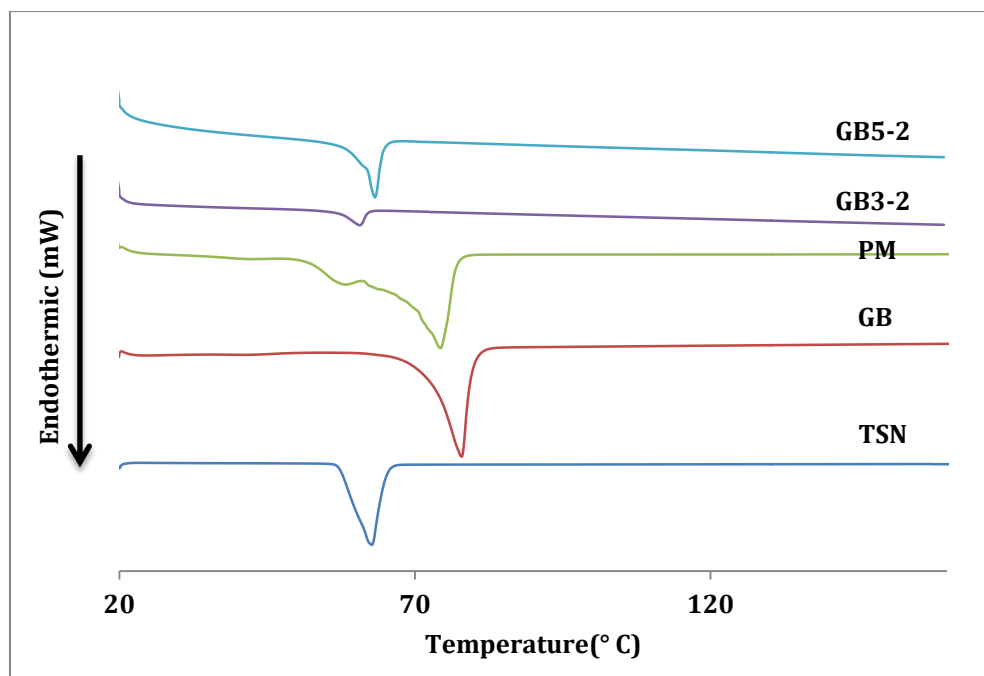


Figure 3.5 DSC thermogram of TSN, GB, physical mixture of GB and TSN, TSN-loaded GB-SLNs (GB3-2, GB5-2).

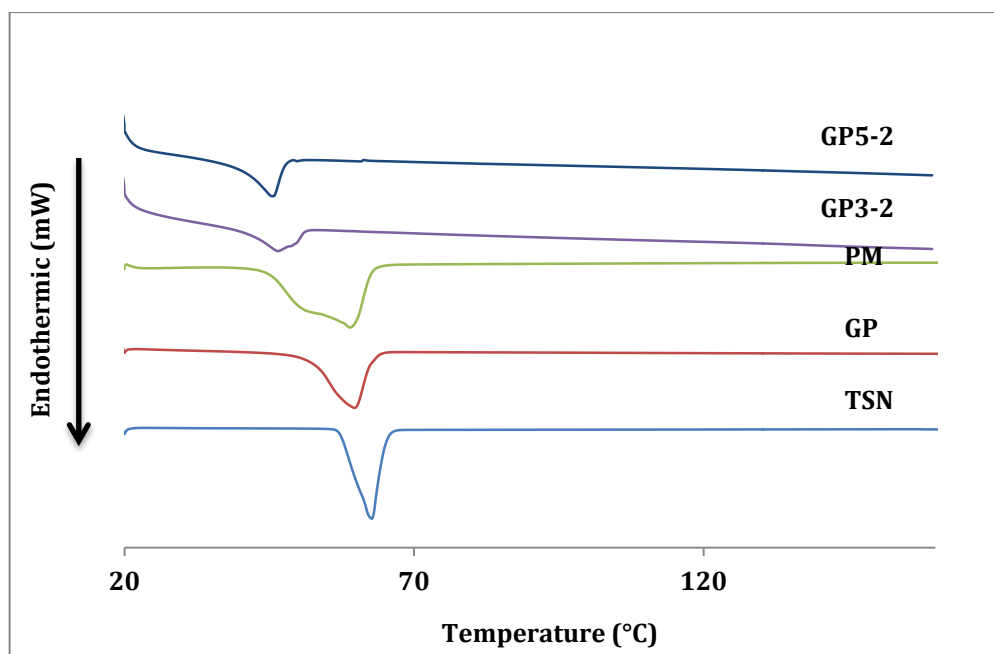


Figure 3.6 DSC thermogram of TSN, GP, physical mixture of GP and TSN, TSN-loaded GP-SLNs (GP3-2, GP5-2).

The melting point depression could be due to polymorphism in the glycerides as they crystallise in different subcell arrangements such as hexagonal, orthorhombic and triclinic. Glycerides display polymorphism with three or more individual forms, including  $\alpha$ ,  $\beta'$  and  $\beta_1$  modifications (Fouad *et al.*, 2011). For TSN-loaded SLNs of both lipids, GB and GP have a broad endothermic peak at 64°C and 45°C for GB and GP respectively. The reduction in melting point for both the lipid formulations is generally due to the nanometric size of the particles, having a specific surface area (Nerella *et al.*, 2014) indicating a reduction in lipid crystallinity. The melting endotherm of TSN was absent in both GB-SLNs and GP-SLNs, which show good homogenous dispersion of TSN in lipid matrix after SLN formation (Negi *et al.*, 2014; Shah *et al.*, 2015).

### 3.4.3.3 Powder X-ray diffraction analysis

XRD is ideally suited for characterisation and identification of polycrystalline forms (Omar, 2013). To study the effect of different glycerides on the crystallinity of TSN in formulations, XRD analysis was carried out on TSN, GB and GP lipids, TSN-loaded GB-SLNs and GP-SLNs.

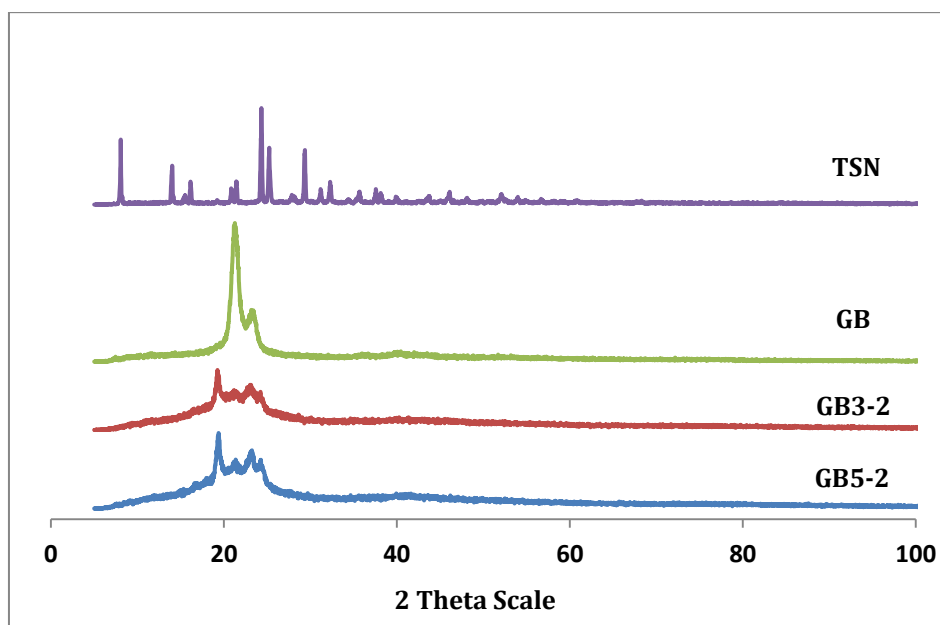


Figure 3.7 XRD pattern showing TSN, GB, TSN-loaded GB-SLNs (GB3-2, GB5-2).

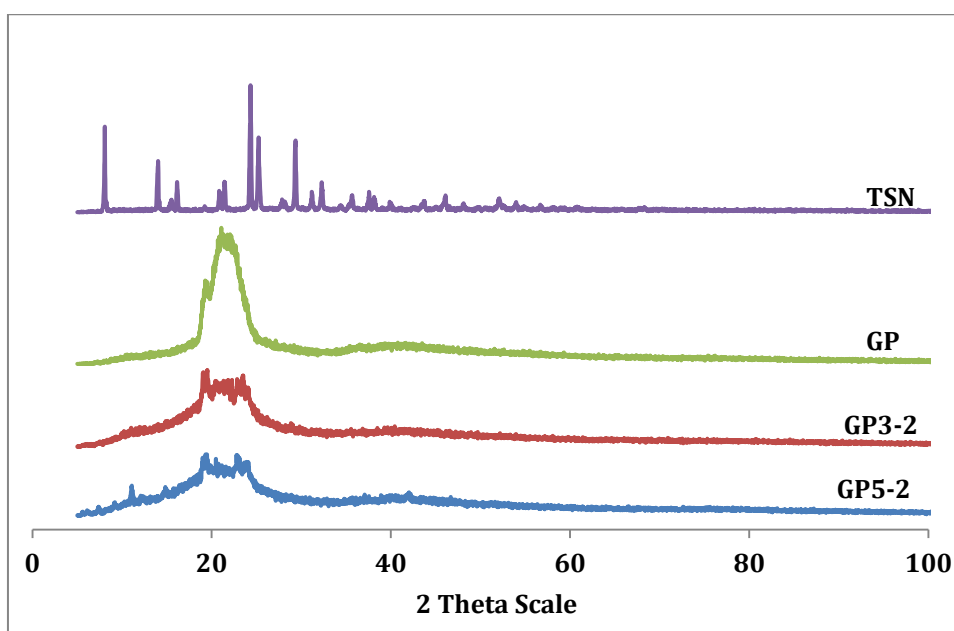


Figure 3.8 XRD pattern showing TSN, GP, TSN-loaded GP-SLNs (GP3-2, GP5-2).



TSN is a crystalline material having major diffraction peaks at  $2\theta$  scattered angles 8.2, 24.4 and 25.4 respectively (Celebioglu *et al.*, 2013). The XRD of GB confirms its semicrystalline nature (Figure 3.7) with a sharp peak at  $2\theta$  angles of 21.18, 23.38 while GP shows peaks at  $2\theta$  angles of 19.5, 21.5 and 23.5 (Figure 3.8). The values are similar to those reported for the lipids in the literature (Bhagwat *et al.*, 2009; Josea *et al.*, 2014). However, a reduction in intensity of TSN peak for both GB-SLNs and GP-SLNs indicates a reduction in crystallinity of TSN, which might be due to encapsulation of the drug in the lipid matrix. Similar results were observed for lipid based nanocarriers prepared using GB and GP lipids, which showed low levels of crystalline decitabine in the final formulation thus confirming a decrease in crystallinity of drug due to molecular dispersion into lipid matrix (Yub *et al.*, 2014). Another study reported the loss of crystallinity of clotrimazole after incorporation into SLNs prepared by GB indicating solubility of drug into lipid matrix and conversion of drug into amorphous forms (Das *et al.*, 2012). XRD results of SLN formulations were in agreement with the DSC analysis (Section 3.4.3.2).

#### 3.4.3.4 Transmission electron microscopy

TEM images of TSN loaded SLNs are shown in Figure 3.9, indicating that the SLNs in aqueous dispersion have a spherical shape and were in the size range 100 nm to 250 nm. This supported the particle size distribution data from NTA (Section 3.4.3.1) and similar results reported for TSN-loaded polymeric nanoparticles (Domínguez-Delgado *et al.*, 2011). GB-SLNs of quercetin was evaluated for brain delivery were also spherical particles in nanometer range (Dhawan *et al.*, 2011). TEM images (Figure 3.9 B) of SLNs showed distribution of drug in lipid rich matrix, which was observed by DSC and XRD analysis of formulations.

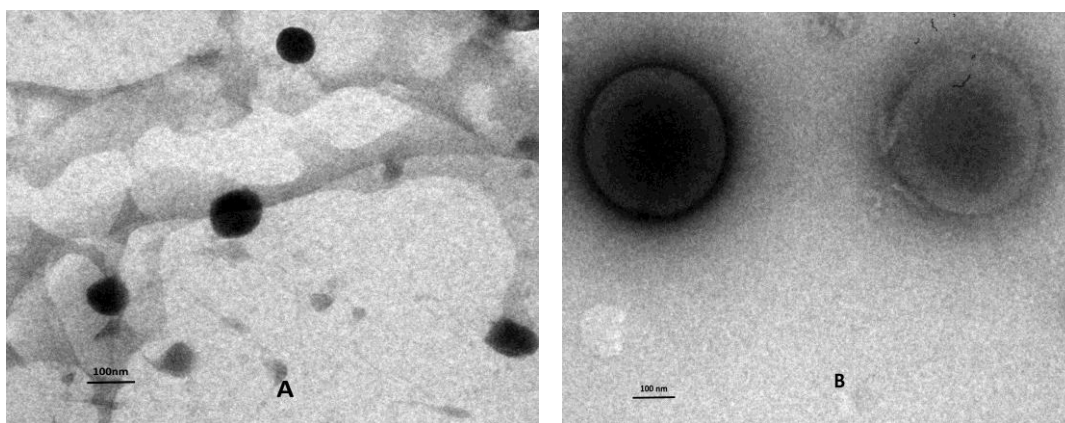


Figure 3.9 TEM images (10,000 x) of TSN loaded SLNs.

### 3.4.3.5 Fourier Transform infrared spectrometry

FTIR spectrometry was used to investigate interactions between drug and lipids during formulation of SLNs. The FTIR spectra of TSN, GB and GP, TSN loaded GB-SLNs and GP-SLNs are shown in Figure 3.10 and Figure 3.11.

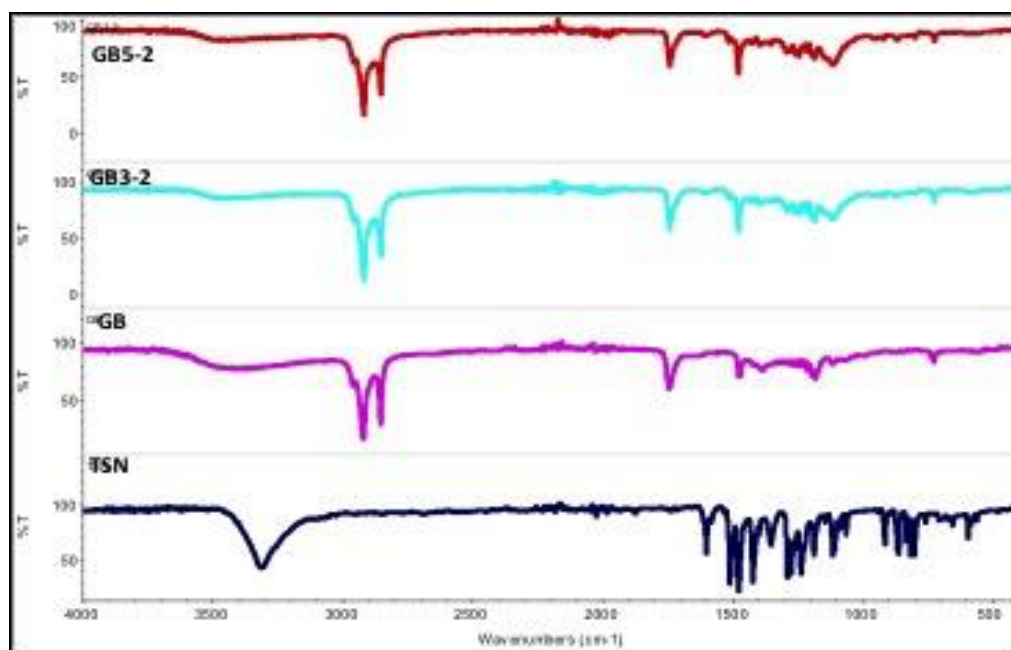


Figure 3.10 FTIR spectrums of TSN, GB and TSN-loaded GB-SLNs (GB3-2, GB5-2).

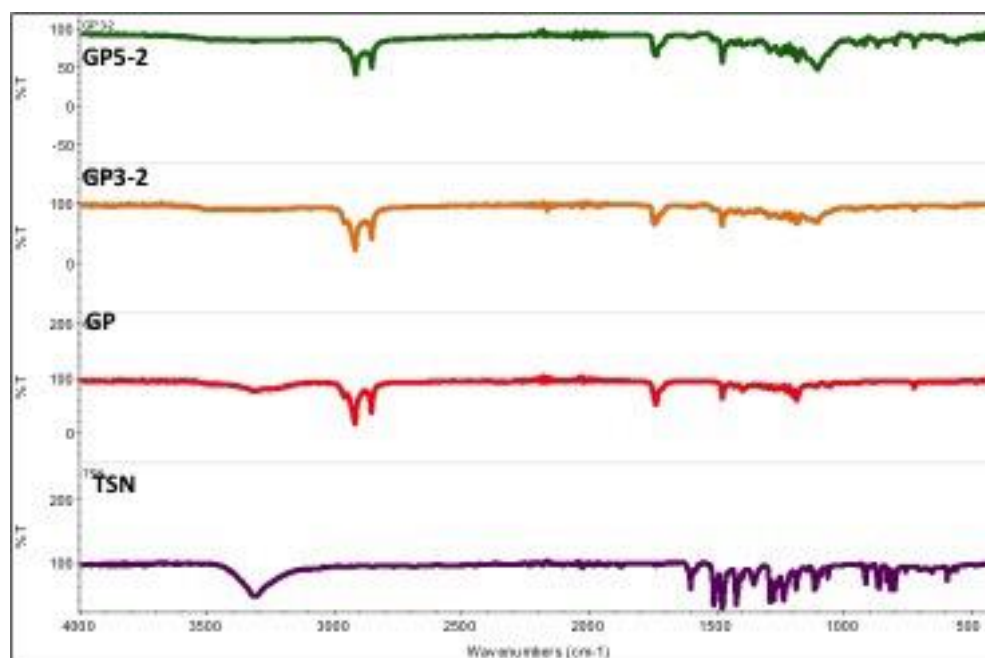


Figure 3.11 FTIR spectrums of TSN, GP and TSN-loaded GP-SLNs (GP3-2, GP5-2).

The FTIR spectra of pure TSN shows strong absorption of halogenated hydrocarbons arising from stretching vibrations of the carbon-halogen bond for the  $\text{CH}_2\text{-Cl}$  group in the  $1300\text{--}1150\text{ cm}^{-1}$  region. The strong absorption bands result from the out-of-plane bending of the ring C-H bonds and in-plane bending bands appeared in the  $1300\text{--}1000\text{ cm}^{-1}$  region. Skeletal vibrations, involving C-C stretching within the ring, are evident in the  $1610\text{--}1585\text{ cm}^{-1}$  and  $1500\text{--}1400\text{ cm}^{-1}$  regions. The FTIR spectra of both the solid lipids, GB and GP, revealed the presence of an absorption band at  $2849$  and  $2917\text{ cm}^{-1}$  due to symmetric and asymmetric C-H stretching; wavenumber  $1702\text{ cm}^{-1}$  depicts C-O stretching and  $2400\text{--}3400\text{ cm}^{-1}$  depicts O-H stretching (Kelidari *et al.*, 2015). However, in the FTIR spectra of TSN loaded GB-SLNs and GP-SLNs the characteristic peaks of TSN are absent. This is due to the overlapping of the characteristics peaks of TSN with other constituents, thus the FTIR results did not suggest any chemical interaction of ingredients (Kumar and Randhawa, 2015; Orhan, 2012).

#### 3.4.3.6 Stability study

Selected batches of GB-SLNs and GP-SLNs were stored in glass vials and placed in a stability cabinet at room temperature ( $20 \pm 2^\circ\text{C}$ ) and under stressed conditions in humidity chamber ( $40^\circ\text{C}/75\% \text{ RH}$ ). The effect of time and storage conditions on the mean particle size, PDI and ZP of SLNs are presented in Table 3.7 and Table 3.8. Results showed no significant difference ( $p>0.05$ ) in PDI and ZP for GB-SLN and GP-SLN formulations under both storage conditions. The particle size of SLNs remained almost stable, with only slight changes in particle size, indicating good stability over room temperature. Study reported by Neupanea *et al.*, (2014) for decitabine lipid nanocarriers prepared with GB and GP as solid lipids, have also shown no significant difference between particle sizes of prepared SLNs after 45 days storage at room temperature.

In case of SLN formulations stored at  $40^\circ\text{C}$  had shown increase in particle size for both GB and GP lipid formulations. Particle size of GP-SLNs and GB-SLNs has significant increase ( $p<0.05$ ) after 60 days of storage, which has been shown by highlighting the data represented in Table 3.6 and Table 3.7 respectively. The reason of increase in particle size might be due to heating of lipids at high temperature for constant long period of time, which disturbs the crystalline structure of lipid carrier (Ghaffari *et al.*, 2011). Study reported by Ruktanonchai *et al.*, (2009) for gamma-oryzanol SLNs have shown significant increase in particle size at storage temperature of  $45^\circ\text{C}$ .

Table 3.7 Particle size, PDI and zeta potential of GP-SLN formulations stored at room temperature and accelerated humidity conditions (Mean  $\pm$  SD, n=3).

Duration	Storage conditions	Formulations	Particle size (nm)	PDI	ZP (mV)
Day 1	Room	GP3-2	193.8 $\pm$ 8.3	0.62 $\pm$ 0.05	-24.4 $\pm$ 0.8
		GP5-2	169.3 $\pm$ 6.2	0.87 $\pm$ 0.04	-29.9 $\pm$ 1.2
	Humidity	GP3-2	193.8 $\pm$ 8.3	0.62 $\pm$ 0.05	-24.4 $\pm$ 0.8
		GP5-2	169.3 $\pm$ 6.2	0.87 $\pm$ 0.04	-29.9 $\pm$ 1.2
Day 30	Room	GP3-2	194.3 $\pm$ 9.5	0.73 $\pm$ 0.03	-29.0 $\pm$ 0.4
		GP5-2	170.6 $\pm$ 7.3	0.89 $\pm$ 0.08	-30.3 $\pm$ 0.9
	Humidity	GP3-2	200.3 $\pm$ 8.4	0.74 $\pm$ 0.05	-29.9 $\pm$ 1.3
		GP5-2	168.9 $\pm$ 6.9	0.85 $\pm$ 0.03	-33.8 $\pm$ 1.8
Day 60	Room	GP3-2	198.2 $\pm$ 9.8	0.83 $\pm$ 0.08	-32.7 $\pm$ 0.7
		GP5-2	179.6 $\pm$ 8.1	0.96 $\pm$ 0.09	-29.4 $\pm$ 0.9
	Humidity	GP3-2	203.2 $\pm$ 8.6	1.24 $\pm$ 0.03	-31.7 $\pm$ 1.9
		GP5-2	174.8 $\pm$ 7.2	1.06 $\pm$ 0.06	-34.9 $\pm$ 2.1
Day 90	Room	GP3-2	216.2 $\pm$ 10.3	0.86 $\pm$ 0.04	-22.6 $\pm$ 0.6
		GP5-2	184.7 $\pm$ 8.6	0.98 $\pm$ 0.06	-28.7 $\pm$ 0.8
	Humidity	GP3-2	220.5 $\pm$ 9.1	1.30 $\pm$ 0.07	-32.4 $\pm$ 2.5
		GP5-2	209.7 $\pm$ 7.8	1.25 $\pm$ 0.05	-34.9 $\pm$ 2.7

Table 3.8 Particle size, PDI and zeta potential of GB-SLN formulations stored at room temperature and accelerated humidity conditions (Mean  $\pm$  SD, n=3).

Duration	Storage conditions	Formulations	Particle size (nm)	PDI	ZP (mV)
Day 1	Room	GB3-2	175.2 $\pm$ 9.2	0.86 $\pm$ 0.03	-20.3 $\pm$ 0.9
		GB5-2	180.1 $\pm$ 7.3	0.89 $\pm$ 0.01	-25.9 $\pm$ 0.6
	Humidity	GB3-2	175.2 $\pm$ 9.2	0.86 $\pm$ 0.03	-20.3 $\pm$ 0.9
		GB5-2	180.1 $\pm$ 7.3	0.89 $\pm$ 0.01	-25.9 $\pm$ 0.6
Day 30	Room	GB3-2	175.3 $\pm$ 10.6	0.86 $\pm$ 0.02	-25.3 $\pm$ 0.6
		GB5-2	188.2 $\pm$ 8.4	0.61 $\pm$ 0.07	-29.1 $\pm$ 0.5
	Humidity	GB3-2	180.3 $\pm$ 10.2	0.93 $\pm$ 0.02	-26.8 $\pm$ 1.2
		GB5-2	195.6 $\pm$ 7.9	0.95 $\pm$ 0.04	-30.2 $\pm$ 1.5
Day 60	Room	GB3-2	180.2 $\pm$ 10.9	0.92 $\pm$ 0.01	-24.6 $\pm$ 0.5
		GB5-2	203.8 $\pm$ 9.3	0.68 $\pm$ 0.04	-26.5 $\pm$ 0.4
	Humidity	GB3-2	189.5 $\pm$ 11.4	1.02 $\pm$ 0.08	-29.4 $\pm$ 1.6
		GB5-2	198.6 $\pm$ 8.3	1.31 $\pm$ 0.04	-32.4 $\pm$ 1.8
Day 90	Room	GB3-2	188.9 $\pm$ 11.2	0.93 $\pm$ 0.03	-28.8 $\pm$ 0.8
		GB5-2	209.6 $\pm$ 9.7	0.72 $\pm$ 0.07	-25.5 $\pm$ 0.3
	Humidity	GB3-2	217.4 $\pm$ 11.6	1.34 $\pm$ 0.01	-32.8 $\pm$ 1.9
		GB5-2	228.1 $\pm$ 9.2	1.45 $\pm$ 0.04	-33.5 $\pm$ 2.3

### 3.4.3.7 Skin permeation study

#### 3.4.3.7.1 *In vitro* skin permeation studies

The influence of type and concentration of lipids and surfactant used, along with other physicochemical parameters on TSN permeation and retention within the skin were evaluated using *in vitro* skin permeation studies. Skin permeation studies were carried out using excised full thickness porcine ear skin with selected (GB3-2, GB5-2, GP3-2, GP5-2) formulations. A saturated aqueous solution of TSN was used as the control and the permeability coefficients and flux from formulations are summarised in Table 3.9. Skin permeation studies are relevant while studying topical drug delivery to ensure that formulations display minimum permeation through skin into the receiver medium and maximum skin deposition. In the present studies, the receiver medium was sampled at pre-determined time intervals up to 24 h to determine TSN permeation through skin.

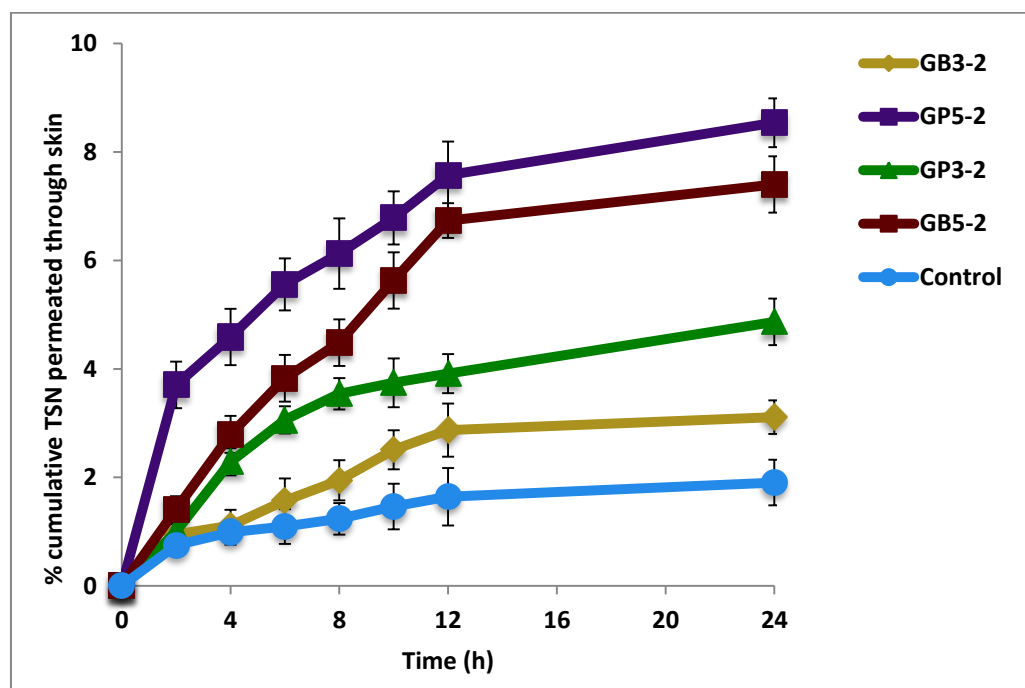


Figure 3.12 *In vitro* cumulative amount of triclosan permeated following 24 h topical application of SLN formulations and control solution through porcine ear skin (Mean  $\pm$  SD, n = 6).

SLNs formulations had a 4.47 fold higher rate of permeation of TSN in comparison with the TSN control solution (Figure 3.12). Similar results were reported for fluconazole GB-SLNs, which had a 1.73-fold higher fluconazole permeation compared to control solution (Gupta and Vyas, 2012). The increased skin delivery of drug can be attributed to the structure and physicochemical properties of SLNs. It has been shown that due to higher occlusive nature and increased skin hydration of SC, SLNs influences the percutaneous permeation of drugs present in the formulations (Gupta and Vyas, 2012; Schäfer-Korting *et al.*, 2007).

GP5-2 exhibited the highest percent cumulative TSN permeation ( $8.23 \pm 0.42$ ) followed by GB5-2 ( $7.64 \pm 0.35$ ), GP3-2 ( $4.37 \pm 0.24$ ) and GB3-2 ( $2.81 \pm 0.09$ ). GB5-2 and GP5-2 resulted in a 2-fold increase in TSN permeation compared to GB3-2 and GP3-2 formulations respectively, which might be due to small particle size, higher % DEE and more occlusive effect due to high content of lipids. Lee *et al.*, (2003) used TP as a cosurfactant to increase permeation of TSN into skin from hydrogel patches, thus allowing TSN accumulation into upper skin layers for localised action. Another studies have also reported increased drug localisation in skin by SLNs formulated using diethyltoluamide (Iscan *et al.*, 2005), glucocorticoids (Jensen *et al.*, 2011) and betamethasone 17-valerate (Zhang and Smith, 2011). Statistical analysis revealed a significant difference ( $P < 0.01$ ) between the steady-state flux values obtained for GB-SLNs and GP-SLNs (Table 3.9). The flux of SLNs formulations and control solutions was in the order of GP5-2 > GP3-2 > GB5-2 > GB3-2 > control.



Table 3.9 *In vitro* permeability parameters of TSN-loaded SLN formulations and control solution in porcine ear skin (Mean  $\pm$  SD, n = 6).

Formulation	Flux ( $J_{ss}$ ) $\mu\text{g}/\text{cm}^2/\text{h}$	Permeability coefficient ( $K_p$ ) $\times 10^{-5}$ cm/h
Control	0.086	0.86
GB3-2	0.202	2.02
GB5-2	0.245	2.45
GP3-2	0.279	2.79
GP5-2	0.536	5.36

#### 3.4.3.7.2 Quantification of triclosan in skin using differential stripping techniques

The amount of TSN retained within skin was determined by adhesive tape stripping method and cyanoacrylate biopsies. Differential stripping technique was used to quantify TSN level in different areas of the skin, including hair follicles, epidermis and dermis and the results are presented in Figure 3.13.

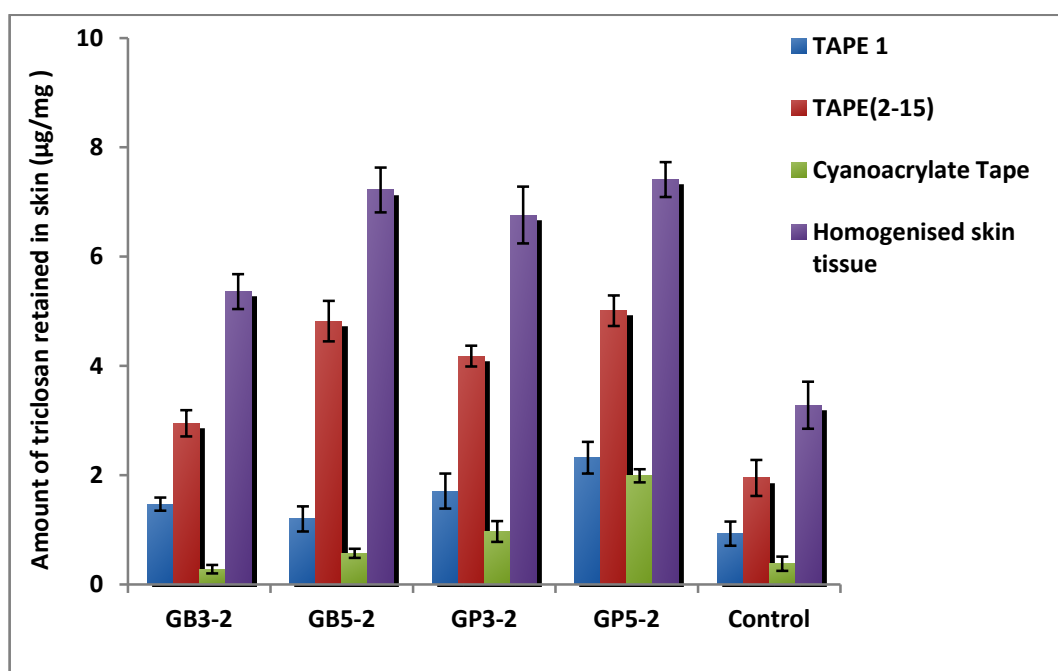


Figure 3.13 Triclosan uptake into skin treated with GB-SLNs (GB3-2, GB5-2), GP-SLNs (GP3-2, GP5-2) and control solution (Mean  $\pm$  SD, n = 6).

The SLN formulations had higher TSN retention within skin compared to the control solution, with the difference being statistically significant ( $p < 0.001$ ). It can be explained by higher occlusive effect and increased hydration of SC commonly associated with lipid nanoparticles (Müller *et al.*, 2007). This is similar to the findings reported for podophyllotoxin-loaded SLNs prepared with tripalmitin lipid and the epidermal targeting was proposed to be due to occlusion and interaction of SLNs with skin lipids (Chen *et al.*, 2006). The amount of TSN recovered from cyanoacrylate tape strip were  $0.28 \pm 0.07 \mu\text{g}/\text{mg}$ ,  $0.57 \pm 0.08 \mu\text{g}/\text{mg}$ ,  $0.97 \pm 0.19 \mu\text{g}/\text{mg}$  and  $1.99 \pm 0.12 \mu\text{g}/\text{mg}$  of tissue for GB3-2, GB5-2, GP3-2 and GP5-2 respectively. The amount of TSN recovered from skin appendages through cyanoacrylate biopsy was observed to be dependent on the concentration of lipid used in the formulations. As lipid concentration increased from 3 % to 5 % (w/w) in GB-SLNs and GP-SLNs, there was a 2-fold increase in TSN retention.

TSN accumulation within the skin was higher for GP-based formulations. This may be due to their smaller particle size, as it has been demonstrated that the penetration depth of the particles can be influenced by their size resulting in the possibility of a differentiated targeting of specific follicular structures (Patzelt *et al.*, 2011). In a similar study, there was a parabolic correlation between skin permeation of econazole nitrate and chain length of the fatty esters present in the lipids used in SLNs. The maximum flux of drug was observed for SLNs containing  $C_{17} - C_{19}$  esters, suggesting that these formulations may constitute a potential carrier for topical delivery of econazole nitrate (Sanna *et al.*, 2009). GB-SLNs prepared with retinol and retinyl palmitate for epidermal drug targeting, resulted in high retinol concentrations in the upper skin layers following application of SLNs, whereas the deeper regions had only very low retinol levels (Jenning *et al.*, 2000). Similarly, vitamin A-loaded GB-SLNs localised the drug in the upper skin layers and it was slowly released into

the viable epidermis in a sustained manner (Pople and Singh, 2006). Isotretinoin-loaded GP-SLNs provided epidermal targeting and reduced systemic uptake of tretinoin. Also, the SLNs formulation minimised direct skin contact thereby preventing skin irritation by the drug (Liu *et al.*, 2007).

### 3.4.3.7.3 *In vitro* comparison studies of follicular penetration using differential stripping technique

The present investigation and the observations by Starcher *et al.*, (2005) explored the theory that the elastic fibres surrounding the hair follicles contract if the skin is excised from cartilage and fatty tissue, possibly leading to a significant reduction of the follicular penetration pathway. However, other factors concerning the reduced follicular penetration must also be taken into consideration, such as loss of humidity and the absence of blood flow in excised skin. These aspects presumably additionally contribute to the differences in the penetration pathways to a certain extent.

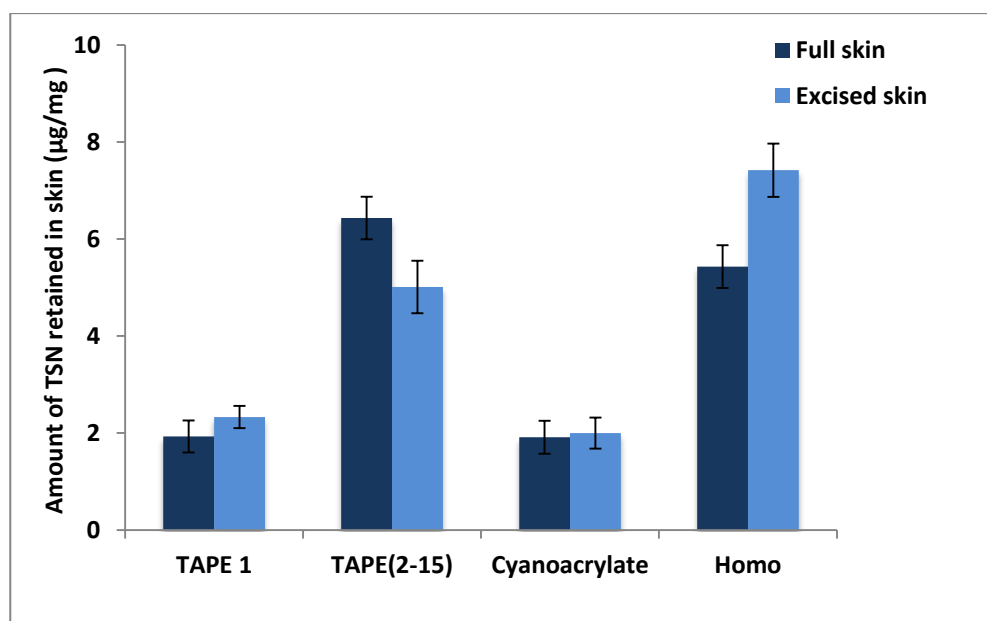


Figure 3.14 Amount of triclosan recovered from full thickness unsliced and excised porcine ear skin (Mean  $\pm$  SD, n = 6).

The present study therefore compared follicular penetration of TSN into full thickness porcine skin from both unsliced and excised porcine ear skin. A similar differential stripping technique was used to quantify the amount of TSN retained into skin and results are presented in Figure 3.14. The total amount of TSN recovered from both adhesive tape strips and cyanoacrylate biopsies for unsliced and excised skin were  $15.93 \pm 1.21 \mu\text{g}/\text{mg}$  and  $16.78 \pm 1.42 \mu\text{g}/\text{mg}$  respectively. To study the difference in follicular penetration of TSN between unsliced and excised full thickness skin only cyanoacrylate biopsy data was considered. The similar amount of TSN ( $2 \mu\text{g}/\text{mg}$ ) was recovered from unsliced and excised skin.

### 3.5 Conclusion

As SLNs have gained popularity as drug delivery systems, there has been increasing interest in understanding the parameters that control drug loading. While studies have provided information on how the choice of lipids and surfactants as well as their concentrations may play a role in determining the extent and localisation of drug loading, information on how the properties of the drug itself may affect its entrapment and permeation remain limited. In this study, encapsulation of TSN was compared with two different solid lipids such as GB and GP. In order to understand how the drug was loaded, the physicochemical properties of SLNs including its particle size, shape along with its interaction with the other component of the formulations were studied. *In vitro* drug permeation studies were also performed to quantify amount of TSN permeated and retained in full thickness porcine ear skin.

TSN was loaded at 10 mg/g of formulation, with encapsulation efficiency ranges between 65- 80 % for both GB and GP lipids, with higher encapsulation in GP-SLNs compared to GB-SLNs. TSN-loaded SLNs exhibited a lipid concentration dependent increase in the particle size and decrease in % DEE. Morphological studies confirmed their spherical shape with a lipid rich matrix. Thermal and structural characterisation was performed to analyse drug and excipient interaction in SLN formulations. From the DSC results, it appears that TSN was molecularly dispersed into the lipid matrix to give a homogenous dispersion within in the formulation. Similarly XRD and FTIR studies also supported homogenous dispersion of TSN into lipid matrix without any specific interaction between drug, lipids and other excipients of formulations.

Formulations containing 3 % and 5 % w/w GB and GP lipids (GB3-2, GB5-2, GP3-2 and GP5-2) were selected for permeation studies using excised full thickness porcine ear skin.

There was less than 8 % of total applied dose of drug permeation over 24 h, thus its permeation into receiver medium was low, which is important for localised action of topical formulations. A differential stripping technique was used to quantify the amount of TSN retained within the skin. Higher amounts of TSN were localised within the skin for GP5-2 indicating a superior ability of GP as a lipid carrier of TSN compared to GB lipid.

## **4. CHAPTER: DESIGNS AND DEVELOPMENT OF ANTIBACTERIAL NANOEMULSIONS FOR TOPICAL DELIVERY**

### 4.1 Introduction

A wound is a breach in the skin that allows access of microbes to the warm, moist and nutritious environment that is favourable to infections caused by bacteria, fungi, etc. MRSA is a common opportunistic microbe found in skin abrasions and open wounds caused by *Staphylococcus aureus*, often acquired due to infections that can occur in hospitals. Such infection prolongs illness and increases the length of stay and cost of hospital treatment. The goal of wound management is to provide the most favourable environment for regeneration of the epidermis. During the period of epidermal renewal, it is imperative to avoid further injury to the skin to minimise wound infection. Popular topical antimicrobial dressings used for wound treatments are iodine (Iodoflex<sup>®</sup>, Iodozyme<sup>®</sup>), silver sulfadiazine (Silvercel<sup>®</sup>, Acticoat<sup>®</sup>) (Neely *et al.*, 2009; Shupp *et al.*, 2010). These antimicrobial dressings have numerous limitations, such as poor skin adherence, short duration of activity against Gram-negative and Gram-positive bacteria and potential toxicity to host immune cells (Hemmila *et al.*, 2010). Hence, there is a need to develop a new generation delivery system, which can deliver topical antimicrobial agent deeper into the skin for controlled drug release for prolonged time.

The term "*nanoemulsion*" refers to a thermodynamically or kinetically stable liquid dispersion of an oil phase and a water phase, in combination with a surfactant. O/W NEs refer to a system in which oil droplets are dispersed in an aqueous phase. This is a favourable delivery system for hydrophobic active substances, whereas W/O NEs are suitable for hydrophilic substances (Henry *et al.*, 2009; Mason *et al.*, 2006). NEs can be

formulated using various methods, including high energy and low energy approaches. The details of various production methods were described in Chapter 1 (Section 1.4.2).

Essential oils derived from plants are well known for their insecticidal, antifungal, and antibacterial properties (Burt, 2004). EO contains 1,8-cineole (eucalyptol), which has been found to possess strong antimicrobial activity against human and food borne pathogens (Bakkali *et al.*, 2008). The intradermal administration of EO increases capillary permeability and favours wound healing (Sarkar, 1994). Olives are the fruit of the olive tree (*Olea europea*), belonging to the family *Oleaceae*. Due to its high content of monounsaturated and polyunsaturated fatty acids, olive oil (OO) has been used extensively in the cosmetics and pharmaceutical products (Eid *et al.*, 2013).

Regarding the selection of surfactants, the efficiency by which the surfactant facilitates NEs fabrication, either alone or in combination with a cosurfactant, is an important consideration (Azeem *et al.*, 2009; Donsi *et al.*, 2012). The surfactant system should effectively stabilise the oil-water interface. During the high energy homogenisation process, it is important to ensure that a sufficient amount of surfactant is rapidly adsorbed to the newly formed droplet surface and covers it well enough to prevent coalescence. With respect to the active ingredient in a formulation, the primary goal using NEs as a carrier system is to protect and deliver the active ingredient. Hence, the compatibility of formulation ingredients with the active ingredient and the capacity of formulation ingredients to solubilise and stabilise the active ingredient must be considered. Prerequisite information, such as the physicochemical properties of the active ingredient, is needed in order to select an appropriate surfactant system and oil phase.

In the present work, EO and OO were used to solubilise TSN for topical applications. NEs were produced containing EO and OO in different concentrations, along with the use of T80 and S80 as a surfactant and cosurfactant mixture ( $S_{\text{mix}}$ ). The effects of the different



formulation excipients were investigated in terms of formulation stability, physicochemical characterisation, and *in vitro* skin permeation.

#### 4.2 Aims of the study

The aims of present study were,

- To formulate NEs of TSN using EO and OO as the oil phase and to study the effects of composition of the liquid lipid phase on physicochemical properties of NE formulations.
- To determine optimised concentration and ratio of oils and surfactants to prepare stable NE formulations using pseudoternary phase diagrams.
- To characterise prepared NE formulations by performing series of experiments to select optimised batches for *in vitro* diffusion study using excised full thickness porcine ear skin.
- To evaluate the ability of SLNs and NEs as nanocarriers drug delivery system for enhanced skin retention of TSN by comparing the amount of TSN recovered from skin using an adhesive tape stripping method.

## 4.3 Materials and Methods

### **Materials:**

Triclosan was a gift from Vivimed Labs (India). Eucalyptus oil, olive oil, Tween<sup>®</sup> 80, Span<sup>®</sup> 80, sodium lauryl sulphate and phosphate buffer saline tablets were purchased from Sigma Aldrich (UK). All other reagents were of analytical grade.

### 4.3.1 Solubility study of triclosan

Aliquots of EO, OO, T80, S80 and deionised water (5 ml) were placed in vials and an excess amount of TSN was added. Samples were kept at a constant temperature ( $25 \pm 0.5^\circ\text{C}$ ) under shaking for 48 h to reach equilibrium (Parveen *et al.*, 2011). The samples were centrifuged at 4000 rpm (Eppendorf AG 5702, Germany) for 15 min and the solubilised TSN in the supernatant was then recovered and quantified by HPLC (Section 2.2.1.1).

### 4.3.2 Construction of pseudoternary phase diagrams

The objective of this study was to identify and select the optimum concentration of surfactant system using HLB values and to investigate the pseudoternary phase diagram behaviour of surfactants with oil and water. HLB is an empirical expression of the relationship between the hydrophilic and lipophilic groups in the surfactant. All surfactant systems comprise entities that combine both hydrophilic and lipophilic groups. HLB values are used to identify suitable surfactant systems for oil and water emulsification. Surfactants having HLB values of  $<10$  are considered to be oil soluble and those with HLB values  $>10$  are water soluble (Aulton and Taylor, 2013). Surfactants with suitable HLB values are selected based on the type of emulsion system to be prepared (O/W emulsion or W/O emulsion).

In present study, OO and EO were used as the oil phases, as they have been successfully used in preparations of NEs for dermal delivery (Eid *et al.*, 2013; Sugumar *et al.*, 2014).

T80 (HLB – 15), S80 (HLB - 4.3) and water were used as surfactant, cosurfactant and aqueous phase respectively. Different mass ratios (1:1, 2:1, 3:1, 4:1) of  $S_{\text{mix}}$  were prepared for phase studies, with increasing concentrations of T80 with respect to S80. Each phase diagram was prepared using EO and OO with  $S_{\text{mix}}$  combinations, at the specific ratios of 1:9, 2:8, 3:7, 4:6, 5:5, 6:4, 7:3, 8:2 and 9:1, in separate vials. This was done to identify clear NE regions, in order to select appropriate concentrations of oils and  $S_{\text{mix}}$  to prepare stable formulations. Aliquots of EO and OO were mixed with each  $S_{\text{mix}}$  at room temperature under gentle magnetic stirring and phase diagrams were constructed using an aqueous titration method in which water was added dropwise to the oil and  $S_{\text{mix}}$ . After equilibration, the systems were visually inspected for transparent fluid system, which were refereed as NE. Highly viscous systems that did not show a change in meniscus after being tilted to an angle of 90° were considered gels. The phase diagrams were constructed using JMP 11 software (SAS Institute Inc., USA).

#### 4.3.3 Formulation of triclosan nanoemulsions

Different batches of NEs were produced using a HSH followed by probe ultrasonication method (Rao and McClements, 2011; Tripathy, 2014). The HSH provides intense disruptive forces that cause the larger droplets of the coarse emulsion to be broken down into smaller ones. The homogenisation speed, time and surfactant concentration all contribute to controlling the droplet size. In practice, to reduce the droplet size to the level required in NEs, it is usually necessary to operate at extremely high speeds to ensure adequate intensity of the disruptive forces.

Droplet size and size distribution served as criteria for the selection of process parameters and NE composition. They not only characterise the NE system, but also serve as indicators of the quality and stability of the formulation. Each NE formulation was prepared by

heating the oil phase containing TSN (loading dose 10 mg/g of formulation) to 40°C to ensure complete dissolution of the drug in oil. The aqueous phase, containing the  $S_{mix}$ , was heated to the same temperature. The hot oil phase was slowly added to the hot aqueous phase under HSH (Silverson, UK). This hot primary emulsion was then subjected to ultrasonication (Sonics and Materials Inc., USA) for 15 min at 70 % frequency amplitude. The compositions of the preliminary NE formulations prepared are shown in Table 4.1.

Table 4.1 Compositions of preliminary TSN-loaded NE formulations

Formulation Code	Oil		T80: S80 (2:1) % w/w	
	Type	Concentration (% w/w)		
EO-5;2.5	Eucalyptus oil	5	2.5	
EO-5;5			5	
EO-5;7.5			7.5	
EO-5;10			10	
EO-10;2.5			10	2.5
EO-10;5				5
EO-10;7.5				7.5
EO-10;10				10
EO-15;2.5			15	2.5
EO-15;5				5
EO-15;7.5				7.5
EO-15;10				10
OO-5;2.5		Olive oil	5	2.5
OO-5;5				5
OO-5;7.5			7.5	
OO-5;10			10	
OO-10;2.5			10	2.5
OO-10;5				5
OO-10;7.5				7.5
OO-10;10				10
OO-15;2.5			15	2.5
OO-15;5				5
OO-15;7.5				7.5
OO-15;10				10

#### 4.3.4 Physicochemical characterisation of the nanoemulsion formulations

Physicochemical characterisation, i.e. determination of droplet size and PDI, ZP, % DEE, thermal analysis, FTIR and morphological studies, were performed using similar methods as described in detail in chapter 3 (Section 3.3.3).

##### 4.3.4.1 Accelerated stability studies

The NE formulations were subjected to temperature stress studies. The composition of the formulation and the ratio of oil and aqueous phase affect the physical stability of NEs. The stress test was carried out in three stages: centrifugation, heating-cooling and freeze-thawing for 3 cycles over 6 days (Loo *et al.*, 2011; Srilatha *et al.*, 2013).

**Centrifugation stage:** All the samples were centrifuged at 4400 rpm for 20 min (Eppendorf AG5702, Germany). The formulations were examined for phase separation, creaming and cracking.

**Heating-cooling stage:** The effect of change in temperature on the stability of NEs was analysed by storing the samples between 4°C and 40°C for a period of 48 h. The stable formulations were then subjected to a freeze thaw cycle.

**Freeze-thaw stage:** The formulations were subjected to -20°C and 25°C for a period of 48 h each. Freeze-thaw cycles were performed in the triplicate and samples were studied for phase separation.

The formulations that were stable under accelerated stability studies were subjected to further characterisation studies.

##### 4.3.4.2 pH determination

The pH of the NEs formulations was measured at ambient temperature using a digital pH meter. Each pH value was measured in triplicate and average value (mean  $\pm$  SD) was recorded.

#### 4.3.4.3 Determination of viscosity

The viscosities of the NEs formulation were evaluated using Bohlin Gemini cone and plate rheometer (Aimil Ltd., India). The viscosities were measured in triplicate at a temperature of 25°C using a shear ramp between 0.1 and 100 s<sup>-1</sup> (Alam *et al.*, 2015).

#### 4.3.4.4 *In vitro* drug release and skin permeation studies

Release and permeation studies for the NE formulations were carried out in Franz diffusion cells. The setup and experimental conditions were similar to those described in the chapter 3 (Section 3.3.3.9). For the release studies, a cellulose acetate membrane (Sigma Aldrich, UK), 23 mm in diameter with a molecular weight cut off of 12-14 kDa was selected. For the skin permeation and retention studies excised full thickness porcine ear skin was used.

A saturated aqueous solution of TSN was used as a control solution. The donor compartment was filled with either the appropriate NE formulation or control solution (equivalent to 10 mg/g of TSN). Subsequently, 500 µl samples were collected from the receiver compartment at 4, 6, 8, 10, 12 and 24 h and replaced by an equal volume of fresh receiver medium. All samples were analysed by the previously validated HPLC method (Section 2.2.1.1). The cumulative amount of TSN released through dialysis membrane and the amount of TSN permeated through the skin were plotted as a function of time.

#### 4.3.4.5 Quantification of triclosan in skin using an adhesive tape stripping method

At the end of the permeation study, the amount of TSN retained within the skin was quantified using the adhesive tape stripping method (Yu *et al.*, 2014). After 24 h of contact, the skin was carefully removed from the cell and washed with distilled water to remove any residual formulation. The tape stripping process was performed and samples were analysed as described in chapter 3 (Section 3.3.3.9.2).

#### 4.3.4.6 Statistical analysis

All the data obtained were reported as the mean  $\pm$  SD and statistically analysed by one way ANOVA and Tukey's test, using GraphPad Prism 5 software. Differences were considered to be statistically significant at  $p < 0.05$ .

## 4.4 Results and Discussion

### 4.4.1 Determination of triclosan solubility

The solubility of the drug in the internal oil phase is an important factor to consider when designing NEs as carriers for lipophilic drugs (Benita and Levy, 1993). TSN is a poorly water soluble drug and thus it is essential to incorporate it into the oil core of the NEs to formulate it for topical drug delivery. Solubility of TSN in selected oils and surfactants i.e. EO, OO, T80 and S80 was investigated and reported in Table 4.2.

Table 4.2 Solubility of triclosan obtained in different oils and surfactants after 48 h equilibration at 25°C (Mean  $\pm$  SD, n = 3).

Solvent	Solubility (mg/g)
EO	5.23 $\pm$ 0.02
OO	3.51 $\pm$ 0.05
T80	41.23 $\pm$ 0.14
S80	29.13 $\pm$ 0.03

Based on solubility data and type of NEs to be prepared (O/W), T80 and S80 were selected as surfactant and cosurfactant respectively. S80 forms a close packed, complex film with T80 at the oil-water interface. Calligaris *et al.* (2015) used T80 as a surfactant in preparation of silybin NEs using OO, sunflower oil and castor oil. Another study reported the use of T80 and S80 (1:1, HLB – 9.65) as  $S_{mix}$  for preparation of NEs using various oils such as isopropyl myristate, EO, OO and mineral oil (Syed and Peh, 2014).



#### 4.4.2 Construction of pseudoternary phase diagrams

The NE formation zone in phase diagrams is controlled by the physicochemical nature of oil and aqueous phase, low interfacial surface tension and association of oil with surfactants at the interfacial surface (El Maghraby, 2008).

Phase diagrams were constructed using EO, OO as the oil phase and T80, S80 as the surfactant and cosurfactant respectively. Nonionic surfactants are generally considered safe due to their relatively compatible behaviour with other excipients in the formulations for skin and in biological tissues (Baroli *et al.*, 2000; Syed and Peh, 2014). A combination of lipophilic and hydrophilic nonionic surfactants can be used to build highly structured emulsions. The effect of the  $S_{mix}$  on NE formation was evaluated for further optimisation of the system. The pseudoternary phase diagrams for EO and OO, with T80 alone or in combination with S80 (1:1, 2:1, 3:1, 4:1) at ambient temperature are represented in Figures 4.1, 4.2 and 4.3 respectively.

In the presence of T80 alone (Figure 4.1), the NE zone occupied about 20 % of the total area of the phase diagram. When S80 is absent, it is possible that the T80 is not able to sufficiently reduce the oil-water interfacial tension due to its hydrophilic nature. At very low oil concentrations, a maximum of 30 % water was solubilised in the surfactant-oil blend. The amount of incorporated water was reduced progressively with increasing oil concentrations. Addition of cosurfactant increased the maximum amount of water incorporated into the oil-surfactant system, with the extent of the NE zone increasing in all cases compared to the cosurfactant-free system.

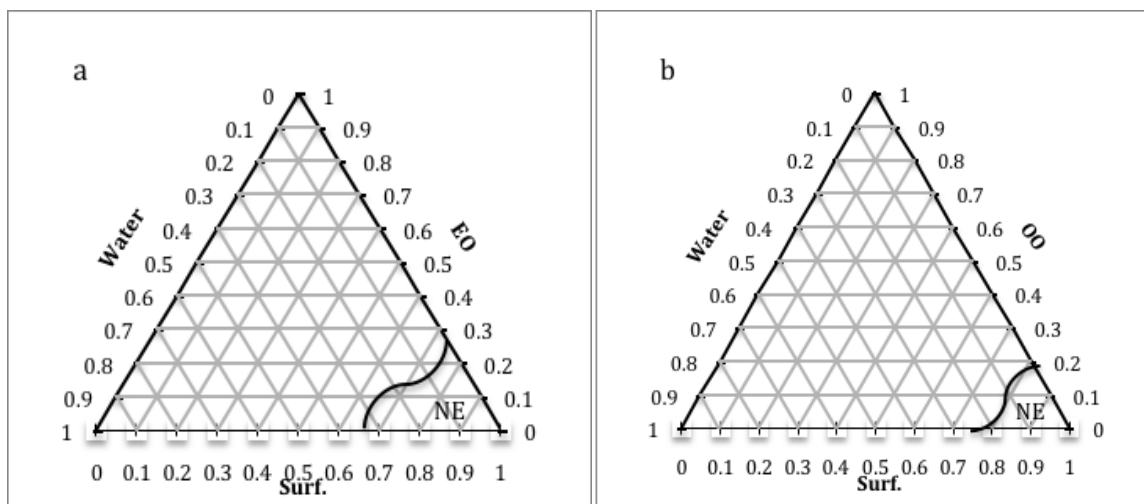


Figure 4.1 Pseudoternary phase diagrams of a) eucalyptus oil and b) olive oil with surfactant (T80) and water.

When T80 with S80 were incorporated in equal amounts ( $S_{\text{mix}}$  1:1; HLB 9.65), a larger NE region was observed, perhaps due to the further reduction in interfacial tension and increased fluidity of the interface (Figures 4.2a and 4.3a). As the surfactant concentration was increased to  $S_{\text{mix}}$  2:1 (HLB 11.57) and  $S_{\text{mix}}$  3:1 (HLB 12.32) (Figure 4.2b, c and Figure 4.3b, c), the NE region increased in size compared to that seen with  $S_{\text{mix}}$  1:1. When the surfactant concentration was further increased to  $S_{\text{mix}}$  4:1 (HLB 12.82) (Figures 4.2d and 4.3d), a decrease in the NE region compared to  $S_{\text{mix}}$  3:1 was observed (Mahdi *et al.*, 2011).

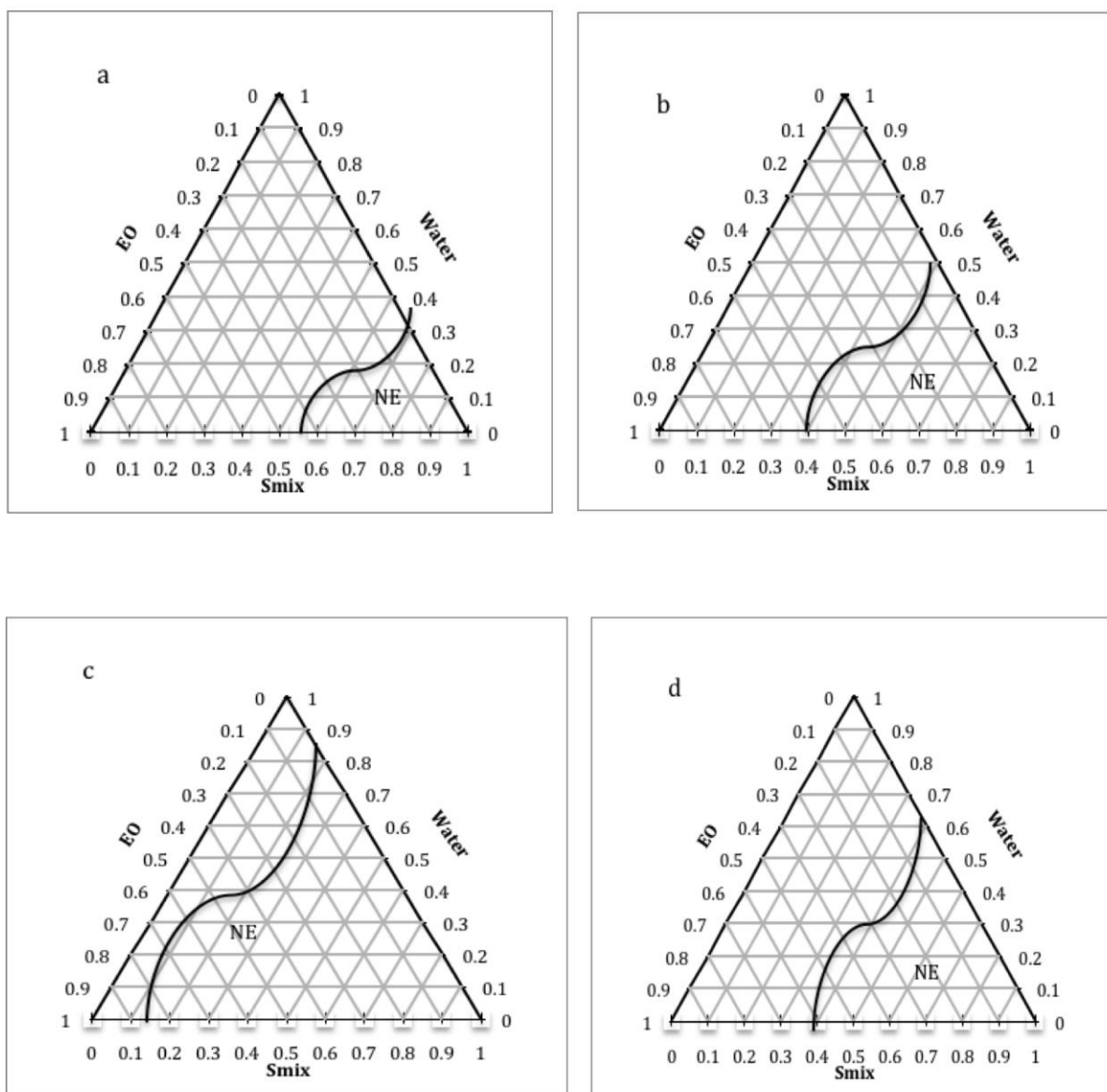


Figure 4.2 Pseudoternary phase diagrams of eucalyptus oil, water and different ratios of surfactant mixture (T80:S80) a) Smix 1:1, b) Smix 2:1, c) Smix 3:1, d) Smix 4:1.

When the surfactant concentration was increased in comparison to cosurfactant, the NE region increased in size up to the 3:1  $S_{mix}$  ratio, but at the 4:1 ratio, the size of the NE region decreased, hence further ratios of  $S_{mix}$  was not evaluated. Reported HLB required for EO and OO is 9.8 and 7 respectively (Orafidiya and Oladimeji, 2002). To obtain the smaller NE droplet size and stable formulations which is related to required HLB, it is proposed that the most stable NE is the one which was formulated with the HLB of  $S_{mix}$  nearest to required

HLB of oil phase (Prinderre *et al.*, 1998; Salager, 2000). Based on this the 2:1  $S_{mix}$  with HLB value 11.57 was selected to prepare NEs using EO and OO as oil phase.

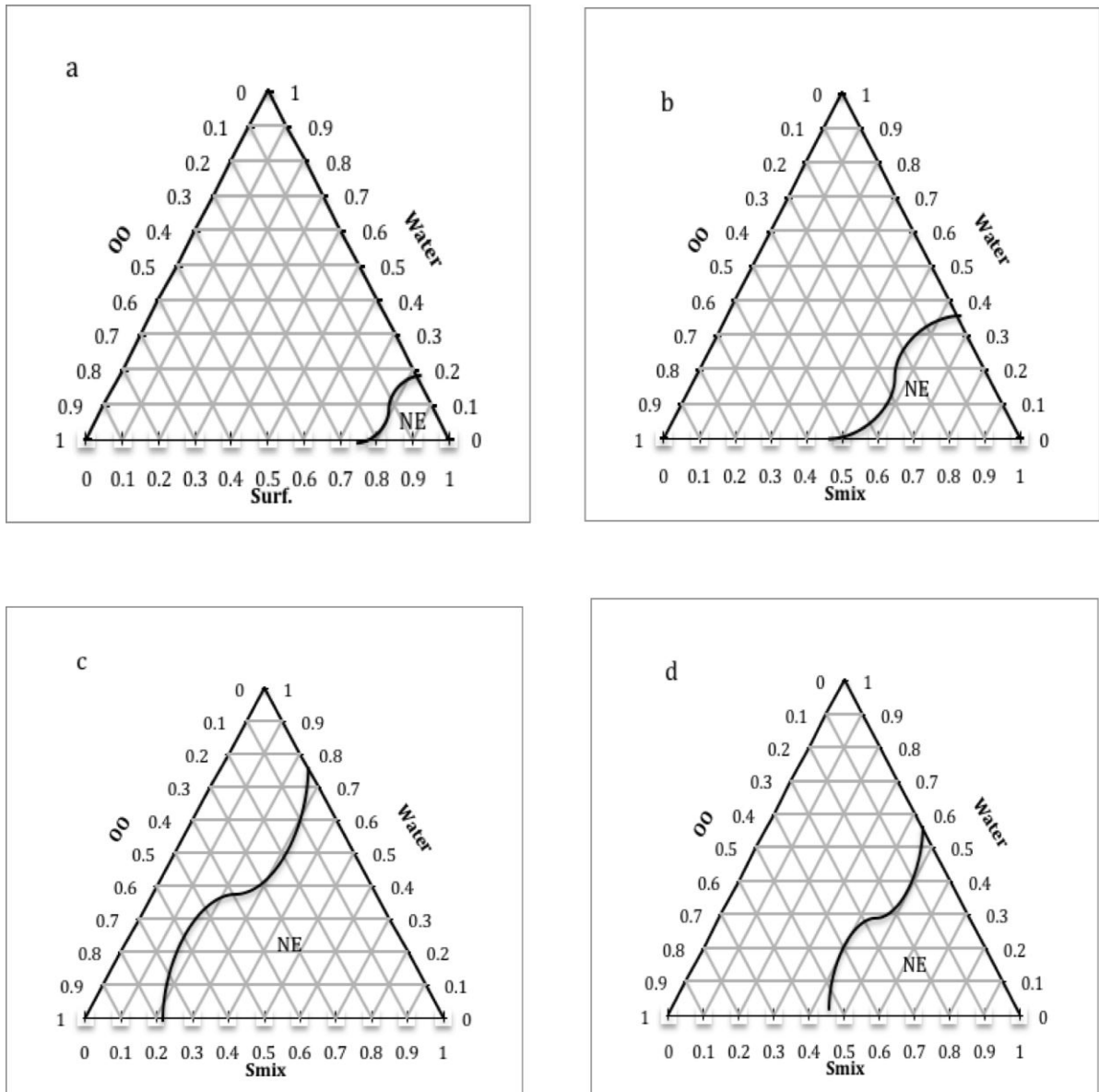


Figure 4.3 Pseudoternary phase diagrams of olive oil, water and different ratios of surfactant mixture (T80:S80) a) Smix 1:1, b) Smix 2:1, c) Smix 3:1, d) Smix 4:1.

#### 4.4.3 Preparation of nanoemulsions

The NEs formulations were prepared using HSH followed by probe ultrasonication. The initial batches of NEs were prepared using different concentrations of oil (5, 10 and 15 % w/w), while concentrations of  $S_{mix}$  (2:1) used were 2.5, 5, 7.5 and 10 % w/w.

##### 4.4.3.1 Impact of homogenisation time

Mean droplet size is a critical parameter of the NEs formulation due to its direct influence on formulation stability, appearance and efficacy of delivery. The effect of different homogenisation times (10, 15, 20, and 25 min) on the mean droplet size was determined for 5 % w/w EO-NEs (EO-5;5) and OO-NEs (OO-5;5) stabilised by 5 % w/w T80 and S80  $S_{mix}$  (2:1).

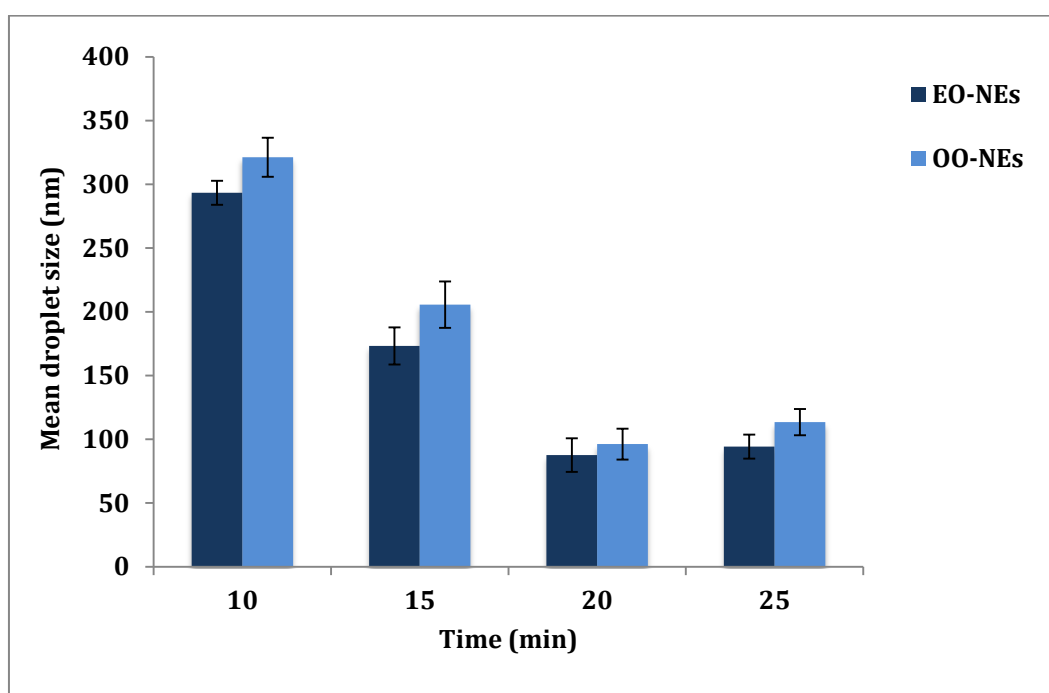


Figure 4.4 Impact of homogenisation time on mean droplet size of EO-NEs and OO-NEs (Mean  $\pm$  SD, n = 3).

Average droplet size decreased with increased homogenisation duration (Figure 4.4) for both NEs. When the duration was increased from 10 min to 20 min, EO-NEs droplet size decreased from  $293.4 \pm 2.9$  nm to  $87.6 \pm 1.2$  nm, while OO-NEs droplet size decreased from  $321.2 \pm 3.2$  nm to  $96.2 \pm 1.7$  nm. When the time was further extended from 20 min to 25 min, no significant change in droplet size was seen for either EO or OO. As the duration of

homogenisation determines the amount of energy input into generating NEs, longer durations mean more energy input, thus enhancing the intense disruptive forces necessary for successful size reduction. Similar results were reported by Shahavi *et al.*, (2015) for clove oil NEs prepared using a  $S_{\text{mix}}$  containing T80 and S80. Their results showed a decrease in droplet size from 160 nm to 40 nm when sonication time was increased from 1 min to 10 min with no further reduction in droplet size when time was increased to 15 min. Hence, based on the data obtained from present study, the homogenisation time for the preparation of TSN-loaded NEs was set at 20 min.

#### 4.4.3.2. Impact of formulation variables

The types and concentrations of oil and surfactants used in the preparation of TSN-loaded NEs are very important because they affect the solubility of lipophilic drug and the physicochemical properties of the formulation, namely its density, viscosity, interfacial tension and phase behaviour (Wooster, 2008). In the present study, the effects of oil and surfactant concentrations on NE droplet size and distribution were studied. EO and OO, at concentrations of 5, 10, and 15 % w/w, were used to prepare NEs containing 2.5, 5, 7.5 and 10 % w/w  $S_{\text{mix}}$  (3:1). The results summarised in Table 4.3 reveal that the concentration of oil greatly influenced the NEs droplet size and its distribution with increasing size when the oil concentration was increased from 5 % to 15% w/w. The efficiency of NE formation decreased with increasing amounts of oil and the formulation became unstable at oil concentrations of 15 % w/w.

Increasing oil concentration reduces the surfactant ability to lower the interfacial tension, which results in instability of the system. Moreover, increasing concentrations of oil increased the collision rate between droplets, promoting increase in rate of flocculation resulting in a droplet size increase (Soleimanpour *et al.*, 2013). With an increase in droplet size, PDI increases, which favours the coalescence of droplets, such that droplets join together to make larger volume with less interfacial area to dissipate the free energy. This eventually leads to phase separation, in which all of the droplets coalesce to form two separated phases (Taylor, 1998).

Table 4.3 Effect of oil and surfactant concentrations on droplet size and distribution in EO-NE and OO-NE formulations (Mean  $\pm$  SD, n = 3).

Formulation Code	Particle size (nm)	PDI	Formulation Code	Particle size (nm)	PDI
EO-5;2.5	139.2 $\pm$ 4.2	0.84 $\pm$ 0.15	OO-5;2.5	145.2 $\pm$ 2.4	0.75 $\pm$ 0.03
EO-5;5	87.5 $\pm$ 2.3	0.74 $\pm$ 0.13	OO-5;5	96.3 $\pm$ 3.5	0.58 $\pm$ 0.06
EO-5;7.5	71.3 $\pm$ 1.3	0.88 $\pm$ 0.03	OO-5;7.5	87.4 $\pm$ 2.1	0.68 $\pm$ 0.04
EO-5;10	69.4 $\pm$ 3.8	0.81 $\pm$ 0.02	OO-5;10	79.1 $\pm$ 1.2	0.63 $\pm$ 0.07
EO-10;2.5	152.4 $\pm$ 2.2	0.92 $\pm$ 0.07	OO-10;2.5	184.1 $\pm$ 4.7	0.89 $\pm$ 0.05
EO-10;5	106.8 $\pm$ 2.8	0.61 $\pm$ 0.15	OO-10;5	121.7 $\pm$ 2.3	0.64 $\pm$ 0.04
EO-10;7.5	95.3 $\pm$ 1.8	0.94 $\pm$ 0.05	OO-10;7.5	106.5 $\pm$ 3.8	0.79 $\pm$ 0.13
EO-10;10	87.5 $\pm$ 1.7	0.66 $\pm$ 0.08	OO-10;10	94.1 $\pm$ 1.4	0.68 $\pm$ 0.15
EO-15;2.5	251.5 $\pm$ 4.6	1.45 $\pm$ 0.17	OO-15;2.5	291.4 $\pm$ 3.2	1.24 $\pm$ 0.21
EO-15;5	208.9 $\pm$ 1.9	1.27 $\pm$ 0.26	OO-15;5	258.1 $\pm$ 2.7	1.84 $\pm$ 0.15
EO-15;7.5	185.1 $\pm$ 2.4	1.37 $\pm$ 0.72	OO-15;7.5	215.4 $\pm$ 4.2	1.47 $\pm$ 0.24
EO-15;10	189.4 $\pm$ 1.5	1.52 $\pm$ 0.83	OO-15;10	210.4 $\pm$ 2.7	1.89 $\pm$ 0.34

The surfactant is the other important component in NE formation, as it controls the rate of adsorption and coalescence by modifying the interface. The concentration, rate of collision and activity at the interface determine the efficiency of NE formation under fixed process parameters (McClement, 2011). During the HSH process, the surfactant molecules adsorb onto the newly formed oil-water interface, reducing the surface tension, facilitating droplet disruption, and restricting the coalescence and aggregation of emulsion droplets (Guzey and McClements, 2006). The adsorption kinetics of the emulsifier have a significant effect on the size and its distribution of droplets.

The results presented in Table 4.3 show a decrease in droplet size when surfactant concentration was increased from 2.5 % w/w to 10 % w/w for both EO and OO. However, there was no significant difference ( $p>0.05$ ) in the droplet size of the NEs when the concentration of surfactant was increased from 5 % w/w to 10 % w/w. Hence, the critical diameter may have been reached, with the distribution then becoming narrower rather than the droplets further fragmenting (Håkansson *et al.*, 2009; Soon *et al.*, 2001). The observed decrease in droplet diameter with increasing surfactant concentration can be attributed to various factors: faster surfactant adsorption to the oil droplets surfaces during homogenisation leads to lower interfacial tension, thereby facilitating droplets breakup; and more surfactant is available to cover the droplets surfaces formed during homogenisation (Jafari *et al.*, 2008; Ziani *et al.*, 2011). Moreover, in practice, it is usually advantageous to use the lowest amount of surfactant required to form stable emulsions, since this reduces both cost and potential toxicity. In addition, high concentrations of non-adsorbed surfactant may decrease emulsion stability by promoting Ostwald ripening or droplet flocculation (Klang and Valenta, 2011; Weiss *et al.*, 2000).

In this study, 5 % w/w of the surfactant mixture was sufficient to enable the newly created surface area resulting from droplets breakup to be coated rapidly during the emulsification process. Based on these data, formulation batches containing 5 % w/w and 10 % w/w EO-NEs (EO-5;2.5 to EO-10;10) and OO-NEs (OO-5;2.5 to OO-10;10) were further subjected to



accelerated stability studies, while the formulations containing 15 % w/w oil were discarded due to instability and phase separation.

#### 4.4.4 Accelerated stability study

Assessment of long term stability of TSN-loaded NEs under environmental storage conditions can be both tedious and time consuming, and is considered uneconomical. Thus, the NE formulations were subjected to a variety of extreme storage conditions, such as centrifugation, heating-cooling cycle and freeze-thaw cycles, to predict the stability of formulations samples over a period of time.

Centrifugation can accelerate the rate of creaming or sedimentation, which demonstrates that the breakdown of an emulsion may be related to the action of gravitational force. O/W NE systems often exhibit creaming rather than sedimentation due to the lower density of oil droplets compared to the aqueous medium. The results from the accelerated stability study of the TSN-loaded EO-NEs and OO-NEs are shown in Table 4.4. Changes in physical appearance were also recorded upon completion of the centrifugation process. EO-5;10, EO-10;7.5, EO-10;10, OO-5;7.5, and OO-10;10 separated into two distinct layers after centrifugation, resulting from instability in the NE system. It is possible that the amount of surfactant used was either too high or was not sufficient to achieve a structured interfacial film in emulsions with a high amount of oily phase.

Only formulations that were stable against centrifugation were subjected to storage at elevated temperatures. The heating-cooling study showed formulations EO-5;2.5, EO-5;7.5, EO-10;2.5, OO-5;7.5, OO-5;10, OO-10;2.5 and OO-10;7.5 underwent phase separation. Sample storage at elevated temperatures contributes to higher kinetic energy in the Brownian motion of oil droplets, speeding up the movement and increasing collisions between the oil droplets. Upon freezing, the oil droplet in the formulations segregated due to the formation of crystallised ice particles, resulting in the disruption of the lipid film

surrounding the droplets. When the samples were thawed, the droplets melted and immediately coalesced with surrounding droplets, resulting in phase separation. After the freeze-thaw cycle, only NEs containing 5 % w/w surfactant mixtures for both EO-NEs (EO-5;5, EO-10;5) and OO-NEs (OO-5;5, OO-10;5) formulations maintained homogeneity.

Table 4.4 Accelerated stability assessment of EO-NE and OO-NE formulations.

Formulation Code	Centrifugation	Heating-cooling cycle		Freeze-thaw cycle
		4°C	25°C	
EO-5;2.5	√	X	X	X
EO-5;5	√	√	√	√
EO-5;7.5	√	√	X	X
EO-5;10	X	N/A	N/A	N/A
EO-10;2.5	√	√	X	X
EO-10;5	√	√	√	√
EO-10;7.5	X	N/A	N/A	N/A
EO-10;10	√	√	√	√
OO-5;2.5	√	√	√	X
OO-5;5	√	√	√	√
OO-5;7.5	√	√	X	X
OO-5;10	√	X	X	X
OO-10;2.5	√	√	X	X
OO-10;5	√	√	√	√
OO-10;7.5	√	√	X	X
OO-10;10	X	N/A	N/A	N/A

Note: √ - stable (no phase separation), X – unstable (phase separation), N/A – (not applicable)

#### 4.4.5 Physicochemical characterisation of nanoemulsions

The NE formulations that passed the accelerated stress testing were then subjected to further characterisation. The measured ZP, % DEE, pH and viscosities of the NEs are shown in Table 4.5. ZP has been identified as an important factor to determine the surface charge, which is important for the stability of the colloidal system (Laouini *et al.*, 2012). In present study, negative ZP values were obtained for all the NEs formulation, which ranged between  $-28.91 \pm 1.23$  mV and  $-37.13 \pm 1.72$  mV. The charge derives from the presence of negatively charged chlorinated poly aromatic phenol groups in TSN. High ZP is required for good colloidal stability, as charged droplets more strongly repel one another, thus overcoming the natural tendency to aggregate (Grosse *et al.*, 2002; Tagne *et al.*, 2008). Thus the obtained ZP values were sufficient to prevent droplet coalescence and indicate stability of the prepared NE formulations.

Measurement of % DEE was carried out to determine the maximum amount of TSN encapsulated in the oil droplets. % DEE of TSN increased with increased oil concentration, for both EO and OO formulations. The % DEE for EO-5;5, EO-10;5, OO-5;5, and OO-10;5 was found to be  $78.61 \pm 1.28$ ,  $86.14 \pm 0.93$ ,  $75.49 \pm 1.16$ , and  $81.19 \pm 2.15$ , respectively. However, no significant differences ( $p > 0.05$ ) in % DEE were observed between the EO-NEs and OO-NEs. The pH range for healthy human skin is between 5.4 to 5.9 (Braun-Falco and Korting, 1986) and the pH of dermal formulations is an important factor in avoiding skin irritation or susceptibility to bacterial infection. The pH of all optimised formulations ranged from 5.23 to 5.91 values compatible with human skin pH and suitable for topical application.

Table 4.5 Physicochemical characterisation of optimised NE formulations (Mean  $\pm$  SD, n = 3).

Formulation Code	ZP (mV)	% DEE	pH	Viscosity (cP)
EO-5;5	-37.13 $\pm$ 1.72	78.83 $\pm$ 1.28	5.23	20.08 $\pm$ 1.14
EO-10;5	-31.84 $\pm$ 0.91	86.14 $\pm$ 0.93	5.71	24.15 $\pm$ 0.94
OO-5;5	-34.56 $\pm$ 1.21	75.49 $\pm$ 1.16	5.54	22.31 $\pm$ 1.29
OO-10;5	-28.91 $\pm$ 1.23	81.19 $\pm$ 2.15	5.91	28.46 $\pm$ 1.73

The shear viscosities of the NEs were measured at a controlled shear rate. Overall, the viscosities of the optimised formulations were low, as expected for O/W NEs (Alvarado *et al.*, 2015). It was observed that increasing the oil concentrations slightly increased the viscosity of the NEs, an effect that could be associated with increased micelle diameter. This phenomenon is usually followed by an increase in the viscosity of systems (Chanamai and McClements, 2000; Chiesa *et al.*, 2008; Mayer *et al.*, 2013). EO-5;5 and OO-5;5 had low viscosities of 20.08  $\pm$  1.14 cP and 22.31  $\pm$  1.29 cP, respectively, perhaps due to higher aqueous content. These results were significantly different from ( $p < 0.05$ ) the EO-10;5 and OO-10;5 formulations.

#### 4.4.6 Morphological study

The NE formulations were examined by TEM to observe the particle shape and verify the droplet size determined by NTA. A TEM micrograph of a TSN-loaded NE formulation is shown in Figure 4.5. The observed droplets are spherical in shape, with an average droplet size of 100 nm. The TEM images for all of the optimised formulations were similar in size and shape. The droplet size results showed good agreement with the results obtained from

droplet size analysis by NTA (Section 4.4.3.2). Similar morphology was reported by Vatsraj *et al.* (2014) for clarithromycin OO-NE formulations.

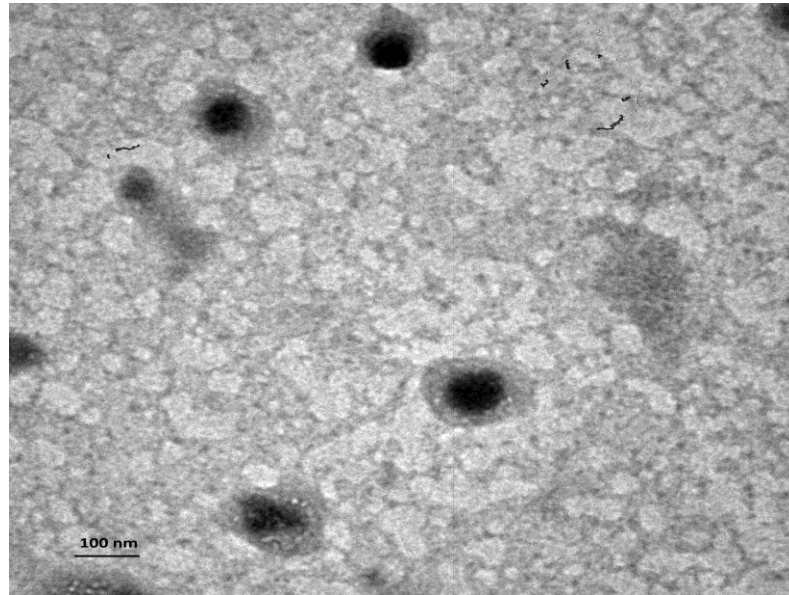


Figure 4.5 TEM image of TSN-loaded NEs (EO-5;5).

#### 4.4.7 Thermal analysis

The effect of drug loading on the thermal behaviour and structural properties of the developed NEs, as well as the potential interactions among ingredients, were examined using DSC. Figures 4.6 and Figure 4.7 shows DSC thermograms for TSN, TSN free NE formulations (Blank EO-NEs and OO-NEs) and the TSN-loaded EO-NE and OO-NE formulations respectively.

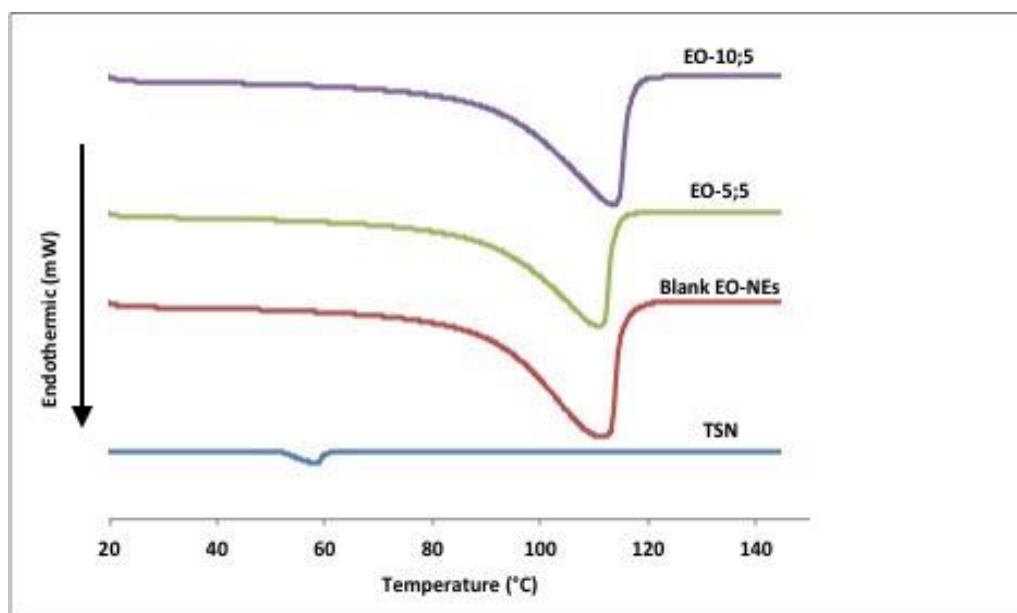


Figure 4.6 DSC thermograms for TSN, blank EO-NEs, and TSN-loaded EO-NEs (EO-5;5, EO-10;5).

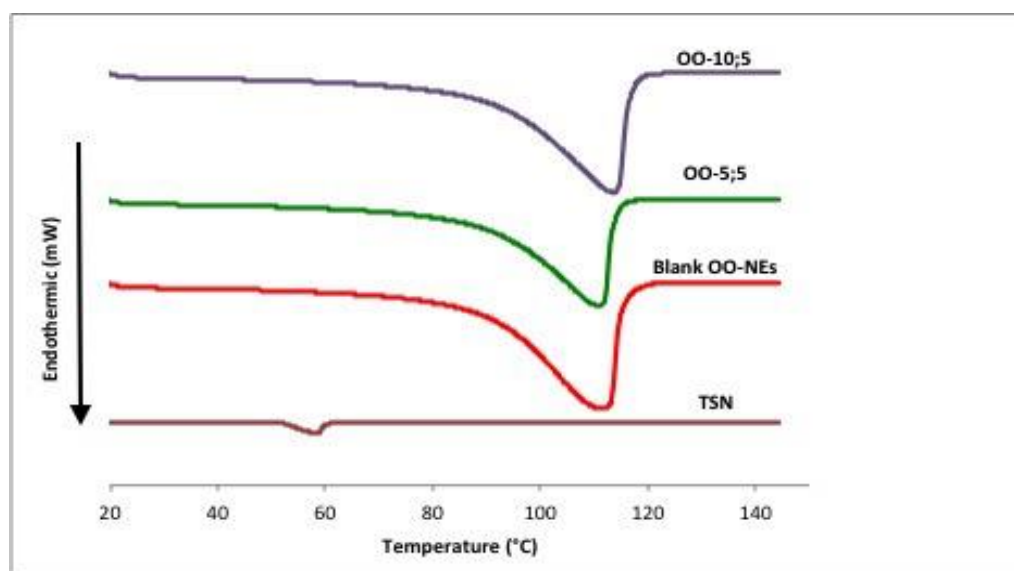


Figure 4.7 DSC thermograms for TSN, blank OO-NEs, and TSN-loaded OO-NEs (OO-5;5, OO-10;5).

The DSC thermogram for TSN has an endothermic peak at 61°C, corresponding to the melting of the drug. In the DSC curves for both blank and the TSN-loaded NEs formulations, a broad endothermic peak was observed around 110°C, most likely due to water evaporation. However, for the TSN-loaded NEs, no melting peak of the drug was detected, suggesting that TSN was molecularly dispersed, i.e. dissolved in the oil phase of the NEs.

#### 4.4.8 Fourier transform infrared analysis

The FTIR spectrum provides valuable information about functional groups and possible intermolecular interactions between the drug and other components in the developed NEs formulations. The FTIR spectra for TSN, EO and OO, TSN free NEs (blank EO-NEs and OO-NEs) and TSN-loaded NEs are shown in Figures 4.8 and 4.9 respectively.

The FTIR spectrum for TSN has strong absorption bands for halogenated hydrocarbons arising from stretching vibrations of the carbon-halogen bond for the CH<sub>2</sub>-Cl group in the 1300–1150 cm<sup>-1</sup> region. Other bands ascribed to out-of-plane bending of the ring C-H bonds, and in-plane bending bands appear in the 1300-1000 cm<sup>-1</sup> region. Skeletal vibrations involving C-C stretching within the ring, are evident in the 1610-1585 cm<sup>-1</sup> and 1500-1400 cm<sup>-1</sup> regions.



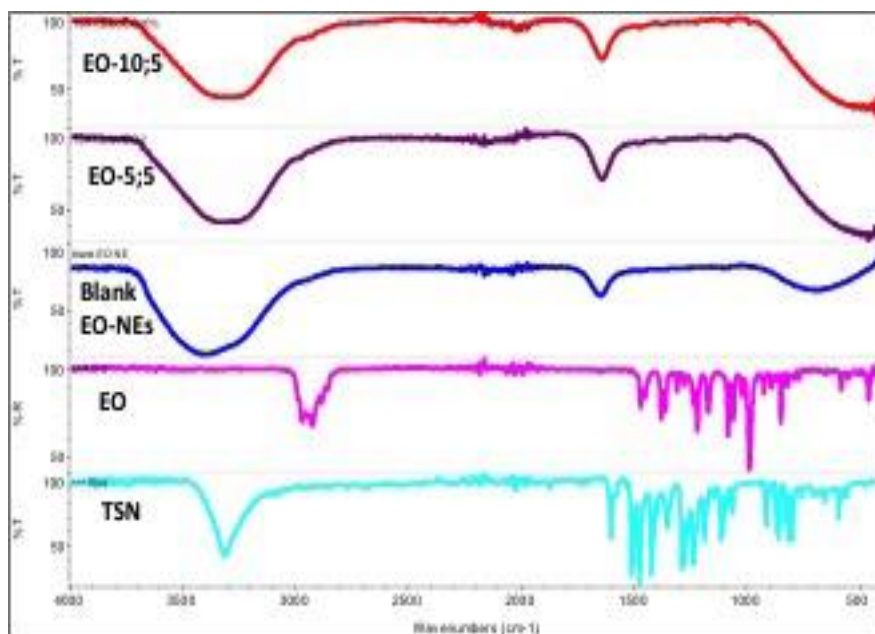


Figure 4.8 FTIR spectra for TSN, EO, Blank EO-NEs and the TSN-loaded EO-NEs (EO-5;5, EO-10;5).

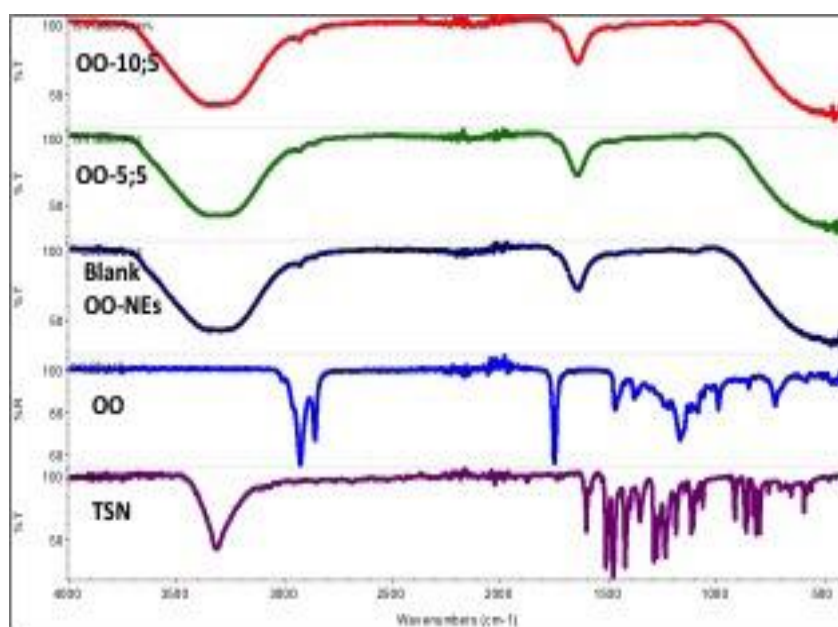


Figure 4.9 FTIR spectra for TSN, OO, Blank OO-NEs and the TSN-loaded OO-NEs (OO-5;5, OO-10;5).

EO has a multiple band at  $2969\text{ cm}^{-1}$ , owing to methylene groups ( $-\text{CH}_2-$ ) (Figure 4.8); at  $1721\text{ cm}^{-1}$  related to carbonyl  $\text{C}=\text{O}$  stretching; at  $1672\text{ cm}^{-1}$  due to  $\text{C}=\text{C}$  stretching of aromatic groups; and at  $1445\text{ cm}^{-1}$  due to  $\text{C}-\text{H}$  deformation (Esteves *et al.*, 2013; Sheet *et al.*, 2007). The FTIR spectra for blank EO-NEs and the TSN-loaded EO-NEs (EO-5;5, EO-10;5) had a broad band in the range of  $2500\text{ cm}^{-1}$  to  $4000\text{ cm}^{-1}$  due to  $\text{O}-\text{H}$  stretching, confirming the presence of water in the formulation. The appearance of a new band at  $1635$

$\text{cm}^{-1}$  and the broadening of bands in the TSN spectrum (in the region of  $1610 - 1585 \text{ cm}^{-1}$  and C-H stretching at  $1649 \text{ cm}^{-1}$ ) indicated that the TSN was molecularly dispersed in oil (Herculano *et al.*, 2015).

Figure 4.9 shows a characteristic FTIR spectra for bulk OO, Blank OO-NEs and the TSN-loaded OO-NEs (OO-5;5, OO-10;5). A weak band is visible near  $3005 \text{ cm}^{-1}$  at the higher wavenumber side of this region, generated by the *cis* double-bond C-H stretching vibration. In addition, this infrared region is dominated by two strong bands at  $2925$  and  $2854 \text{ cm}^{-1}$ , resulting from the respective asymmetric and symmetric stretching vibrations of the acyl  $\text{CH}_2$  groups (Guillen and Cabo, 1997; Voort *et al.*, 2001). Peaks observed at  $1465 \text{ cm}^{-1}$  and  $1377 \text{ cm}^{-1}$  are due to bending vibrations of methyl and methylene groups. The large peak around  $1740 \text{ cm}^{-1}$  is due to C=O double bond stretching vibration and stretching vibration of C-O result in peaks in the  $1500-650 \text{ cm}^{-1}$  region (Rohman and Che Man, 2012). FTIR spectra for the TSN-loaded NEs showed significant broadening of the  $2925 \text{ cm}^{-1}$  band compared to bulk OO, which may be due to stretching of C=C bond in the aromatic ring of TSN. The NEs also showed a characteristic peak between  $1700 \text{ cm}^{-1}$  and  $1500 \text{ cm}^{-1}$  resulting in the appearance of superimposed peaks for TSN and OO in these regions. This confirmed the successful encapsulation of TSN with retained stability, as well as the absence of any significant interaction between drug and oils (Devi and Kakati, 2013; Herrero *et al.*, 2011).

#### 4.4.9 *In vitro* release study

The *in vitro* release of TSN from the optimised NE formulations and a control solution was investigated and the percentage cumulative TSN release was plotted against time (Figure 4.10). All NE formulations showed higher drug release compared to control solution, indicating that the formulation plays an important role in the process of drug release into the receiver medium (Costa and Lobo, 2001). After 24 h, drug release from the NEs was less

than 2 % of total applied dose, which is advantageous for localised effect of topical formulations.

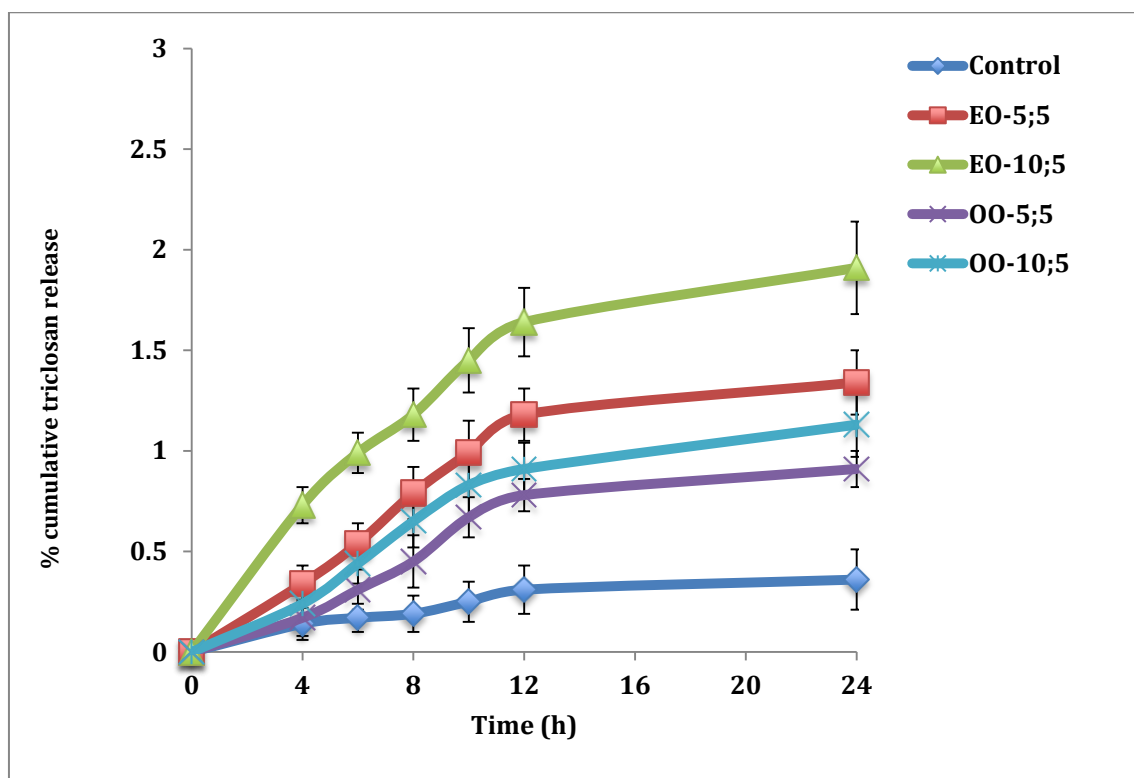


Figure 4.10 *In vitro* release profiles of TSN from EO-NEs (EO-5;5, EO-10;5), OO-NEs (OO-5;5, OO-10;5) and control solution (Mean  $\pm$  SD, n = 6).

Drug release from EO-NEs was higher compared to the OO-NEs and control, which might be due to smaller droplet size and lower viscosity compared to the OO-NEs. Similar results were reported by Rajan and Vasudevan (2012) for atorvastatin NEs prepared with oleic acid and having a droplet size and viscosity range similar to EO-NEs obtained in the present study. Another study reported increased ketoconazole drug release from a topical hydrogel prepared with EO, which enhanced drug release (Jain *et al.*, 2013).

#### 4.4.10 *In vitro* skin permeation study

Skin permeation studies were performed to compare the permeation of drug from optimised NE formulations (EO-5;5, EO-10;5, OO-5;5, OO-10;5) and control solution. The cumulative amount of TSN permeated, flux and permeability coefficients for the NEs and

control solution are presented in Table 4.5. The cumulative amounts of TSN that permeated through excised full thickness porcine ear skin from the NEs and control solution are shown in Figure 4.11. More drug permeated from the NE formulations compared to control, indicating the suitability of NEs as a carrier for use in dermal delivery of lipophilic drugs. Several mechanisms have been proposed to explain NEs ability to improve dermal permeation and retention. Solubility of TSN is increased by NE formulations due to presence of a lipophilic oil phase, which favours drug partition into the skin because only the fraction of the drug dissolved in the vehicle can enter the skin (Heuschkel *et al.*, 2008). NE formulations may interact with lipid layers of SC, enhancing drug permeation and retention into the skin (Malcolmson *et al.*, 1998). Also, it is proposed that NEs can carry drug through the skin due to their small droplet size (McClements and Xiao, 2012).

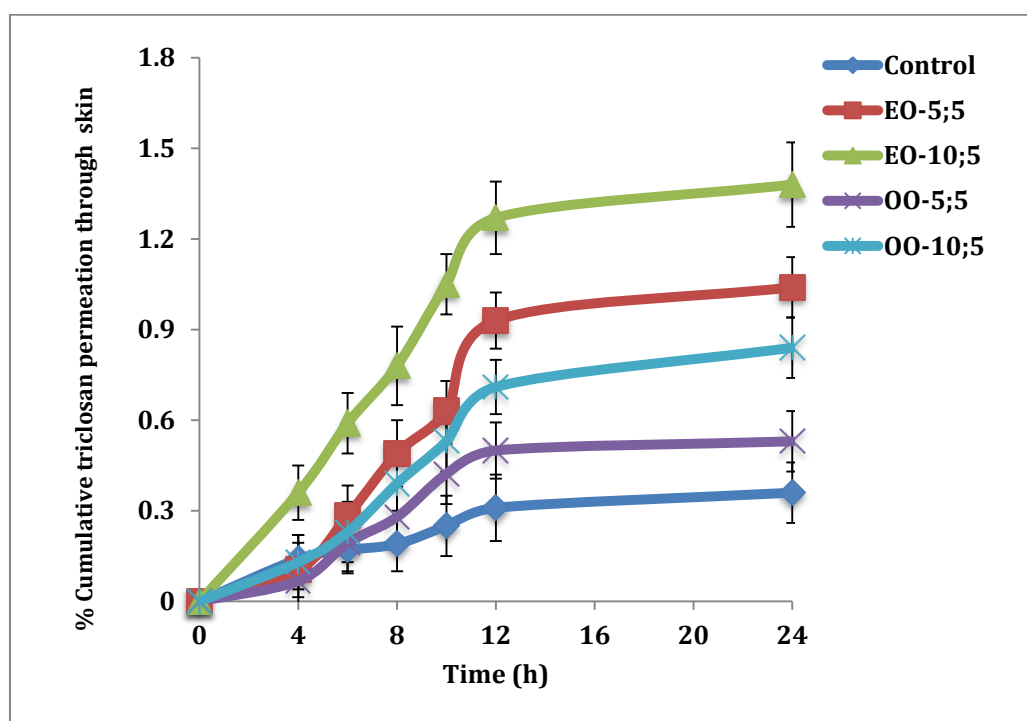


Figure 4.11 *In vitro* skin permeation profile of NE formulations (EO-5;5, EO-10;5, OO-5;5, OO-10;5) and control solution (Mean  $\pm$  SD, n = 6).

The EO-NEs showed higher drug permeation through the skin compared to the OO-NEs.

This might be due to the physicochemical properties of NEs, including higher solubility of

TSN in EO, smaller droplet size, lower viscosity and the permeation enhancing effect of EO. The *in vitro* permeation studies showed percent cumulative TSN permeated through skin is higher for EO-10;5 ( $1.38 \pm 0.02$ ) provides greater drug permeation than EO-5;5 ( $1.13 \pm 0.05$ ), OO-5;5 ( $0.48 \pm 0.006$ ), and OO-10;5 ( $0.83 \pm 0.002$ ).

Similar permeation results were reported by Shafaat *et al.* (2013) for transdermal delivery of clozapine NEs. Results showed formulation with small droplet size and low viscosity had increased the permeation uptake of clozapine through skin. Another study reported increase in the *in vitro* percutaneous delivery of sumatriptan succinate formulation using EO by a mechanism in which the terpenes modify the barrier properties of the SC, improving drug partitioning into the tissue (Femenía-Fonta *et al.*, 2005; Williams and Barry, 1991). In the present study, statistical analysis showed significant differences ( $p < 0.05$ ) between the steady-state flux values obtained for EO-NEs and those of the OO-NEs (Table 4.6)

Table 4.6 *In vitro* skin permeation parameters for NEs and control solution (Mean  $\pm$  SD, n = 6).

Formulation Code	Flux ( $J_{ss}$ ) $\mu\text{g}/\text{cm}^2/\text{h}$	Permeability coefficient ( $K_p$ ) $\times 10^{-5}$ cm/h
Control	0.086	0.86
EO-5;5	0.497	4.97
EO-10;5	0.315	3.15
OO-5;5	0.195	1.95
OO-10;5	0.236	2.36

#### 4.4.10.1 Quantification of triclosan in skin using adhesive tape stripping method

Tape stripping method is used to quantify the amount of drug retained within the skin. Adhesive tapes were used to remove the superficial layers of SC, which were then analysed for drug content (Lademann *et al.*, 2009; Weigmann *et al.*, 2009). TSN levels in different layers of skin were studied using the adhesive tape stripping method and the results are presented in Figure 4.12.

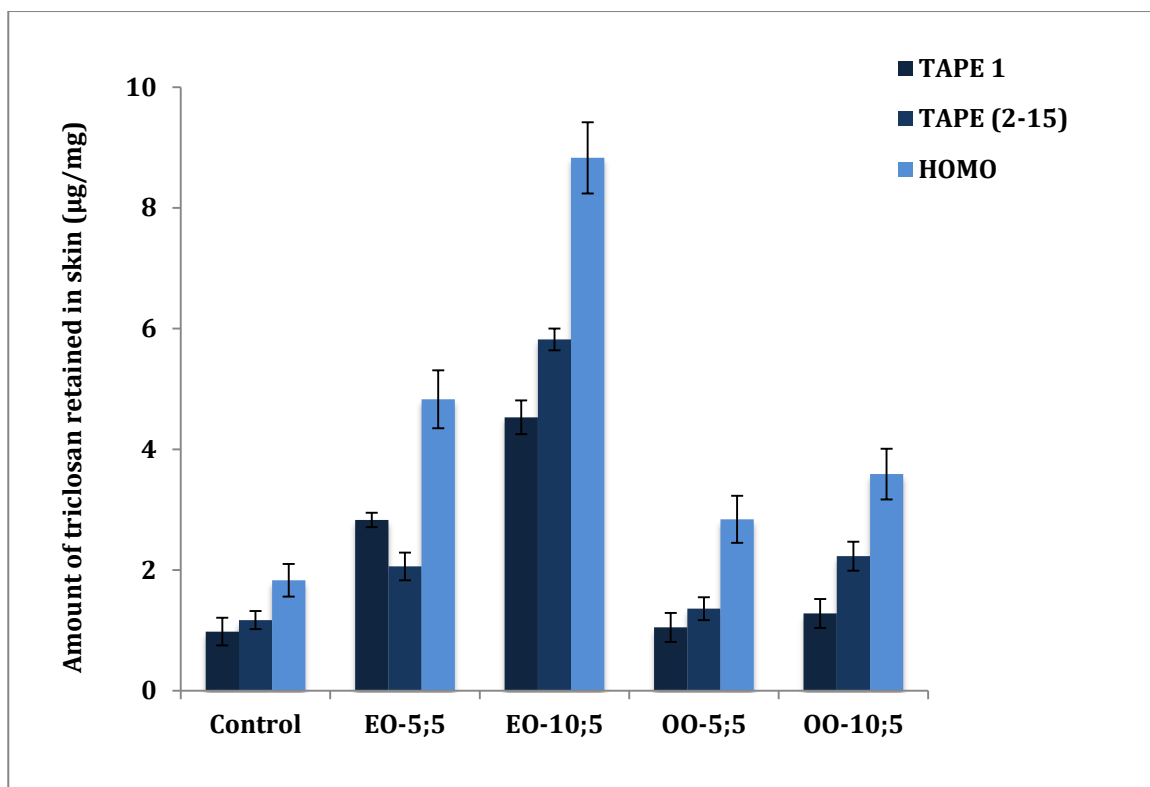


Figure 4.12 *In vitro* profile of TSN accumulation in skin layers 24 h following topical application of control, EO-NEs (EO-5;5, EO-10;5) and OO-NEs (OO-5;5, OO-10;5) (Mean  $\pm$  SD, n = 6). HOMO refers to homogenised tissue after removal of the SC layers.

The NE formulations resulted in higher amounts of TSN retained in the skin compared to the control, with the difference being statistically significant ( $p < 0.05$ ). Encapsulation of TSN into nanosized oil droplets increases skin hydration, improving the delivery of drug through the skin. The large surface area of the NE systems enhances the penetration of drug through the skin surface (Tharwat *et al.*, 2004). The data obtained from adhesive tape stripping method (Tape 1 – Tape 15) shows difference in TSN retention between the EO-NEs and OO-NEs. The TSN level for the control solution was  $2.15 \pm 0.03$   $\mu\text{g}/\text{mg}$ , compared to the NE formulations, which were  $4.89 \pm 0.15$   $\mu\text{g}/\text{mg}$ ,  $10.35 \pm 0.05$   $\mu\text{g}/\text{mg}$ ,  $2.41 \pm 0.07$   $\mu\text{g}/\text{mg}$  and  $3.51 \pm 0.08$   $\mu\text{g}/\text{mg}$  for EO-5;5, EO-10;5, OO-5;5 and OO-10;5, respectively.

TSN retention in skin was higher for EO-NEs compared to the OO-NEs, which aligns with the *in vitro* drug release and skin permeation data discussed in previous study (Sections 4.4.9 and 4.4.10). EO contains about 80 % cineole, which has been reported to be a skin penetration enhancer (Amin *et al.*, 2008; Saify *et al.*, 2000; Shen *et al.*, 2013). A study by Williams and Barry (1989) reported the penetration enhancement activities of EO through excised human skin using 5-fluorouracil as a model drug.

#### 4.4.11 Comparison of skin penetration of lipid nanocarriers for topical delivery of triclosan using *in vitro* diffusion studies

Nanocarriers such as SLNs and NEs were prepared and characterised individually to evaluate their ability to deliver TSN into skin. GP-SLNs and EO-NEs were found to have better skin retention ability compared to other prepared formulations hence, similar formulations containing 5 % w/w solid lipid (GP5-2) and 5 % w/w liquid lipid EO-NEs (EO-5;5) were selected. Figure 4.13 depicts the amount of TSN in the skin obtained using adhesive tape stripping method for SLNs and NEs.

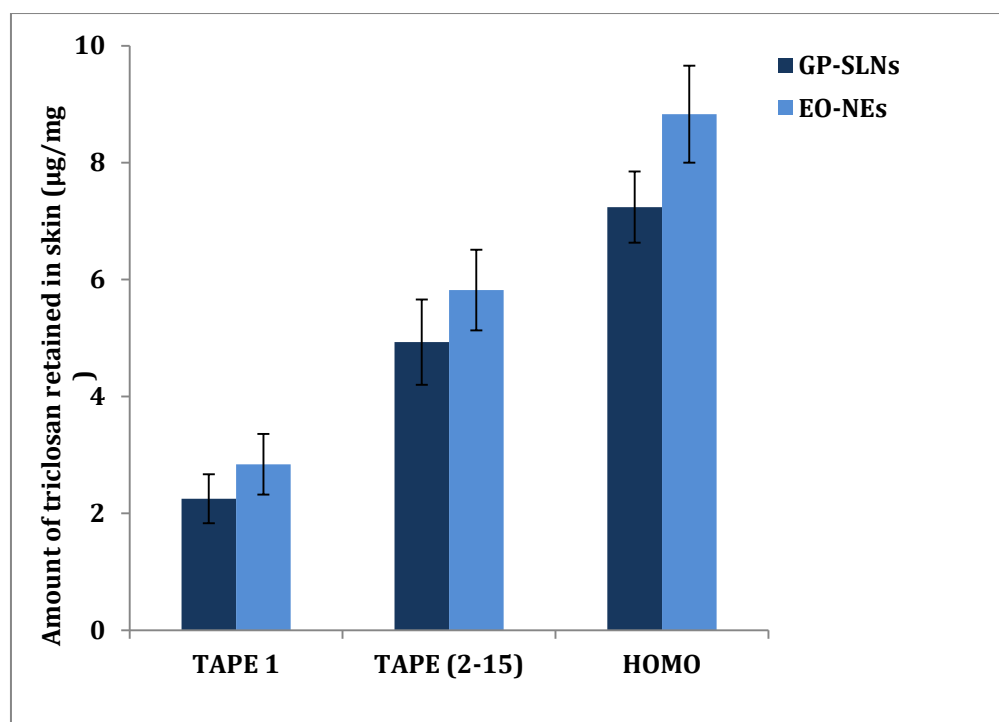


Figure 4.13 Amount of triclosan in the skin following application of GP-SLNs (GP5-2) and EO-NEs (EO-5;5) (Mean  $\pm$  SD, n = 6).

The total amount of TSN recovered from the skin was higher for NEs ( $17.49 \pm 0.16 \mu\text{g/mg}$ ) compared to SLNs ( $14.42 \pm 0.27 \mu\text{g/mg}$ ) with the difference being statistically significant ( $p < 0.05$ ). This might be due to the difference in composition and physical state of lipids used in preparation of SLNs and NEs. SLNs were composed of lipids containing mono and diglycerides whereas NEs were produced using oils composed of mixtures of mono-, di- and triglycerides. In addition, SLNs contains a solid lipid core compared to the soft flexible core in NEs.

A similar study reported by Aditya *et al.*, (2014) evaluated the effect of composition and physical state on the quercetin bioaccessibility in simulated intestinal conditions using different lipid nanocarriers. They found lower bioaccessibility from SLNs compared to NEs. This may be attributed by the formation of a less ordered lattice defect in NEs with more space for guest molecules (Nayak *et al.*, 2010; Severino *et al.*, 2012). This is in line with other studies reported by Clares *et al.*, (2014), in which retinyl palmitate was encapsulated in SLNs and NEs, and drug permeation was higher from NEs. It was reported that the



penetration enhancement of vehicles through the skin depends on the flexibility of the carrier (Garduno-Ramirez *et al.*, 2012).

#### 4.5 Conclusion

The NE formulations containing TSN were formulated using EO and OO by HSH followed by ultrasonication. Pseudoternary phase diagrams studies allowed the identification of different regions, as well as the selection of maximum and minimum concentrations of each component required for obtaining stable formulations. The effect of different concentrations of oil phase and surfactant on droplet size distribution and other physicochemical parameters were studied. Amount of TSN released and permeated through artificial membrane and full thickness porcine skin was evaluated by diffusion studies.

TSN-loaded NEs were prepared successfully using EO and OO, with EO-NEs having smaller droplet size and higher % DEE compared to OO-NEs. Concentrations of oil and surfactant had opposing actions on droplet size, with an increase in the oil phase increasing droplet size while an increase in surfactant concentration caused a decrease in droplet size. Morphological studies confirmed the formation of spherical NEs droplet while thermal and structural characterisation demonstrated the molecular dispersion of drug within the oil phase of the formulation. Optimised formulations containing 5 % w/w and 10 % w/w EO-NEs and OO-NEs (EO-5;5, EO-10;5, OO-5;5, OO-10;5) were selected for further *in vitro* drug release and permeation studies. EO-NEs demonstrated higher drug permeation through skin compared to OO-NEs due to the influence of physicochemical properties such as higher solubility of TSN in EO, smaller droplet size, low viscosity and permeation enhancement effects of EO. Higher amounts of TSN were recovered from skin following application of NE formulation EO-10;5 ( $10.35 \pm 0.05$   $\mu\text{g}/\text{mg}$ ) compared to other NE formulations. The results reported in this work clearly demonstrate the potential of these NEs for enhanced topical dermal delivery.

## **5. CHAPTER – NANOEMULSIONS AS CARRIERS OF HYDROPHILIC COMPOUNDS FOR TOPICAL DELIVERY**

### 5.1 Introduction

HAIs are caused either by a medical intervention such as a surgical procedure or from contact within a healthcare setting. Although they cover a wide range of infections, SSIs are the most commonly reported nosocomial infections, accounting for 14–16 % of all nosocomial infections among hospital patients (Smyth and Emmerson, 2000). SSIs are the result of contamination of skin during pre or post-surgical procedure by microorganisms originated either from patient's own flora or any contaminated item in the sterile surgical field, including a device or the hubs of an intravascular device.

CHG has been an important components as a topical antiseptic agent for more than 50 years to reduce the risk of HAIs (Edmiston *et al.*, 2007; Hibbard, 2005; Holder and Zellinger, 2009). It is used as either in the form of aqueous or alcoholic solution in surgical environment to disinfect the skin prior to surgery. CHG is a bisbiguanide with broad spectrum antiseptic activity against a wide range of both Gram-positive and Gram-negative bacteria and lipophilic viruses (Pratt *et al.*, 2007). The effectiveness and widespread use of CHG has led to some concern over the emergence of bacterial resistance. Many studies have been performed to understand the CHG resistance over various microorganisms (Barry *et al.*, 1999; Zhang *et al.*, 2011).

Karpanen *et al.* (2008) reported poor permeation of CHG from 2 % w/v aqueous solution into the deeper layers of the skin. Therefore, there is a need to develop an effective carrier system or formulations in order to achieve effective skin antiseptics to permeate CHG deeper into skin. This includes potentially using CHG with a combination of other antimicrobial agents or permeation enhancers.

EO has been used medicinally and is recognised as possessing broad spectrum antimicrobial and permeation enhancement activities (Edris, 2007). Due to its antibacterial properties, EO is a common ingredient in topical antiseptics, soaps and mouthwashes. Furthermore, it is generally considered safe when applied topically (Higgins *et al.*, 2015). The addition of EO to CHG was shown to significantly enhance skin penetration of CHG into the epidermis and dermis (Karpanen *et al.*, 2010). Another oil, OO has been used for health and personal care for thousands of years: Egyptian pharaohs used it to moisturise their skin and hair, whereas the Romans used it to treat wounds. Badiu *et al.* (2010) reported beneficial effects of OO on capillary blood flow and endothelial function, the exact mechanism of which is currently unknown.

Altrazeal<sup>®</sup>, a flexible methacrylate dressing (Uluru Inc., Addison, TX, USA), supplied as powder, contains a hydrophilic polymer consisting of a methacrylate backbone and terminal hydroxyl group. Altrazeal can be directly applied into a wound, or can be hydrated with saline or another sterile solution, resulting in rapid hydration of methacrylate particles to form a strong uniform gel material that can conform to surfaces in the wound bed. Altrazeal has also been studied as a drug delivery vehicle for various cationic and anionic wound antiseptics, such as povidone-iodine, polyhexamethylene biguanide and octenidine dihydrochloride (Forstner *et al.*, 2013).

Human skin has been widely used as a model for studying *in vitro* diffusion of transdermal and topical formulations. However, human skin suffers from high biological variability such as thickness of the skin, lipid content and lipid composition (Schmook *et al.*, 2001; Trauera *et al.*, 2014). Recently, Strat-M<sup>®</sup> membrane (Merck Millipore, UK) has become available commercially as an artificial skin mimic membrane. As a synthetic membrane, it has low batch-to-batch variability, thus providing more consistent data. Takashi *et al.*, (2015) evaluated the permeation of parabens, lidocaine hydrochloride, antipyrine, aminopyrine and isosorbide dinitrate using Strat-M membrane. Results showed similar

permeability coefficients and partition coefficient values as human and animal skin models. Hence, in the present research work Strat-M membrane was used to analyse CHG permeation and was compared with permeability coefficient data obtained using porcine ear skin as an *in vitro* skin model.

The present work includes the formulation and evaluation of various CHG-NE formulations using oils such as EO and OO, and S80 and T80 as a surfactant and cosurfactant mixture ( $S_{\text{mix}}$ ). *In vitro* drug release and skin permeation of CHG were studied using different synthetic membranes and excised full thickness porcine ear skin, respectively.

## 5.2 Aims of the study

The aims of this study were,

- To evaluate NEs as hydrophilic drug carriers for CHG by preparing various compositions of NEs using EO and OO as oil phase for topical dermal delivery.
- To characterise the prepared NE formulations based on their physicochemical properties and to compare the drug release, skin permeation and retention of CHG using dialysis membrane, Strat-M membrane and excised full thickness porcine ear skin.
- To study the impact of damage SC on drug permeation using adhesive tape stripping method to mimic wound condition by *in vitro* skin diffusion study.
- To evaluate a methacrylate powder dressing as a drug delivery vehicle to control the release of CHG by *in vitro* skin diffusion study.

### 5.3 Materials and Method

#### Materials:

Chlorhexidine digluconate solution (20 % w/v), eucalyptus oil, olive oil, Tween<sup>®</sup> 80, Span<sup>®</sup> 80 and dialysis membrane were purchased from Sigma Aldrich (UK). Altrazeal<sup>®</sup> powder was a gift from Uluru Inc, UK. Strat-M<sup>®</sup> membrane was purchased from Merck Millipore, UK. All other reagents used were of analytical grade.

#### 5.3.1 Construction of pseudoternary phase diagrams

Pseudoternary phase diagrams for the development of NEs were prepared using water, S80, T80, and EO or OO as the aqueous, surfactant, cosurfactant and oil phases, respectively. W/O type NEs were prepared using an oil phase titration method (Shakeel and Ramadan, 2010; Shakeel *et al.*, 2013). S80 and T80 were mixed in mass ratios of 1:0, 1:1, 2:1, 3:1 and 4:1. Aqueous phase and specific ratios of  $S_{mix}$  were combined using a vortex mixer in mass ratios ranging from 1:9 to 9:1. The mixtures of aqueous phase and  $S_{mix}$  were titrated using the slow addition of the oil phase (EO, OO), and pseudoternary phase diagrams were constructed using JMP 11 software (SAS Institute Inc., USA) and NE regions were identified based on visual observations.

#### 5.3.2 Formulation of chlorhexidine digluconate nanoemulsions

CHG-NEs were prepared using the previously described HSH followed by probe ultrasonication (Urban and Wagner, 2006). The hot oil phase was prepared using either EO or OO with S80 by heating at 40°C to ensure effective mixing, while the hot aqueous phase was prepared by mixing CHG (equivalent to 20 mg/g of formulations) with T80 and water at same temperature. The hot aqueous phase was slowly added into the hot oil phase under HSH (Silverson, UK). This primary hot emulsion was subjected to ultrasonication (Sonics and Materials Inc., USA) for 10 min using 70 % frequency amplitude for further size reduction of the droplets. The preliminary composition of the NE mixtures, as defined in the

isotropic regions of the pseudoternary phase diagrams, were prepared using different ratios of  $S_{mix}$  and are presented in Table 5.1.

Table 5.1 Composition of preliminary CHG-loaded NE formulations.

Formulation Code	Oil		S80: T80 (2:1) % w/w
	Type	Concentration (% w/w)	
C-EO-70(5)	Eucalyptus oil	70	5
C-EO-70(10)			10
C-EO-70(15)			15
C-EO-75(5)		75	5
C-EO-75(10)			10
C-EO-75(15)			15
C-OO-70(5)		Olive oil	70
C-OO-70(10)			10
C-OO-70(15)			15
C-OO-75(5)	75		5
C-OO-75(10)			10
C-OO-75(15)			15



### 5.3.3 Physicochemical characterisation of nanoemulsion formulations

All physicochemical characterisation, i.e., determination of droplet size, PDI, ZP, % DEE, pH, viscosity, morphological examination using TEM, FTIR, and accelerated thermal stress testing were carried out as described in detail in the chapter 4 (Section 4.3.4).

#### 5.3.3.1 *In vitro* drug release and skin permeation studies

*In vitro* drug release and skin permeation studies for the CHG-NE formulations were carried out using Franz diffusion cells. The setup and experimental conditions were similar to those described in the chapter 3 (Section 3.3.3.9), except for the receiver medium, which contained PBS (pH 7.4) without the use of SLS. For the release studies, a cellulose acetate membrane (Sigma Aldrich, UK), 23 mm in diameter, with a molecular weight cut off of 12-14 kDa was selected and for the skin permeation studies excised full thickness porcine ear skin was used.

An aqueous solution of CHG (2 % w/v) was used as a control solution. The dialysis membrane or skin was equilibrated for 30 min before loading NE formulations (equivalent to 20 mg/g CHG concentration) or similar concentration of control solution to donor compartment and covered with Parafilm to prevent evaporation. Subsequently, 500 µl samples were collected from the receiver compartment at 4, 6, 8, 10, 12 and 24 h and replaced by an equal volume of fresh receiver medium to maintain sink conditions. All samples were analysed for amount of CHG released or permeated using HPLC (Section 2.2.1.1). The cumulative amount of CHG released, or the amount that permeated through the artificial membrane or porcine ear skin was plotted as a function of time.

### 5.3.3.2 Quantification of chlorhexidine digluconate in skin using adhesive tape stripping method

The amount of CHG retained within the skin following application of the NE formulations and the control solution was quantified using the adhesive tape stripping method. The tape stripping method was performed and the samples were analysed as similar as described in chapter 3 (Section 3.3.3.9.2).

### 5.3.3.3 *In vitro* skin diffusion studies of chlorhexidine digluconate nanoemulsions using methacrylate dressing powder

Altrazeal dressing powder was studied as a drug delivery vehicle for CHG using the *in vitro* Franz diffusion cells. Accurately weighed Altrazeal powder (500 mg) was placed in the donor compartment and loaded with NE formulations or control solution (equivalent to 20 mg/g CHG concentration) using a micropipette. Addition of cationic CHG caused hydration of methacrylate polymer particles, transforming the powder into a porous gel matrix (Figure 5.1), for detailed gelation mechanism refer Section 5.1. The amount of CHG that permeated into receiver compartment after 24 h and the amount retained within skin was analysed using HPLC.



Figure 5.1 Hydrogel conversion of methacrylate powder dressing following the addition of CHG-NEs [C-EO-70(10)].

#### 5.3.3.5 *In vitro* diffusion studies of chlorhexidine digluconate permeation using porcine ear skin and Strat- M<sup>®</sup> membrane

In the present study, *in vitro* permeation was performed with Strat-M membrane and excised full thickness porcine ear skin, in order to compare the permeability coefficient and flux of the applied CHG-NE formulations and control solution (equivalent to 20 mg/g CHG concentration). The experimental set up and conditions was as similar as described in previous study (Section 5.3.3.1) and the amount of CHG released or permeated into receiver medium was analysed by HPLC (Section 2.2.1.2).

#### 5.3.3.6 Studies of chlorhexidine digluconate penetration into barrier-intact and barrier-impaired porcine ear skin

The treatment of skin infections and wounds implies the application of a drug to skin having a damaged or completely removed epidermal barrier, which is likely to affect the penetration profile of the carrier and drug substance into the skin. To mimic this effect, the skin barrier was disrupted using 15 successive adhesive tape strips using surgical tape (3M Transpore, UK) as described by Simonsen and Fullerton (2007). *In vitro* diffusion studies were carried out as described in Section 5.3.3.1 using barrier-intact and barrier-impaired excised full thickness porcine ear skin. The influence of skin barrier properties on the penetration profile of CHG from NE formulations and control solution was studied.

#### 5.3.3.7 Statistical analysis

All measurements were repeated at least three times and the data are reported as the mean  $\pm$  SD. Data obtained was statically analysed by one way ANOVA using GraphPad Prism 5 software. Differences were considered to be statistically significant at  $p < 0.05$ .

## 5.4 Results and Discussion

### 5.4.1 Pseudoternary phase diagrams

Various CHG-NEs were prepared by constructing pseudoternary phase diagrams with water, S80, T80, and EO or OO as the aqueous, surfactant, cosurfactant and oil phases, respectively. The pseudoternary phase diagrams were developed using the oil titration method for each  $S_{mix}$  to identify the NE zones. The resulting diagrams are presented in Figures 5.2, 5.3 and 5.4.

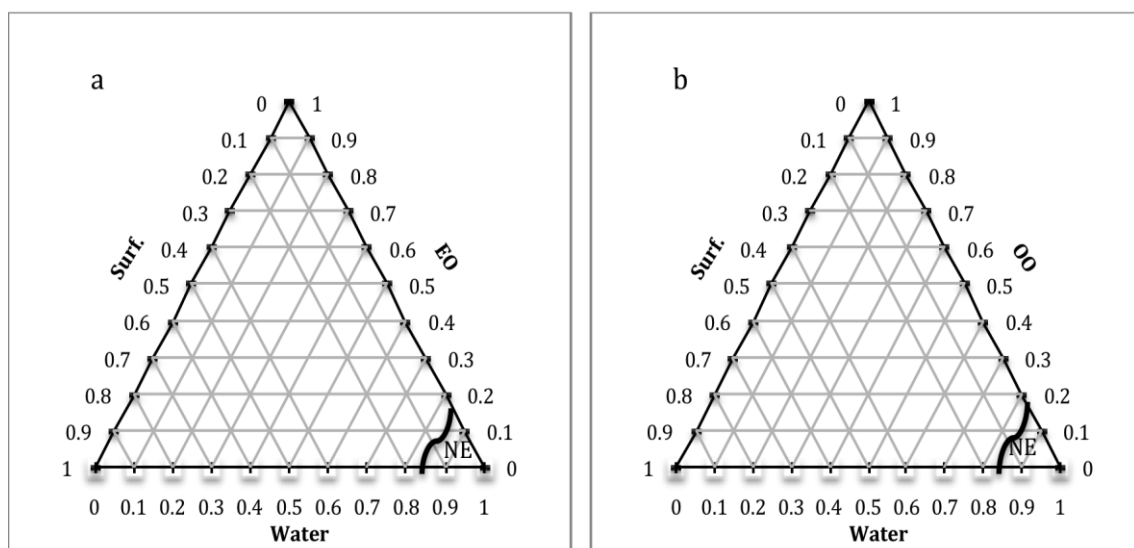


Figure 5.2 Pseudoternary phase diagrams of a) eucalyptus oil and b) olive oil with surfactant (S80) and water.

It was observed that when S80 was used alone without T80 ( $S_{mix}$  ratio 1:0), only a small amount of aqueous phase was incorporated at higher concentrations of S80 for both EO and OO (Figure 5.2). The maximum amount of water that could be added was found to be 10 % w/w at a high (81 % w/w)  $S_{mix}$  concentration. However, when S80 and T80 concentrations were kept equal ( $S_{mix}$  ratio 1:1), the NEs zones increased slightly as compared to the 1:0 ratio. The aqueous phase found to be solubilised to only 17 % w/w when the  $S_{mix}$  concentration was 63 % w/w (Figures 5.3a and 5.4a).

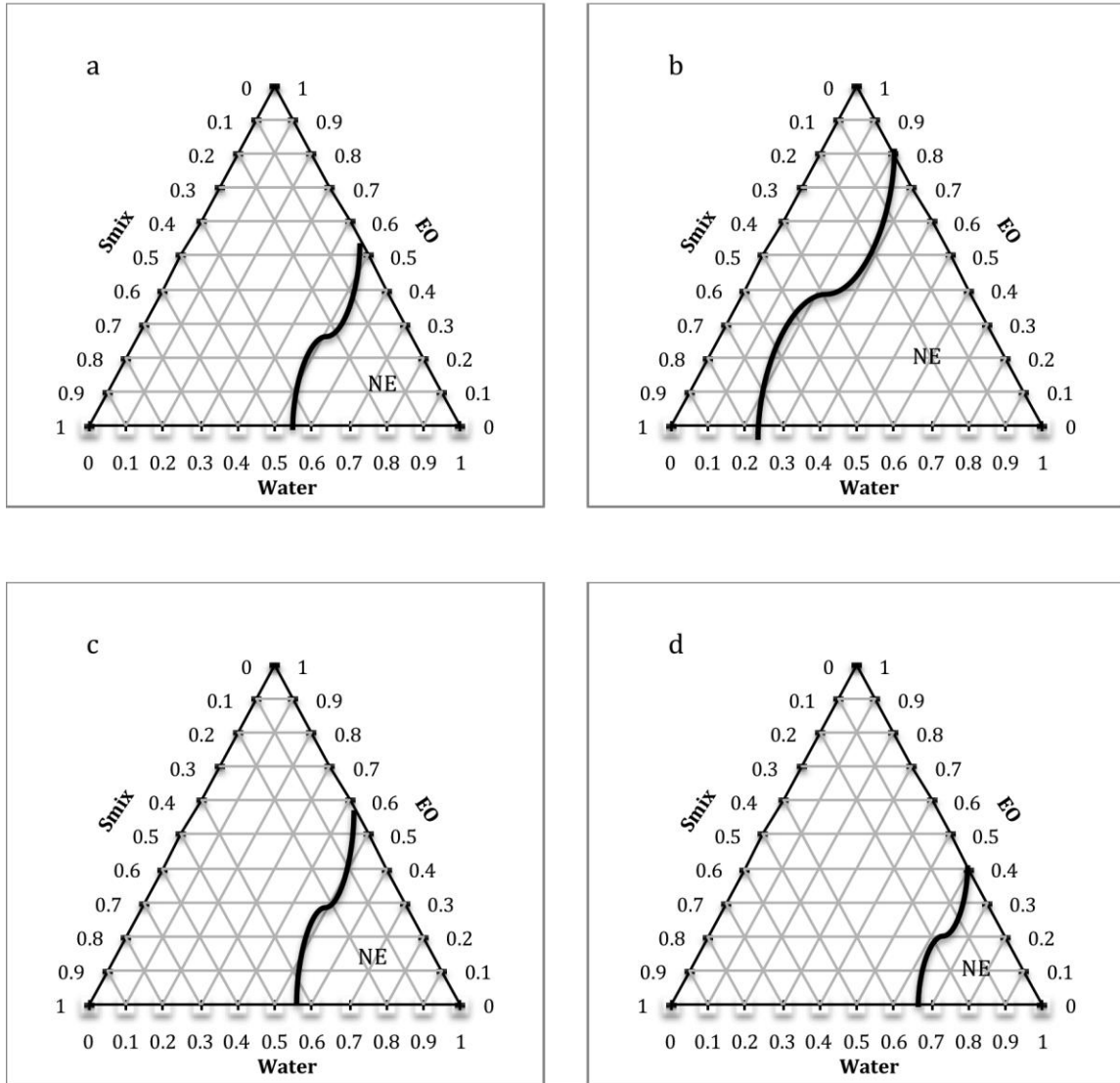


Figure 5.3 Pseudoternary phase diagrams of eucalyptus oil, water and different ratios of surfactant mixture (S80:T80) a) Smix 1:1, b) Smix 2:1, c) Smix 3:1, d) Smix 4:1.

When the  $S_{mix}$  ratio was increased to 2:1, it was observed that the NE zone increased markedly as compared to  $S_{mix}$  ratio 1:1 (Figures 5.3b and 5.4b), allowing 31 % w/w incorporation of the aqueous phase with a lower concentration (20 % w/w) of  $S_{mix}$ . However, when the  $S_{mix}$  ratio was increased to 3:1, the NE zone decreased compared to the 2:1 ratio (Figure 5.3c and 5.4c). The maximum amount of aqueous phase solubilised was 26 % w/w when incorporating 45 % w/w  $S_{mix}$ . Upon further increasing the  $S_{mix}$  ratio to 4:1, the NE zone decreased further compared to the 2:1 and 3:1 ratios (Figure 5.3d and 5.4d). As

indicated by the phase diagrams, the maximum NE zone was achieved at a  $S_{mix}$  ratio of 2:1.

Therefore, this ratio was used in the preliminary NE formulations.

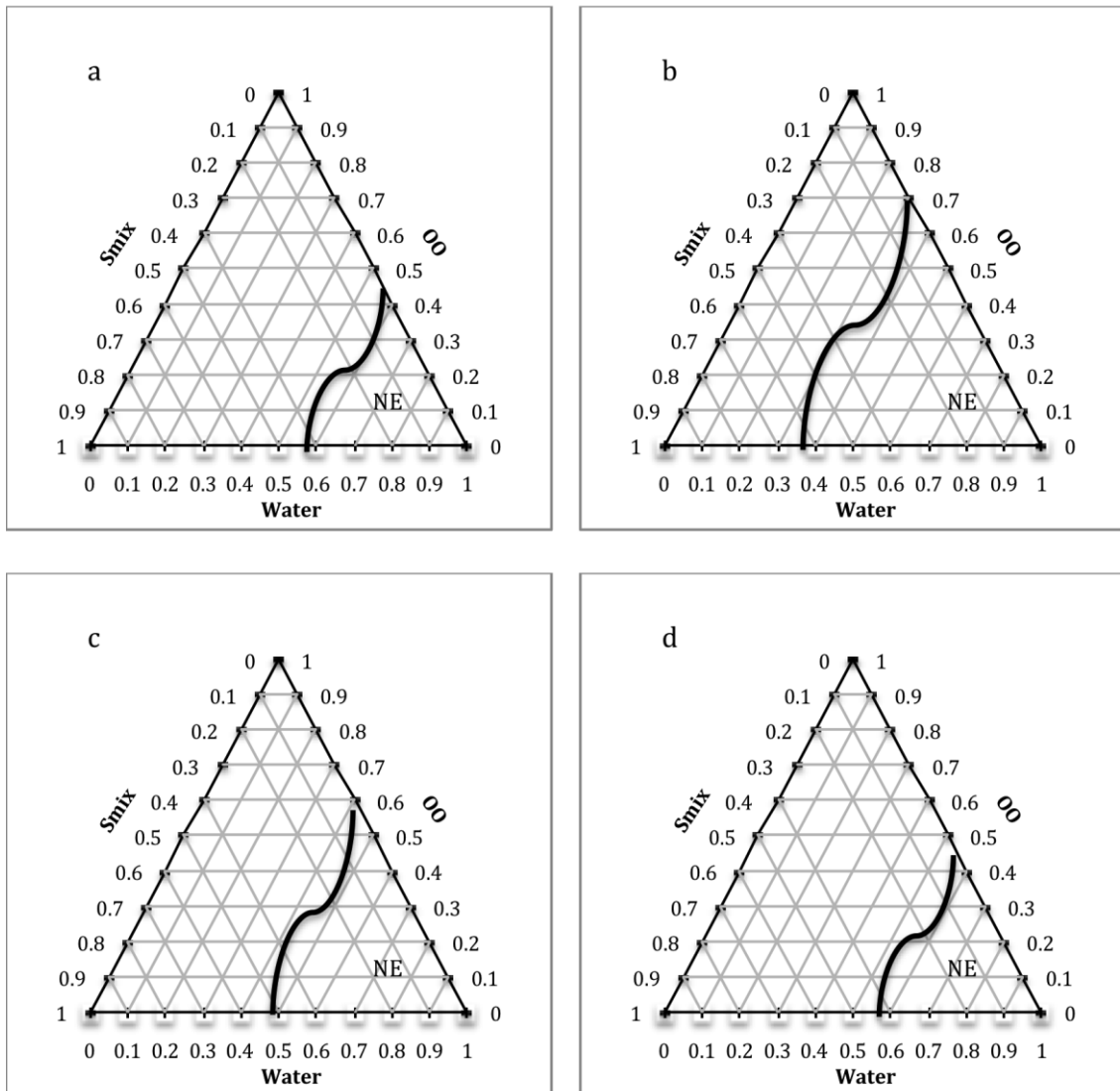


Figure 5.4 Pseudoternary phase diagrams of olive oil, water and different ratios of surfactant mixture (S80:T80) a)  $S_{mix}$  1:1, b)  $S_{mix}$  2:1, c)  $S_{mix}$  3:1, d)  $S_{mix}$  4:1.

#### 5.4.2 Preparation and characterisation of nanoemulsions

W/O NEs of CHG were prepared using a HSH followed by ultrasonication method. The initial batches of CHG-EO and CHG-OO NEs were prepared using different concentrations of  $S_{\text{mix}}$  2:1 (5, 10 and 15 % w/w), while the concentrations of oil used were 70 and 75 % w/w to maintain CHG concentrations (loading dose of 20 mg/g CHG) in final formulation. The low weight percentage of water was selected to minimise droplet collision, and excess surfactant was used (up to 15 % w/w) to minimise coalescence.

##### 5.4.2.1 Influence of homogenisation stirring speed and processing time

It has been reported that droplet size depends on the energy input, e.g. stirring speed and time of homogenisation (Jasińska *et al.*, 2014). The effect of different homogenisation speeds (4000 to 10,000 rpm) and time (10, 15 and 20 min) on the mean droplet size was determined for CHG-EO [C-EO-70(10)] and CHG-OO [C-OO-70(10)] NE formulations are shown in Figure 5.5.

As homogenisation speed increased from 4000 rpm to 10,000 rpm, there was a decrease in droplet size, due to higher deformation stress. The decrease in mean droplet size measured immediately after preparation of NEs was from  $764 \pm 12.24$  nm to  $273 \pm 17.51$  nm for the CHG-EO NEs, while in case of the CHG-OO NEs, mean droplet size decreased from  $851 \pm 13.47$  nm to  $308 \pm 9.36$  nm. Differences in droplet size may be due to the different physicochemical properties of EO and OO such as their chemical composition, viscosity and HLB values (Orafidiya and Oladimeji, 2002). It may be possible to decrease the droplet size further using HSH but due to the specification of homogeniser used, the highest available speed was 10,000 rpm hence, the homogenisation speed used for preparation of NEs was 10,000 rpm.

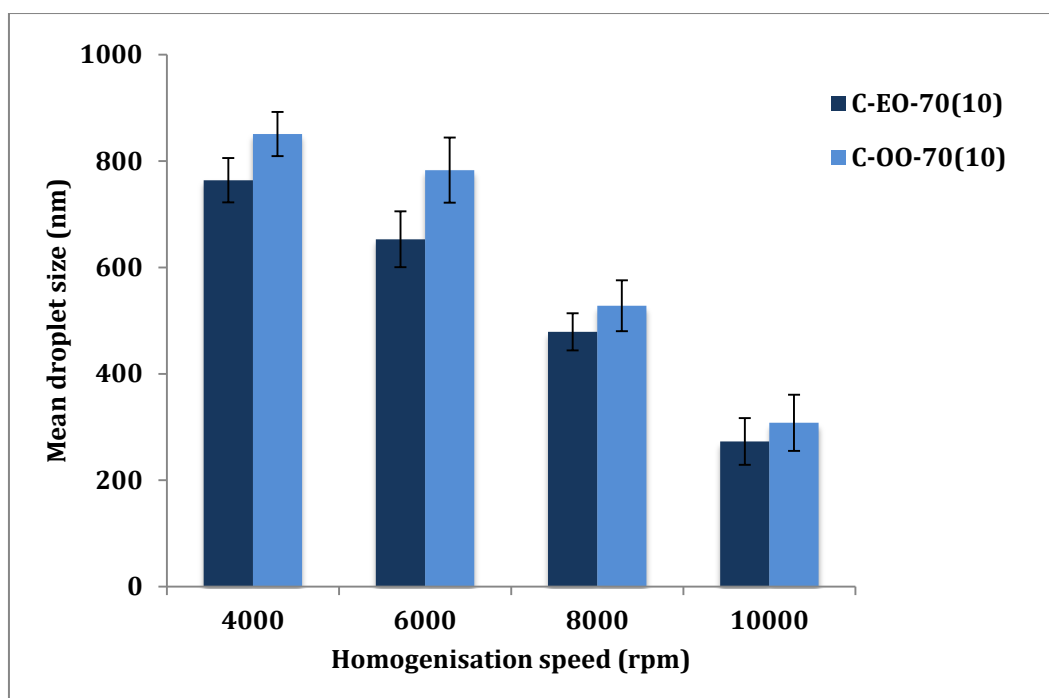


Figure 5.5 Influence of homogenisation speed on droplet size of CHG-loaded EO-NEs [C-EO-70(10)] and CHG-OO NEs [C-OO-70(10)] (Mean  $\pm$  SD, n = 3).

Droplet size reduced as homogenisation time was extended for both CHG-EO and CHG-OO NEs (Figure 5.6). When the homogenisation time increased from 10 min to 15 min, the droplet size of the CHG-EO NEs decreased from  $492 \pm 10.34$  nm to  $271 \pm 14.31$  nm, while the CHG-OO NEs droplet size decreased from  $574 \pm 18.24$  nm to  $315 \pm 16.71$  nm. However, when the duration was further increased to 20 min, there was a slight increase in droplet size for both the CHG-EO NEs and CHG-OO NEs. Similar results were reported by Tang *et al.*, (2013) for the formulation of an aspirin NEs using an ultrasonication method, which showed increase in processing duration led to a decrease in NEs droplet size. Qian and McClements, (2011) reported that, with certain types of emulsifiers extended durations of homogenisation may lead to “over-processing” which caused an increase in droplet size. The preliminary CHG-NEs were formulated using 10,000 rpm homogenisation speed for 15 min followed by ultrasonication for 10 min at 70 % frequency amplitude.



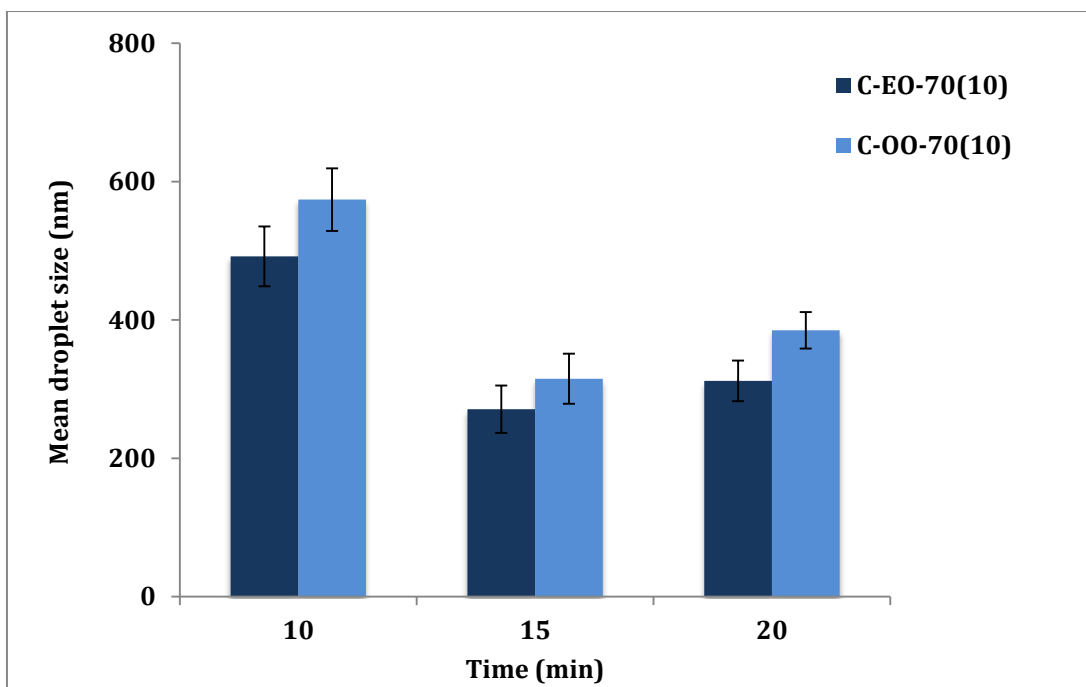


Figure 5.6 Influence of duration of homogenisation on droplet size of CHG-loaded OO-NEs [C-EO-70(10)] and CHG-OO NEs [C-OO-70(10)] (Mean  $\pm$  SD, n = 3).

#### 5.4.2.2. Influence of surfactant concentration

The type and concentration of surfactants used to prepare W/O CHG-NEs are very important because they affect the droplet size and its distribution, along with formulation stability. A series of NEs containing 5, 10 and 15 % w/w  $S_{mix}$  (2:1) in the oil phase were prepared and the effects of surfactant concentration on droplet size and PDI was determined by using NTA, which are shown in Table 5.2.

Droplet size decreased when surfactant concentration was increased from 5 to 10 % w/w for both CHG-EO and CHG-OO NE formulations. This effect demonstrates the dynamic equilibrium between droplet break up and coalescence present in the emulsion (Niknafs *et al.*, 2011). At low concentrations, the levels of surfactant in the water-oil interfacial layer are not sufficient to completely cover the surface of the drops causing coalescence and flocculation of droplets, thus leading to increased size.

Table 5.2 Influence of surfactant concentration on droplet size and distribution of CHG-loaded EO-NEs and OO-NEs (Mean  $\pm$  SD, n = 3).

Formulation	Droplet size (nm)	PDI	Formulation	Droplet size (nm)	PDI
C-EO-70(5)	389.2 $\pm$ 9.2	0.74 $\pm$ 0.15	C-OO-70(5)	415.2 $\pm$ 10.5	0.85 $\pm$ 0.03
C-EO-70(10)	257.5 $\pm$ 12.4	0.56 $\pm$ 0.13	C-OO-70(10)	285.3 $\pm$ 13.4	0.61 $\pm$ 0.06
C-EO-70(15)	291.3 $\pm$ 15.8	0.62 $\pm$ 0.24	C-OO-70(15)	338.2 $\pm$ 12.4	0.69 $\pm$ 0.04
C-EO-75(5)	438.4 $\pm$ 13.9	0.81 $\pm$ 0.02	C-OO-75(5)	485.1 $\pm$ 14.8	0.73 $\pm$ 0.07
C-EO-75(10)	305.4 $\pm$ 12.2	0.59 $\pm$ 0.07	C-OO-75(10)	348.1 $\pm$ 4.7	0.64 $\pm$ 0.05
C-EO-75(15)	341.8 $\pm$ 17.5	0.63 $\pm$ 0.15	C-OO-75(15)	382.7 $\pm$ 18.4	0.74 $\pm$ 0.04

Increasing the surfactant concentration results in a greater number of surfactant molecules migrating from the aqueous phase to the oil phase, producing nanodroplets (Saber *et al.*, 2013). However, increasing the surfactant concentration up to 15 % w/w both increased droplet size and resulted in a broader PDI. By increasing the surfactant concentration, the surfactant can form micelles in the continuous phase rather than orienting at the particle surface, resulting in increased local osmotic pressure, thus causing depletion of the continuous phase between droplets. Consequently, aggregation takes place and particle size increases (Wulff-Perez and Torcello-Gomez, 2009).

#### 5.4.3 Thermal stability study

Thermodynamic stability tests were performed to identify any unstable or metastable NEs compositions (Shakeel *et al.*, 2014a, 2014b). All of the prepared formulations were

subjected to stability studies that included centrifugation, heating-cooling and freeze-thaw cycles, as described in detail in chapter 4 (Section 4.4.4).

The C-EO-75(5) NE formulation underwent phase separation following centrifugation, while the other formulations were stable (Table 5.3). These were then subjected to thermal stress under two different conditions, 4°C and 25°C. Only the formulations that remained stable were then subjected to the freeze-thaw cycle. The formulations containing 10 % w/w  $S_{\text{mix}}$  for both EO [C-EO-70(10), C-EO-75(10)] and OO [C-OO-70(10), C-OO-75(10)] were found to be stable under all three testing conditions.

Based on the results obtained from studies of effect of different homogenisation speed, time and stability studies, the CHG-EO NEs [C-EO-70(10), C-EO-75(10)] and CHG-OO NEs [C-OO-70(10), C-OO-75(10)] each containing a surfactant concentration of 10 % w/w, were found to have the smallest droplet size, PDI and stable under all thermal stress studies, thus these formulations were selected for further physicochemical characterisation and *in vitro* diffusion studies.

Table 5.3 Thermal stability assessments of CHG-loaded EO-NE and OO-NE formulations.

Formulation Code	Centrifugation	Heating-cooling cycle		Freeze-thaw cycle
		4°C	25°C	
C-EO-70(5)	√	X	X	N/A
C-EO-70(10)	√	√	√	√
C-EO-70(15)	√	√	X	X
C-EO-75(5)	X	N/A	N/A	N/A
C-EO-75(10)	√	√	√	√
C-EO-75(15)	√	√	X	N/A
C-OO-70(5)	√	X	N/A	N/A
C-OO-70(10)	√	√	√	√
C-OO-70(15)	√	√	X	N/A
C-OO-75(5)	√	√	√	X
C-OO-75(10)	√	√	√	√
C-OO-75(15)	√	√	X	N/A

**Note:** √ - stable (no phase separation), X – unstable (phase separation), N/A – (not applicable)

#### 5.4.4 Physicochemical characterisation of nanoemulsions

The formulations that passed the thermal stability testing were further characterised for ZP, % DEE, pH and viscosity and results are presented in Table 5.4. High zeta values have been suggested as an indicator of the physical stability of NEs, as they can ensure the creation of a high energy barrier against coalescence of the inner phase droplets (Zhao *et al.*, 2010). All formulations had high positive ZPs, ranging from  $39.53 \pm 1.21$  mV to  $47.16 \pm 1.72$  mV. This indicates a reasonable electrostatic repulsion between the droplets (Baspinar *et al.*, 2010). The positive charge of NE formulations was likely due to the presence of water soluble, positively charged CHG. The % DEE of all the NEs formulations were C-EO-70(10), C-EO-75(10), C-OO-70(10) and C-OO-75(10) were  $79.83 \pm 2.28$ ,  $82.14 \pm 1.93$ ,  $73.49 \pm 2.06$  and  $78.19 \pm 1.35$  respectively. The % DEE for both EO and OO formulations were found to be almost similar with C-EO-75(10) having the highest entrapment efficiency.

Table 5.4 Physicochemical characterisation of NE formulation (Mean  $\pm$  SD, n = 3).

Formulation	ZP (mV)	% DEE	pH	Viscosity (cP)
C-EO-70(10)	$47.16 \pm 1.72$	$79.83 \pm 2.28$	5.78	$23.08 \pm 1.14$
C-EO-75(10)	$44.82 \pm 0.91$	$82.14 \pm 1.93$	5.65	$25.15 \pm 0.94$
C-OO-70(10)	$39.53 \pm 1.21$	$73.49 \pm 2.06$	5.41	$29.31 \pm 1.29$
C-OO-75(10)	$41.91 \pm 1.23$	$78.19 \pm 1.35$	5.36	$33.46 \pm 1.73$

The pH of skin ranges between 5 and 6, with 5.5 considered to be average pH of the skin (Ohman and Vahlquist, 1998). Therefore, formulations intended for application to skin should have a pH close to this range. The pH values for all the NEs formulations prepared were found to be in the range of 5.36 to 5.78, suitable for topical application.

Viscosity of EO and OO reported in literature is 30 cP and 40 cP at 40°C respectively (Diamante and Lan, 2014; Tarabet *et al.*, 2012). Viscosities of the both CHG-EO NEs and CHG-OO NEs were less than the respective oils due to the presence of water in formulations. Similar results were reported by Shakeel *et al.*, (2015), using W/O EO-NEs, which showed a direct relationship between oil concentration and viscosities of NEs formulations.

#### 5.4.5 Morphological study

The CHG-NEs were examined using TEM to observe the droplet shape and verify the droplets size determined by NTA. The droplets of the CHG-NEs appeared dark, and the surrounding liquid appeared bright, as shown in Figure 5.7. As seen in the displayed image, the observed droplets were spherical in shape, and ranged in size from 200 nm – 300 nm. The TEM images for all the formulated NEs were similar in shape, and the droplet size range was in agreement with the NTA results (Section 5.4.2.2).

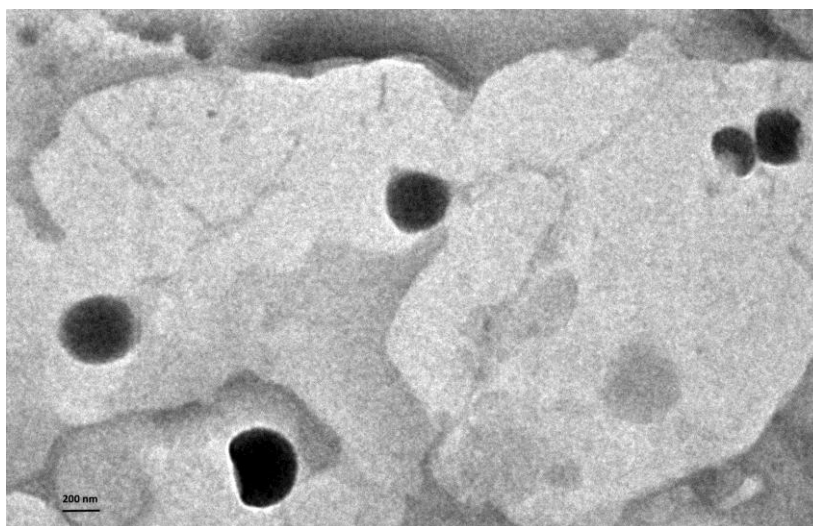


Figure 5.7 TEM image of CHG-loaded NEs [C-EO-70(10)].

Li *et al.* (2015) reported a similar droplet shape for a chlorhexidine acetate NE designed to improve chlorhexidine solubility and to enhance its antimicrobial activity against *Spreptococcus mutans in vitro* and *in vivo*. They reported minimum inhibitory concentration

(MIC) of a chlorhexidine acetate control solution was 0.8  $\mu\text{g/ml}$ , which was two times higher than chlorhexidine acetate NEs (0.4  $\mu\text{g/ml}$ ). Also the NE formulations exhibited a fast-acting bactericidal activity against *Spreptococcus mutans*, causing over 95 % death within 5 min, compared to chlorhexidine acetate solution (73 %). These data showed the potential role of NE formulation to prevent bacterial infection during the wound healing process.

#### 5.4.6 Fourier transform infrared spectrometry

The FTIR absorption spectra were obtained to study the drug and excipient interaction in the NE formulations. The FTIR spectra of CHG, EO and OO, CHG free formulations (blank EO-NEs and OO-NEs) and CHG-loaded NEs are shown in Figures 5.8 and Figure 5.9 respectively.

The FTIR spectrum of CHG had a broad symmetrical absorption peak between 3700–2700  $\text{cm}^{-1}$ , representing OH stretching due to the presence of water. Sharper amide bands were seen at 1650  $\text{cm}^{-1}$  (C = O stretch), 1538  $\text{cm}^{-1}$  (secondary N-H bend and C-N stretch) corresponding presence of CHG characteristic peaks. As seen in Figures 5.8 and 5.9, EO and OO had multiple absorption bands, which are described in detail in the previous chapter (Section 4.4.8).

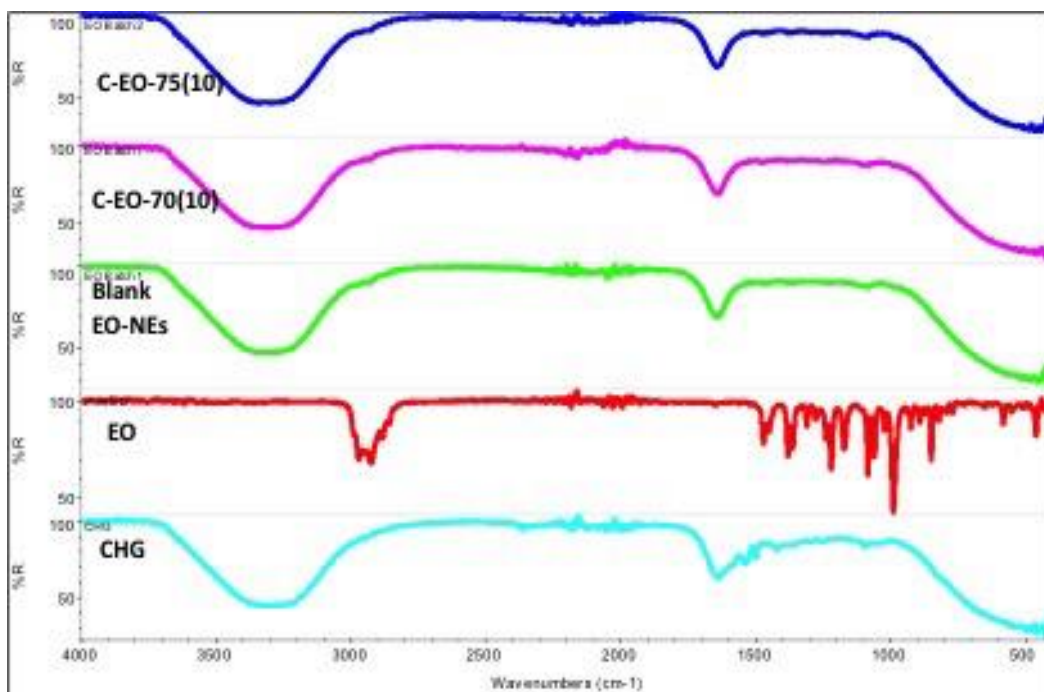


Figure 5.8 FTIR spectra for CHG, EO, Blank EO-NEs and CHG-loaded EO-NEs [C-EO-70(10), C-EO-75(10)].

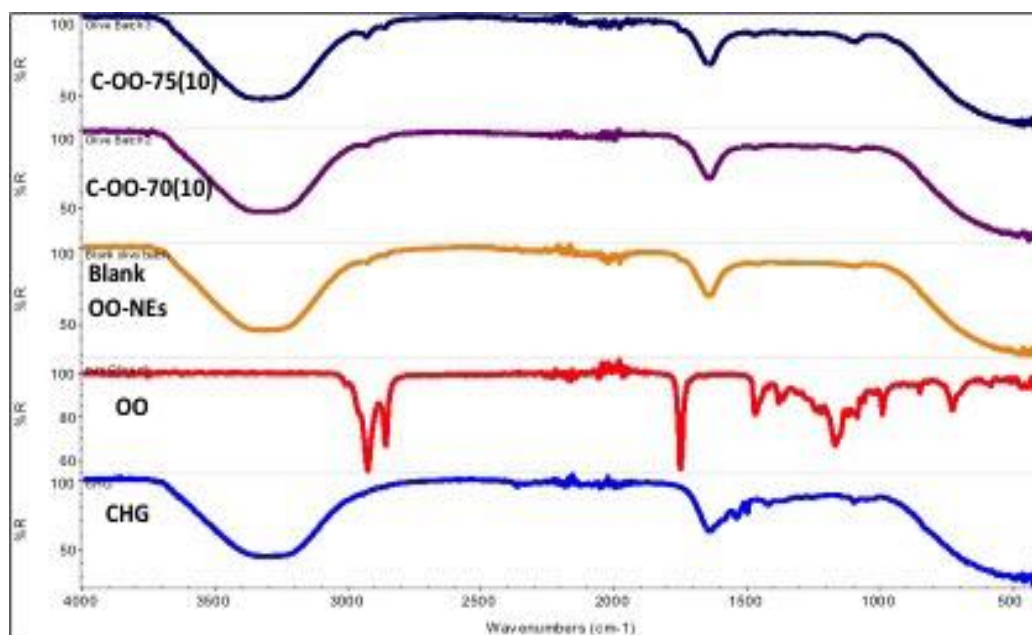


Figure 5.9 FTIR spectra for CHG, OO, Blank OO-NEs and CHG-loaded OO-NEs [C-OO-70(10), C-OO-75(10)].

The FTIR spectra for both blank and CHG-loaded NEs of EO and OO (Figure 5.8 and Figure 5.9) had a broad symmetrical absorption peak between 3700–2700  $\text{cm}^{-1}$ , representing the OH stretching mode of water superimposed over the CHG bands. The



broad peak seen between  $1500\text{ cm}^{-1}$  and  $1700\text{ cm}^{-1}$  in the blank and the CHG-loaded NEs formulations is due to the C=O double bond stretching vibration, resulting in superimposed peaks for CHG and EO and OO in this region (Kim *et al.*, 2008). Results obtained from FTIR spectra does not show any new peaks or modification of existing peaks between prepared NEs and individual components of NE system, which represents no chemical interaction between drug and excipients during formulation.

#### 5.4.7 *In vitro* drug release study

The *in vitro* release of CHG from the NE formulations and control solution (loading dose for both equivalent to 20 mg/g CHG concentration) was investigated using dialysis membrane, and the amount of CHG released was plotted against time (Figure 5.10). The data shows an initial burst release of CHG from the NEs and control solution for up to 4 h, the first time point, followed by a slow release up to 24 h.

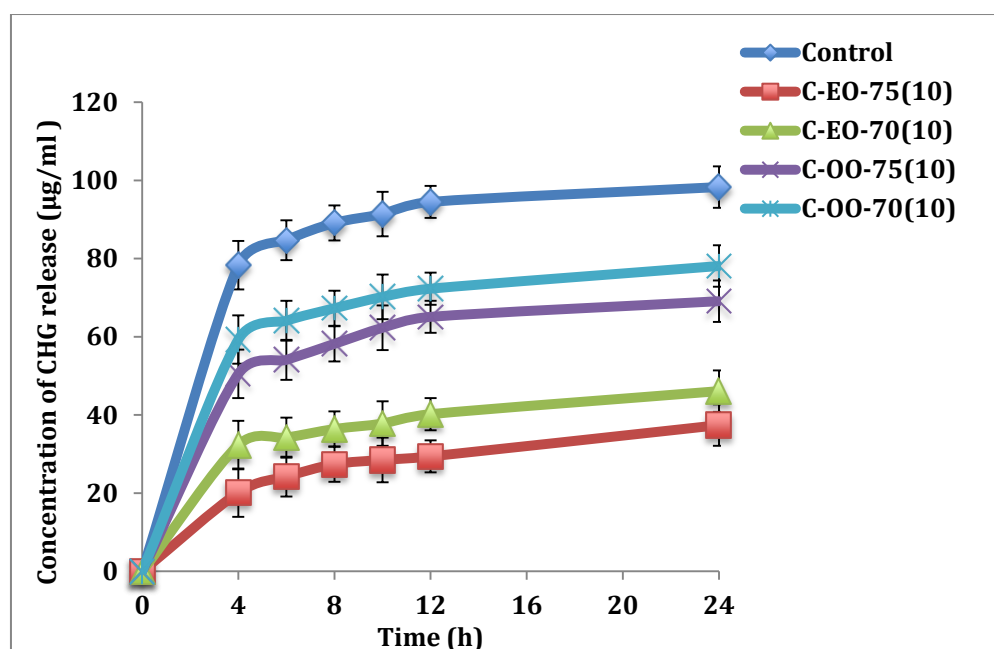


Figure 5.10 *In vitro* release profiles of CHG from NE formulations [C-EO-70(10), C-EO-75(10), C-OO-70(10), C-OO-75(10)] and control solution (Mean  $\pm$  SD, n = 6).

Release data shows lower CHG release from NE formulations compared to control solution, which might be due to the effect of formulation excipients. The amount of oil in the formulation restricts partitioning of the drug between the oil and water interface and

dialysis membrane controls the rate of drug release (Sandhu *et al.*, 2012). Literature study reported by Syed (2013) for *in vitro* evaluation of docetaxel OO-NEs (10 % w/w oil) formulated using similar production method. Results showed lower release of docetaxel from NE formulations compared to its control solution. Another study reported evaluation of *in vitro* release and epidermal permeation of dapsone NEs for topical delivery (Borges *et al.*, 2013). Release of dapsone was found to be less from NEs compared to a control solution, confirming the role of formulation excipients and composition in controlled release of drug into receiver.

#### 5.4.8 *In vitro* skin diffusion studies

*In vitro* skin permeation of all CHG-NE formulations and control solution was performed using Franz diffusion cells to study the localisation of drug within the skin layers and to determine if the formulation had any influence on this. Cumulative permeation was plotted against time (Figure 5.11), and permeability coefficient and steady state flux were calculated (Table 5.5). After 24 h less than 1 % w/w of the total applied dose of CHG reached the receiver compartment from NE formulations compared to 1.6 % w/w from the control solution. The reduced permeation through the skin may be as a result of altering the pathway into the skin. It has been reported that NEs may more effectively target hair follicles, thus differences will be seen between lipid formulations and the solution. The positive charge on the NEs in this study may also influence interactions with protein residues compared to non-charged equivalents (Yilmaz and Borchert, 2005).

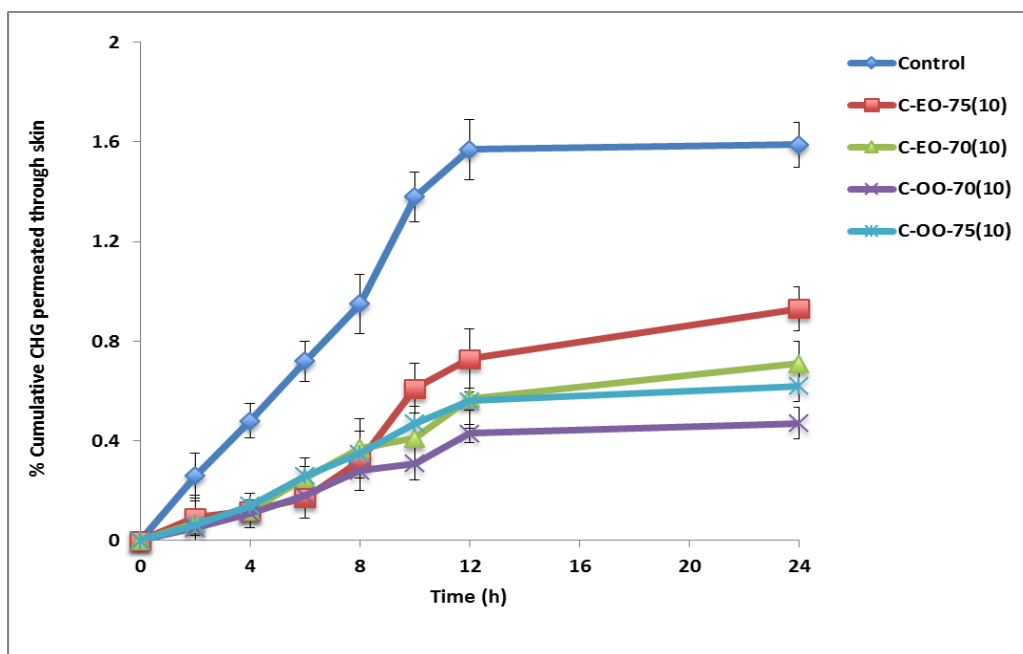


Figure 5.11 *In vitro* skin permeation of CHG from NE formulations [C-EO-70(10), C-EO-75(10), C-OO-70(10), C-OO-75(10)] and control solution (Mean  $\pm$  SD, n = 6).

In our study, permeation graphs show slow release of CHG from NEs, which unexpectedly plateaued after 12 h of diffusion experiment for CHG-OO NEs and control solution. Based on the literature study, CHG has been found to be stable at experimental conditions such as pH and temperature and also sink condition was maintained throughout experiment to establish concentration gradient across skin. The possible explanation could be binding of CHG with lipids and ceramides present in the SC of the epidermis, which enhances CHG penetration and retention after its application to the skin reducing its permeation into receiver compartment (Lorian, 2005). Similar permeation results were reported by Karpanen *et al.* (2008) in evaluation of CHG penetration into human skin, which had showed less CHG permeation into receiver compartment. Another study reported by Tsai *et al.*, (2014) showed effect of NEs as carrier for hydrophilic ropinirole hydrochloride. Skin permeation study showed no detectable level of drug in receiver compartment after 12 h of diffusion experiment. Less permeation of CHG from NE formulations compared to control solution might be due to the presence of formulation excipients such as oil, surfactant and

cosurfactant which enhances the penetration of CHG into skin by interacting and disrupting barrier properties of SC (Makraduli *et al.*, 2013; Tsai *et al.*, 2013).

Statistical analysis revealed a significant difference ( $p < 0.05$ ) in steady state flux values obtained for CHG-EO NEs and CHG-OO NEs. The flux of NEs and control solution was in order of control > C-EO-75(10) > C-EO-70(10) > C-OO-75(10) > C-OO-70(10).

Table 5.5 *In vitro* permeability parameters of CHG from NE formulations and control solution (Mean  $\pm$  SD, n = 6).

Formulation Code	Flux ( $J_{ss}$ ) $\mu\text{g}/\text{cm}^2/\text{h}$	Permeability coefficient ( $K_p$ ) $\times 10^{-4}$ cm/h
Control	1.23	2.81
C-EO-75(10)	0.91	1.29
C-EO-70(10)	0.87	1.52
C-OO-75(10)	0.84	0.26
C-OO-70(10)	0.76	0.22

#### 5.4.8.1 Quantification of chlorhexidine digluconate in skin using adhesive tape stripping method

The adhesive tape stripping method is used for quantification of topically applied substances in the skin. It removes the superficial layers of SC and allows the determination of the amount of drug that has penetrated into the skin. The CHG levels found in the skin are presented in Figure 5.12.

CHG penetration into the skin was higher for NE formulations compared to the control, with the differences being statistically significant ( $p < 0.05$ ). In addition, CHG skin penetration was significantly higher ( $p < 0.05$ ) for CHG-EO NEs compared to CHG-OO NEs and the control solution. The amount of CHG recovered from the skin for the control

solution was  $3.01 \pm 0.02 \mu\text{g}/\text{mg}$ , compared to  $6.15 \pm 0.12 \mu\text{g}/\text{mg}$ ,  $5.31 \pm 0.08 \mu\text{g}/\text{mg}$ ,  $4.39 \pm 0.04 \mu\text{g}/\text{mg}$  and  $3.98 \pm 0.06 \mu\text{g}/\text{mg}$  for C-EO-75(10), C-EO-70(10), C-OO-75(10) and C-OO-70(10) respectively. The C-EO-75(10) formulation had the CHG retention in skin, which is above the MIC range ( $2 \mu\text{g}/\text{ml}$ ) required to inhibit the growth of many Gram-positive and Gram-negative microorganisms reported in literature (Kärpänen, 2008; Popovich *et al.*, 2012).

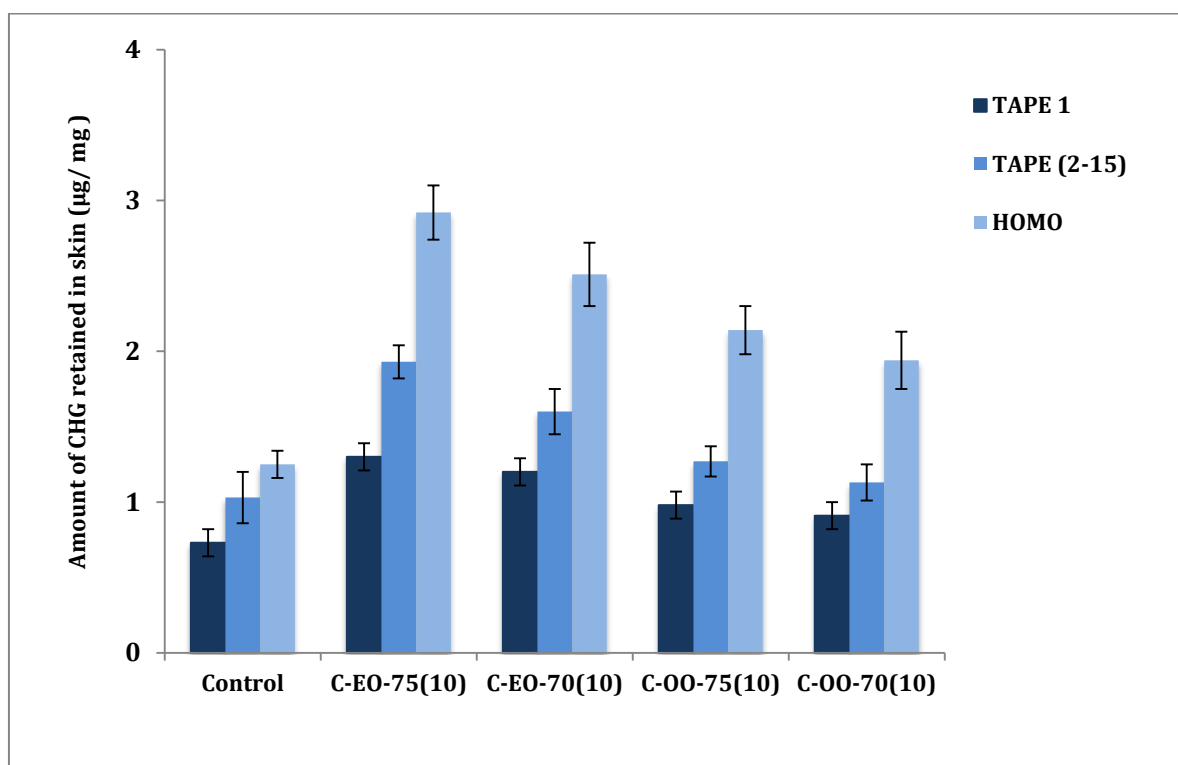


Figure 5.12 Penetration profiles showing the concentrations of CHG ( $\mu\text{g}/\text{mg}$  tissue) in porcine ear skin after 24 h exposure to the NE formulations [C-EO-70(10), C-EO-75(10), C-OO-70(10), C-OO-75(10)] and control solution (Mean  $\pm$  SD,  $n = 6$ ). HOMO refers to homogenised tissue after removal of the SC layers.

EO enhances the permeation of CHG into the skin, suggesting that a combination of CHG and EO may be a potential method to improve skin antiseptics in clinical practice. EO contains 1,8-cineole, which has been shown to bind in large quantities to the SC (Cornwell *et al.*, 1996). It is thought to enhance lipophilic drug penetration by increasing the partition coefficient (partitioning of drug between vehicle and SC), as well as hydrophilic drug penetration by increasing the diffusion coefficient (Cal *et al.*, 2001). Williams *et al.*, (2006) also showed that 1,8-cineole partitioning in the skin lipids is heterogeneous, leading to both

ordered and disordered areas in SC lipids. Furthermore, it has been shown in *in vitro* assays that cineole does not permeate through the skin but is retained in the skin (Cal *et al.*, 2006). Biruss *et al.*, (2007) reported increased skin penetration of steroid hormones using an EO (45 % v/v) microemulsion for topical delivery with EO shown to enhance percutaneous absorption by SC lipid extraction and loosening the hydrogen bond between the ceramides leading to fluidisation of lipid bilayers (Chena *et al.*, 2014). Topical application of EO and other essential oil mixtures on necrotic ulcers on the neck areas of cancer patients, resulted in not only antibacterial but also an anti-inflammatory activity (Warnke *et al.*, 2006). EO exhibited low toxicity and greater efficacy in reduction of morbidity associated with neoplastic ulcers. These studies indicate the potential of EO as a topical skin penetration enhancer and also suggest useful future work to determine the antibacterial effect of CHG-NE formulations in the prevention of bacterial skin infections. Another study reported amount of CHG recovered from top layers of human skin (100  $\mu\text{m}$  thickness) with combination of EO with CHG was 0.157  $\mu\text{g}/\text{mg}$ , which was higher than the concentration required to kill many common skin microorganisms (Kärpänen, T., 2008).

#### 5.4.9 *In vitro* skin diffusion studies of chlorhexidine digluconate nanoemulsions using methacrylate dressing powder

The amount of CHG permeated into and retained within the skin using a methacrylate powder dressing as a drug delivery vehicle are presented in Figure 5.13 and Figure 5.14. The amount of CHG permeated through skin using methacrylate powder dressing is <1 % w/w of total applied dose from NEs and control solution, which is lower than corresponding results obtained without use of the methacrylate powder dressing as discussed in previous study (Section 5.4.8).

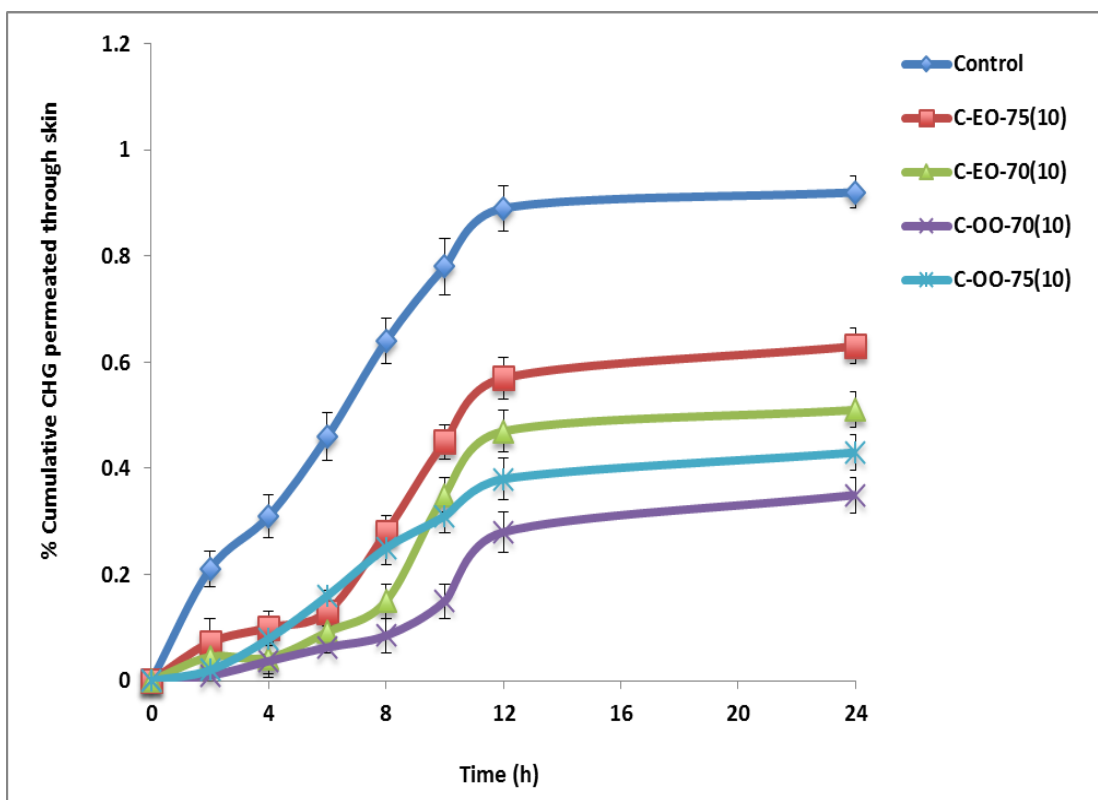


Figure 5.13 *In vitro* skin permeation of CHG in presence of methacrylate powder dressing from NE formulations [C-EO-70(10), C-EO-75(10), C-OO-70(10), C-OO-75(10)] and control solution (Mean  $\pm$  SD, n = 6).

The amount of CHG penetrated into the skin was higher from CHG-EO NEs [C-EO-75(10)] compared to other NEs and the control solution. The amount of CHG recovered from skin for the control solution was  $1.64 \pm 0.07$   $\mu\text{g}/\text{mg}$ , compared to  $3.43 \pm 0.09$   $\mu\text{g}/\text{mg}$ ,  $2.87 \pm 0.05$   $\mu\text{g}/\text{mg}$ ,  $2.93 \pm 0.08$   $\mu\text{g}/\text{mg}$  and  $2.84 \pm 0.03$   $\mu\text{g}/\text{mg}$  for C-EO-75(10), C-EO-70(10), C-OO-75(10) and C-OO-70(10) respectively (Figure 5.14). A previous study by Forstner *et al.*, (2013) evaluated the antibacterial efficacy of various antiseptic agents, polyhexamethylene biguanide, povidone-iodine and octenidine dihydrochloride alone and in combination, using a methacrylate dressing as the drug delivery vehicle. Without the antiseptic agent, the dressing did not prevent bacterial growth but it reduced bacterial multiplication, whereas the inclusion of the antiseptic led to a greater reduction in bacterial growth.

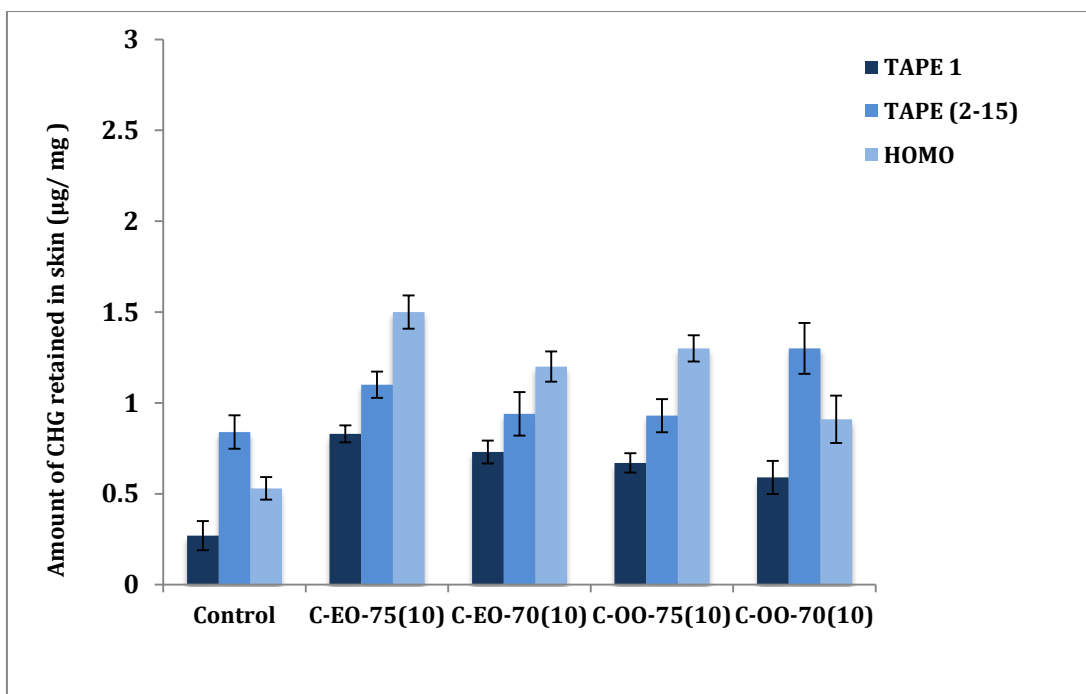


Figure 5.14 Penetration profiles showing the concentrations of CHG ( $\mu\text{g}/\text{mg}$  tissue) in presence of methacrylate powder dressing from NE formulations [C-EO-70(10), C-EO-75(10), C-OO-70(10), C-OO-75(10)] and control solution (Mean  $\pm$  SD,  $n = 6$ ) HOMO refers to homogenised tissue after removal of the SC layers.

St. John (2010) used a methacrylate dressing powder containing silver sulfadiazine to evaluate antimicrobial efficacy and wound management properties. The methacrylate dressing was applied to surgical wounds in a porcine model over 14 days using multiple bacterial strains. The silver rapidly converted to silver chloride on addition of saline solution to hydrate the methacrylate powder. The dressing was able to release the silver over prolonged period of time for complete recovery of wound.

Biocompatibility testing performed by Forstner *et al.*, (2013) found the methacrylate powder to be non-toxic, non-irritant and non-sensitising with a preclinical study found a faster time to reepithelialisation when compared to cellulose dressings in a surgical porcine wound healing model. They also reported methacrylate dressing contain approximately 68 % water, which is similar to the water content of the skin (72 % – 74 %), further increasing its biological compatibility

In present study, when CHG was added to methacrylate powder dressing, the cationic nature of CHG caused gelation of methacrylate polymer to form a porous flexible gel



structure, which allowed controlled release of CHG. The amount of CHG recovered from skin following application of the NEs with methacrylate dressing (Figure 5.14) was lower than the without use of methacrylate dressing (Figure 5.12). Hence, the methacrylate dressing might holds the drug within its porous gel structure for extended periods and this may be advantageous for prevention of bacterial growth during the surgical wound healing process.

#### 5.4.10 *In vitro* diffusion studies of chlorhexidine digluconate permeation using porcine ear skin and Strat- M<sup>®</sup> membrane

The percent cumulative amounts of CHG permeated from control solution and NE formulations [C-EO-75(10), C-OO-75(10)] were plotted against time (Figure 5.15) and were similar to the amount of CHG permeated through porcine ear skin i.e., for the control solution, C-EO-75(10) and C-OO-75(10) was  $1.64 \pm 0.12$ ,  $1.08 \pm 0.09$  and  $0.85 \pm 0.17$  respectively, while in case of porcine skin, the cumulative amount permeated was  $1.59 \pm 0.17$ ,  $0.93 \pm 0.13$  and  $0.62 \pm 0.07$  for control, C-EO-75(10) and C-OO-75(10) respectively (Figure 5.11). Thus NEs reduced CHG permeation in both skin and the Strat-M membrane model.

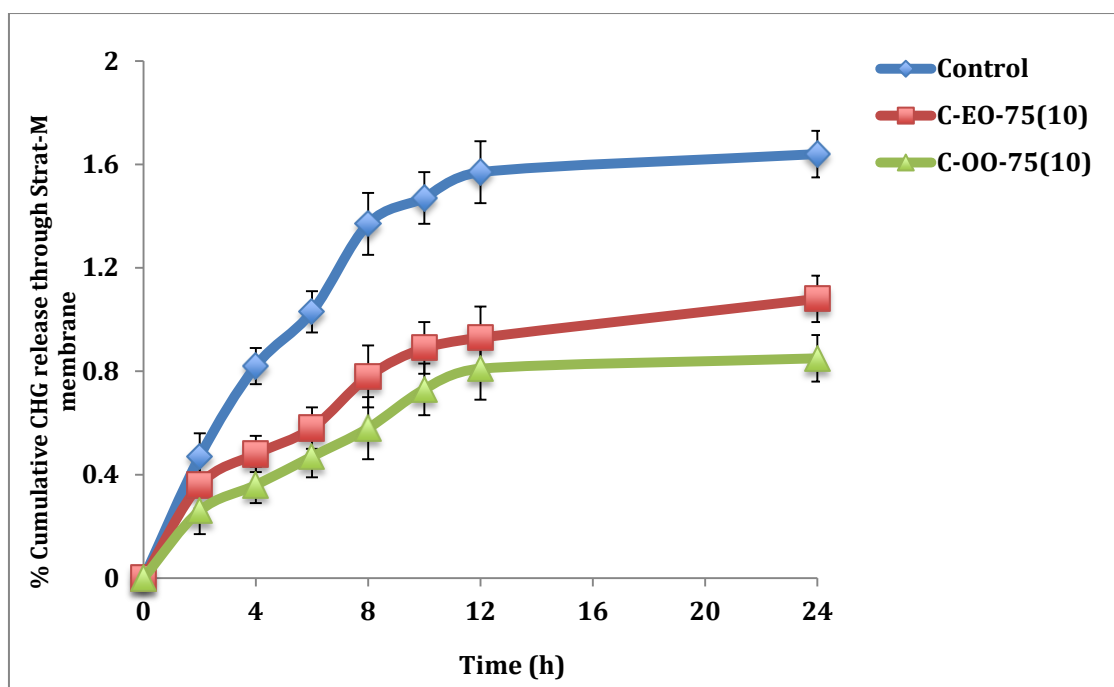


Figure 5.15 *In vitro* skin diffusion studies of CHG through Strat-M membrane from NE formulations [C-EO-75(10), C-OO-75(10)] and control solution (Mean  $\pm$  SD, n = 6).

The flux and permeability coefficients of CHG through porcine skin and Strat-M are not significantly different ( $p > 0.05$ ) (Table 5.6). Similar results were reported for a NE based gel formulation of diclofenac diethylamine using Strat-M membrane (Hamed *et al.*, 2015), with results from *in vitro* diffusion studies showing a good correlation between the permeability coefficient in human skin and Strat-M membrane. Study reported using Strat-M membrane, human skin and hairless rat skin to compare permeability coefficients and partition coefficients of various chemical compounds applied as an aqueous solution (Uchida *et al.*, 2015) also found very similar results for Strat-M to those in human and rat skin.

These reports indicate the suitability of Strat-M membrane as a substitute for *in vitro* diffusion studies for human and animal skin for laboratory use in certain circumstances. Strat-M contains two layers of polyethersulfone that are resistant to diffusion and a top layer of polyolefin which more open and diffusive, thus mimicking the SC barrier structure and composition of human and animal skin. Further experiments need to be conducted with

various formulations in order to verify that Strat-M can be used to screen the impact of formulation design on the topical and/or transdermal delivery of compounds.

Table 5. 6 Permeability parameters for CHG from control solution and NEs in porcine ear skin and Strat-M membrane (Mean  $\pm$  SD, n = 6).

Formulations	% CHG permeation		Permeability coefficient (Kp) (cm/h)	
	Porcine skin	Strat-M membrane	Porcine skin	Strat-M membrane
Control	1.26	0.96	$2.85 \times 10^{-3}$	$2.82 \times 10^{-3}$
C-EO-75(10)	0.66	0.54	$1.52 \times 10^{-3}$	$1.15 \times 10^{-3}$
C-OO-75(10)	0.11	0.13	$0.22 \times 10^{-3}$	$0.31 \times 10^{-3}$

#### 5.4.11 Studies of chlorhexidine digluconate penetration into barrier-intact and barrier-impaired porcine ear skin

The amount of CHG permeated and recovered from control solution and NE formulations using barrier-impaired, full thickness porcine ear skin was analysed and plotted against time (Figure 5.16).

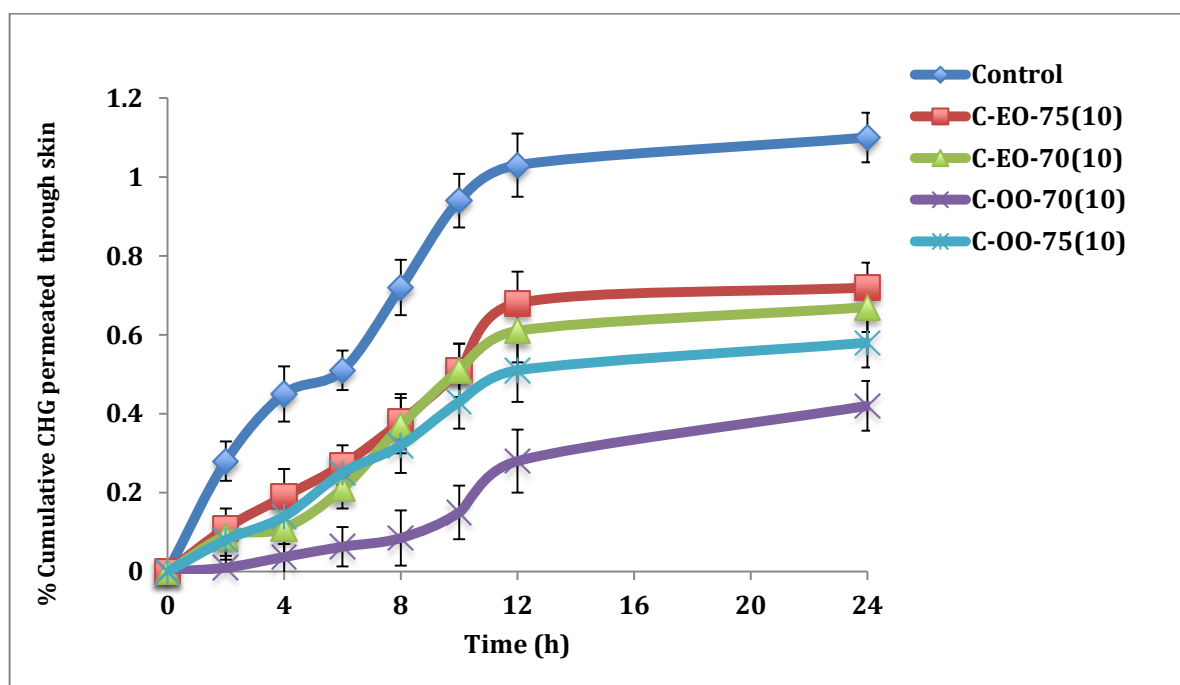


Figure 5.16 *In vitro* skin diffusion of CHG through barrier impaired skin from NE formulations [C-EO-70(10), C-EO-75(10), C-OO-70(10), C-OO-75(10)] and control solution (Mean  $\pm$  SD, n = 6).

The permeation data obtained from both barrier-intact and barrier-impaired skin showed no significant difference ( $p > 0.05$ ) between amount of CHG permeated through skin, while the amount of CHG recovered from barrier-impaired skin was significantly higher ( $p < 0.05$ ) than the amount recovered from intact skin (Table 5.6). Both CHG-EO NEs and CHG-OO NEs caused a 2-fold increase in CHG retention in barrier-impaired skin compared to barrier-intact skin, while retention of the CHG was only slightly increased for the control solution.

Table 5. 7 Amount of CHG recovered from the SC (15 tapes) and homogenised tissue following barrier-intact and barrier-impaired skin permeation studies (Mean  $\pm$  SD, n = 6).

Formulations	Amount of CHG recovered ( $\mu\text{g}/\text{mg}$ )	
	Barrier-intact skin	Barrier-impaired skin
Control	3.01 $\pm$ 0.02	4.45 $\pm$ 0.19
C-EO-75(10)	6.15 $\pm$ 0.12	12.07 $\pm$ 0.23
C-EO-70(10)	5.31 $\pm$ 0.08	9.85 $\pm$ 0.35
C-OO-75(10)	4.39 $\pm$ 0.04	8.37 $\pm$ 0.15
C-OO-70(10)	3.98 $\pm$ 0.06	7.16 $\pm$ 0.28

Spagnul *et al.*, (2011) investigated uranium penetration through barrier-impaired and barrier intact porcine ear skin following application of a calixarene NE formulations. Skin barrier properties was disrupted by using application of 60 adhesive tape strips to confirm the removal of SC. After skin permeation study they found increase in steady state flux of uranium about 55 times higher across barrier-impaired skin compared to barrier-intact skin indicating removal of SC had a greater influence on uranium skin penetration. Another study evaluated release and antimicrobial efficacy of chlorhexidine phosphanilate (CHP) cream formulation by analysing chlorhexidine penetration through barrier-intact and barrier-impaired human skin (Wang *et al.*, 1990). To remove the SC from epidermis skin was incubated in 0.2 % trypsin solution at 37 °C for 30 min. Data obtained after diffusion experiment showed that a negligible amount of CHP permeated to receiver compartment through barrier-intact skin, while barrier impaired skin showed 107  $\mu\text{g}/\text{ml}$  of CHP permeation (2 %w/w CHP cream formulation). It showed the rate-limiting step in barrier-impaired skin is the release and dissolution rate of CHP from cream formulation. CHG

binds to the proteins present in the skin and mucous membranes with limited systemic or body absorption (Edmiston *et al.*, 2013). Though in present study, we did not observe massive increase in concentration of CHG between barrier-intact and barrier-impaired skin compared to the data reported in literature. The reason might be the tape stripping method was used in present study to disrupt SC using 15 strips might not be sufficient and robust enough to remove and damage SC completely but data obtained from barrier-impaired skin shows some degree of damage to SC due to increase in CHG retention into skin.

Removal and damage of SC might also enhance the systemic absorption of active drugs causing risk of toxic effects in body. In case of CHG, being topical antiseptic agent several studies have reported anaphylactic reactions following parenteral and mucosal application (Bae *et al.*, 2008; Okano *et al.*, 1989), but very limited data is available on topical dermal application (Autegarden *et al.*, 1999).

## 5.5 Conclusion

NEs were produced by HSH and ultrasonication for topical drug delivery of the hydrophilic CHG, an antimicrobial agent. W/O NEs were formulated using S80 and T80 as surfactant and cosurfactant at various ratios with EO and OO as oil phase, in an attempt to enhance its skin penetration and provide controlled drug release. NEs droplet size were affected by use of S80 and T80 mixtures at various concentration levels with different HLB values. Pseudoternary phase diagram was constructed to select a suitable surfactant and cosurfactant ratio to prepare stable NE formulations. A ratio of 2:1 (S80 and T80) was found to produce NEs with mean droplet size below 350 nm for both EO and OO, with positively charged NEs, most likely as a consequence of presence of cationic CHG.

CHG-EO NEs [C-EO-70(10), C-EO-75(10)] and CHG-OO NEs [C-OO-70(10), C-OO-75(10)] formulations were used for *in vitro* drug release and skin permeation studies using Franz diffusion cells. Results from *in vitro* permeation studies showed a good correlation between permeability coefficients for Strat-M membrane (a synthetic model) and porcine ear skin. An *in vitro* skin permeation study carried out using full thickness porcine ear skin showed less than 2 % w/w of total applied CHG permeated into the receiver compartment making it a potential drug delivery system for localised topical antiseptic action. The concentration of CHG recovered from skin following application of CHG-EO NEs [C-EO-75(10)] was  $6.15 \pm 0.12$   $\mu\text{g}/\text{mg}$ , which is above the MIC level for many microorganisms.

Nanostructured methacrylate dressing was applied to the skin and formed a flexible, porous gel structure on contact with cationic CHG. *In vitro* diffusion studies showed the potential of the methacrylate dressing to hold the CHG within polymer matrix and facilitate controlled release of CHG over a prolonged period of time. This opens new possibilities for topical antimicrobial treatment and prophylactic strategies in wound care management,

which needs to be elucidated in future studies, as to whether these effects correlate with the clinical situation in infected or contaminated wounds.



## 6. CHAPTER: FINAL DISCUSSION AND FUTURE WORK

Effective skin antisepsis is imperative prior to incision of the skin, for example during surgery, insertion of intravascular devices and other invasive procedures. HAIs are a major concern within the health services as they inflict a significant financial burden and time constraints on the healthcare system due to increased morbidity and mortality rates, prolonged hospital occupancy and intensified treatment regimes, including repeated surgical procedures (Vilela *et al.*, 2007). SSIs are responsible for an estimated 15 % of HAIs, represent a considerable proportion of all nosocomial infections, and are the most common infection occurring in surgical patients (Stevens, 2009). Whilst post-operative care can reduce infection rates, an effective pre-operative procedure is crucial to avoid development of many preventable infections.

In the majority of SSIs cases, microorganisms such as *Staphylococcus aureus* and *Staphylococcus epidermidis* are the most common pathogens derived from surgical sites. When skin is incised, underlying tissue is exposed to the overlying endogenous flora, resulting in an increasing proportion of such infections (Piette and Verschraegen, 2009). The ability of these microorganisms to grow within skin despite using a prior skin antiseptic procedure creates additional complications due to their reduced susceptibility to antimicrobial agents. Current evidence based guidelines recommend that 2 % w/v CHG, preferably in 70 % (v/v) IPA, is used for skin antisepsis prior to incision of the skin (Loveday *et al.*, 2014). Microorganisms have been shown to persist within the skin following skin antisepsis, and the poor skin permeation of many antiseptic agents may contribute to SSIs (Hendley and Ashe, 2003; Karpanen *et al.*, 2008). It is therefore proposed to have a carrier system, which can enhance skin penetration of an antimicrobial agent for a

prolonged period of time prior to surgical procedure to inhibit bacterial growth and prevent skin infections.

In this study, the efficiency of lipid-based carriers was to accessed enhance skin retention of antimicrobial agents such as TSN and CHG for topical drug delivery. Among the lipid-based delivery systems, were SLNs and NEs are extensively studied due to relative easy production methods, non-toxicity and biocompatibility of lipids, easy availability of excipients and scale-up possibilities made these systems academically and industrially attractive. In addition, by manipulating surfactants to have a suitable HLB, it is possible to fabricate stable nanosized carriers (Chen *et al.*, 2010; Severino *et al.*, 2012b). Among these nanocarriers, SLNs are produced using lipids, which are solid at room and body temperature. If these solid lipids are exchanged for liquid lipid, NEs can be produced. Thus, even though SLNs and NEs are composed of lipids, but they differ in their physical state and composition of lipids. Therefore, the key purposes of this study were to produce SLNs and NEs using HSH followed by probe ultrasonication and to study the effect of differences in composition of each delivery system on various physicochemical properties of nanocarrier formulations and their skin retention properties using *in vitro* diffusion studies.

In chapter 3, SLNs of TSN (equivalent to TSN concentration to 10 mg/g of formulation) was formulated using GB and GP as solid lipids. GP-SLNs had smaller particle size with higher % DEE compared GB-SLNs made under the same conditions. SLNs of both lipids showed lipid concentration dependent increase in the particle size and decrease in % DEE. Morphological and thermal studies confirmed the presence of spherical particles with no chemical interaction between drug and other excipients. SLN formulations with 3 % w/w and 5 % w/w of both GB and GP lipids were used to assess skin targeting behavior and TSN skin permeation was higher with SLNs compared to TSN solution. This increased skin

delivery by SLNs is a result of the large surface area due to small particle size, an occlusive effect of lipids and a penetration enhancement effect of surfactants into the skin. The amount of TSN retained within the skin was evaluated by differential stripping technique by combining adhesive tape stripping and cyanoacrylate biopsies. The amount of TSN retained within skin was higher from SLNs compared to the control solution, with the difference being statistically significant ( $p < 0.001$ ). It can be explained by higher occlusive effect and increased hydration of SC commonly associated with lipid nanoparticles (Müller *et al.*, 2007). Lipid concentration dependent increases in TSN retention were observed, as lipid concentration increased from 3 % to 5 % (w/w) in GB-SLNs and GP-SLNs, there was a 2-fold increase in TSN retention. Skin retention of TSN was higher for GP-SLNs (5 % w/w GP lipid) formulations compared to the others, indicating a superior ability of GP as a lipid carrier of TSN compared to GB solid lipid.

In addition to SLNs, skin penetration of TSN was also evaluated by preparation of TSN-loaded NEs using EO and OO as the internal oil phase and T80 and S80 as surfactant and cosurfactant mixture (chapter 4). The aim of these work was to find better nanocarrier system for TSN delivery to skin with enhance skin penetration properties. NEs are one of the most promising formulations for enhancing the percutaneous absorption of an active substance, as they are a thermodynamically and kinetically stable liquid dispersion of an oil phase and a water phase, in combination with a surfactant. EO has been shown to enhance skin permeation of both lipophilic and hydrophilic compounds, which is thought to be due to its terpene constituents. EO contains 1,8-cineole which has also demonstrated skin penetration enhancing properties (Aqil *et al.*, 2007; Narishetty and Panchagnula, 2005). OO due to its high content of monounsaturated and polyunsaturated fatty acids has been used extensively in cosmetics and pharmaceutical products (Eid *et al.*, 2013). Pseudoternary phase diagrams behavior studies allowed the identification of different regions, as well as

the selection of maximum and minimum concentrations of each component required for obtaining stable formulations. EO-NEs had a smaller droplet size and higher % DEE compared to OO-NEs. Concentrations of oil and surfactant had opposing actions on droplet size, with an increase in the oil phase increasing droplet size while an increase in surfactant concentration caused a decrease in droplet size.

Formulations prepared with 5 % w/w and 10 % w/w oil phase and 5 % w/w surfactant mixture were selected for further *in vitro* skin permeation studies. EO-NEs demonstrated higher drug permeation through skin compared to OO-NEs due to the influence of physicochemical properties such as higher solubility of TSN in EO, smaller droplet size and low viscosity of formulation with permeation enhancement effects of EO. Higher amounts of TSN ( $10.35 \pm 0.05 \mu\text{g}/\text{mg}$ ) were recovered from skin following administration of EO-NEs [EO-10(5)] compared to other EO-NE and OO-NE formulations. NEs and previous findings of SLNs for topical delivery of TSN in chapter 3 were compared for better retention of solid and liquid lipid nanocarriers was compared using *in vitro* skin permeation studies and quantifying amount of TSN recovered from skin using adhesive tape stripping method. The SLN and NE formulations containing equal amount of lipids i.e. GP-SLNs (GP5-2) and EO-NEs [EO-5(5)] were selected for *in vitro* skin diffusion study using porcine ear skin. The amount of TSN recovered from skin was higher for NEs ( $17.49 \pm 0.16 \mu\text{g}/\text{mg}$ ) compared to SLNs ( $14.42 \pm 0.27 \mu\text{g}/\text{mg}$ ) with the difference being statistically significant ( $p < 0.05$ ). This might be due to difference in composition and physical state of lipids used and difference in the physicochemical properties of nanocarriers. The results reported in this work have clearly demonstrated the suitability of NEs for enhanced skin retention of TSN upon topical administration.

In chapter 5 of this thesis, another commonly used antimicrobial agent CHG was selected to formulate into NEs to enhance its skin retention properties. W/O NEs of CHG (equivalent of CHG concentration to 20 mg/g of formulation) were formulated and evaluated using EO and OO as external oil phase due to hydrophilic nature of CHG. Pseudoternary phase diagrams study helped to select a surfactant and cosurfactant ratio of 2:1 (S80 and T80) to produce stable NEs with mean droplet size less than 350 nm for both EO and OO up to 83 % drug encapsulation efficiency. Selected formulations of EO-NEs and OO-NEs were used to study *in vitro* drug release and skin permeation using synthetic membranes such as dialysis membrane, Strat-M membrane and excised full thickness porcine ear skin. Release and permeation studies detected < 2 % w/w of the total applied dose of CHG after 24 h of contact, thus making it advantageous for localised topical delivery of CHG. EO-NEs showed significantly greater ( $p < 0.05$ ) CHG skin penetration than the OO-NEs and control. The results demonstrate that EO enhances the permeation of CHG into the skin, suggesting that a combination of CHG and EO may be used to improve skin penetration in clinical practice. EO contains 1,8-cineole, which has been shown to bind in large quantities to the SC (Cornwell *et al.*, 1996). The results from this study clearly demonstrate the enhanced skin delivery of CHG with EO-NEs into the deeper layers of the skin, therefore enhancing skin retention. These results clearly lay the foundation for future work. However, the penetration of EO into the skin, its potential side effects and skin tolerability need to be investigated before *in vivo* studies are undertaken in the clinical setting.

In the healthcare environment the increasing numbers of resistant microorganisms is a major concern. The extensive use of many antimicrobial agents has contributed to the acquired resistance among many pathogens. Thus it is important to search for new drug delivery systems for better and prolonged skin penetration activity of antimicrobial agents without increasing systemic absorption. Potential future work may be the incorporation of

prepared lipid nanoformulations into suitable hydrogels or polymers for easy skin application, evaluation of antimicrobial efficacy of prepared SLNs and NEs using various microbial strains and to study the skin penetration enhancement ability of SLN and NE formulations prepared with different types of solid lipids and oils. The main findings of this thesis are the enhanced skin penetration of TSN and CHG from lipid nanoformulations using GB, GP as solid lipids and EO and OO as oils, with special emphasis on NEs as lipid carriers for the enhanced skin delivery of TSN are exciting and clearly lay the foundation for future work.

## 7. REFERENCES

- Abd, E., 2015. Targeted skin delivery of topically applied drugs by optimised formulation design. PhD Thesis. University of Queensland, Australia.
- Abdelbary, G., Fahmy, R.H., 2009. Diazepam loaded solid lipid nanoparticles: Design and characterisation. *AAPS PharmSciTech*, 10, 211–219.
- Aditya, N.P., Macedo, A.S., Doktorovova, S., Souto, E.B., Kim, S., Pahn-Shick, C., Ko, S., 2014. Development and evaluation of lipid nanocarriers for quercetin delivery: A comparative study of solid lipid nanoparticles (SLN), nanostructured lipid carriers (NLC), and lipid nanoemulsions (LNE). *Food Science and Technology*, 59, 115–121.
- Aguiar, J., Carpena, P., Molina-Bolívar, J. a., Carnero Ruiz, C., 2003. On the determination of the critical micelle concentration by the pyrene 1:3 ratio method. *Journal of Colloid and Interface Science*, 258, 116–122.
- Alam, M.S., Ali, M.S., Alam, M.I., Anwar, T., Safhi, M.M., 2015. Stability testing of beclomethasone dipropionate nanoemulsion. *Tropical Journal of Pharmaceutical Research*, 14, 15–20.
- Alvarado, H.L., Abrego, G., Souto, E.B., Garduño-Ramirez, M.L., Clares, B., García, M.L., Calpena, A.C., 2015. Nanoemulsions for dermal controlled release of oleanolic and ursolic acids: *In vitro*, *ex vivo* and *in vivo* characterisation. *Colloids and Surfaces B: Biointerfaces*, 130, 40–47.
- Alvarez-Román, R., Naik, A., Kalia, Y.N., Fessi, H., Guy, R.H., 2004. Visualisation of skin penetration using confocal laser scanning microscopy. *European Journal of Pharmaceutics and Biopharmaceutics*, 58, 301–316.
- Alyautdin, R.N., Tezikov, E.B., Ramge, P., Kharkevich, D.A., Begley, D.J., Kreuter, J., 1998. Significant entry of tubocurarine into the brain of rats by adsorption to polysorbate 80 coated polybutylcyanoacrylate nanoparticles: An *in situ* brain perfusion study. *Journal of Microencapsulation*, 15, 67–74.
- Amin, S., Kohli, K., Khar, R.K., Mir, S.R., Pillai, K.K., 2008. Mechanism of *in vitro* percutaneous absorption enhancement of carvedilol by penetration enhancers. *Pharmaceutical Development and Technology*, 13, 533–539.
- Aqil, M., Ahad, A., Sultana, Y., Ali, A., 2007. Status of terpenes as skin penetration enhancers. *Drug Discovery Today*, 12, 1061–1067.

- Aruoma, O.I., Spencer, J.P., Rossi, R., Aeschbach, R., Khan, A., Mahmood, N., Munoz, A., Murcia, A., Butler, J., Halliwell, B., 1996. An evaluation of the antioxidant and antiviral action of extracts of rosemary and provencal herbs. *Food and Chemical Toxicology*, 34, 449–456.
- Ashton, P., Hadgraft, J., Stevens, J., 1986. Some effects of a non-ionic surfactant on topical availability. *Journal of Pharmacy and Pharmacology*, 38, 70.
- Aulton, M.E., Taylor, K., 2013. Emulsions and creams, in: *Aulton's Pharmaceuticals: The Design and Manufacture of Medicines*. Edinburgh: Churchill Livingstone, pp. 436–448.
- Autegarden, J.E., Pecquet, C., Huet, S., Bayrou, O., Leynadier, F., 1999. Anaphylactic shock after application of chlorhexidine to unbroken skin. *Contact Dermatitis*, 40, 215.
- Azeem, A., Rizwan, M., Ahmad, F.J., Khar, R.K., Iqbal, Z., Talegaonkar, S., 2009. Components screening and influence of surfactant and cosurfactant on nanoemulsion formation. *Current Nanoscience*, 5, 220–226.
- Azevedo, R.C., Barreto, S.M., Ostrosky, E.A., Rocha-Filho, P.A., Veríssimo, L.M., Ferrari, M., 2015. Production and characterisation of cosmetic nanoemulsions containing opuntia ficus-indica (L.) mill extract as moisturising agent. *Molecules*, 20, 2492–2509.
- Aziz, Z., Abu, S.F., Chong, N.J., 2012. A systematic review of silver-containing dressings and topical silver agents (used with dressings) for burn wounds. *Burns*, 38, 307–318.
- Baboota, S., Shakeel, F., Ahuja, A., Ali, J., Shafiq, S., 2007. Design, development and evaluation of novel nanoemulsion formulations for transdermal potential of celecoxib. *Acta Pharmaceutica*, 57, 315–332.
- Badiu, D., Luque, R., Rajendram, R., 2010. The effects of olive oil on the skin., in: Preedy, V.R. & Watson, R.R. (Ed.), *Olives and Olive Oil in Health and Disease Prevention*. London:Elsevier, pp. 1125–1132.
- Bae, Y.J., Chan, S.P., Jae, K.L., Jeong, E., Kim, T.B., You, S.C., Moon, H.B., 2008. A case of anaphylaxis to chlorhexidine during digital rectal examination. *Journal of Korean Medical Science*, 23, 526–528.
- Bakkali, F., Averbeck, S., Averbeck, D., Idaomar, M., 2008. Biological effects of essential oils: A review. *Food and Chemical Toxicology*, 46, 446–475.
- Bali, V., Ali, M., Ali, J., 2010. Study of surfactant combinations and development of a novel nanoemulsion for minimising variations in bioavailability of ezetimibe. *Colloids and surfaces B: Biointerfaces*, 76, 410–20.
- Barbero, A.M., Frasch, H.F., 2009. Pig and guinea pig skin as surrogates for human *in vitro*



penetration studies: A quantitative review. *Toxicology in Vitro*, 23, 1–13.

Barbour, M.E., Maddocks, S.E., Wood, N.J., Collins, A.M., 2013. Synthesis, characterisation, and efficacy of antimicrobial chlorhexidine hexametaphosphate nanoparticles for applications in biomedical materials and consumer products. *International Journal of Nanomedicine*, 8, 3507–3519.

Barkvold, P., Rolla, G., 1994. Triclosan protects the skin against dermatitis caused by sodium lauryl sulphate exposure. *Journal of Clinical Periodontology*, 21, 717–719.

Barnea, Y., Amir, A., Leshem, D., Zaretski, A., Weiss, J., Shafir, R., Gur, E., 2004. Clinical comparative study of aquacel and paraffin gauze dressing for split-skin donor site treatment. *Annals of Plastic Surgery*, 53, 132–136.

Baroli, B., López-Quintela, M.A., Delgado-Charro, M.B., Fadda, A.M., Blanco-Méndez, J., 2000. Microemulsions for topical delivery of 8-methoxsalen. *Journal of Controlled Release*, 69, 209–218.

Barrett, C.W., Hadgraft, J.W., Caron, G.A., Sarkany, I., 1965. The effect of particle size on the percutaneous absorption of fluocinolone acetonide. *British Journal of Dermatology*, 77, 576–578.

Barry, A.L., Fuch, P.C., Brown, S.D., 1999. Lack of effect of antimicrobial resistance on susceptibility of microorganisms to chlorhexidine gluconate or povidone iodine. *Diagnostic Microbiology and Infectious Disease*, 18, 920–92.

Barry, B.W., 1987. Mode of action of penetration enhancers in human skin. *Journal of Controlled Release*, 6, 85–97.

Basketter, D.A., Marriott, M., Gilmour, N.J., White, I.R., 2004. Strong irritants masquerading as skin allergens: the case of benzalkonium chloride. *Contact Dermatitis*, 50, 213–217.

Baspinar, Y., Keck, C.M., Borchert, H.H., 2010. Development of a positively charged prednicarbate nanoemulsion. *International Journal of Pharmaceutics*, 383, 201–208.

Belly, R.T., Kydd, G.C., 1982. Silver resistance in microorganisms. *Developments in Industrial Microbiology*, 23, 567–577.

Benita, S., Levy, M.Y., 1993. Submicron emulsions as colloidal drug carriers for intravenous administration: Comprehensive physicochemical characterisation. *Journal of Pharmaceutical Sciences*, 82, 1069–1079.

- Bethell, E., 2003. Why gauze dressing should not be the first choice to manage most acute surgical cavity wounds. *Journal of Wound Care*, 12, 237–239.
- Bhagwat, D.A., Kawtikwar, P.S., Sakarkar, D.M., 2009. Formulation and the *in vitro* and biopharmaceutical evaluation of sustained release tablet of verapamil HCL using precirol ATO 5 through melt granulation technique. *Asian Journal of Pharmaceutics*, 3, 278–285.
- Bhargava, H. N., Leonard, P. A., 1995. Triclosan: Applications and Safety. *American Journal of Infection Control*, 24, 209-218.
- Biruss, B., Kahliq, H., Valenta, C., 2007. Evaluation of an eucalyptus oil containing topical drug delivery system for selected steroid hormones. *International Journal of Pharmaceutics*, 328, 142–151.
- Blam, O.G., Vaccaro, A.R., Vanichkachorn, J.S., Albert, T.J., Hillibrand, A.S., Minnich, J.M.,
- Murphey, S.A., 2003. Risk factors for surgical site infection in the patient with spinal injury. *Spine*, 28, 1475–1480.
- Blanpain, C., Fuchs, E., 2009. Epidermal homeostasis: A balancing act of stem cells in the skin. *Nature Reviews Molecular Cell Biology*, 10, 207–217.
- Block, S.S., 1991. Chlorhexidine, in: Denton, G.W. (Ed.), *Disinfection, Sterilization, and Preservation*. Lea & Febiger, Philadelphia, pp. 274–285.
- Boateng, J.S., Matthews, K.H., Stevens, H.N.E., Eccleston, G.M., 2008. Wound healing dressings and drug delivery systems: A review. *Journal of Pharmaceutical Sciences*, 97, 2892–2923.
- Borges, V.R., Simon, A., Sena, A.R., Cabral, L.M., de Sousa, V.P., 2013. Nanoemulsion containing dapsone for topical administration: A study of *in vitro* release and epidermal permeation. *International Journal of Nanomedicine*, 8, 535–544.
- Bouchemal, K., Briançon, S., Perrier, E., Fessi, H., 2004. Nanoemulsion formulation using spontaneous emulsification: Solvent, oil and surfactant optimisation. *International Journal of Pharmaceutics*, 280, 241–51.
- Bragg, P.D., Rainnie, D.J., 1974. The effect of silver ions on the respiratory chain of *Escherichia coli*. *Canadian Journal of Microbiology*, 20, 883–889.
- Braun-Falco, O., Korting, H.C., 1986. Der normale pH-Wert der menschlichen Haut. *Hautarzt* 37, 126–129.
- Brayfield, A., 2014. Martindale: The Complete Drug Reference, 38th ed.
- Brendan, P., Sally, J.A., Carolana, V.A., Mortonb, J., Clench, M.R., 2007. Sample preparation and data interpretation procedures for the examination of xenobiotic compounds

- in skin by indirect imaging MALDI-MS. *International Journal of Mass Spectrometry*, 260, 243–251.
- Broex, E.C., Van Asselt, A.D., Bruggeman, C.A., VanTiel, F.H., 2009. Surgical site infections: How high are the costs? *Journal of Hospital Infection*, 72, 193–201.
- Brophy, J.J., Lassak, E. V, Toia, R.F., 1985. The steam volatile leaf oil of eucalyptus pulverulenta. *Planta Medica*, 51, 170–171.
- Brossard, C., 1991. Modelling of theophylline compound release from hard gelatin capsules containing gelucire matrix granules. *Drug Development and Industrial Pharmacy*, 17, 1267–1277.
- Broughton, G., Janis, J.E., Attinger, C.E., 2006. The basic science of wound healing. *Plastic and Reconstructive Surgery*, 117, 12S – 34S.
- Brown, M.B., Martin, G.P., Jones, S.A., Akomeah, F.K., 2006. Dermal and transdermal drug delivery systems: Current and future prospects. *Drug Delivery*, 13, 175–187.
- Brown, M.R.W., Anderson, R.A., 1968. The bactericidal effect of silver ions on *Pseudomonas aeruginosa*. *Journal of Pharmaceutics and Pharmacology*, 20, S1–S3.
- Bunge, A.L., Guy, R.H., Hadgraft, J., 1999. The determination of a diffusional pathlength through the stratum corneum. *International Journal of Pharmaceutics*, 188, 121–124.
- Burt, S.A., 2004. Essential oils, their antibacterial properties and potential applications in foods: A review. *International Journal of Food Microbiology*, 94, 223–253.
- Caelli, M., Porteous, J., Carson, C.F., Heller, R., Riley, T. V, 2000. Tea tree oil as an alternative topical decolonisation agent for *methicillin-resistant Staphylococcus aureus*. *Journal of Hospital Infection*, 46, 236–237.
- Cal, K., Janicki, S., Sznitowska, M., 2001. *In vitro* studies on penetration of terpenes from matrix-type transdermal systems through human skin. *International Journal of Pharmaceutics*, 224, 81–88.
- Cal, K., Kupiec, K., Sznitowska, M., 2006. Effect of physicochemical properties of cyclic terpenes on their *ex vivo* skin absorption and elimination kinetics. *Journal of Dermatological Science*, 41, 137–142.
- Calabrese, V., Randazzo, S.D., Catalano, C., Rizza, V., 1999. Biochemical studies on a novel antioxidant from lemon oil and its biotechnological application in cosmetic dermatology. *Drugs Under Experimental and Clinical Research*, 25, 219–225.
- Calligaris, S., Comuzzo, P., Bot, F., Lippe, G., Zironi, R., Anese, M., Nicoli, M., 2015.

Nanoemulsions as delivery systems of hydrophobic silybin from silymarin extract: Effect of oil type on silybin solubility, *in vitro* bioaccessibility and stability. *Food Science and Technology*, 63, 77–84.

Celebioglu, A., Umu, O.C., Tekinay, T., Uyar, T., 2013. Antibacterial electrospun nanofibers from triclosan/cyclodextrin inclusion complexes. *Colloids and Surfaces B: Biointerfaces*, 116, 612–619.

Cevc, G., Vierl, U., 2010. Nanotechnology and the transdermal route: A state of the art review and critical appraisal. *Journal of Controlled Release*, 141, 277–299.

Chanamai, R., McClements, D.J., 2000. Dependence of creaming and rheology of monodisperse oil-in-water emulsions on droplet size and concentration. *Colloids and Surfaces A: Physicochemical and Engineering Aspects*, 172, 79–86.

Charcosset, C., EI-Harati, A., Fessi, H., 2005. Preparation of solid lipid nanoparticles using a membrane contactor. *Journal of Controlled Release*, 108, 112–120.

Chen, C., Tung-Hu, T., Zih-Rou, H., Fang, J.F., 2010. Effects of lipophilic emulsifiers on the oral administration of lovastatin from nanostructured lipid carriers: Physicochemical characterisation and pharmacokinetics. *European Journal of Pharmaceutics and Biopharmaceutics*, 74, 474–482.

Chen, H., Chang, X., Du, D., Liu, W., Liu, J., Weng, T., Yang, Y., Xu, H., Yang, X., 2006. Podophyllotoxin loaded solid lipid nanoparticles for epidermal targeting. *Journal of Controlled Release*, 110, 296–306.

Chen, M.L., 2008. Lipid excipients and delivery systems for pharmaceutical development: A regulatory perspective. *Advanced Drug Delivery Reviews*, 60, 768–777.

Chena, Y., Quana, P., Liua, X., Wangb, M., Fang, L., 2014. Novel chemical permeation enhancers for transdermal drug delivery. *Asian Journal of Pharmaceutical Sciences*, 9, 51–64.

Chiesa, M., Garg, J., Kang, Y.T., Chen, G., 2008. Thermal conductivity and viscosity of water-in-oil nanoemulsions. *Colloids and Surfaces A: Physicochemical and Engineering Aspects*, 326, 67–72.

Chimmiri, P., Rajalakshmi, R., Mahitha, B., Ramesh, V.H., Ahmed, N., 2012. Solid lipid nanoparticles: A novel carrier for cancer therapy. *International Journal of Biological and Pharmaceutical Research*, 3, 405–413.

Chopra, I., 1987. Microbial resistance to veterinary disinfectants and antiseptics, in: Linton, A.H., Hugo, W.B., Russell, A.D. (Eds.), *Disinfection in Veterinary and Farm Animal Practice*. Blackwell Scientific Publications Ltd., Oxford, England.

Cimanga, K., Kambu, K., Tona, L., Apers, S., Bruyne, T. De, Hermans, N., Totte, J., Pieters,

- L., Vlietinck, A.J., 2002. Correlation between chemical composition and antibacterial activity of essential oils of some aromatic medicinal plants growing in the Democratic Republic of Congo. *Journal of Ethnopharmacology*, 79, 213–220.
- Clares, B., Calpena, A.C., Parra, A., Abrego, G., Alvarado, H., Fangueiro, J.F., Souto, E.B., 2014. Nanoemulsions (NEs), liposomes (LPs) and solid lipid nanoparticles (SLNs) foretinyl palmitate: Effect on skin permeation. *International Journal of Pharmaceutics*, 473, 591–598.
- Coldman, M.F., Kalinovsky, T., Poulsen, B.J., 1971. The *in vitro* penetration of fluocinonide through human skin from different volumes of DMSO. *British Journal of Dermatology*, 85, 457–461.
- Cornwell, P.A., Barry, B.W., 1994. Sesquiterpene components of volatile oils as skin penetration enhancers for the hydrophilic permeant 5-fluorouracil. *Journal of Pharmacy and Pharmacology*, 46, 261–269.
- Cornwell, P.A., Barry, B.W., Bouwstra, J.A., Gooris, G.S., 1996. Modes of action of terpene penetration enhancers in human skin: Differential scanning calorimetry, small angle X-ray diffraction and enhancer uptake studies. *International Journal of Pharmaceutics*, 127, 9–26.
- Costa, P., Lobo, J.M.S., 2001. Modelling and comparison of dissolution profiles. *European Journal of Pharmaceutics and Biopharmaceutics*, 13, 123–133.
- Cowan, M.M., 1999. Plant products as antimicrobial agents. *Clinical Microbiology Reviews*, 12, 564–584.
- Dai, T., Tegos, G.P., Burkatovskaya, M., Castano, A.P., Hamblin, M.R., 2009. Chitosan acetate bandage as a topical antimicrobial dressing for infected burns. *Antimicrobial Agents and Chemotherapy*, 53, 393–400.
- Das, S., Ng, W.K., Tan, R.B.H., 2012. Are nanostructured lipid carriers (NLCs) better than solid lipid nanoparticles (SLNs): Development, characterisations and comparative evaluations of clotrimazole loaded SLNs and NLCs? *European Journal of Pharmaceutical Sciences*, 47, 139–151.
- De Lissovoy, G., Fraeman, K., Hutchins, V., Murphy, D., Song, D., Vaughn, B.B., 2009. Surgical site infection: Incidence and impact on hospital utilisation and treatment costs. *American Journal of Infection Control*, 37, 387–397.
- Degreef, H., 1998. How to heal a wound fast. *Dermatology Clinics*, 16, 365–375.
- Devi, N., Kakati, D.K., 2013. Smart porous microparticles based on gelatin/sodium alginate polyelectrolyte complex. *Journal of Food Engineering*, 117, 193–204.
- Dhawan, S., Kapil, R., Singh, B., 2011. Formulation development and systematic

- optimisation of solid lipid nanoparticles of quercetin for improved brain delivery. *The Journal of Pharmacy and Pharmacology*, 63, 342–351.
- Diamante, L.M., Lan, T., 2014. Absolute viscosities of vegetable oils at different temperatures and shear rate range of 64 . 5 to 4835 s<sup>-1</sup>. *Journal of Food Processing*, 1–6.
- Dias, M., Hadgraft, J., Lane, M.E., 2007. Influence of membrane-solvent-solute interactions on solute permeation in model membranes. *International Journal of Pharmaceutics*, 336, 108–114.
- Dick, I.P., Scott, R.C., 1992. Pig ear skin as an *in vitro* model for human permeability. *Journal of Pharmaceutics and Pharmacology*, 44, 640–645.
- Diegelmann, R.F., Evans, M.C., 2004. Wound healing: An overview of acute, delayed and fibrotic healing. *Frontiers in Bioscience*, 1, 283–189.
- Domínguez-Delgado, C.L., Rodríguez-Cruz, I.M., Escobar-Chávez, J.J., Calderón-Lojero, I.O., Quintanar-Guerrero, D., Ganem, A., 2011. Preparation and characterisation of triclosan nanoparticles intended to be used for the treatment of acne. *European Journal of Pharmaceutics and Biopharmaceutics*, 79, 102–107.
- Donsi, F., Annunziata, M., Vincensi, M., Ferrari, G., 2012. Design of nanoemulsion based delivery systems of natural antimicrobials: Effect of the emulsifier. *Journal of Biotechnology*, 159, 342–350.
- Dryden, M.S., Dailly, S., Crouch, M., 2004. A randomised, controlled trial of tea tree topical preparations versus a standard topical regimen for the clearance of MRSA colonisation. *Journal of Hospital Infection*, 56, 283–286.
- Edimo, A., 1993. Capacity of lipophilic auxiliary substances to give spheres by extrusion-spheronisation. *Drug Development and Industrial Pharmacy*, 19, 827–842.
- Edmiston, C.E., Bruden, B., Rucinski, M.C., Henen, C., Graham, M.B., Lewis, B.L., 2013. Reducing the risk of surgical site infections: Does chlorhexidine gluconate provide a risk reduction benefit? *American Journal of Infection Control*, 41, S49–S55.
- Edmiston, C.E., Seabrook, G.R., Johnson, C.P., Paulson, D.S., Beausoleil, C., 2007. Comparative of a new and innovative 2 % chlorhexidine gluconate-impregnated cloth with 4 % chlorhexidine gluconate as a topical antiseptic for preparation of the skin prior to surgery. *American Journal of Infection Control*, 35, 89–96.
- Edris, A.E., 2007. Pharmaceutical and therapeutic potentials of essential oils and their individual volatile constituents: A review. *Phytotherapeutic Research*, 21, 308–323.
- Edward, R., Harding, K.G., 2004. Bacteria and wound healing. *Current Opinion in Infectious Disease*, 17, 91–96.

- Eid, A.M., Elmarzugi, N.A., El-Enshasy, H.A., 2013. Preparation and evaluation of olive oil nanoemulsion using sucrose monoester. *International Journal of Pharmacy and Pharmaceutical Sciences*, 5, 434–440.
- Ekambaram, P., Abdul, H.A., Kailasa, P., 2012. Solid lipid nanoparticles: A review. *Scientific Reviews and Chemical Communications*, 2, 80–102.
- El Maghraby, G.M., 2008. Transdermal delivery of hydrocortisone from eucalyptus oil microemulsion: Effects of cosurfactants. *International Journal of Pharmaceutics*, 355, 285–292.
- El Nabarawi, M.A., Dalia, S.S., Dalia, A.A., Shereen, A.H., 2013. *In vitro* skin permeation and biological evaluation of lornoxicam monolithic transdermal patches. *International Journal of Pharmacy and Pharmaceutical Sciences*, 5, 242–248.
- El-Kattan, A.F., Asbill, C.S., Michniak, B.B., 2000. The effect of terpene enhancer lipophilicity on the percutaneous permeation of hydrocortisone formulated in HPMC gel systems. *International Journal of Pharmaceutics*, 198, 179–189.
- Elisabet, F., Clara, R., Martí, R., Elisabeth, B., 2005. Critical micelle concentration of surfactants in aqueous buffered and unbuffered systems. *Analytica Chimica Acta*, 548, 95–100.
- Eming, S.A., Smoler, H., Krieg, T., 2002. Treatment of chronic wounds: State of the art and future concepts. *Cells, Tissues and Organs*, 172, 105–117.
- Essa, S., Rabanel, J.M., Hildgen, P., 2011. Characterisation of rhodamine loaded PEG-g-PLA nanoparticles (NPs): Effect of poly(ethyleneglycol) grafting density. *International Journal of Pharmaceutics*, 411, 178–187.
- Esteves, B., Marques, A. V., Domingos, I., Pereira, H., 2013. Chemical changes of heat treated pine and eucalyptus wood monitored by FTIR. *Maderas. Ciencia y Tecnologia*, 15, 245–258.
- Fahr, A., Liu, X., 2007. Drug delivery strategies for poorly water soluble drugs. *Expert Opinion on Drug Delivery*, 4, 403–416.
- Falabella, A.F., 2006. Debridement and wound bed preparation. *Dermatology and Therapy*, 19, 317–325.
- Faller, B., 2008. Artificial membrane assays to assess permeability. *Current Drug Metabolism*, 9, 886–892.
- Fan, H., Lin, Q., Morrissey, G.R., Khavari, P.A., 1999. Immunization *via* hair follicles by topical application of naked DNA to normal skin. *Nature Biotechnology*, 17, 870–872.
- Fan, K., Tang, J., Escandon, J., Kirsner, R.S., 2011. State of the art in topical wound healing

- products. *Plastic and Reconstructive Surgery*, 127, 44–59.
- Fang, J.Y., Fang, C.L., Lui, C.H., Su, Y.H., 2008. Lipid nanoparticles as vehicles for topical psoralen delivery. *European Journal of Pharmaceutics and Biopharmaceutics*, 70, 633–640.
- Fatouros, D.G., Karpf, D.M., Nielsen, F.S., Mullertz, A., 2007. Clinical studies with oral lipid based formulations of poorly soluble compounds. *Therapeutics and Clinical Risk Management*, 3, 591–604.
- Femenía-Fonta, A., Balaguer-Fernández, C., Merinob, V., Rodillaa, V., López-Castellano, A., 2005. Effect of chemical enhancers on the *in vitro* percutaneous absorption of sumatriptan succinate. *European Journal of Pharmaceutics and Biopharmaceutics*, 61, 50–55.
- Filipe, V., Hawe, A., Jiskoot, W., 2010. Critical evaluation of nanoparticle tracking analysis (NTA) by NanoSight for the measurement of nanoparticles and protein aggregates. *Pharmaceutical Research*, 27, 796–810.
- Filon, F.L., Mauro, M., Adami, G., Bovenzi, M., Crosera, M., 2015. Nanoparticles skin absorption: New aspects for a safety profile evaluation. *Regulatory Toxicology and Pharmacology*, 72, 310–322.
- Fitzgerald, R.H., Bharara, M., Mills, J.L., Armstrong, D.G., 2009. Use of nanoflex powder dressing for wound management following debridement for necrotising fasciitis in the diabetic foot. *International Wound Journal*, 6, 133–139.
- Flaten, G.E., Palac, Z., Engesland, A., Filipović-Grčić, J., Vanić, Ž., Škalko-Basnet, N., 2015. *In vitro* skin models as a tool in optimisation of drug formulation. *European Journal of Pharmaceutical Sciences*, 75, 10–24.
- Flores, A., Kingsley, A., 2007. Topical antimicrobial dressings: An overview. *Wound Essential*, 2, 182–185.
- Fonder, M.A., Lazarus, G.S., Cowan, D.A., Aronson-Cook, B., Kohli, A.R., Mamelak, J.A., 2008. Treating the chronic wound: A practical approach to the care of non healing wounds and wound care dressings. *Journal of American Academy of Dermatology*, 58, 185–206.
- Forstner, C., Leitgeb, J., Schuster, R., Dosch, V., Kramer, A., Cutting, K., Leaper, D., Assadian, O., 2013. Bacterial growth kinetics under a novel flexible methacrylate dressing serving as a drug delivery vehicle for antiseptics. *International Journal of Molecular Sciences*, 14, 10582–10590.
- Fouad, E.A., El-Badry, M., Mahrous, G.M., Alsarra, I.A., Alashbban, Z., Alanazi, F.K., 2011. *In vitro* investigation for embedding dextromethorphan in lipids using spray drying. *Digest Journal of Nanomaterials and Biostructures*, 6, 1129–1139.



- Freitas, C., Müller, R.H., 1999. Correlation between long term stability of solid lipid nanoparticles (SLNs) and crystallinity of the lipid phase. *European Journal of Pharmaceutics and Biopharmaceutics*, 47, 125–132.
- Friend, D., Catz, P., Heller, J., Reid, J., Baker, R., 1988. Transdermal delivery of levonorgestrel I. alkanols as permeation enhancers. *Journal of Controlled Release*, 7, 243–250.
- Furr, J.R., Russell, A.D., Turner, T.D., Andrews, A., 1994. Antibacterial activity of Actisorb Plus, Actisorb and silver nitrate. *Journal of Hospital Infection*, 27, 201–208.
- Fuguet, E., Ràfols, C., Rosés, M., Bosch, E., 2005. Critical micelle concentration of surfactants in aqueous buffered and unbuffered systems. *Analytica Chimica Acta*, 548, 95–100.
- Gao, Z.H., 1995. Controlled release of contraceptive steroids from biodegradable and injectable gel: *In vivo* evaluation. *Pharmaceutical Research*, 12, 864–868.
- García-Fuentes, M., Torres, D., Alonso, M., 2002. Design of lipid nanoparticles for the oral delivery of hydrophilic macromolecules. *Colloids and Surfaces B: Biointerfaces*, 27, 159–168.
- Garduno-Ramirez, M.L., Clares, B., Dominguez-Villegas, V., Peraire, C., Ruiz, M.A., Garcia, M.L., Calpena, A.C., 2012. Skin permeation of cacalol, cacalone and 6-epicacalone sesquiterpenes from a nanoemulsion. *Natural Product Communications*, 7, 821–823.
- Gawkroder, D.J., Arden-Jones, M.R., 2002. *Dermatology: An illustrated colour text*.
- Gemmell, C.G., Edwards, D.I., Fraise, A.P., Gould, F.K., Ridgway, G.L., Warren, R.E., 2006. Guidelines for the prophylaxis and treatment of *methicillin-resistant staphylococcus aureus* (MRSA) infections in the UK. *Journal of Antimicrobial Chemotherapy*, 57, 589–608.
- Ghaffari, S., Varshosaz, J., Saadat, A., Atyabi, F., 2011. Stability and antimicrobial effect of amikacin-loaded solid lipid nanoparticles. *International Journal of Nanomedicine*, 6, 35–43.
- Ghalem, B.R., Mohamed, B., 2008. Antibacterial activity of leaf essential oils of eucalyptus globulus and eucalyptus camaldulensis. *African Journal of Pharmacy and Pharmacology*, 2, 211–215.
- Ghosh, T., Yum, S., Pfister, W., 1997. Dermal drug delivery products, in: *Transdermal and Topical Delivery Systems*. Interpharm Press, Buffalo Grove, IL, pp. 78–95.
- Gilbane, A.J., Denton, C.P., Holmes, A.M., 2013. Scleroderma pathogenesis: A pivotal role for fibroblasts as effector cells. *Clinical and Experimental Dermatology*, 15, 215.
- Godin, B., Touitou, E., 2007. Transdermal skin delivery: Predictions for human from *in vivo*, *ex vivo* and animal models. *Advanced Drug Delivery Reviews*, 59, 1152–1161.

- Goff, H.D., 1997. Colloidal aspects of ice cream: A review. *International Dairy Journal*, 7, 363–373.
- Gomes, M.J., Martins, S., Ferreira, D., Segundo, M.A., Reis, S., 2014. Lipid nanoparticles for topical and transdermal application for alopecia: Development, physicochemical characterisation, and *in vitro* release and penetration studies. *International Journal of Nanomedicine*, 9, 1231–1242.
- Grosse, C., Pedrosa, S., Shilov, V.N., 2002. On the influence of size, zeta potential, and state of motion of dispersed particles on the conductivity of a colloidal suspension. *Journal of Colloid and Interface Science*, 251, 304–310.
- Grove, C., Wilna, L., Jan L, D., Wenzhan, Y., Melgardt, M.D., 2003. Improving the aqueous solubility of triclosan by solubilization, complexation and *in situ* salt formation. *Journal of Cosmetic Science*, 54, 537–550.
- Guenther, E., 1948. The essential oils. Vol I, D. Van Norstrand Company, Inc., New York.
- Guillen, M.D., Cabo, N., 1997. Characterisation of edible oils and lard by fourier transform infrared spectroscopy: Relationships between composition and frequency of concrete bands in the fingerprint region. *Journal of American Oil Chemists' Society*, 74, 1281–1286.
- Guo, S., Dipietro, L.A., 2010. Factors affecting wound healing. *Journal of Dental Research*, 89, 219–229.
- Gupta, M., Vyas, S.P., 2012. Development, characterisation and *in vivo* assessment of effective lipodic nanoparticles for dermal delivery of fluconazole against cutaneous candidiasis. *Chemistry and Physics of Lipids*, 165, 454–461.
- Guy, R.H., Hadgraft, J., 1987. The effect of penetration enhancers on the kinetics of percutaneous absorption. *Journal of Controlled Release*, 5, 43–51.
- Guzey, D., McClements, D.J., 2006. Formation, stability and properties multilayer emulsions for application in the food industry. *Advances in Colloid and Interface Science*, 128, 227–248.
- Gysler, A., Kleuser, B., Sippl, W., Lange, K., Korting, H.C., Hölting, H.D., Korting, H.C., 1999. Skin penetration and metabolism of topical glucocorticoids in reconstructed epidermis and in excised human skin. *Pharmaceutical Research*, 16, 1386–1391.
- Haftek, M., Teillon, M.H., Schmitt, D., 1998. Stratum corneum, corneodesmosomes and *ex vivo* percutaneous penetration. *Microscopy Research and Technique*, 43, 242–249.
- Haigh, J.M., Smith, E.W., 1994. The selection and use natural and synthetic membranes for *in vitro* diffusion experiments. *European Journal of Pharmaceutical Sciences*, 2, 311–330.
- Håkansson, A., Trägårdh, C., Bergenståhl, B., 2009. Dynamic simulation of emulsion formation in a high pressure homogeniser. *Chemical Engineering Science*, 64, 2915–2925.

- Hamdani, J., 2003. Physical and thermal characterisation of precirrol and compritol as lipophilic glycerides used for the preparation of controlled release matrix pellets. *International Journal of Pharmaceutics*, 260, 47–57.
- Hamed, R., Basil, M., Albaraghthi, T., Sunoqrot, S., 2015. Nanoemulsion based gel formulation of diclofenac diethylamine: Design, optimisation, rheological behavior and *in vitro* diffusion studies. *Pharmaceutical Development and Technology*, 1–10.
- Hamishehkar, H., Ghanbarzadeh, S., Sepehran, S., Javadzadeh, Y., Adib, Z.M., Kouhsoltani, M., 2015. Histological assessment of follicular delivery of flutamide by solid lipid nanoparticles: Potential tool for the treatment of androgenic alopecia. *Drug Development and Industrial Pharmacy*, 7, 1–8.
- Hammer, K.A., Carson, C.F., Riley, T. V, Nielsen, J.B., 2006. A review of the toxicity of melaleuca alternifolia (tea tree) oil. *Food and Chemical Toxicology*, 44, 616–625.
- Han, F., Li, S., Yin, R., Liu, H., Xu, L., 2008. Effect of surfactants on the formation and characterisation of a new type of colloidal drug delivery system: Nanostructured lipid carriers. *Colloids and Surfaces A: Physicochemical and Engineering Aspects*, 315, 210–216.
- Harding, K., Cutting, K., Price, P., 2000. The cost effectiveness of wound management protocols of care. *British Journal of Nursing*, 9, 6–10.
- Harold, F.M., Baarda, J.R., Baron, C., Abrams, A., 1969. Dio 9 and chlorhexidine. Inhibition of membrane bound ATPase and of cation transport in *Streptococcus faecalis*. *Biochimica et Biophysica Acta*, 183, 129–136.
- Harrison, J.E., Watkinson, A.C., Green, D.M., Hadgraft, J., Brain, K., 1996. The relative effect of azone and transcutool on permeant diffusivity and solubility in human stratum corneum. *Pharmaceutical Research*, 13, 542–546.
- Hart, J., 2002. Inflammation: Its role in the healing of acute wounds. *Journal of Wound Care*, 11, 205–209.
- Hausen, B.M., Reichling, J., Harkenthal, M., 1999. Degradation products of monoterpenes are the sensitising agents in tea tree oil. *American Journal of Contact Dermatitis*, 10, 68–77.
- Hemmila, M.R., Mattar, A., Taddonio, M.A., Arbabi, S., Hamouda, T., Ward, P.A., Wang, S.C., Baker, J.R., 2010. Topical nanoemulsion therapy reduces bacterial wound infection and inflammation after burn injury. *Surgery*, 148, 499–509.
- Hendley, J.O., Ashe, K.M., 2003. Effect of topical antimicrobial treatment on aerobic bacteria in the stratum corneum of human skin. *Antimicrobial Agents and Chemotherapy*, 47, 1988–1990.
- Hendry, E.R., Worthington, T., Conway, B.R., Lambert, P.A., 2009. Antimicrobial efficacy of eucalyptus oil and 1,8-cineole alone and in combination with chlorhexidine digluconate

- against microorganisms grown in planktonic and biofilm cultures. *Journal of Antimicrobial Chemotherapy*, 64, 1219–1225.
- Henry, J.V.L., Fryer, P.J., Frith, J., Ian, T., 2009. Emulsification and storage instabilities of hydrocarbon-in-water sub micron emulsions stabilised with tweens 20 and 80, Brij 96v and sucrose monoesters. *Journal of Colloid and Interface Science*, 338, 201–206.
- Herculano, E.D., de Paula, H.C.B., de Figueiredo, E.T., Dias, F.G.B., De, P.V.A., 2015. Physicochemical and antimicrobial properties of nanoencapsulated eucalyptus staigeriana essential oil. *Food Science and Technology*, 61, 484–491.
- Herrero, a. M., Carmona, P., Pintado, T., Jiménez-Colmenero, F., Ruíz-Capillas, C., 2011. Olive oil-in-water emulsions stabilised with caseinate: Elucidation of protein lipid interactions by infrared spectroscopy. *Food Hydrocolloids*, 25, 12–18.
- Heurtault, B., Saulnier, P., Pech, B., Proust, J.E., Benoit, J.P., 2002. A novel phase inversion based process for the preparation of lipid nanocarrier. *Pharmaceutical Research*, 19, 875–880.
- Heuschkel, S., Goebel, A., Neubert, R.H.H., 2008. Microemulsions-morden colloidal carrier for dermal and transdermal drug delivery. *Journal of Pharmaceutical Sciences*, 97, 603–631.
- Hibbard, J.S., 2005. Analysis comparing the antimicrobial activity and safety of current antiseptic agents: A review. *Journal of Infusion Nursing*, 28, 194–207.
- Higgins, C., Palmer, A., Nixon, R., 2015. Eucalyptus oil: Contact allergy and safety. *Contact Dermatitis*, 52, 344–346.
- Hiom, S.J., Furr, J.R., Russell, A.D., Hann., A.C., 1996. The possible role of yeast cell walls in modifying cellular response to chlorhexidine diacetate. *Cytobios*, 86, 123–135.
- Hoelgaard, A., Mollgaard, B., 1985. Dermal drug delivery improvement by choice of vehicle or drug derivative. *Journal of Controlled Release*, 2, 111–120.
- Holder, C., Zellinger, M., 2009. Daily bathing with chlorhexidine in the ICU to prevent central line associated infections. *Journal of Clinical Outcomes Management*, 16, 509–513.
- Humar, A., Ostromecki, A., Direnfeld, J., Marshall, J.C., Lazar, N., Houston, P.C., Boiteau, P., Conly, J.M., 2000. Prospective randomised trial of 10 % povidone-iodine versus 0.5 % tincture of chlorhexidine as cutaneous antiseptics for prevention of central venous catheter infection. *Clinical Infectious Diseases*, 31, 1001–1007.
- Hung, C., Chen, W., Hsu, C., Aljuffali, I., Shih, H., Fang, J., 2015. Cutaneous penetration of soft nanoparticles via photodamaged skin: Lipid based and polymer based nanocarriers for drug delivery. *European Journal of Pharmaceutics and Biopharmaceutics*, 94, 94–105.
- Ibrahim, S.A., Li, K.S., 2010. Efficiency of fatty acids as chemical penetration enhancers:

Mechanisms and structure enhancement relationship. *Pharmaceutical Research*, 27, 115–125

ICH Harmonised Tripartite Guideline, 2005, Validation of analytical procedures: Text and methodology Q2(R1). The International Conference on Harmonisation of Technical Requirements for Registration of Pharmaceuticals for Human Use June 02, 2014. Available online: <http://somatek.com/content/uploads/2014/06/sk140605h.pdf>

Iscan, Y., Wissing, S.A., Hekimoglu, S., Müller, R.H., 2005. Solid lipid nanoparticles (SLN) for topical drug delivery: Incorporation of the lipophilic drugs N,N-diethyl-m-toluamide and Vitamin K. *Pharmazie*, 60, 905–909.

Ishihara, M., Nakanishi, K., Ono, K., Sato, M., Kikuchi, M., Saito, Y., Yura, H., Matsui, T., Hattori, H., Uenoyama, M., Kurita, A., 2002. Photocrosslinkable chitosan as a dressing for wound occlusion and accelerator in healing process. *Biomaterials*, 23, 833–840.

Jafari, S.M., Assadpoor, E., He, Y.H., Bhandari, B., 2008. Re-coalescence of emulsion droplets during high-energy emulsification. *Food Hydrocolloids*, 22, 1191–1202.

Jain, A.K., Thomas, N.S., Panchagnula, R., 2002. Transdermal drug delivery of imipramine hydrochloride: I. Effect of terpenes. *Journal of Controlled Release*, 79, 93–101.

Jain, K., Kumar, S.R., Sood, S., Gowthamarajan, K., 2013. Enhanced oral bioavailability of atorvastatin via oil-in-water nanoemulsion using aqueous titration method. *Journal of Pharmaceutical Sciences and Research*, 5, 18–25.

Jakate, A.S., Einhaus, C.M., DeAnglis, A.P., Retzinger, G.S., Desai, P.B., 2003. Preparation, characterisation, and preliminary application of fibrinogen-coated olive oil droplets for the targeted delivery of docetaxol to solid malignancies. *Cancer Research*, 63, 7314–7320.

Jakubovic, H.R., Ackerman, A.B., 1992. Structure and function of skin: Development, morphology and physiology, in: Moschella, S.L., Hurley, H.J. (Eds.), *Dermatology*. Saunders, W B, Philadelphia, pp. 3–87.

Jana, P., Hommos, A., Müller, R.H., 2009. Lipid nanoparticles (SLN,NLC) in cosmetic and pharmaceutical dermal products. *International Journal of Pharmaceutics*, 366, 170–184.

Jannin, V., Bérard, V., Diaye, A., Andrès, C., Pourcelot, Y., 2003. Comparative study of the lubricant performance of compritol<sup>®</sup> 888 ATO either used by blending or by hot melt coating. *Indian Journal of Pharmaceutical Sciences*, 262, 39–45.

Jasińska, M., Baldyga, J., Hallb, S., Pacek, A.W., 2014. Dispersion of oil droplets in rotor stator mixers: Experimental investigations and modeling. *Chemical Engineering and Processing: Process Intensification*, 84, 45–53.

Jenning, V., Gysler, A., Schafer-Korting, M., Gohla, S.H., Scha, M., 2000. Vitamin A loaded solid lipid nanoparticles for topical use: Occlusive properties and drug targeting

- to the upper skin. *European Journal of Pharmaceutics and Biopharmaceutics*, 49, 211–218.
- Jensen, L.B., Petersson, K., Nielsen, H.M., 2011. *In vitro* penetration properties of solid lipid nanoparticles in intact and barrier impaired skin. *European Journal of Pharmaceutics and Biopharmaceutics*, 79, 68–75.
- Jones, V.J., 2006. The use of gauze: Will it ever change. *International Wound Journal*, 3, 79–86.
- Josea, S., Anjua, S.S., Cinua, T.A., Aleykuttya, N.A., Thomasc, S., Souto, E.B., 2014. *In vivo* pharmacokinetics and biodistribution of resveratrol-loaded solid lipid nanoparticles for brain delivery. *International Journal of Pharmaceutics*, 20, 6–13.
- Joshi, V., Brewster, D., Colonero, P., 2012. *In vitro* diffusion studies in transdermal research:  
A synthetic membrane model in place of human skin. *Drug Development & Delivery*, 12, 40–42.
- Judd, A.M., Scurr, D.J., Heylings, J.R., Wan, K.W., Moss, G.P., 2013. Distribution and visualisation of chlorhexidine within the skin using ToF-SIMS: A potential platform for the design of more efficacious skin antiseptic formulations. *Pharmaceutical Research*, 30, 1896–1905.
- Jung, W.K., Kim, H.S., Koo, S., Shin, S., Kim, J.M., Park, Y.K., Hwang, Y.S., Yang, H., Park., Y.H., 2007. Antifungal activity of the silver ion against contaminated fabric. *Mycoses*, 50, 265–269.
- Junyaprasert, V.B., Singhsa, P., Jintapattanakit, A., 2013. Influence of chemical penetration enhancers on skin permeability of ellagic acid-loaded niosomes. *Asian Journal of Pharmaceutical Sciences*, 8, 110–117.
- Kakadia, P.G., Conway, B.R., 2014. Solid lipid nanoparticles: A potential approach for dermal drug delivery. *American Journal of Pharmacological Sciences*, 2, 1–7.
- Kansy, M., Senner, F., Gubernator, K., 1998. Physicochemical high throughput screening: Parallel artificial membrane permeation assay in the description of passive absorption processes. *Journal of Medicinal Chemistry*, 41, 1007–1010.
- Karadzovska, D., Riviere, J.E., 2013. Assessing vehicle effects on skin absorption using artificial membrane assays. *European Journal of Pharmaceutical Sciences*, 50, 569–576.
- Karn-orachaia, K., Smithb, S.M., Saesooc, S., Treethongc, A., Puttipipatkachornd, S., Pratontepe, S., Ruktanonchai, U.R., 2016. Surfactant effect on the physicochemical characteristics of  $\gamma$ -oryanol-containing solid lipid nanoparticles. *Colloids and Surfaces A: Physicochemical and Engineering Aspects*, 488, 118–128.
- Kärpänen, T., 2008. Studies on skin antisepsis and enhanced skin penetration of

- chlorhexidine. PhD Thesis. Aston University, U.K.
- Karpanen, T.J., Conway, B.R., Worthington, T., Hilton, A.C., Elliott, T.S.J., Lambert, P.A., 2010. Enhanced chlorhexidine skin penetration with eucalyptus oil. *BMC Infectious Disease*, 10, 278–283.
- Karpanen, T.J., Worthington, T., Conway, B.R., Hilton, A.C., J, E.T.S., Lambert, P.A., 2008. Penetration of chlorhexidine into human skin. *Antimicrobial Agents and Chemotherapy*, 52, 3633–3636.
- Kaye, E.T., 2000. Topical antimicrobial agents. *Infectious Disease Clinics of North America*, 14, 321–339.
- Kazarian, S.G., Chan, K.L., 2013. ATR-FTIR spectroscopic imaging: Recent advances and applications to biological systems. *The Analyst*, 138, 1940–1951.
- Kelidari, H.R., Saeedi, M., Akbari, J., Morteza-Semnani, K., Gill, P., Valizadeh, H., Nokhodchi, A., 2015. Formulation optimisation and *in vitro* skin penetration of spironolactone loaded solid lipid nanoparticles. *Colloids and Surfaces B: Biointerfaces*, 128, 473–479.
- Kennedy-Evans, K.L., Lutz, J.B., 2010. Hydrogel dressings. *Advances in Wound Care*, 1, 131–136.
- Khalil, R.M., El-bary, A.A., Kassem, M.A., Ghorab, M.M., Ahmed, M.B., 2013. Solid lipid nanoparticles for topical delivery of meloxicam : Development and *in vitro* characterisation, in: 1st Annual International Interdisciplinary Conference 24–26.
- Khurana, S., Bedi, P.M.S., Jain, N.K., 2010. Development of nanostructured lipid carriers (NLC) for controlled delivery of meloxicam. *International Journal of Biomedical Nanoscience and Nanotechnology*, 1, 247–266.
- Kim, J., Uchiyamab, T., Carrilhac, M., Ageed, K.A., Mazzonie, A., Breschif, L., Carvalhog, R.M., Leo, T., Looneyi, S., Wimmeri, C., Tezvergil-Mutluayj, A., Tayk, F.R., Pashley, D.H., 2008. Chlorhexidine binding to mineralised versus deminaralised dentin powder. *Dental Materials*, 42, 157–162.
- Klang, V., Valenta, C., 2011. Lecithin based nanoemulsions. *Journal of Drug Delivery Science and Technology*, 21, 55–76.
- Klasen, H.J., 2000. Historical review of the use of silver in the treatment of burns I. Early uses. *Burns*, 26, 117–130.
- Klimek, J.J., 1985. Treatment of wound infection. *Cutis: Cutaneous Medicine for the Practitioner*, 36, 21–24.
- Knaggs, H., 2007. Cell biology of pilocebaseous unit, in: Webster, G., Rawlings, A. (Eds.),

- Acne and Its Therapy*. Informa Healthcare, New York, pp. 12–36.
- Knorr, F., Lademann, J., Patzelt, A., Sterry, W., Blume-Peytavi, U., Vogt, A., 2009. Follicular transport route - Research progress and future perspectives. *European Journal of Pharmaceutics*, 71, 173–180.
- Koletzko, B., Göbel, Y., Böhles, H.J., Engelsberger, I., Forget, D., Le Brun, A., Peters, J., Zimmermann, A., 2003. Parenteral fat emulsion based on olive and soybean oils. *Journal of Pediatric Gastroenterology and Nutrition*, 37, 161–167.
- Korting, H.C., Schöllmann, C., White, R.J., 2011. Management of minor acute cutaneous wounds: Importance of wound healing in a moist environment. *Journal of the European Academy of Dermatology and Venereology*, 25, 130–137.
- Kotikalapudi, L.S., Adepu, L., VijayaRatna, J., Diwan, P. V., 2012. Formulation and *in vitro* characterisation of domperidone loaded solid lipid nanoparticles. *International Journal of Pharmaceutical and Biomedical Research*, 3, 22–29.
- Kreilgaard, M., Pedersen, E., Jaroszewski, J.W., 2000. NMR characterisation and transdermal drug delivery potential of microemulsion systems. *Journal of Controlled Release*, 69, 421–433.
- Küchler, S., Radowski, M.R., Blaschke, T., Dathe, M., Plendl, J., Haag, R., Schäfer-Korting, M Kramer, K.D., 2009. Nanoparticles for skin penetration enhancement - A comparison of a dendritic core multishell nanotransporter and solid lipid nanoparticles. *European Journal of Pharmaceutics and Biopharmaceutics*, 71, 243–250.
- Kumar, A., Samarth, R.M., Yasmeen, S., Sharma, A., Sugahara, T., Terado, T., Kimura, H., 2004. Anticancer and radioprotective potentials of mentha piperita. *Biofactors*, 22, 87–91.
- Kumar, S., Randhawa, J.K., 2015. Solid lipid nanoparticles of stearic acid for the drug delivery of paliperidone. *Royal Society of Chemistry*, 5, 68743–68750.
- Kupetz, E., Bunjes, H., 2014. Lipid nanoparticles: Drug localisation is substance specific and achievable load depends on the size and physical state of the particles. *Journal of Controlled Release*, 189, 54–64.
- Kushla, G.P., Zatz, J.L., 1991. Correlation of water and lidocaine flux enhancement by cationic surfactants *in vitro*. *Journal of Pharmaceutical Sciences*, 80, 1079–1083.
- Lademan, J., Richter, H., Teichmann, A., Otberg, N., Blume-Peytavi, U., Luengo, J., Weiss, B., Schaefer, U., Lehr, C.M., Wepf, R., Sterry, W., 2007. Nanoparticles: An efficient carrier for drug delivery into the hair follicles. *European Journal of Pharmaceutics and Biopharmaceutics*, 66, 159–164.
- Lademann, J., Jacobi, U., Surber, C., Weigmann, H.J., Fluhr, J.W., 2009. The tape stripping procedure - Evaluation of some critical parameters. *European Journal of Pharmaceutics and Biopharmaceutics*, 72, 317–323.



- Lambers, H., Piessens, S., Bloem, A., Pronk, H., Finkel, P., 2006. Natural skin surface pH is on average below 5, which is beneficial for its resident flora. *International Journal of Cosmetic Science*, 28, 359–370.
- Lane, M.E., 2013. Skin penetration enhancers. *International Journal of Pharmaceutics*, 447, 12–21.
- Laouini, A., Fessi, H., Charcosset, C., 2012. Membrane emulsification: A promising alternative for vitamin E encapsulation within nanoemulsion. *Journal of Membrane Science*, 423-424, 85–96.
- Larese, F., Mauro, M., Adami, G., Bovenzi, M., Crosera, M., 2015. Nanoparticles skin absorption: New aspects for a safety profile evaluation. *Regulatory Toxicology and Pharmacology*, 72, 310–322.
- Lau, W.M., White, A.W., Gallagher, S.J., Donaldson, M., McNaughton, G., Heard, C.M., 2008. Scope and limitations of the co-drug approach to topical drug delivery. *Current Pharmaceutical Design*, 14, 794–802.
- Lauer, A.C., 2005. Percutaneous drug delivery to the hair follicle, in: Bronaugh, R.L., Maibach, H.I. (Eds.), *Percutaneous Absorption: Drugs, Cosmetics, Mechanisms, Methods*. Marcel Dekker, pp. 427–450.
- Lauterbach, A., Müller-goymann, C., 2014. Comparison of rheological properties, follicular penetration, drug release, and permeation behavior of a novel topical drug delivery system and a conventional cream. *European Journal of Pharmaceutics and Biopharmaceutics*, 88, 614–624.
- Lawrence, W.T., 1998. Physiology of acute wound. *Clinics in Plastic Surgery*, 25, 321 – 340.
- Lawrence, W.T., Diegelmann, R.F., 1994. Growth factors in wound healing. *Clinics in Dermatology*, 12, 157–169.
- Leaper, D., 2006. Silver dressings: Their role in wound management. *International Wound Journal*, 3, 282–294.
- Lee, T.W., Kim, J.C., Hwang, S.J., 2003. Hydrogel patches containing triclosan for acne treatment. *European Journal of Pharmaceutics and Biopharmaceutics*, 56, 407–412.
- Leive, L., 1974. The barrier function of the Gram-negative envelope. *Annals of the New York Academy of Sciences*, 235, 109–129.
- Leveque, J.L., de Rigal, J., Saint-Leger, D., Billy, B., 1993. How does sodium lauryl sulfate alter the skin barrier function in man? A multiparametric approach. *Skin Pharmacology*, 6, 111–115.
- Li, J., Chen, J., Kirsner, R., 2007. Pathophysiology of acute wound healing. *Clinics in*

*Dermatology*, 25, 9–18.

Li, P., Ghosh, A., Wagner, R.F., Krill, S., Joshi, Y.M., Serajjudin, A.M., 2005. Effect of combined use of non ionic surfactant on formation of oil-in-water nanoemulsion.

*International Journal of Pharmaceutics*, 288, 27–34.

Li, Y.F., Sun, H.W., Gao, R., Liu, K.Y., Zhang, Q., Fu, Q.H., Li, S., Guo, G., Ming, Q., 2015.

Inhibited biofilm formation and improved antibacterial activity of a novel nanoemulsion against cariogenic streptococcus mutans *in vitro* and *in vivo*. *International Journal of Nanomedicine*, 447–462.

Liedtke, S., Wissing, S., Müller, R.H., Mader, K., 2000. Influence of high pressure homogenisation equipment on nanodispersions characteristics. *International Journal of Pharmaceutics*, 196, 183–185.

Lin, G.H., Hemming, M., 1996. Ocular and dermal irritation studies of some quaternary ammonium compounds. *Food and Chemical Toxicology*, 34, 177–182.

Liu, D., Ge, Y., Tang, Y., Yuan, Y., Zhang, Q., Li, R., Xu, Q., 2010a. Solid lipid nanoparticles for transdermal delivery of diclofenac sodium: Preparation, characterisation and *in vitro*

studies. *Journal of Microencapsulation*, 27, 726–734.

Liu, D., Liu, C., Zou, W., Zhang, N., 2010b. Enhanced gastrointestinal absorption of N3-O-toluyfl-fluorouracil by cationic solid lipid nanoparticles. *Journal of Nanoparticle Research*, 12, 975–984.

Liu, J., Gong, T., Wang, C., Zhong, Z., Zhang, Z., 2007. Solid lipid nanoparticles loaded with insulin by sodium cholate phosphatidylcholine based mixed micelles: Preparation and characterisation. *International Journal of Pharmaceutics*, 340, 153–162.

Liu, J., Hu, W., Chen, H., Ni, Q., Xu, H., Yang, X., 2007. Isotretinoin-loaded solid lipid nanoparticles with skin targeting for topical delivery. *International journal of pharmaceutics*, 328, 191–5.

Loo, C.H., Basri, M., Tejo, B.A., Ismail, R., Nang, H.L.L., Hassan, H.A., Choo, Y.M., 2011. An improved method for the preparations of nanostructured lipid carriers containing heat sensitive bioactives. *Colloids and Surfaces B: Biointerfaces*, 87, 180–186.

Lorian, V., 2005. Disinfectants and antiseptics, modes of action, mechanisms of resistance and testing, in: *Antibiotics in Laboratory Medicine*. Lippincott Williams & Wilkins, PA, pp. 628–630.

Loveday, H.P., Wilson, J.A., Pratt, R.J., Golsorkhi, M., Tingle, A., Bak, A., Browne, J., Prieto, J., Wilcox, M., 2014. National evidence-based guidelines for preventing healthcare associated infections in NHS hospitals in england. *Journal of Hospital*

*Infection*, 86, S1–S70.

Mahdi, E.S., Sakeena, M.H., Abdulkarim, M.F., Abdullah, G.Z., Sattar, M.A., Noor, A.M., 2011. Effect of surfactant and surfactant blends on pseudoternary phase diagram behavior of newly synthesised palm kernel oil esters. *Drug Design, Development and Therapy*, 5, 311–323.

Mahe, B., Vogt, A., Liard, C., Duffy, D., Abadie, V., Bonduelle, O., Boissonnas, A., W., S., Verrier, B., Blume-Peytavi, U. Combadiere, B., 2009. Nanoparticle based targeting of vaccine compounds to skin antigen presenting cells by hair follicles and their transport in mice. *Journal of Investigative Dermatology*, 129, 1156–1164.

Mahmood, M.E., Al-Koofee, D.A.F., 2013. Effect of temperature changes on critical micelle concentration for tween series surfactant. *Global Journal of Science Frontier Research Chemistry*, 13, 1–7.

Maibach, H.I., Feldmann, R., 1967. The effect of DMSO on percutaneous penetration of hydrocortisone and testosterone in man. *Annals of the New York Academy of Sciences*, 141, 423–427.

Makraduli, L., Crcarevska, M.S., Geskovski, N., Dodov, M.G., Goracinova, K., 2013. Factorial design analysis and optimisation of alginate-Ca-chitosan microspheres. *Journal of Microencapsulation*, 30, 81–92.

Malcolmson, C., Satra, C., Kantaria, S., Sidhu, A., Lawrence, M.J., 1998. Effect of oil on the level of solubilisation of testosterone propionate into non-ionic oil-in-water microemulsions. *Journal of Pharmaceutical Sciences*, 87, 109–116.

Mangram, J.A., Horan, C.T., Pearson, L.M., Silver, C.L., Jarvis, R.W., 1999. Guideline for prevention of surgical site infection. *Infection Control and Hospital Epidemiology*, 20, 247–278.

Mao, G., Flach, C.R., Mendelsohn, R., Walters, R.M., 2012. Imaging the distribution of sodium dodecyl sulfate in skin by confocal raman and infrared microspectroscopy. *Pharmaceutical Research*, 29, 2189–2201.

Marcia, R.-E.-S., Castro, M., 2002. New dressings, including tissue engineered living skin. *Clinics in Dermatology*, 20, 715–723.

Mason, T.G., Wilking, J.N., Meleson, K., Chang, C.B., Graves, S.M., 2006. Nanoemulsions:

Formation, structure and physical properties. *Journal of Physics: Condensed Matter*, 18, 635–

666.

Mayer, S., Weiss, J., McClements, D.J., 2013. Behavior of vitamin E acetate delivery systems

under simulated gastrointestinal conditions: Lipid digestion and bioaccessibility of low energy nanoemulsions. *Journal of Colloid and Interface Science*, 404, 215–222.

McClement, D.J., 2011. Edible nanoemulsions: Fabrication, properties and functional performance. *Soft Matter*, 7, 2297.

McClements, D.J., Xiao, H., 2012. Potential biological fate of ingested nanoemulsions: Influence of particle characteristics. *Food and Function*, 3, 202–220.

McDonnell, G., Russell, A.D., 1999. Antiseptics and disinfectants: Activity, action and resistance. *Clinical Microbiology Reviews*, 12, 147–149.

Mehnert, W., Mäder, K., Wolfgang, M., 2001a. Solid lipid nanoparticles production, characterisation and applications. *Advanced Drug Delivery Reviews*, 47, 83–101.

Mehnert, W., Mäder, K., Wolfgang, M., Madar, K., Mader, K., 2001b. Solid lipid nanoparticles production, characterisation and applications. *Advanced Drug Delievery Reviews*, 47, 83–101.

Meidan, V.C., Bonner, M., Michniak, B., 2005. Transfollicular drug delivery - is it a reality?

*International Journal of Pharmaceutics*, 306, 1 – 14.

Michell, L.R., Yunsheng, H., Kwokei, N., Walter, A.K., Richard, M.C., 2003. Direct analysis

of drug candidates in tissue by matrix-assisted laser desorption/ionisation mass spectrometry.

*Journal of Mass Spectroscopy*, 38, 1081–1092.

Miki, R., Ichitsuka, Y., Yamada, T., Kimura, S., Egawa, Y., Seki, T., Juni, K., Ueda, H., Morimoto, Y., 2015. Development of a membrane impregnated with a

poly(dimethylsiloxane)/poly(ethylene glycol) copolymer for a high throughput screening of the permeability of drugs, cosmetics, and other chemicals across the human skin. *European Journal of Pharmaceutical Sciences*, 66, 41–49.

Mills, S.E., Cross, P.C., 2006. Transdermal drug delivery: Basic principles for the veterinarian. *The Veterinary Journal*, 172, 218–233.

Mittal, A., Schulze, K., Ebensen, T., Weissmann, S., Hansen, S., Guzmán, C., Lehr, C., 2015.

Inverse micellar sugar glass (IMSG) nanoparticles for transfollicular vaccination. *Journal of Controlled Release*, 206, 140–152.

- Monaco, J.L., Lawrence, W.T., 2003. Acute wound healing an overview. *Clinics in Plastic Surgery*, 30, 1–12.
- Morgan, D.A., 2002. Wounds-What should a dressing formulary include? *Hospital Pharmacist*, 9, 261–266.
- Morgan, D.A., 1999. Wound management products in the drug tariff. *Pharmaceutical Journal*, 263, 820–825.
- Morimoto, H., Wada, Y., Seki, T., Sugibayashi, K., 2002. *In vitro* skin permeation of morphine hydrochloride during the finite application of penetration enhancing system containing water, ethanol and L-menthol. *Biological and Pharmaceutical Bulletin*, 25, 134–136.
- Morse, A., 2009. Reducing healthcare associated infections in hospitals in England. National Audit Office.
- Morton, H.E., 1983. Alcohols, in: S. S. Bloch (ed.) (Ed.), *Disinfection, Sterilization, and Preservation*,. Lea & Febiger, Philadelphia, pp. 225–239.
- Mukerjee, P., Mysels, K.J., 1971. Critical micelle concentration of aqueous surfactant systems. US. Government Printing Office, Washington, D.C., *NSRDS-NBS 36*,.
- Müller, R.H., Mäder, K., Gohla, S.H., Muller, R.H., Mader, K., 2000. Solid lipid nanoparticles for controlled drug delivery: A review of the state of the art. *European Journal of Pharmaceutics and Biopharmaceutics*, 50, 161–177.
- Müller, R.H., Mehnert, W., Lucks, J.S., Schwarz, C., Mühlen, A. zur, Weyhers, H., Freitas, C., Rühl, D., 1995. Solid lipid nanoparticles (SLN) - An alternative colloidal carrier system for controlled drug delivery. *European Journal of Pharmaceutics and Biopharmaceutics*, 41, 62–69.
- Müller, R.H., Petersen, R.D., Hommoss, A., Pardeike, J., 2007. Nanostructured lipid carriers (NLC) in cosmetic dermal products. *Advanced Drug Delivery Reviews*, 59, 522–30.
- Mulyaningsih, S., Sporer, F., Reichling, J., Wink, M., 2011. Antibacterial activity of essential oils from eucalyptus and of related components against multi-resistant bacterial pathogens. *Pharmaceutical Biology*, 49, 893–899.
- Nagelreitera, C., Mahrhausera, D., Wiatschkaa, K., Skipiola, S., Valenta, C., 2015. Importance of a suitable working protocol for tape stripping experiments on porcine ear

skin: Influence of lipophilic formulations and strip adhesion impairment. *International Journal of Pharmaceutics*, 491, 162-169.

Nakano, M., Patel, N.K., 1970. Release, uptake, and permeation behavior of salicylic acid in

ointment bases. *Journal of Pharmaceutical Sciences*, 59, 985–988.

Narishetty, S.T.K., Panchagnula, R., 2005. Effect of L-menthol and 1,8-cineole on phase behavior and molecular organisation of SC lipids and skin permeation of zidovudine. *Journal*

*of Controlled Release*, 102, 59–70.

Nayak, A.P., Tiyaboonchai, W., Patankar, S., Madhusudhan, B., Souto, E.B., 2010.

Curcuminoids-loaded lipid nanoparticles: Novel approach towards malaria treatment. *Colloids and Surfaces B: Biointerfaces*, 81, 263–273.

Neely, A.N., Gardner, J., Durkee, P., Warden, G.D., Greenhalgh, D.G., Gallagher, J.J., Herndon, D.N., Tompkins, R.G., Kagan, R.J., 2009. Are topical antimicrobials effective against bacteria that are highly resistant to systemic antibiotics? *Journal of Burn Care & Research*, 30, 19–29.

Negi, J.S., Chattopadhyay, P., Sharma, A.K., Ram, V., 2014. Development and evaluation of

glyceryl behenate based solid lipid nanoparticles (SLNs) using hot self-nanoemulsification (SNE) technique. *Archives of Pharmacal Research*, 37, 361–370.

Nerella, A., Basava, R., Devi, A., 2014. Formulation, optimisation and *in vitro* characterisation of letrozole loaded solid lipid nanoparticles. *International Journal of Pharmaceutical Sciences and Drug Research*, 6, 183–188.

Nerurkar, M.M., 1996. The use of surfactants to enhance the permeability of peptides through

Caco-2 cells inhibition of an apically polarised efflux system. *Pharmaceutical Research*, 13, 528–534.

Neupanea, Y.R., Srivastavaa, M., Ahmada, N., Kumarb, N., Bhatnagarb, A., Kohli, K., 2014. Lipid based nanocarrier system for the potential oral delivery of decitabine: Formulation design, characterisation, *ex vivo*, and *in vivo* assessment. *International Journal of Pharmaceutics*, 477, 601–612.

Ngawhirunpat, T., Opanasopit, P., Rojanarata, T., Panomsuk, S., Chanchome, L., 2008.

Evaluation of simultaneous permeation and metabolism of methyl nicotinate in human, snake

and shed snake skin. *Pharmaceutical Development and Technology*, 13, 75–83.

Niknafs, N., Spyropoulos, F., Norton, I.T., 2011. Development of a new reflectance technique to investigate the mechanism of emulsification. *Journal of Food Engineering*, 104, 603–611.

O’Toole, E.A., 2001. Extracellular matrix and keratinocyte migration. *Clinical Experimental Dermatology*, 26, 525–530.

Ogunwande, I.A., Olawore, N.O., Adeleke, K.A., Konig, W.A., 2003. Chemical composition of the essential oils from the leaves of three eucalyptus species growing in Nigeria. *Journal of Essential Oil Research*, 15, 297–301.

Ohman, H., Vahlquist, A., 1998. The pH gradient over the stratum corneum differs in X-linked recessive and autosomal dominant Ichthyosis: A clue to molecular origin of ‘acid skin mantle’? *The Journal of Investigative Dermatology*, 111, 674–677.

Okano, M., Nomura, M., Hata, S., Okada, N., Sato, K., Kitano, Y., Tashiro, M., Yoshimoto, Y., Hama, R., Aoki, T., 1989. Anaphylactic symptoms due to chlorhexidine gluconate. *Archives of Dermatology*, 125, 50–52.

Oliveira, G., Beezer, A., Hadgraft, J., Lane, M.E., 2011. Alcohol enhanced permeation in model membranes. Part II. Thermodynamic analysis of membrane partitioning. *International Journal of Pharmaceutics*, 420, 216–222.

Omar, M., 2013. Studying the release of diclofenac sodium from glycerides. *International Journal of Pharmacy and Pharmaceutical Sciences*, 5, 119–127.

Orafidiya, L.O., Oladimeji, F.A., 2002. Determination of the required HLB values of some essential oils. *International Journal of Pharmaceutics*, 237, 241–249.

Orhan, M., 2012. Determination and characterisation of triclosan on polyethylene terephthalate fibres. *Journal of Textiles and Engineer*, 19, 27–30.

Osborne, D.W., 2011. Diethylene glycol monoethyl ether: An emerging solvent in topical dermatology products. *Journal of Cosmetic Dermatology*, 10, 324–329.

Otberg, N., Richter, H., Schaefer, H., Blume-Peytavi, U., Sterry, W., Lademann, J., 2004. Variations of hair follicle size and distribution in different body sites. *Journal of Investigative Dermatology*, 122, 14–19.

- Otberg, N., Teichmann, A., Rasuljev, U., Sinkgraven, R., Sterry, W., Lademann, J., 2007. Follicular penetration of topically applied caffeine *via* a shampoo formulation. *Skin pharmacology and physiology*, 20, 8.
- Padhye, S.G., Nagarsenker, M.S., 2013. Simvastatin solid lipid nanoparticles for oral delivery: Formulation development and *in vivo* evaluation. *Indian Journal of Pharmaceutical Sciences*, 75, 591–598.
- Pandey, A., Mittal, A., Chauhan, N., Alam, S., 2014. Role of surfactants as penetration enhancer in transdermal drug delivery system. *Journal of Molecular Pharmaceutics & Organic Process Research*, 02, 109–113.
- Parveen, R., Baboota, S., Ali, J., Ahuja, A., Vasudev, S.S., Ahmad, S., 2011. Oil based nanocarrier for improved oral delivery of silymarin: *In vitro* and *in vivo* studies. *International Journal of Pharmaceutics*, 413, 245–253.
- Patel, D., Dasgupta, S., Dey, S., Ramani, Y.R., Ray, S., Mazumder, B., 2012. Nanostructured lipid carriers (NLC) based gel for the topical delivery of aceclofenac: Preparation, characterisation, and *in vivo* evaluation. *Scientia Pharmaceutica*, 80, 749–764.
- Patzelt, A., Richter, H., Buettemeyer, R., Huber, H.J., Blume-Peytavi, U., Sterry, W., Lademann, J., 2008. Differential stripping demonstrates a significant reduction of the hair follicle reservoir *in vitro* compared to *in vivo*. *European Journal of Pharmaceutics and Biopharmaceutics*, 70, 234–238.
- Patzelt, A., Richter, H., Knorr, F., Schäfer, U., Lehr, C.M., Dähne, L., Sterry, W., Lademann, J., 2011. Selective follicular targeting by modification of the particle sizes. *Journal of Controlled Release*, 150, 45–48.
- Paulson, D.S., 2014. Current topical antimicrobials, in: *Topical Antimicrobials Testing and Evaluation*. CRS Press, pp. 85–88.
- Percival, S.L., Emanuel, C., Cutting, K.F., Williams, D.W., 2012. Microbiology of the skin and the role of biofilms in infection. *International wound journal*, 14–32.
- Pershing, L.K., Lambert, L.D., Knutson, K., 1990. Mechanism of ethanol enhanced estradiol permeation across human skin *in vivo*. *Pharmaceutical Research*, 7, 170–175.
- Peter, T.C., Dong, C.Y., Masters, B.R., Berland, K.M., 2000. Two-photon excitation fluorescence microscopy. *Annual Review of Biomedical Engineering*, 2, 399–429.



- Philippa, J.H., Francese, S., Emmanuelle, C.M., Nicola, W., Malcolm, C.R., 2011. MALDI-MS imaging of lipids in *ex vivo* human skin. *Analytical and Bioanalytical Chemistry*, 401, 115–125.
- Piette, A., Verschraegen, G., 2009. Role of coagulase-negative *staphylococci* in human disease. *Veterinary Microbiology*, 134, 45–54.
- Pillai, O., Nair, V., Panchagnula, R., 2004. Transdermal iontophoresis of insulin: IV. Influence of chemical enhancers. *International Journal of Pharmaceutics*, 269, 109–120.
- Pinkus, H., 1951. Examination of the epidermis by the strip method of removing horny layers.  
I. Observations on thickness of the horny layer, and on mitotic activity after stripping. *Journal of Investigative Dermatology*, 16, 383–386.
- Pool, J.G., 1977. Normal hemostatic mechanisms: A review. *American Journal of Medical Technology*, 43, 776–780.
- Pople, P. V, Singh, K.K., 2006. Development and evaluation of topical formulation containing solid lipid nanoparticles of vitamin A. *AAPS PharmSciTech*, 1–7.
- Popovich, K.J., Lyles, R., Hayes, R., Hota, B., Trick, W., Weinstein, R.A., Hayden, M.K., 2012. Relation of chlorhexidine gluconate skin concentration to microbial density on skin of critically III patients bathed daily with chlorhexidine gluconate. *Infection Control and Hospital Epidemiology*, 33, 889–896.
- Prajapati, S.T., Joshi, H.A., Patel, C.N., 2013. Preparation and characterisation of self-microemulsifying drug delivery system of olmesartan medoxomil for bioavailability improvement. *Journal of Pharmaceutics*, 2013, 1–9.
- Prasanthi, D., Lakshmi, P.K., 2012. Effect of chemical enhancers in transdermal permeation of alfuzosin hydrochloride. *International Scholarly Research Network*, 1–8.
- Pratt, R.J., Pellowe, C.M., Wilson, J.A., Harper, P.J., Jones, S. R. L. J., McDougall, C., Wilcox, M.H., 2007. National evidence-based guidelines for preventing healthcare associated infection in NHS hospitals in England. *Journal of Hospital Infection*, 65, S1–64.
- Prausnitz, M.R., Mitragotri, S., Langer, R., 2004. Current status and future potential of transdermal drug delivery. *Nature Reviews Drug Discovery*, 3, 115–124.
- Priano, L., Esposti, D., Esposti, R., Castagna, G., Medici, C.D., Fraschini, F., Gasco, M.R., Mauro, A., 2007. Solid lipid nanoparticles incorporating melatonin as new model for sustained oral and transdermal delivery systems. *Journal of Nanoscience and*

*Nanotechnology*, 7, 3596–3601.

Prinderre, P., Piccerelle, P.H., Cauture, E., Kalantzis, G., Reynier, J.P., Joachim, J., 1998. Formulation and evaluation of o/w emulsions using experimental design. *International Journal of Pharmaceutics*, 163, 73–79.

Priyanka, K., Abdul, H.S., 2012. Preparation and evaluation of montelukast sodium loaded solid lipid nanoparticles. *Journal of Young Pharmacists*, 4, 129–137.

Priyanka, K., Sathali, A.A., 2012. Preparation and evaluation of montelukast sodium loaded solid lipid nanoparticles. *Journal of Young Pharmacists*, 4, 129–37.

Puglia, C., Bonina, F., 2008. Effect of polyunsaturated fatty acids and some conventional penetration enhancers on transdermal delivery of atenolol. *Drug Delivery*, 15, 107–112.

Puglia, C., Filosa, R., Peduto, A., de Caprasiis, P., Rizza, L., Bonina, F., Blasi, P., 2006. Evaluation of alternative strategies to optimise ketorolac transdermal delivery. *AAPS PharmSciTech*, 7, 1–9.

Purner, S.K., Babu, M., 2000. Collagen based dressings- A review. *Burns*, 26.

Qian, C., McClements, D.J., 2011. Formation of nanoemulsions stabilised by model food grade emulsifiers using high pressure homogenisation: Factors affecting particle size. *Food Hydrocolloids*, 25, 1000 – 1008.

Queen, D., Orsted, H., Sanada, H., Sussman, G., 2004. A dressing history. *International Wound Journal*, 1, 59–77.

Quinn, K.J., Courtney, J.M., Evans, J.H., Gaylor, J.D., Reid, W.H., 1985. Principles of burn of dressings. *Biomaterials*, 6, 369–377.

Rahman, S.M.H., Telny, T.C., Ravi, T.K., Kuppusamy, S., 2009. Role of surfactant and pH in dissolution of curcumin. *Indian Journal of Pharmaceutical Sciences*, 71, 139–142.

Rahman, Z., Zidan, A.S., Khan, M.A., 2010. Non destructive methods of charcaterisation of risperidone solid lipid nanoparticles. *European Journal of Pharmaceutics and Biopharmaceutics*, 76, 127–137.

Rai, V., Ghosh, I., Bose, S., Silva, S.-M.-C., Chandra, P., Michiniak-Kohn, B., 2010. A transdermal review on permeation of drug formulations, modifier compounds and delivery methods. *Journal of Drug Delivery Science and Technology*, 20, 75–87.

Rajan, R., Vasudevan, D.T., 2012. Effect of permeation enhancers on the penetration mechanism of transdermal gel of ketoconazole. *Journal of Advanced Pharmaceutical Technology and Research*, 3, 112–116.

Ramadan, A.A., 2010. A study of some lipid based drug delivery systems. PhD Thesis. University of Alexandria, Egypt.

- Ramasasthy, S.S., 2005. Acute wounds. *Clinical Plastic Surgery*, 32, 195–208.
- Ramshaw, J., Werkmeister, J.A., Glatteur, V., 1995. Collagen based biomaterials. *Biotechnology Review*, 13, 336–382.
- Rao, J., McClements, D.J., 2011. Formation of flavor oil microemulsions, nanoemulsions and emulsions: Influence of composition and preparation method. *Journal of Agricultural and Food Chemistry*, 59, 5026–5035.
- Rassua, G., Cossua, M., Langascoa, R., Cartaa, A., Cavallib, R., Giunchedia, P., Gavinia, E., 2015. Propolis as lipid bioactive nanocarrier for topical nasal drug delivery. *Colloids and Surfaces B: Biointerfaces*, 136, 908–917.
- Raymond, C.R., Paul, J.S., Marian, E.Q., 2009. Handbook of pharmaceutical excipients.
- Realdon, N., Ragazzi, E., Ragazzi, E., 2001. Effect of gelling conditions and mechanical treatment on drug availability from lipogel. *Drug Development and Industrial Pharmacy*, 27, 165–170.
- Reddy, L.H., Kute, V.B., Bakshi, N., Murthy, R.S.R., 2006. Tamoxifen citrate loaded solid lipid nanoparticles (SLN): Preparation, characterisation, *in vitro* drug release, and pharmacokinetic evaluation. *Pharmaceutical Development and Technology*, 11, 167–177.
- Reichman, D.E., Greenberg, J.A., 2009. Reducing surgical site infections: A review. *Reviews in Obstetrics & Gynaecology*, 2, 212–221.
- Richards, R.M.E., Odelola, H.A., Anderson, B., 1984. Effect of silver on whole cells and spheroplasts of a silver resistant pseudomonas aeruginosa. *Microbios*, 39, 151–158.
- Richardson, M., 2004. Acute wounds: An overview of physiological healing process. *Nursing Times*, 100, 50–53.
- Rigg, P.C., Barry, B.W., 1990. Shed snake skin and hairless mouse skin as model membranes for human skin during permeation studies. *Journal of Investigative Dermatology*, 94, 235–240.
- Robson, M.C., Steed, D.L., Franz, M.G., 2001. Wound healing: Biologic features and approaches to maximise healing trajectories. *Current Problems in Surgery*, 38, 72–140.
- Rohman, A., Che Man, Y.B., 2012. Quantification and classification of corn and sunflower oils as adulterants in olive oil using chemometrics and FTIR spectra. *The Scientific World Journal*, 2012, 1–6.

- Romero-García, J.M., Niño, L., Martínez-Patiño, C., Álvarez, C., Castro, E., Negro, M.J., 2014. Biorefinery based on olive biomass: State of the art and future trends. *Bioresource Technology*, 159, 421–432.
- Rosenberg, A., Alatary, S.D., Peterson, A.F., 1976. Safety and efficacy of the antiseptic chlorhexidine gluconate. *The Journal of Surgery, Gynecology and Obstetrics*, 143, 789–792.
- Rosso, J.Q., Levin, J., 2011. Clinical relevance of maintaining the structural and functional integrity of the stratum corneum: Why is it important to you? *Journal of Drugs in Dermatology*, 10, 5–12.
- Roth, S.H., Fuller, P., 2011. Diclofenac sodium topical solution 1.5 % w/w with dimethyl sulfoxide compared with placebo for the treatment of osteoarthritis: Pooled safety results. *Postgraduate Medical Journal*, 123, 180–188.
- Rowe, R.C., Sheskey, P.J., Cook, W.G., Fenton, M.E., 2012. Sorbitan esters, in: *Handbook of Pharmaceutical Excipients*. Washington, DC, pp. 675–681.
- Ruktanonchai, U., Sakulkhua, U., Bejraphaa, P., Opanasopitb, P., Bunyapraphatsarac, N., Junyaprasertc, V., Puttipipatkachorn, S., 2009. Effect of lipid types on physicochemical characteristics, stability and antioxidant activity of gamma-oryzanol-loaded lipid nanoparticles. *Journal of Microencapsulation: Micro and Nano Carriers*, 26, 614–626.
- Rupenganta, A., Somasundaram, I., Ravichandiram, V., Kausalya, J., Senthilnathan, B., 2011.
- Solid lipid nanoparticles - A versatile carrier system. *Journal of Pharmacy Research*, 4, 2069–2075.
- Russell, A.D., Hugo, W.B., 1994. Antimicrobial activity and action of silver. *Progress in Medicinal Chemistry*, 31, 351–371.
- Russell, A.D., Hugo, W.B., Ayliffe, G.A.J., 2013. Sensitivity of protozoa to disinfection B. acanthamoeba and contact lens solutions, in: Fraiese, A.P., Maillard, J.Y., Sattar, S. (Eds.), *Principles and Practice of Disinfection, Preservation and Sterilisation*. Willey Blackwell, Oxford, England, pp. 241–260.
- Ryan, K.J., Mezei, M., 1975. *In vivo* method for monitoring polysorbate 85 effect on epidermal permeability. *Journal of Pharmaceutical Sciences*, 64, 671–673.
- Saberi, A.M., Fang, Y., McClements, D.J., 2013. Fabrication of vitamin E enriched nanoemulsions: Factors affecting particle size using spontaneous emulsification. *Journal of Colloid and Interface Science*, 391, 95–102.
- Sadlon, A.E., Lamson, D.W., 2010. Immune-modifying and antimicrobial effects of eucalyptus oil and simple inhalation devices. *Alternative Medicine Review*, 15, 33–47.

- Saify, Z.S., Ahsan, O., Dayo, A., 2000. Cineole as skin penetration enhancer. *Pakistan Journal of Pharmaceutical Sciences*, 13, 29–32.
- Salager, J.L., 2000. Formulation concepts for the emulsion makers., In: Nielloud F, MartiI-Mestres G. (Ed.), *Pharmaceutical Emultions and Suspensions: Drugs and the Pharmaceutical Sciences*. New York: Marcel Dekker, pp. 19–72.
- Salari, M.H., Amine, G., Shirazi, M.H., Hafezi, R., Mohammadypour, M., 2006. Antibacterial effects of eucalyptus globulus leaf extract on pathogenic bacteria isolated from specimens of patients with respiratory tract disorders. *Clinical Microbiology and Infection*, 12, 194–196.
- Salminen, H., Helgason, T., Aulbach, S., Kristinsson, B., Kristbergsson, K., Weiss, J., 2014. Influence of cosurfactants on crystallisation and stability of solid lipid nanoparticles. *Journal of Colloid and Interface Science*, 426, 256–263.
- Salunkhe, S.S., Thorat, J.D., Mali, S.S., Hajare, A.A., Bhatia, N.M., 2013. Formulation, development and evaluation of artemisia pallens (davana) oil based topical microemulsion. *World Journal of Pharmacy and Pharmaceutical Sciences*, 2, 5725–5736.
- Sandhu, P., Bilandi, A., Kumar, S., Kapoor, B., Kataria, S., Rathore, D., Bhardwaj, S., 2012. Additives in topical dosage forms. *International Journal of Pharmaceutical, Chemical and Biological Sciences*, 2, 78–96.
- Sanna, V., Mariani, A., Caria, G., Sechi, M., 2009. Synthesis and evaluation of different fatty acid esters formulated into precinol ATO based lipid nanoparticles as vehicles for topical delivery. *Chemical and Pharmaceutical Bulletin*, 57, 680–684.
- Sapra, B., Jain, S., Tiwary, A.K., 2008. Percutaneous permeation enhancement by terpenes: Mechanistic view. *American Association of Pharmaceutical Scientists Journal*, 10, 120–132.
- Saraiya, K., Bolton, S., 1990. Use of precinol to prepare sustained release tablets of theophylline and quinidine gluconate. *Drug Development and Industrial Pharmacy*, 16, 1963–1969.
- Sarkar, S.N., 1994. Capillary permeability increasing effect of eucalyptus hybrid leaf and a seseli indicum seed oils in rabbit. *Indian Journal of Pharmacology*, 26, 55–56.
- Savage, C.A., 1971. A new bacteriostat for skin care products. *Drug and Cosmetic Industry*,

109, 161–163.

Schaberg, D.R., 1994. Resistant Gram-positive organisms. *Annals of Emergency Medicine*, 24, 462–464.

Schaberg, D. R., Culver, D. H., Gaynes, R. P., 1991. Major trends in the microbial etiology of nosocomial infection. *The American Journal of Medicine*, 91, 72S-75S.

Schaefer, H., Lademann, J., 2001. The role of follicular penetration - A differential view. *Skin*

*Pharmacology and Applied Skin Physiology*, 14, 23–27.

Schäfer-Korting, M., Wolfgang, M., Hans-Christian, K., 2007. Lipid nanoparticles for improved topical application of drugs for skin diseases. *Advanced Drug Delivery Reviews*, 59, 427–443.

Schaefer, U.F., Hansen, S., Schneider, M., Luengo, C.J., Lehr, C.M., 2008. Models for skin absorption and skin toxicity testing., in: *Drug Absorption Studies*. pp. 3–33.

Schmook, F.P., Meingassner, J.G., Billich, A., 2001. Comparison of human skin or epidermis

models with human and animal skin in *in vitro* percutaneous absorption. *International Journal of Pharmaceutics*, 215, 51–56.

Schubert, M., 2003. Solvent injection as a new approach for manufacturing lipid nanoparticles - Evaluation of the method and process parameters. *European Journal of Pharmaceutics and Biopharmaceutics*, 55, 125–131.

Schultz, G.S., Barillo, D.J., Mozingo, D.W., and Chin, G.A., 2004. Wound bed preparation and brief history of time. *International Wound Journal*, 1, 19–32.

Schultz, G.S., Sibbald, R.G., Falanga, V., Ayello, E.A., Dowsett, C., Harding, K., Romanelli,

M., Stacey, M.C., Teot, L., Vanscheidt, W., 2003. Wound bed preparation: A systematic approach to wound management. *Wound Repair and Regeneration*, 11, 1–28.

Sepideh, A.B., Moujan, M., Rezayat, S.M., Mitra, K., Amir, A., Parisa, Z., 2013. Toxicity assessment of nanosilver wound dressing in wistar rat. *Acta Medica Iranica*, 51, 203–208.

Severino, P., Andreani, T., Macedo, A.S., Fangueiro, J.F., Santana, M.H., Silva, A.M., 2012. Current state-of-art and new trends on lipid nanoparticles (SLN and NLC) for oral drug delivery. *Journal of Drug Delivery*, 750–891.

Shafaat, K., Kumar, B., Das, S.K., Hasan, R.U., Prajapati, S.K., 2013. Novel nanoemulsion as vehicles for transdermal delivery of clozapine: *In vitro* and *in vivo* studies. *International Journal of Pharmacy and Pharmaceutical Sciences*, 5, 126–134.

Shah, B., Khunt, D., Bhatt, H., Misra, M., Padh, H., 2015. Application of quality by design

approach for intranasal delivery of rivastigmine loaded solid lipid nanoparticles: Effect on formulation and characterisation parameters. *European Journal of Pharmaceutical Sciences*, 78, 54–66.

Shahavi, M.H., Hosseini, M., Jahanshahi, M., Meyer, R.L., Darzi, G.N., 2015. Evaluation of critical parameters for preparation of stable clove oil nanoemulsion. *Arabian Journal of Chemistry*, .

Shaikh, N.H., 1991. Effect of different binders on release characteristics of theophylline from compressed microspheres. *Drug Development and Industrial Pharmacy*, 17, 793–804.

Shakeel, F., Haq, N., Al-Dhfyhan, A., Alanazi, F.K., Alsarra, I.A., 2013. Chemoprevention of skin cancer using low HLB surfactant nanoemulsion of 5-fluorouracil: A preliminary study. *Drug Delivery*, 22, 573–580.

Shakeel, F., Haq, N., Alanazi, F.K., Alsarra, I.A., 2015. Removal of glibenclamide from aqueous solution using water/PEG-400/ethanol/eucalyptus oil green nanoemulsions. *Journal of Molecular Liquids*, 203, 120–124.

Shakeel, F., Haq, N., Alanazi, F.K., Alsarra, I.A., 2014a. Removal of xylenol orange from its aqueous solution using SDS-self microemulsifying systems: Optimisation by Box–Behnken statistical design., *Environmental Science and Pollution Research*, 21, 5187–5200.

Shakeel, F., Haq, N., F.K. Alanazi, I., Alsarra, A., 2014b. Box–Behnken statistical design for removal of methylene blue from aqueous solution using sodium dodecyl sulfate self-microemulsifying systems. *Journal of Industrial and Engineering Chemistry*, 53, 1179–1188.

Shakeel, F., Ramadan, W., 2010. Transdermal delivery of anticancer drug caffeine from water-in-oil nanoemulsions. *Colloids and Surfaces B: Biointerfaces*, 75, 356–362.

Sharma, N., Bansal, M., Visht, S., Sharma, P.K., Kulkarni, G.T., 2010. Nanoemulsion : A new concept of delivery system. *Chronicles of Young Scientists*, 1, 2–6.

Sheet, E.M., Saleh, S.M., Hamed, A.Y., 2007. Primary identification of eucalyptus (eucalyptus camaldulensis) wood lignina monomers by FTIR spectroscopy. *Mesopotamia Journal of Agriculture*, 35, 10–17.

- Shegokar, R., Singh, K.K., Müller, R.H., 2011. Production and stability of stavudine solid lipid nanoparticles - from lab to industrial scale. *International Journal of Pharmaceutics*, 416, 461–470.
- Shen, T., Xu, H., Weng, W., Zhang, J., 2013. Development of a reservoir type transdermal delivery system containing eucalyptus oil for tetramethylpyrazine. *Drug Delivery*, 20, 19–24.
- Shenoy, V.S., Gude, R.P., Murthy, R.S., 2009. Paclitaxel-loaded glyceryl palmitostearate nanoparticles: *In vitro* release and cytotoxic activity. *Journal of Drug Targeting*, 17, 304–310.
- Sherry, E., Reynolds, M., Sivananthan, S., Mainawalala, S., Warnke, P.H., 2004. Inhalational phytochemicals as possible treatment for pulmonary tuberculosis: Two case reports. *American Journal of Infection Control*, 32, 369–370.
- Sherry, E., Sivananthan, S., Warnke, P.H., Eslick, G.D., 2003. Topical phytochemicals used to salvage the gangrenous lower limbs of type 1 diabetic patients. *Diabetes Research and Clinical Practice*, 62, 65–66.
- Sherry, E., Warnke, P.H., 2004. Successful use of an inhalational phytochemical to treat pulmonary tuberculosis: A case report. *Phytomedicine*, 11, 95–97.
- Shumaia, P., Rafshanjani, A.S., Kader, A., 2014. Formulation and evaluation of dexamethasone loaded stearic acid nanoparticles by hot homogenisation method. *International Current Pharmaceutical Journal*, 3, 331–335.
- Shupp, J.W., Nasabzadeh, T.J., Rosenthal, D.S., Jordan, M.H., Fidler, P., Jeng, J.C., 2010. A review of local pathophysilologic bases of burn wound progression. *Journal of Burn Care & Research*, 31, 849–873.
- Sikkema, J., De Bont, J.A., Poolman, B., 1995. Mechanisms of membrane toxicity of hydrocarbons. *Microbiological Reviews*, 59, 201–222.
- Silva, J., Abebe, W., Sousa, S.M., Duarte, V.G., Machado, M.I.L., Matos, F.J.A., 2003. Analgesic and anti-inflammatory effects of essential oils of eucalyptus. *Bioresource Technology*, 89, 277–283.
- Silver, S.L., Phung, T., 1996. Bacterial heavy metal resistance: New surprises. *Annual Review of Microbiology*, 50, 753–789.
- Simonsen, L., Fullerton, A., 2007. Development of an *in vitro* skin permeation model



- simulating atopic dermatitis skin for the evaluation of dermatological products. *Skin Pharmacology and Physiology*, 20, 230–236.
- Singh, S., Majumdar, D.K., 1999. Effect of *Ocimum sanctum* fixed oil on vascular permeability and leucocytes migration. *Indian Journal of Experimental Biology*, 37, 1136–1138.
- Sinko, B., Garrigues, T.M., Balogh, G.T., Nagy, Z., Tsinman, O., Avdeef, A., Takacs-Novak, K., 2012. Skin-PAMPA: A new method for fast prediction of skin penetration. *European Journal of Pharmaceutics*, 45, 698–707.
- Sinko, B., Kokosi, J., Avdeef, A., Takacs-Novak, K., 2009. A PAMPA study of the permeability enhancing effect of new ceramide analogues. *Chemical Biodiversity*, 6, 1867–1874.
- Siramon, P., Ohtani, Y., 2007. Antioxidative and antiradical activities of eucalyptus *camaldulensis* leaf oils from Thailand. *Journal of Wood Science*, 53, 498–504.
- Small, H., Adams, D., Casey, A.L., Crosby, C.T., Lambert, P.A., Elliott, T., 2008. Efficacy of Adding 2 % (w/v) chlorhexidine gluconate to 70 % (v/v) isopropyl alcohol for skin disinfection prior to peripheral venous cannulation. *Infection Control and Hospital Epidemiology*, 29, 963–5.
- Smyth, E.T.M., Emmerson, A.M., 2000. Surgical site infection surveillance. *The Journal of Hospital Infection*, 45, 173–184.
- Soares, S., Fonte, P., Costa, A., Andrade, J., Seabra, V., Ferreira, D., Reis, S., Sarmiento, B., 2013. Effect of freeze-drying, cryoprotectants and storage conditions on the stability of secondary structure of insulin-loaded solid lipid nanoparticles. *International Journal of Pharmaceutics*, 456, 370–381.
- Soleimanpour, M., Koocheki, A., Kadkhodae, R., 2013. Influence of main emulsion components on the physical properties of corn oil in water emulsion: Effect of oil volume fraction, whey protein concentrate and *lepidium perfoliatum* seed gum. *Food Research International*, 50, 457–466.
- Soon, S.Y., Harbidge, J., Titchener-Hooker, N.J., Shamlou, P.A., 2001. Prediction of drop breakage in an ultra high velocity jet homogeniser. *Journal of chemical Engineering of Japan*, 34, 640–646.

- Spagnul, A., Bouvier-Capely, C., Phan, G., Landon, G., Tessier, C., Suhard, D., Rebière, F., Agarande, M., Fattal, E., 2011. *Ex vivo* decrease in uranium diffusion through intact and excoriated pig ear skin by a calixarene nanoemulsion. *European Journal of Pharmaceutics and Biopharmaceutics*, 79, 258–267.
- Srilatha, R., Aparna, C., Srinivas, P., Sadananda, M., 2013. Formulation, evaluation and characterisation of glipizide nanoemulsion. *Asian Journal of Pharmaceutical and Clinical Research*, 6, 66–71.
- St. John, J. V., 2010. Antimicrobial effectiveness and exudate management from novel silver containing powder dressing, in: WHS Meeting.
- Starcher, B., Aycock, R.L., Hill, C.H., 2005. Multiple roles for elastic fibers in the skin. *Journal of Histochemistry and Cytochemistry*, 53, 431–443.
- Stevens, D.L., 2009. Bacteria, Treatments for skin and soft-tissue and surgical site infections due to MDR Gram-positive. *The Journal of Infection*, 59, S32–S39.
- Stoughton, R.B., McClure, W.O., 1983. Azone: A new non-toxic enhancer of cutaneous penetration. *Drug Development and Industrial Pharmacy*, 9, 725–744.
- Strickley, R.G., 2004. Solubilising excipients in oral and injectable formulations. *Pharmaceutical Research*, 21, 201–230.
- Su, Y.C., Ho, C.L., Wang, E.I., Chang, S.T., 2006. Antifungal activities and chemical compositions of essential oils from leaves of four eucalyptus. *Taiwan Journal of Forest Science*, 21, 49–61.
- Sugumar, S., Ghosh, V., Nirmala, M.J., Mukherjee, A., Natarajan, C., 2014. Ultrasonic emulsification of eucalyptus oil nanoemulsion: Antibacterial activity against *Staphylococcus aureus* and wound healing activity in wistar rats. *Ultrasonics Sonochemistry*, 21, 1044–1049.
- Syed, H.K., Peh, K.K., 2014. Identification of phases of various oil, surfactant/cosurfactants and water system by ternary phase diagram. *Acta Poloniae Pharmaceutica. Drug Research*, 71, 301–309.
- Syed, M.A. V., 2013. Biodegradable preparation, characterisation and *in vitro* evaluation of stealth docetaxel lipid nanoemulsions for efficient cytotoxicity. *International Journal of Drug Delivery*, 5, 188–195.
- Szycher, M., Lee, S.J., 1992. Modern wound dressings: A systemic approach to wound healing. *Journal of Biomaterials Applications*, 7, 142–213.

- Tagne, J.B., Kakurnanu, S., Nicolosi, R.J., 2008. Nanoemulsion preparations of the anticancer drug dacarbazine significantly increase its efficacy in a xenograft mouse melanoma model. *Molecular pharmaceutics*, 5, 1055–1063.
- Takahashi, T., Kokubo, R., Sakaino, M., 2004. Antimicrobial activities of eucalyptus leaf extracts and flavonoids from eucalyptus maculate. *Letters in Applied Microbiology*, 39, 60–64.
- Takashi, U., Wesam, R.K., Sayumi, K., Hiroaki, T., Takeshi, O., Kenji, S., 2015. Prediction of skin permeation by chemical compounds using the artificial membrane, Strat-M (TM). *European Journal of Pharmaceutical Sciences*, 67, 113–118.
- Tang, S.Y., Shridharan, P., Sivakumar, M., 2013. Impact of process parameters in the generation of novel aspirin nanoemulsions - Comparative studies between ultrasound cavitation and microfluidizer. *Ultrasonics Sonochemistry*, 20, 485–497.
- Tanja, M.G., Kristine, B.A., Nielsen, O.F., Anders, E., 2010. FTIR imaging and ATR-FT-Far-IR synchrotron spectroscopy of pig ear skin. *Spectroscopy*, 24, 105–111.
- Tarabet, L., Loubar, K., Lounici, M.S., Hanchi, S., Tazerout, M., 2012. Eucalyptus biodiesel as an alternative to diesel fuel: Preparation and tests on DI diesel engine. *Journal of Biomedicine and Biotechnology*, 2012, 235485.
- Taylor, P., 1998. Ostwald ripening in emulsions. *Advances in Colloid and Interface Science*, 75, 107–163.
- Teichmann, A., Jacobi, U., Ossadnik, M., Richter, H., Koch, S., Sterry, W., Lademann, J., 2005. Differential stripping: Determination of the amount of topically applied substances penetrated into the hair follicles. *Journal of Investigative Dermatology*, 125, 264–269.
- Teichmann, A., Otberg, N., Jacobi, U., Sterry, W., Lademann, J., 2006. Follicular penetration: Development of a method to block the follicles selectively against the penetration of topically applied substances. *Skin Pharmacology and Physiology*, 19, 216–223.
- Tenjarla, S., 1999. Microemulsions: An overview and pharmaceutical applications. *Critical Reviews in Therapeutic Drug Carrier Systems*, 16, 461–521.
- Tharwat, T., Izquierdob, P., Esquenab, J., Solans, C., 2004. Formation and stability of nanoemulsions. *Advances in Colloid and Interface Science*, 108, 303–318.
- Thomas, S., 2000. Alginate dressings in surgery and wound management- part 1. *Wound Care*, 9, 56–60.

- Tobin, D.J., 2001. Biochemistry of human skin-our brain on the outside. *Chemical Society Review*, 14, 23–27.
- Trauera, S., Richter, H., Kuntschec, J., Büttemeyere, R., Liebsch, M., Linscheidf, M., Fahr, A., Schäfer-Korting, M., Lademanna, J., Patzelta, A., 2014. Influence of massage and occlusion on the *ex vivo* skin penetration of rigid liposomes and invasomes. *European Journal of Pharmaceutics and Biopharmaceutics*, 86, 301–306.
- Traunter, B.W., Clarridge, J.E., Darouiche, R.O., 2002. Skin antiseptics kits containing alcohol and chlorhexidine gluconate or tincture of iodine are associated with low rates of blood culture contamination. *Journal of Hospital Infection*, 23, 397–401.
- Traversa, B., Sussman, G., 2001. The role of growth factors, cytokines and protease in wound management. *Primary Intention*, 9, 161–167.
- Triantafyllopoulos, G., Stundner, O., Memtsoudis, S., Poultsides, L.A., 2015. Patient, surgery and hospital related risk factors for surgical site infections following total hip arthroplasty. *The Scientific World Journal*, 1–9.
- Tripathy, M., 2014. Comparison of process parameter optimisation using different designs in nanoemulsion based formulation for transdermal delivery of fullerene. *International Journal of Nanomedicine*, 9, 4375–4386.
- Trotta, M., Debernardi, F., Caputo, O., 2003. Preparation of solid lipid nanoparticles by a solvent emulsification - Diffusion technique. *International Journal of Pharmaceutics*, 257, 153–160.
- Tsai, M.J., Fu, Y.S., Lin, Y.H., Huang, Y.B., Wu, P.C., 2014. The effect of nanoemulsion as a carrier of hydrophilic compound for transdermal delivery. *PLoS ONE*, 9, 1–8.
- Tsai, P.J., Huang, C.T., Lee, C.C., Li, C.L., Huang, Y.B., 2013. Isotretinoin oil-based capsule formulation optimisation. *Scientific World Journal*, 2013, 1–8.
- Tsinman, K., Sinko, B., 2013. A high throughput method to predict skin penetration and screen topical formulations. *Cosmetic and Toiletries*, 128, 192–199.
- Uchida, T., Kadhum, W.R., Kanai, S., Todo, H., Oshizaka, T., Sugibayashi, K., 2015. Prediction of skin permeation by chemical compounds using the artificial membrane, Strat-M. *European Journal of Pharmaceutical Sciences*, 67, 113–118.
- Ueno, H., Yamada, H., Tanaka, I., Kaba, N., Matura, M., Okumura, M., Kadosawa, T.,

- Fujinaga, T., 1999. Accelerating effects of chitosan for healing at early phase of experimental open wound in dogs. *Biomaterials*, 20, 1407–1414.
- Urban, K., Wagner, G., 2006. Rotor stator and disc systems for emulsification processes. *Chemical Engineering Technology*, 29, 24–31.
- Van Rijswijk, L., 2006. Ingredient based wound dressing classification: A paradigm shift that is passe´ and in need of replacement. *Journal of Wound Care*, 15, 11–14.
- Van-der Valk, P.G., Kruis-de Vries, M.H., Nater, J.P., Bleumink, E., De Jong, M.C., 1985. Eczematous (irritant and allergic) reactions of the skin and barrier function as determined by water vapour loss. *Clinical Experimental Dermatology*, 10, 185–193.
- Vatsraj, S., Chauhan, K., Pathak, H., 2014. Formulation of a novel nanoemulsion system for enhanced solubility of a sparingly water soluble antibiotic, clarithromycin. *Journal of Nanoscience*, 1–7.
- Vilela, R., Jacomo, A.D.N., Tresoldi, A.T., 2007. Risk factors for central venous catheter-related infections in paediatric intensive care. *Clinical Science*, 62, 537.544.
- Visscher, M.O., 2009. Update on the use of topical agents in neonates. *Newborn and Infant Nursing Reviews*, 9, 31–47.
- Vogt, A., Combadiere, B., Hadam, S., Stieler, K.M., Lademann, J., Schaefer, H., B., A., Sterry, W., Blume-Peytavi, U., 2006. 40 nm, but not 750 or 1500 nm, nanoparticles enter epidermal CD1a+ cells after transcutaneous application on human skin. *Journal of Investigative Dermatology*, 126, 1316–1322.
- Voort, F.R. van de, Sedman, J., Russin, T., 2001. Lipids analysis by vibrational spectroscopy. *European Journal of Lipid Science and Technology*, 103, 815–840.
- Waalder, S.M., Rolla, G., Skjorland, K.K., Ogaard., B., 1993. Effects of oral rinsing with triclosan and sodium lauryl sulfate on dental plaque formation: Pilot study. *Scandinavian Journal of Dental Research*, 101, 192–195.
- Waller, J.M., Maibach, H.I., 2009. A quantitative approach to age and skin structure and function: Protein, glycosaminoglycan, water, and lipid content and structure., in: *Handbook of Cosmetic Science and Technology*. pp. 145–154.
- Waller, J.M., Maibach, H.I., 2005. Age and skin structure and function, a quantitative approach (I): Blood flow, pH, thickness, and ultrasound echogenicity. *Skin Research and*

*Technology*, 11, 221–235.

Wang, J.C.T., Williams, R.R., Wang, L., Loder, J., 1990. *In vitro* skin penetration of and bioassay of chlorhexidine phosphanilate, a new antimicrobial agent. *Pharmaceutical Research*, 7, 995 – 1002.

Weigmann, H.J., Schanzer, S., Patzelt, A., Bahaban, V., Durat, F., Sterry, W., Lademann, J., 2009. Comparison of human and porcine skin for characterisation of sunscreens. *Journal of Biomedical Optics*, 14, 24–27.

Weiss, J., Canceliere, C., McClements, D.J., 2000. Mass transport phenomena in oil-in-water emulsions containing surfactant micelles: Ostwald ripening. *Langmuir*, 16, 6833–6838.

Westesen, K., Bunjes, H., Koch, M.H., 1997. Physicochemical characterisation of lipid nanoparticles and evaluation of their drug loading capacity and sustained release potential. *Journal of Controlled Release*, 48, 223–236.

Wichterle, O., Lim, D., 1960. Hydrophilic gels for biological use. *Nature*, 185, 117–118.

Wiechers, J.W., Drenth, B.F., Jonkman, J.H., de Zeeuw, R.A., 1987. Percutaneous absorption and elimination of the penetration enhancer azone in humans. *Pharmaceutical Research*, 4, 519–523.

Wild, T., Rahbarnia, A., Kellenar, M., Sobotka, L., Eberlein, T., 2010. Basics in nutrition and wound healing. *Nutrition*, 26, 862–866.

Williams, A.C., Barry, B.W., 2004. Penetration enhancers. *Advanced Drug Delivery Reviews*, 56, 603–618.

Williams, A.C., Barry, B.W., 1991. Terpenes and the lipid-protein partitioning theory of skin penetration enhancement. *Pharmaceutical Research*, 8, 17–24.

Williams, A.C., Barry, B.W., 1991. Terpenes and the lipid–protein partitioning theory of skin penetration enhancers. *Pharmaceutical Research*, 8, 17–24.

Williams, A.C., Barry, B.W., 1989a. Essential oils as novel human skin penetration enhancers.

*International Journal of Pharmaceutics*, 57, R7–R9.

Williams, A.C., Barry, B.W., 1989b. Essential oils as novel human skin penetration enhancers.

- International Journal of Pharmaceutics*, 57, 7–9.
- Williams, A.C., Edwards, H.G.M., Lawson, E.E., Barry, B.W., 2006. Molecular interactions between the penetration enhancer 1,8-cineole and human skin. *Journal of Raman Spectroscopy*, 37, 361–366.
- Williford, P.M., 1999. Opportunities for mupirocin calcium cream in the emergency department. *Journal of Emergency Medicine*, 17, 213–220.
- Wilson, J., Wloch, C., Saei, A., McDougall, C., Harrington, P., Charlett, A., Lamagni, T., Elgohari, S., Sheridan, E., 2015. Inter-hospital comparison of rates of surgical site infection following caesarean section delivery: Evaluation of a multicentre surveillance study. *Journal of Hospital Infection*, 84, 44–51.
- Witte, M.B., Barbul, A., 1997. General principles of wound healing. *Surgical Clinics of North America*, 77, 509–528.
- Wooster, T.J., 2008. Impact of oil type on nanoemulsion formation and ostwald ripening stability. *Langmuir*, 24, 12758–12765.
- Wosika, H., Cal, K., 2010. Targeting to hair follicles: Current status and potential. *Journal of Dermatological Science*, 57, 83–89.
- Wulff-Perez, A., Torcello-Gomez, M.J., 2009. Stability of emulsions for parenteral feeding: Preparation and characterisation of o/w nanoemulsions with natural oils and pluronic F68 as surfactant. *Food Hydrocolloids*, 23, 1096–1102.
- Yadav, N., Khatak, S., Singh, U.S., 2013. Solid lipid nanoparticles: A review. *International Journal of Applied Pharmaceutics*, 5, 8–18.
- Yamane, M.A., Williams, A.C., Barry, B.W., 1995. Terpene penetration enhancers in propylene glycol/water co-solvent systems: Effectiveness and mechanism of action. *Journal of Pharmacy and Pharmacology*, 47, 978–989.
- Yang, R., Gao, R.C., Cai, C.F., Xu, H., Li, F., He, H.B., Tang, X., 2010. Preparation of gel core solid lipid nanoparticle: A novel way to improve the encapsulation of protein and peptide. *Chemical and Pharmaceutical Bulletin*, 58, 1195–1202.
- Yilmaz, E., Borchert, H.H., 2005. Design of a phytosphingosine containing, positively charge nanoemulsion as a colloidal carrier system for dermal application of ceramides. *European Journal of Pharmaceutics and Biopharmaceutics*, 60, 91–98.

- Yokomizo, Y., Sagitani, H., 1996. The effects of phospholipids on the percutaneous penetration of indomethacin through the dorsal skin of guinea pig *in vitro*. 2. The effects of the hydrophobic group in phospholipids and a comparison with general enhancers. *Journal of Controlled Release*, 42, 37–46.
- Yu, M., Ma, H., Lei, M., Li, N., Tan, F., 2014. *In vitro/in vivo* characterisation of nanoemulsion formulation of metronidazole with improved skin targeting and anti rosacea properties. *European Journal of Pharmaceutics and Biopharmaceutics*, 88, 92–103.
- Zhang, H., 2003. Commonly used surfactant, tween 80, improves absorption of p-glycoprotein substrate, digoxin, in rats. *Archives of Pharmacal Research*, 26, 768–772.
- Zhang, J., Smith, E., 2011. Percutaneous permeation of betamethasone 17-valerate incorporated in lipid nanoparticles. *Journal of Pharmaceutical Sciences*, 100, 896–903.
- Zhang, M., O'Donoghue, M.M., Ito, T., Hiramatsu, K., Boost, M.V., 2011. Prevalence of antiseptic-resistance genes in *Staphylococcus aureus* and coagulase-negative *staphylococci* colonising nurses and the general population in Hong Kong. *Journal of Hospital Infection*, 78, 113–117.
- Zhao, Y., Wang, C., Chowb, A.H., Ren, K., Gong, T., Zhang, Z., Zheng, Y., 2010. nanoemulsifying drug delivery system (SNEDDS) for oral delivery of Zedoary essential oil: Formulation and bioavailability studies. *International Journal of Pharmaceutics*, 383.
- Ziani, K., Barish, J.A., McClements, D.J., Goddard, J.M., 2011. Manipulating interactions between functional colloidal particles and polyethylene surfaces using interfacial engineering. *Journal of Colloid and Interface Science*, 360, 31–38.



## **8. PUBLICATIONS AND PROFESSIONAL ACTIVITIES**

### **Publications**

Kakadia, P. G., Conway, B. R., 2016. Design, optimisation and evaluation of solid lipid nanoparticles as potential dermal drug delivery system. – Manuscript ready for submission.

Kakadia, P. G., Conway, B. R., 2015. Lipid nanoparticles for dermal drug delivery. *Current Pharmaceutical Design*, 21(20), 2823 – 2829.

Kakadia, P. G., Conway, B. R., 2014. Solid lipid nanoparticles: A novel approach for dermal drug delivery. *American Journal of Pharmaceutical Sciences*, 2(5A), 1 – 7.

### **Oral Presentation**

Kakadia, P. G., Conway, B. R., 2013. Formulations of solid lipid nanoparticles for topical delivery of triclosan. 4<sup>th</sup> APS International PharmSci Conference, Heriot Watt University, Edinburgh, U.K.

### **Posters**

Kakadia, P. G., Conway, B. R., 2015. Comparative permeation of chlorhexidine digluconate using excised skin and artificial membrane. American Association of Pharmaceutical Scientists Annual Meeting, Orlando Convention Centre, Florida, U.S.A.

Kakadia, P. G., Conway, B. R., 2015. Assessing follicular delivery of triclosan formulations using tape stripping techniques. American Association of Pharmaceutical Scientists Annual Meeting, Orlando Convention Centre, Florida, U.S.A.

Kakadia, P. G., Conway, B. R., 2015. Chlorhexidine digluconate nanoemulsions for topical antiseptis. Controlled Release Society Annual Meeting and Exposition, Edinburgh, U.K.

Kakadia, P. G., Conway, B. R., 2014. Topical delivery of nanoencapsulated triclosan. American Association of Pharmaceutical Scientists Annual Meeting, San Diego Convention Centre, California, U.S.A.

Kakadia, P. G., Conway, B. R., 2014. Topical delivery of nanoencapsulated triclosan by lipid based carriers. 5<sup>th</sup> APS International PharmSci Conference, University of Hertfordshire, U.K.

Kakadia, P. G., Conway, B. R., 2014. Topical drug delivery of nanoencapsulated antibacterial agents. Controlled Release Society Annual Meeting and Exposition, Convention centre at Hilton, Chicago, U.S.A.

### **Professional Activities**

Oct 2014 – Oct 2015: Worked as Vice-chair of American Association of Pharmaceutical Scientists (AAPS) student chapter at University of Huddersfield.

Oct 2013 – Oct 2014: Designed and supervised undergraduate research projects.

Oct 2013 – Oct 2015: Attended and participated in national and international scientific conferences.